

# Differences and Similarities in the Regulation of RAF Isoforms: Identification of Novel A-RAF Phosphorylation Sites

Dissertation zur Erlangung des  
naturwissenschaftlichen Doktorgrades  
der Bayerischen Julius-Maximilians-Universität Würzburg



vorgelegt von

**Angela Baljuls**

aus

Koktschetaw, Kasachstan

Würzburg, 2008

Eingereicht am: \_\_\_\_\_

Mitglieder der Promotionskommission:

Vorsitzender: Prof. Dr. Martin J. Müller

Gutachter: Prof. Dr. Ulf R. Rapp

Gutachter: Prof. Dr. Ricardo Benavente

Tag des Promotionskolloquiums: \_\_\_\_\_

Doktorurkunde ausgehändigt am: \_\_\_\_\_

Meiner Familie  
zum Dank für Eure Liebe und Unterstützung

*Basic research is like shooting an arrow into the air and, where it lands,  
painting a target.*

*Homer Burton Adkins*

---

# TABLE OF CONTENTS

|  |    |
|--|----|
| <b>1. SUMMARY</b>  | 5  |
| <b>2. ZUSAMMENFASSUNG</b>  | 6  |
| <b>3. INTRODUCTION</b>   | 7  |
| <b>3.1. MAP kinase signaling pathways</b>                                    | 7  |
| <b>3.2. Key components of the classical MAP kinase cascade</b>               | 11 |
| <b>3.2.1. EGF receptor as an example of receptor tyrosine kinases (RTKs)</b> | 11 |
| <b>3.2.2. Ras-GTPase</b>   | 12 |
| <b>3.2.3. Lck as an example of Src family kinases</b>                        | 15 |
| <b>3.2.4. MEK</b>  | 17 |
| <b>3.2.5. ERK</b>  | 19 |
| <b>3.2.6. Scaffolds</b>  | 22 |
| <b>3.2.7. RAF kinases</b>  | 24 |
| 3.2.7.1. Structure of RAF proteins   | 26 |
| 3.2.7.2. Regulation of RAF activity by 14-3-3 proteins                       | 28 |
| 3.2.7.3. Mechanism of Ras–RAF coupling                                       | 31 |
| 3.2.7.4. Current mechanism of RAF activation                                 | 34 |
| 3.2.7.5. Regulation of RAF activity by phosphorylation                       | 36 |
| <b>3.3. Isoform-specific properties of A-RAF</b>                             | 37 |
| <b>3.3.1. A-RAF gene</b>   | 37 |
| 3.3.1.1. Localization of A-RAF gene  | 37 |
| 3.3.1.2. Molecular organization of A-RAF gene                                | 38 |
| <b>3.3.2. A-RAF protein</b>  | 39 |
| 3.3.2.1. Splicing variants of A-RAF  | 39 |
| 3.3.2.2. Expression of A-RAF   | 39 |
| 3.3.2.3. Localization of A-RAF protein                                       | 41 |
| 3.3.2.4. Physiological role of A-RAF   | 42 |
| 3.3.2.5. Interaction partners of A-RAF                                       | 43 |
| <b>4. AIM OF THE PROJECT</b>   | 46 |
| <b>5. MATERIALS AND METHODS</b>  | 47 |
| <b>5.1. Materials</b>  | 47 |
| <b>5.1.1. Instruments</b>  | 47 |
| <b>5.1.2. Chemical reagents and general materials</b>                        | 48 |
| <b>5.1.3. Software</b>   | 49 |
| <b>5.1.4. Cell culture materials</b>   | 49 |
| <b>5.1.5. Antibodies used for Western blotting and immunoprecipitation</b>   | 50 |
| <b>5.1.6. Enzymes</b>  | 51 |
| <b>5.1.7. Kits</b>   | 51 |
|  | 1  |

---

|  |    |
|--|----|
| <b>5.1.8. Plasmids</b>   | 51 |
| <b>5.1.9. Oligonucleotides</b>   | 52 |
| <b>5.1.10. Cell lines and bacterial strains</b>                                    | 54 |
| <b>5.2. Solutions and buffers</b>  | 55 |
| <b>5.3. Methods</b>  | 60 |
| <b>5.3.1. Bacterial manipulation</b>   | 60 |
| 5.3.1.1. Preparation of chemocompetent cells (CaCl <sub>2</sub> method)            | 60 |
| 5.3.1.2. Transformation of chemocompetent bacteria                                 | 60 |
| <b>5.3.2. Methods of molecular biology</b>   | 61 |
| 5.3.2.1. Amplification of DNA fragments by PCR                                     | 61 |
| 5.3.2.2. Agarose gel electrophoresis of DNA  | 62 |
| 5.3.2.3. Isolation of DNA fragments from agarose gel                               | 63 |
| 5.3.2.4. Purification of DNA fragments   | 63 |
| 5.3.2.5. Digestion of DNA with restriction endonucleases                           | 63 |
| 5.3.2.6. DNA ligation  | 64 |
| 5.3.2.7. Mini-preparation of plasmid DNA   | 65 |
| 5.3.2.8. Midi-preparation of plasmid DNA   | 65 |
| 5.3.2.9. Determination of DNA concentration and quality                            | 65 |
| 5.3.2.10. DNA sequencing (Sanger's Dideoxynucleotide<br>Synthetic Method)          | 66 |
| 5.3.2.11. Site-directed mutagenesis  | 67 |
| <b>5.3.3. Biochemical methods</b>  | 69 |
| 5.3.3.1. Preparation of cell lysates   | 69 |
| 5.3.3.2. Determination of protein concentration (Bradford Assay)                   | 70 |
| 5.3.3.3. Sodium dodecyl sulfate polyacrylamide gel<br>electrophoresis (SDS-PAGE)   | 70 |
| 5.3.3.4. Immunoblotting  | 71 |
| 5.3.3.5. Immunoblot stripping  | 72 |
| 5.3.3.6. Immunoprecipitation   | 72 |
| 5.3.3.7. RAF <i>in vitro</i> kinase assay  | 73 |
| 5.3.3.8. Purification of GST-fusion RAF proteins from Sf9 and<br>COS7 cell lysates | 74 |
| 5.3.3.9. Purification of GST-fusion 14-3-3 proteins from <i>E. coli</i>            | 74 |
| 5.3.3.10. Purification of His-tagged RAF proteins from Sf9 cell<br>lysates         | 74 |
| 5.3.3.11. Subcellular fractionation  | 75 |
| 5.3.3.12. Mass spectrometry measurements   | 76 |
| 5.3.3.13. BIAcore's SPR technology   | 77 |
| <b>5.3.4. Cell culture methods</b>   | 78 |
| 5.3.4.1. Cultivation and passaging of eukaryotic cells                             | 78 |
| 5.3.4.2. Cell counting   | 79 |
| 5.3.4.3. Freezing, long-term storage and thawing of cells                          | 80 |
| 5.3.4.4. Transfection of mammalian adherent cells                                  | 80 |
| 5.3.4.5. Infection of insect cells   | 80 |

|  |     |
|--|-----|
| <b>5.3.5. Bioinformatic methods</b>  | 84  |
| 5.3.5.1. Modeling of the N-region interactions with the catalytic part of RAF kinases  | 84  |
| 5.3.5.2. Modeling of the three-dimensional structure of the IH-segment in A-RAF  | 84  |
| <b>6. RESULTS</b>  | 86  |
| <b>6.1. MS analysis of A-RAF phosphorylation</b>   | 86  |
| 6.1.1. Phosphorylation sites within the kinase domain of A-RAF   | 86  |
| 6.1.2. Phosphorylation sites within the regulatory part of A-RAF   | 88  |
| <b>6.2. A-RAF kinase activity is regulated by 14-3-3 proteins</b>  | 92  |
| 6.2.1. Regulation of A-RAF activity by 14-3-3 in Sf9 cells   | 93  |
| 6.2.2. Regulation of A-RAF activity by 14-3-3 in COS7 cells  | 93  |
| 6.2.3. Mammalian 14-3-3 proteins associate with RAF kinases in isoform-specific manner   | 95  |
| 6.2.4. 14-3-3 binding sites of RAF kinases differ in their binding affinities  | 98  |
| <b>6.3. Phosphorylation of MEK binding sites is critical for A-RAF kinase activity</b>   | 100 |
| <b>6.4. Phosphorylation of the activation segment is necessary for maximal activation of A-RAF</b>   | 101 |
| <b>6.5. N-region determines low basal activity and limited inducibility of A-RAF kinase</b>  | 102 |
| 6.5.1. Substitution of serine 299 to alanine in A-RAF abrogates its activation   | 104 |
| 6.5.2. Phosphorylation of the conserved serine in the N-region is predicted to depend on amino acid at position -3                         | 105 |
| 6.5.3. Mutation in the N-region leads to a constitutively active form of A-RAF kinase  | 106 |
| 6.5.4. C-RAF behaves similar to A-RAF: mutations at the positions 335 and 339 in the N-region of C-RAF modulate its kinase activity        | 111 |
| 6.5.5. Active forms of C-RAF mutants are located preferentially at membranes   | 115 |
| 6.5.6. A model derived from the tertiary structure of RAF reveals a tight contact between the N-region of A-RAF and its catalytic domain   | 118 |
| 6.5.7. R398/K399 in C-RAF and analogous residues R359/K360 in A-RAF are indispensable for their activation                                 | 121 |
| 6.5.8. Substitution of R398 in C-RAF and R359 in A-RAF by alanine induces mobility shift-associated hyperphosphorylation of these proteins | 125 |
| <b>6.6. Feedback regulation of A-RAF</b>   | 129 |

|  |     |
|--|-----|
| 6.6.1. Phosphorylation within the IH-domain positively regulates activation process of A-RAF                                     | 129 |
| 6.6.2. Spatial model reveals charge reversal at the molecular surface of IH-segment of A-RAF upon phosphorylation                | 133 |
| <b>7. DISCUSSION</b>   | 136 |
| 7.1. Isoform-specific regulation of A-RAF by 14-3-3 proteins   | 136 |
| 7.1.1. Phosphorylation of the N-region may support the association of A-RAF with 14-3-3 dimers                                   | 136 |
| 7.1.2. Differences in subcellular localization of RAF isoforms may explain the isoform-specific association with 14-3-3 proteins | 138 |
| 7.2. Maximal activation of A-RAF kinase requires phosphorylation of both MEK binding sites, S432 and T442                        | 139 |
| 7.3. Negative charge of the N-region is a prerequisite for phosphorylation of activation segment                                 | 140 |
| 7.4. Non-conserved residues within the N-region determine activation properties of RAF kinases                                   | 141 |
| 7.4.1. PKA and RSK are predicted to phosphorylate RAF on the conserved serine within the N-region                                | 142 |
| 7.4.2. Tyrosine 296 determines the low activating potency of A-RAF by sterical reasons   | 144 |
| 7.4.3. Disruption of interaction between the N-region and the PABR facilitates binding to lipids                                 | 145 |
| 7.4.4. Regulation of RAF activity by PABR is similar for A- and C-RAF  | 146 |
| 7.5. ERK-mediated feedback phosphorylation is proposed to participate in A-RAF activation  | 148 |
| 7.6. Molecular modeling of the IH-segment suggests a “switch-of-charge” mechanism for A-RAF regulation                           | 150 |
| <b>8. REFERENCES</b>   | 153 |
| <b>9. APPENDIX</b>   | 171 |
| 9.1. <i>Mascot</i> <sup>TM</sup> results pages of the phosphopeptide spectra from Table 3  | 171 |
| 9.2. Abbreviations   | 184 |
| <b>ACKNOWLEDGMENTS</b>   | 188 |
| <b>CURRICULUM VITAE</b>  | 189 |
| <b>ERKLÄRUNG</b>   | 192 |



# 1. SUMMARY

In mammals, the RAF family of serine/threonine kinases consists of three members, A-, B- and C-RAF. Activation of RAF kinases involves a complex series of phosphorylations. Although the most prominent phosphorylation sites of B- and C-RAF are well characterized, little is known about regulatory phosphorylation of A-RAF. Using mass spectrometry, we identified here a number of novel *in vivo* phosphorylation sites in A-RAF. The physiological role and the function of these sites were investigated subsequently by amino acid exchange at the relevant positions. In particular, we found that S432 participates in MEK binding and is indispensable for A-RAF signaling. On the other hand, phosphorylation within the activation segment does not contribute to epidermal growth factor-mediated activation. Regarding regulation of A-RAF activity by 14-3-3 proteins, we show that A-RAF activity is regulated differentially by its C-terminal and internal 14-3-3 binding domain. Furthermore, by use of SPR technique, we found that 14-3-3 proteins associate with RAF in an isoform-specific manner.

Of importance, we identified a novel regulatory domain in A-RAF (referred to as IH-segment) positioned between amino acids 248 and 267, which contains seven putative phosphorylation sites. Three of these sites, serines 257, 262 and 264, regulate A-RAF activation in a stimulatory manner. The spatial model of the A-RAF fragment including residues between S246 and E277 revealed a “switch of charge” at the molecular surface of the IH-region upon phosphorylation, suggesting a mechanism in which the high accumulation of negative charges may lead to an electrostatic destabilization of protein/membrane interaction resulting in depletion of A-RAF from the plasma membrane.

Activation of B- and C-RAF is regulated by phosphorylation at conserved residues within the negative-charge regulatory region (N-region). Identification of phosphopeptides covering the sequence of the N-region led to the conclusion that, similar to B- and C-RAF, kinase activity of A-RAF is regulated by phosphorylation of the N-region. Abrogation of A-RAF activity by S299A substitution and elevated activity of the A-RAF-Y301D-Y302D mutant confirmed this conclusion. In addition, we studied the role of the non-conserved residues within the N-region in the activation process of RAF kinases. The non-conserved amino acids in positions -3 and +1 relative to the highly conserved S299 in A-RAF and S338 in C-RAF have so far not been considered as regulatory residues. Here, we demonstrate that Y296R substitution in A-RAF led to a constitutively active kinase. In contrast, G300S substitution (mimicking B- and C-RAF) acts in an inhibitory manner. These data were confirmed by analogous mutations in C-RAF. Based on the three-dimensional structure of the catalytic domain of B-RAF, a tight interaction between the N-region residue S339 and the catalytic domain residue R398 was identified in C-RAF and proposed to inhibit the kinase activity of RAF proteins. Furthermore, Y296 in A-RAF favors a spatial orientation of the N-region segment, which enables a tighter contact to the catalytic domain, whereas a glutamine residue at this position in C-RAF abrogates this interaction. Considering this observation, we suggest that Y296, which is unique for A-RAF, is a major determinant of the low activating potency of this RAF isoform. Finally, the residues R359 in A-RAF and R398 in C-RAF, which interact with the N-region, are also involved in binding of phosphatidic acid. Substitution of this conserved arginine by alanine resulted in accumulation of hyper-phosphorylated form of RAF, suggesting that this residue play a crucial role in phosphorylation-mediated feedback regulation of A- and C-RAF.

Collectively, we provide here for the first time a detailed analysis of *in vivo* A-RAF phosphorylation status and demonstrate that regulation of A-RAF by phosphorylation exhibits unique features compared with B- and C-RAF.

## 2. ZUSAMMENFASSUNG

Die Protein-Familie der Serin/Threonin-spezifischen RAF-Kinasen umfasst in Säugetieren drei Mitglieder, A-, B- und C-RAF. Bei der Aktivierung dieser Kinasen spielen Phosphorylierungsereignisse eine entscheidende Rolle. Im Gegensatz zu B- und C-RAF, deren Phosphorylierungsstellen ausgiebig charakterisiert sind, blieb die Phosphorylierung von A-RAF weitgehend unerforscht. In der vorliegenden Arbeit wurden unter Verwendung der massenspektrometrischen Analyse zahlreiche neue *in vivo* A-RAF-Phosphorylierungsstellen identifiziert. Die physiologische Relevanz und die Funktion dieser Stellen wurden anschließend durch Aminosäureaustausch an den relevanten Positionen untersucht. Dabei wurde festgestellt, dass S432 in der A-RAF-Bindung zu MEK involviert und für die Signalweiterleitung unverzichtbar ist. Hingegen ist die EGF-bedingte A-RAF-Aktivierung nicht von der Phosphorylierung innerhalb des Aktivierungssegments abhängig. Hinsichtlich der Regulation von A-RAF-Aktivierung durch 14-3-3-Proteine, wurde hier gezeigt, dass die katalytische Aktivität von A-RAF durch die C-terminale und die interne 14-3-3-Bindungsdomänen unterschiedlich reguliert wird. Weiterhin wurde mittels SPR-Verfahren festgestellt, dass die Interaktion von 14-3-3-Proteinen mit RAF-Kinasen einen isoformspezifischen Charakter trägt.

Von entscheidender Bedeutung war die Entdeckung einer neuen regulatorischen Domäne (hier als IH-Segment bezeichnet), die in der A-RAF-Sequenz die Aminosäuren 248 bis 267 umfasst und sieben A-RAF-spezifische Phosphorylierungsstellen enthält. Drei dieser Stellen, S257, S262 und S264, erwiesen sich als positive Regulatoren der A-RAF-Aktivierung. Das räumliche Modell dieses A-RAF-Fragments deckte eine „Ladungsumkehr“ an der molekularen Oberfläche der IH-Region infolge der Phosphorylierung auf. Dieser Befund begründete den Vorschlag eines Regulationsmechanismus, in dem die starke Akkumulierung der negativen Ladungen zu einer elektrostatischen Destabilisierung der Protein-Membran-Interaktion führt, was die Verdrängung der A-RAF-Kinase von der Plasma-Membran zur Folge haben könnte.

Die Aktivierung von B- und C-RAF wird durch Phosphorylierung der sogenannten „negativ geladenen“ Region (N-Region) reguliert. Die Identifizierung mehrerer Phosphopeptide aus der N-Region von A-RAF veranlasste die Schlussfolgerung, dass die A-RAF-Aktivität ebenfalls durch die Phosphorylierung innerhalb dieser Region gesteuert werden könnte. In der Tat, die Aufhebung der A-RAF-Aktivität durch die S299A-Substitution und die erhöhte Aktivität der A-RAF-Y301D-Y302D-Mutante bestätigen diese Aussage. Darüberhinaus wurde die Rolle der nichtkonservierten Aminosäuren an den Positionen -3 und +1 relativ zum S299 in A-RAF und S338 in C-RAF im Aktivierungsprozess der RAF-Kinasen untersucht, nachdem diese ursprünglich nicht als regulatorische Stellen erkannt wurden. Es wird hier demonstriert, dass Y296R-Substitution der A-RAF-Kinase eine konstitutive Aktivität verleiht. Hingegen wirkte die G300S-Substitution, die von B- und C-RAF abgeleitet wurde, inhibitorisch. Diese Befunde wurden durch die analogen Mutationen in C-RAF bestätigt. Basierend auf der dreidimensionalen Struktur der katalytischen Domäne von B-RAF wurde eine Interaktion zwischen der N-Region und der katalytischen Domäne in A- und C-RAF festgestellt, die zu einer Inhibierung der Aktivität führen soll. Darüberhinaus wurde gezeigt, dass die räumliche Ausrichtung von Y296 in der N-Region von A-RAF einen engen Kontakt mit der katalytischen Domäne ermöglicht; dagegen hebt Glutamin in dieser Position die Interaktion auf. In Anbetracht dieser Befunde wurde vorgeschlagen, dass das A-RAF-spezifische Y296 das niedrige Aktivierungspotential dieser RAF-Isoform determiniert. In diesem Zusammenhang wurde auch gefunden, dass die Aminosäuren R359 in A-RAF und R398 in C-RAF eine duale Funktion besitzen, indem sie sowohl mit der N-Region als auch mit Lipiden in Wechselwirkung treten können. Substitution dieser konservierten Arginine durch Alanin führte zur Akkumulierung der hyperphosphorylierten Formen der RAF-Kinasen, was die Schlussfolgerung erlaubt, dass diese Reste eine wichtige Rolle in der ERK-vermittelten Feedback-Regulation von A- und C-RAF spielen.

Insgesamt wird hier zum ersten Mal eine detaillierte Analyse der *in vivo* A-RAF-Phosphorylierung geliefert und gezeigt, dass die phosphorylierungsvermittelte Regulation von A-RAF einzigartige Merkmale innerhalb der Familie von RAF-Kinasen aufweist.

## 3. INTRODUCTION

### 3.1. MAP kinase signaling pathways

Mitogen-activated protein kinases (MAPKs) are serine/threonine-specific protein kinases that respond to extracellular stimuli (mitogens) and regulate various cellular processes, such as proliferation, differentiation, transformation, motility and apoptosis. The MAP kinases (also referred to as extracellular signal-regulated protein kinases or ERKs) are the terminal enzymes in a three-kinase cascade. The reiteration of three-kinase cascades for related but distinct signaling pathways gave rise to the concept of a MAPK pathway as a modular, multifunctional signaling element that acts sequentially within one pathway, where each enzyme phosphorylates and thereby activates the next member in the sequence. A canonical MAPK module consists of three protein kinases: a MAPK kinase kinase (MAP3K or MEKK) that is activated by extracellular stimuli. This kinase activates a MAPK kinase (MAP2K or MEK) through phosphorylation on its serine and threonine residues. MEK, in turn, activates a MAPK/ERK enzyme through phosphorylation on its highly conserved serine/threonine and tyrosine residues. MAP kinases are conserved in plants, fungi and animals, and all eukaryotic cells use multiple MAP kinase modules for signal transduction [1-3]. In mammals, fourteen MAP kinase genes have been identified that define seven distinct MAP kinase pathways (**Fig. 1**). MAPKs can be classified into conventional or atypical enzymes, based on their ability to get phosphorylated and activated by members of the MAP2K family. Conventional MAP kinases comprise ERK1/ERK2, p38s, JNKs and ERK5. Atypical MAP kinases include ERK3/ERK4, NLK and ERK7.

ERK1 and ERK2, also known as classical MAP kinases, were the first members of the MAPK superfamily whose cDNAs were cloned [4,5]. They can be stimulated by a huge number of ligands and cellular perturbations [6]. For example, in fibroblasts they are activated by serum, growth factors, cytokines, certain stresses, ligands for G-protein-coupled receptors and transforming agents. Activation of ERK1/2 can be initiated through activation of transmembrane receptors with intrinsic or associated protein tyrosine kinase (PTK) activity [7]. Binding of extracellular ligands to their respective cell surface receptors leads to autophosphorylation of the receptor and enhanced PTK activity. The subsequent association of the Src homology 2 (SH2) domains of adaptor proteins, such as Grb2 and Shc, with the autophosphorylated receptors or with additional docking proteins provides the molecular interactions that bring the required signal transduction molecules into close proximity (**Fig. 2**). Receptors without intrinsic PTK activity but which harbor sites for tyrosine phosphorylation may also activate the cascade via association of their phosphotyrosine residues with adaptor molecules. For example, the SH3 domain of Grb2 (growth factor receptor-binding protein 2) binds a proline-rich region of the guanine nucleotide exchange protein SOS (“son of sevenless”) that, in turn, increases loading of Ras with GTP [8,9]. The GTP-bound form of Ras binds to RAF (a MAP3K) (**Fig. 2**). This action leads to activation of membrane-prebound RAF [10-12]. MAPK kinases (MEK1 and MEK2) are phosphorylated and activated by RAF. MEK1/2 are dual specificity protein kinases that phosphorylate the

ERK enzymes on threonine and tyrosine residues of the conserved T-X-Y motif (where X is any amino acid) within the activation loop (e.g. T183 and Y185 in ERK2), thereby increasing their enzymatic activity by approximately 1000-fold over the activity found with the basal or monophosphorylated forms [8,9]. Phosphorylation of these residues induces conformational changes that alter the alignment of the two kinase halves (N-terminal and C-terminal domains) of the folded protein and enhance access to substrate, which together increase enzymatic activity [13,14].

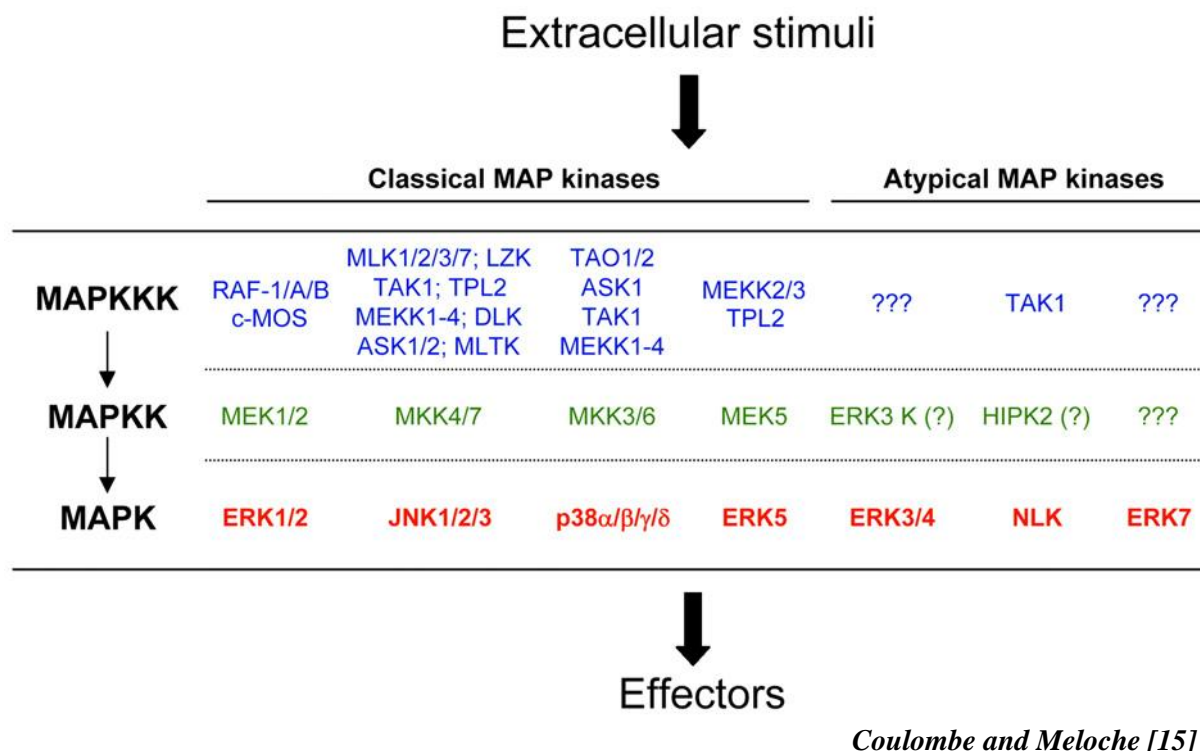


**FIGURE 1: Human MAP kinase pathways [15].**

JNKs/SAPKs (c-Jun N-terminal kinases/stress activated protein kinases) are originally identified as kinases that bind and phosphorylate transcription factor c-Jun. JNKs are responsive to stress stimuli, such as ultraviolet light, cytokines, osmotic and heat shock, as well as inhibitors of DNA, RNA and protein synthesis. In contrast to activation of ERK1/2, upstream signal transduction mechanism for the JNK cascade is less well understood. JNKs are activated through phosphorylation on threonine and tyrosine residues by MKK4 and MKK7 (also known as SEK1 and SEK2, respectively). The direct upstream regulators of this cascade module are several different MAP3Ks. These include members of the MEKK group (MEKK1 though 4), the mixed-lineage protein kinase group (MLKs, DLK and LZK), the ASK group (ASKs), TAK1 and TPL2. MEKK can be activated by upstream module p21-activated kinases (PAKs). Several lines of evidence indicate that Rho family GTPases, such as Rac and Cdc42, mediate the initiation of the JNK cascade (**Fig. 1**) [16-21].

Beside the JNK pathway, constitutively activated forms of Rac and Cdc42 are efficient activators of a p38/HOG cascade. p38 MAP kinase is the mammalian orthologue of the yeast HOG kinase. In parallel to JNK cascade, p38 signaling pathway is strongly

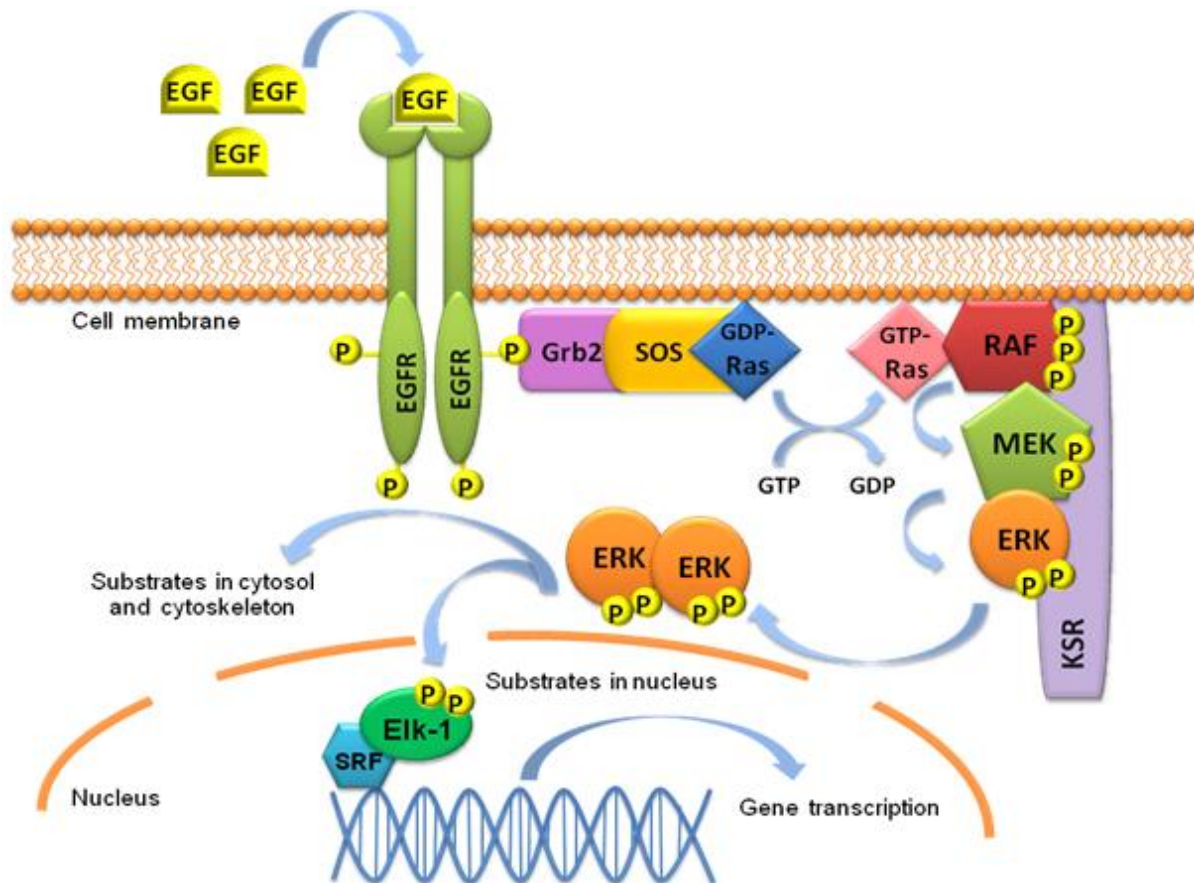


**FIGURE 2: Organization and function of the Ras–RAF–MEK–ERK pathway (simplified presentation).** The binding of epidermal growth factor (EGF) induces receptor dimerization and autophosphorylation (P) on tyrosine residues. These phosphotyrosines function as docking sites for signaling molecules, including the Grb2-SOS complex which activates the small G-protein Ras by stimulating the exchange of guanosine diphosphate (GDP) for guanosine triphosphate (GTP). This exchange induces a conformational change in Ras, enabling it to associate with RAF at the cell membrane, where RAF activation takes place. RAF activation is a multi-step process that involves the dephosphorylation of inhibitory sites by protein phosphatase 2A (PP2A) as well as the phosphorylation of activating sites by PAK, Src, CK2 and yet unknown other kinases. Activated RAF phosphorylates and activates MEK, which in turn phosphorylates and activates ERK. The interaction between RAF and MEK can be disrupted by RKIP (RAF kinase inhibitor protein; not shown). The three-tiered kinase cascade is scaffolded by KSR (kinase suppressor of Ras). Activated ERK has many substrates in the cytosol, such as cytoskeletal proteins and phospholipase A2 [6,22]. It can also enter the nucleus to control gene expression by phosphorylating transcription factors, such as Elk-1 family proteins [23]. SRF, serum response factor.

responsive to stress stimuli, such as inflammatory cytokines, ultraviolet irradiation, heat shock and osmotic shock, and less to serum and growth factors [6,24-31]. The canonical activation of p38 MAPKs occurs via dual phosphorylation of their T-G-Y motif in the activation loop by MKK3 and MKK6 that are strongly selective for p38 MAPKs and do not activate JNKs or ERK1/2 [32-37]. MKK3/6 can be phosphorylated and activated by several MAP3Ks, including MLKs, ASK1, TAK1 and some members of the MEKK family [33,38-41]. The low molecular weight GTP-binding proteins from the Rho subfamily, such as Rac1, Cdc42, Rho

and Rit, and heterotrimeric G-protein-coupled receptors contribute to p38 activation upstream of MAP3Ks (**Fig. 1**) [42-45]. A large body of evidence indicates that p38 MAPK activity is critical for normal immune and inflammatory response as well as for the control of many aspects of the physiology of the cell, such as control of cell cycle or cytoskeleton remodeling [46].

ERK5 was initially documented as a MAPK family member that is activated by stress stimuli [47,48]. Subsequently, it was shown that ERK5 can be activated in response to serum [49] and nerve growth factor (NGF) [50]. Following stimulation, MEKK2 and MEKK3, members of the MAP3K family, activate MEK5, a specific MAP2K for ERK5, although these two MAP3Ks are associated differently with upstream signaling pathways [51,52]. Subsequently, MEK5 phosphorylates and activates ERK5, and then the activated ERK5 phosphorylates substrates including myocyte enhancer factor 2 (MEF2) [49], c-Myc and RSK (**Fig. 1**) [50,53-55].

ERK3 and ERK4 are structurally related atypical MAPKs possessing S-E-G motif instead of T-E-Y in activation loop and displaying major differences only in the C-terminal extension. Little is known about the biological function of ERK3/4 and its cellular targets. Recent studies have shown that ERK3 interacts with and activates the MAP kinase-activated protein kinase MK5, suggesting a physiological relationship between the two protein kinases (**Fig. 1**) [56-58]. Several lines of evidence suggest a role for ERK3 in the control of cell differentiation, acting as a negative regulator of cell cycle progression in certain cellular contexts [15].

ERK7 and ERK8 are the newest members of MAPKs and behave like atypical MAPKs. They possess a long C-terminus similar to ERK3/4. [59-62]. How physiological agonists regulate ERK7/8 activity is unclear. Recent studies showed, however, that oxidative stress and mitogens stimulate the phosphorylation of activation loop in ERK7. Activated Src and RET tyrosine kinases were also found to induce ERK7 phosphorylation and activation (**Fig. 1**) [15].

Various extracellular ligands, such as the Wnt ligand Wnt-1, the cytokines interleukin-6 and granulocyte colony-stimulating factor, and transforming growth factor- $\beta$  (TGF- $\beta$ ) family members activate the atypical MAP kinase NLK (nemo-like kinase) [63-66]. Genetic and biochemical evidence has implicated the MAP3K TGF- $\beta$ -activated kinase 1 (TAK1) and its regulatory subunit TAK1-binding protein 1 (TAB1) in NLK activation [64,65]. More recently, homeodomain-interacting protein kinase (HIPK2), a member of the CMGC group of protein kinases, was shown to interact with and phosphorylate NLK *in vitro*. The phosphorylation of NLK by HIPK2 is associated with an increase in phosphotransferase activity [63]. These findings suggest that HIPK2 may represent the MAP2K in the TAK1–NLK signaling pathway (**Fig. 1**).

## 3.2. Key components of the classical MAP kinase cascade

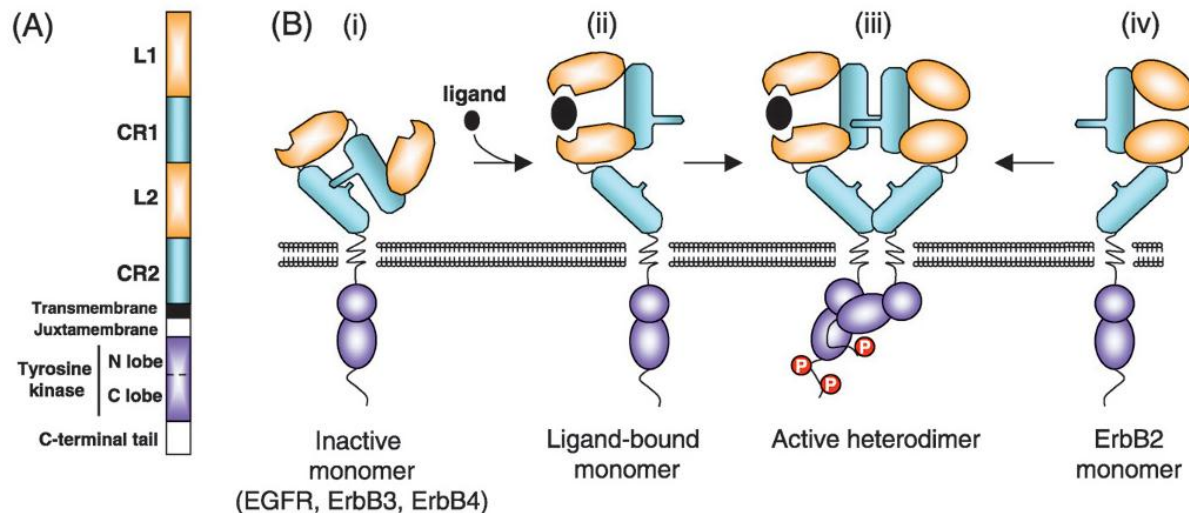
### 3.2.1. EGF receptor as an example of receptor tyrosine kinases (RTKs)

The epidermal growth factor receptor (EGFR) plays a central role in initiating the signaling that directs the behavior of epithelial cells and tumors of epithelial cell origin. The EGF family of receptor tyrosine kinases consists of four members, ErbB1, ErbB2, ErbB3 and ErbB4 [67,68]. These structurally related receptors are single chain transmembrane glycoproteins. Generally, they consist of an extracellular ligand-binding ectodomain, a transmembrane domain, a short juxtamembrane section, a tyrosine kinase domain and a tyrosine-containing C-terminal tail [69]. The ectodomain is composed of four subdomains termed L1 (leucine-rich repeat 1), CR1 (cysteine-rich 1), L2 and CR2 (**Fig. 3A**). In the inactive, ligand-free state, the ectodomain adopts a “tethered” conformation, in which the beta hairpin loop of CR1 interacts with CR2, sequestering the dimerization loop [70]. Binding of ligand to the L1 and L2 domains induces a conformational change, in which the receptor adopts an extended form that exposes the dimerization loop and allows the interaction of receptor ectodomains [71,72]. This mechanism is common for ErbB1, ErbB3 and ErbB4 (**Fig. 3B**). In contrast, ErbB2 is locked in the extended conformation, rendering ligand binding unnecessary for interaction with other receptors [73]. The extended conformation abolishes the potential ligand-binding site by fixing domains L1 and L2 in close proximity. Ligand binding to the ErbB ectodomain and receptor dimerization induce conformational changes in the intracellular tyrosine kinase domain that lead to receptor autophosphorylation. The tyrosine kinase domain comprises a bilobed structure with binding of ATP between these two lobes. Activation of the RTK induces interaction between the N-lobe of one tyrosine kinase domain with C-lobe of its partner (**Fig. 3B**) [74].

Multiple ligands bind to and activate the EGFR, including epidermal growth factor (EGF), transforming growth factor- $\alpha$ , amphiregulin, heparin-binding EGF and betacellulin [75]. EGF and transforming growth factor- $\alpha$  are believed to be the most important ligands for EGFR. Transmembrane signaling of the EGF receptor depends on the intrinsic tyrosine kinase activity of the receptor molecule. Phosphorylated tyrosine residues serve as binding sites for the recruitment of signal transducers and activators of intracellular substrates, such as Ras, which then stimulate an intracellular signal transduction cascade. Multiple signal transduction pathways lie downstream of activated EGFRs. The Ras–RAF mitogen-activated protein kinase pathway [76,77], and the phosphatidylinositol 3-kinase and Akt pathway [78-80] are two major signaling routes for EGFR. These pathways regulate multiple biological processes, such as gene expression, cellular proliferation and inhibition of apoptosis, which contribute to the development of malignancy [81,82]. Stimulation of EGFR pathways has also been shown to promote tumor cell motility, adhesion, metastasis and angiogenesis [83-87].

Immediate negative regulation of signaling can occur through dephosphorylation and internalization of the activated receptors. Delayed signal attenuation through the expression of negative regulators and lysosomal degradation of receptors also helps keep ErbB signaling under control. Tyrosine dephosphorylation of active receptors has the capacity to inhibit the downstream signaling through abolishment of binding sites for intermediates and adaptor

proteins. Internalization of activated receptors plays a central role in dampening signaling by targeting receptors for lysosomal degradation or in some cases promoting ligand dissociation. Once in early endosomes, unoccupied EGFR tends to quickly recycle back to the cell surface, whereas ligand-bound receptor recycles more slowly or is degraded in lysosomes [69].



Wieduwilt and Moasser [69]

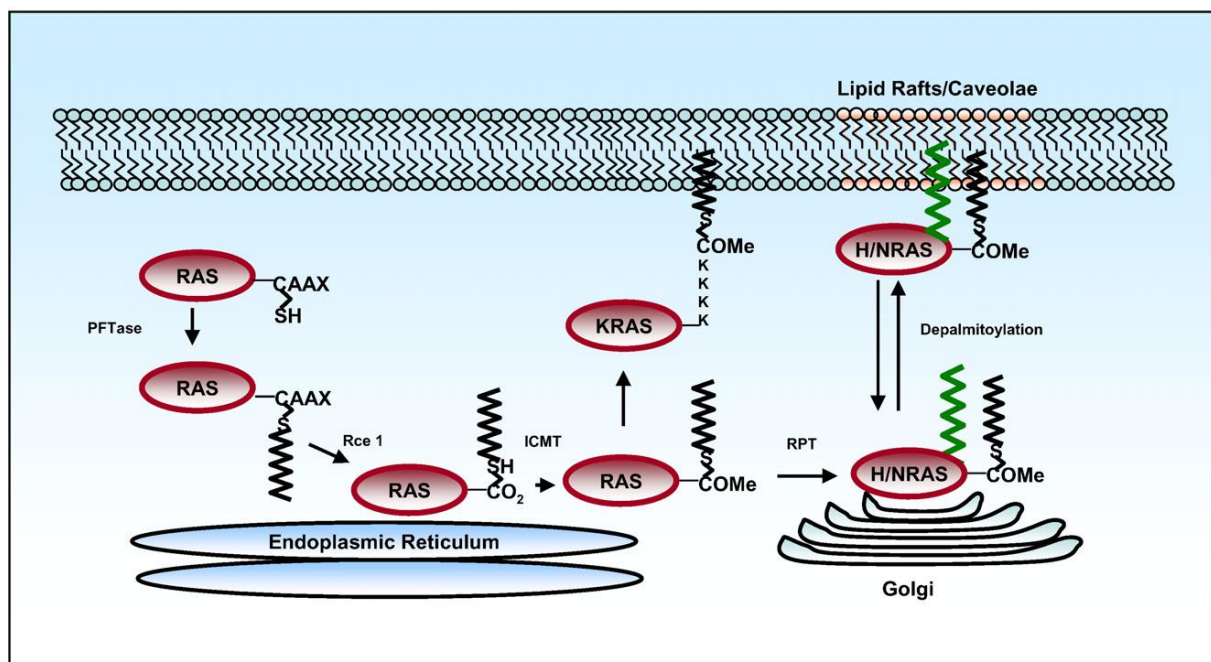
**FIGURE 3: Structure and activation mechanism of epidermal growth factor receptor (EGFR).** (A) Linear representation of ErbB receptor domains. The ErbB receptor consists of several domains: the ligand-binding leucine-rich domains L1 and L2; the cysteine-rich domain CR1 that contains the dimerization loop responsible for receptor dimerization; the CR2 domain; the short transmembrane and juxtamembrane domains that connect the extracellular part with the bilobed tyrosine kinase domain; and the C-terminal tail. (B) Schematic overview of the structural basis for ErbB receptor dimerization and activation [69]. For more details, see text.

### 3.2.2. Ras-GTPase

Ras proteins belong to the family of small GTPases that control a lot of signaling cascades responsible for cell growth, migration, adhesion, cytoskeletal integrity, survival and differentiation (**Fig. 5C**) [12,88]. Their primary role is to assemble transient signaling complexes at the membrane that activate signal transduction pathways. Three different *ras* genes are present in the human genome, named *Ha(rvey)-ras*, *K-(irsten)-ras* and *N(euroblastoma)-ras*. They give rise to four gene products, H-, N-, K-Ras4A and K-Ras4B. K-Ras4A and K-Ras4B are splice variants of the *K-ras* gene that use alternative fourth exon. The Ras isoforms are highly homologous. Their G-domain (residues 1–165), which binds guanine nucleotides and is required for the “switch” function and for effector binding, is nearly identical. On the other hand, their C-termini (last 24–25 amino acids), termed the hypervariable region (HVR), are highly variable. The HVR region, which can be divided into the lipid anchor (the most C-terminal region) and the preceding linker domain, contains the sequences responsible for the membrane anchoring of Ras as well as for its intracellular trafficking.



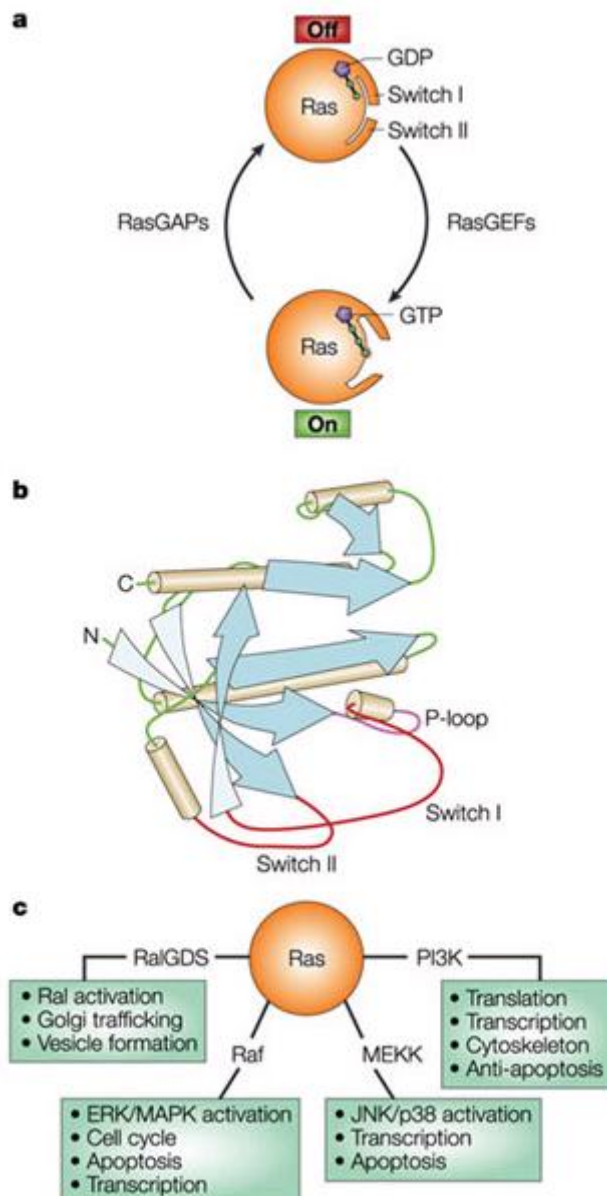
Ras proteins are synthesized as cytosolic precursors that undergo posttranslational processing to be able to associate with cell membranes. Localization of Ras at the cytosolic leaflet of cellular membranes is believed to be required for their biological activity. The initial set of modifications, which is common to all Ras proteins, is directed by the carboxy-terminal CAAX motif, in which C is cysteine, A is usually but not always an aliphatic amino acid and X is any amino acid. The CAAX sequence is recognized by cytosolic prenyltransferases: farnesyltransferase (FTase) or geranylgeranyltransferase type I (GGTase I). The amino acid in the X position determines which prenyltransferase modifies the protein (S, M, A or Q for FTase and L for GGTase I). In the case of H-, N- and K-Ras, farnesyltransferase attaches a farnesyl group to the cysteine residue of the CAAX motif. The farnesylated CAAX sequence targets Ras to the cytosolic surface of the ER, where an endopeptidase, Rce1 (Ras and  $\alpha$ -factor converting enzyme), removes the AAX tripeptide. The now C-terminal farnesylcysteine is then recognized by a third enzyme, isoprenylcysteine carboxyl methyltransferase (Icmt), that methylates the  $\alpha$ -carboxyl group. Finally, after methylation, Ras proteins take one of two routes to the cell surface, which is dictated by a second targeting signal that is located immediately amino-terminal to the farnesylated cysteine. Whereas H- and N-Ras undergo palmitoylation on cysteine residues in their HVRs and enter the exocytic pathway trafficking through the Golgi to the plasma membrane, K-Ras, which has a polylysine sequence instead of cysteine residues, bypasses the Golgi and reaches the plasma membrane by a yet uncharacterized pathway [89]. Notably, the isoform K-Ras4B has been shown to interact with microtubules via the polybasic domain. Depalmitoylation of H- and N-Ras leads to the localization of these two isoforms in the Golgi (Fig. 4) [12,90-92].



*Rajalingam et al. [12]*

**FIGURE 4: Processing and trafficking of H-, N- and K-Ras.** For details, see text. PFTase, protein farnesyltransferase; Rce 1, Ras converting enzyme 1; Icmt, isoprenylcysteine carboxyl methyltransferase; RPT, Ras palmitoyltransferase.

Ras proteins alternate between GTP- and GDP-bound conformations, whereby the GTP-bound conformation represents the “On” and GDP-bound the “Off” state [93,94] (**Fig. 5A**). The docking platform for effectors comprises the so-called “switch regions” (switch I, switch II and the P-loop) of Ras GTPases, which are three short segments that border the nucleotide-binding site. The P-loop coordinates nucleotide binding, whereas the switch I and II regions make up a mobile binding surface that conforms to the nature of a bound nucleotide. The effector loop is a fingerprint of small GTPases, determining the specificity of effector binding to a given GTPase (**Fig. 5B**) [95].



Kinbara et al. [95]

**FIGURE 5: Structure and biochemistry of small GTPases.** (A) Schematic diagram of the structural changes in Ras molecules upon nucleotide binding. (B) Schematic diagram of the G-domain of Ras. (C) Ras effectors. For details, see text.

Ras GTPases bind magnesium complexes of guanine nucleotides with high affinities and remarkable selectivity [96]. As the “switch-on” and “switch-off” reactions in the cycle of Ras are intrinsically very slow, the regulatory input by guanine nucleotide exchange factors (GEFs) and GTPase-activating proteins (GAP) determines the lifetime of the two states. It is activated by the action of GEF, catalyzing dissociation of GDP, thus, facilitating the loading with GTP, which is the more prevalent guanine nucleotide in the living cell. In the GTP-bound state, Ras interacts with effectors, which are defined as proteins that interact specifically with the GTP-bound state and transmit a signal. The signal is terminated by the GTPase reaction on Ras, which is very slow but is accelerated by Ras-specific GAP. Ras in the GDP-bound state is no longer able to interact with the effectors (**Fig. 5A**) [93,94,97-99].

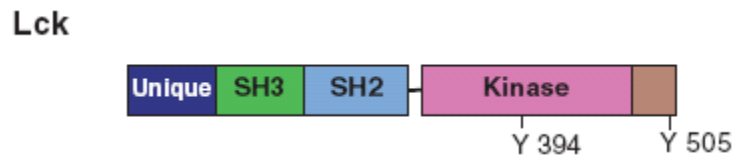
*Ras* genes encoded by rat sarcoma viruses, *v-H-ras* and *v-K-ras*, were among the first oncogenes to be recognized. These viral genes are mutant forms of cellular proto-oncogenes. The transformation of *ras* gene from a proto-oncogene to an oncogene is the result of a point mutation at either position 12, 13 or 61. Oncogenic mutations of Ras, such as G12V, make the GTPase insensitive to the action of GAPs and thereby lock it in the GTP-bound active state [100,101].

Binding of Ras effector proteins to GTP-Ras triggers distinct signaling cascades (**Fig. 5C**). RAF kinase was first discovered as a Ras effector followed by Ral guanine nucleotide dissociation stimulator (RalGDS) and phosphatidylinositol 3-kinase (PI3K). The family of Ras effectors expanded over the past years and includes currently more than ten different proteins: RAF, PI3K, RalGDS, p120GAP, Rin1, Tiam, Af6, Nore1, PLC $\epsilon$  and PKC $\zeta$  [12]. Furthermore, the notion that GDP-bound Ras does not have any functional role has been challenged by the recent observation that GDP-Ras indeed interacts with several effector proteins and modulates downstream signaling events. For instance, the transcription factor Aiolos has been found to interact with GDP-Ras. This interaction modulates the nuclear translocation of Aiolos and the expression of anti-apoptotic protein Bcl2 [102,103]. The common feature of Ras effector proteins is the presence of a Ras binding domain or RBD. At least three distinct RBDs are recognized: (I) the RBD of RAF and Tiam 1, (II) the RBD of PI3K and (III) the Ras association (RA) domains of RalGDS and AF6. The structures of the four RBDs solved so far displayed the same topology, the ubiquitin fold ( $\beta\beta\alpha\beta\beta\alpha\beta$ ), suggesting a similar mode of interaction of Ras with its effectors [12].

### 3.2.3. Lck as an example of Src family kinases

The Src family of protein tyrosine kinases is a closely related group of non-receptor kinases, which are involved in signaling pathways that control the growth and differentiation of cells in response to the activation of cell surface receptors by growth factors, cytokines or cell surface ligands. This protein family includes nine mammalian members: c-Src, Lck, Hck, Blk, Fyn, Lyn, Fgr, Yes and Yrk. Whereas c-Src is expressed in a wide range of tissues and most probably has a variety of functions, other members of the family are restricted in their expression [104].

Lck or p56<sup>Lck</sup> is a T-lymphocyte-specific member of the Src family. The structure of Lck is typical of the Src kinase family. It consists of myristoylation sequence, unique amino-terminal region followed by Src homology domains SH3 and SH2, a tyrosine kinase catalytic domain and C-terminal regulatory domain (**Fig. 6**). Lck is a membrane protein that associates with the inner surface of the plasma membrane through its N-terminus. This interaction is mediated by both, myristic and palmitic acid that are covalently bound to the N-terminal glycine and cysteine 3 and/or 5. The unique region of Lck represents the domain possessing the greatest sequence diversity within this group of enzymes. This domain is thought to be involved in the interaction of Lck with specific cellular proteins, including its substrates. In T-cells, it is known to mediate association with the cytoplasmic tail of T-cell coreceptors CD4 and CD8. SH3 domain is mainly implicated in the regulation of protein-protein interactions, recognizing proline-rich region found in GEFs and GAPs. SH2 domain of Lck recognizes phosphorylated tyrosine residues on other proteins, thereby facilitating the formation of tyrosine phosphorylation-induced multimeric complexes. The tyrosine kinase domain of Lck catalyzes the transfer of the gamma-phosphate from ATP to tyrosine residues on proteins [105,106].



| Molecules shown to associate with Lck |  |
|---------------------------------------|--|
| cell surface                          | CD4 & CD8, CD45, CD2, IL-2R  |
| intracellular                         | ZAP-70, PI-3K, c-cbl, SAM68, MAPK, RasGAP, RAF, LckBP1, Lad/TSA <sub>d</sub> |

*Zamoyska et al. [107], modified*

**FIGURE 6: Domain structure and interaction partners of Lck.** For details, see text.

The structure of the catalytic domain of Lck is typical for protein kinases. It consists of two lobes: the smaller N-terminal lobe (N-lobe) contains a five-stranded  $\beta$ -sheet and one important  $\alpha$ -helix ( $\alpha$ C); the larger C-terminal lobe (C-lobe) consists mainly of  $\alpha$ -helices and provides the surface for interactions with peptide substrates. ATP binding occurs at the interface between the two lobes with a glycine-rich “strand-turn-strand” segment, providing a number of important contacts.

Two polypeptide segments in the core of the catalytic domain are important for catalytic reaction and for regulation. Several side chains of the highly conserved “catalytic segment” bind metal ions or contact directly the phosphate groups of ATP. The adjacent “activation segment” is very divergent, and in most kinases, it contains one or more phosphorylation sites that control catalytic activity. In the activated form of Lck, the activation segment is autophosphorylated at Y394 (**Fig. 6 and 7**) [104,105].

The C-terminal regulatory domain contains a second important *in vivo* phosphorylation site (Y505, see also **Fig. 6**). When phosphorylated, the regulatory Y505 interacts with its own SH2 domain, maintaining a closed conformation and keeping the kinase in an inactive state. Consequently, the substitution of Y505 by phenylalanine converts Lck to an efficient oncogene [105,107].

Lck is involved in T-cell development and activation [107]. Recent studies have revealed that Lck is also required for activation-induced T-cell death (AICD) [108] and for initiating the mitochondrial apoptosis pathway [109]. Activation of Lck occurs in response to stimulation of TCR (T-cell receptor) and IL-2R (interleukin-2 receptor) [110]. Both receptors are found on the surface of the T-lymphocytes. TCR is responsible for recognition of antigens bound to major histocompatibility complex (MHC) molecules, whereas IL-2R binds and responds to a cytokine called interleukin-2. Activation of Lck by TCR is the most studied process. In normal T-cells, the C-terminal negative regulatory Y505 is normally not phosphorylated, rendering Lck in a so-called “primed” state, ready to be activated. Upon TCR-MHC/peptide interactions, Lck is recruited to the complex via its non-covalent association with either CD8 or CD4 co-receptors. It is likely that Lck molecules trans-phosphorylate Y394 within their activation loop upon clustering of the co-receptors during antigen recognition. After coligation of the TCR and either of the co-receptors, active Lck is proximally positioned to phosphorylate specific tyrosine residues within ITAMs (immunoreceptor tyrosine-based activation motifs) located within the CD3 and TCR $\zeta$  signaling chains of the TCR. This allows binding of Syk family kinases (ZAP-70 in T-cells) to the ITAMs. Lck then phosphorylates and activates ZAP-70, which in turn

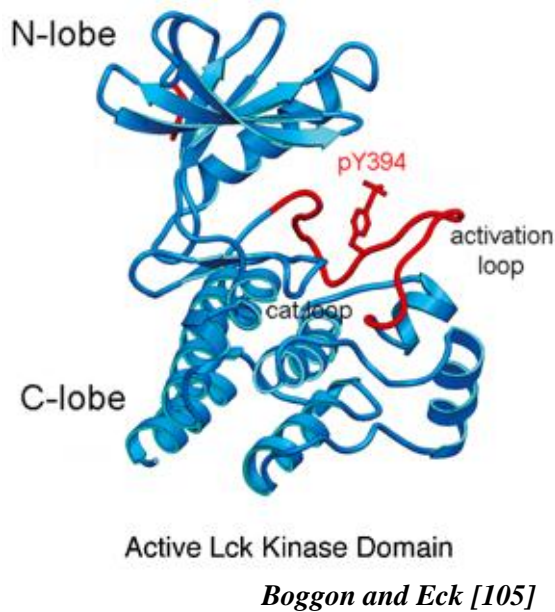


**FIGURE 7: Three-dimensional structure of the Lck kinase domain in its active conformation.**

phosphorylates T-cell-specific adapters, such as LAT and SLP-76 that generate a signaling platform for the subsequent activation of downstream signaling pathways, including the Ras–RAF–MEK–ERK signaling cascade. T-cell activation is characterized by entry into cell cycle and changes in gene expression consistent with T-cells achieving full effector function [106].

Beside the indirect activation of RAF kinases through Lck, the direct association of RAF and Lck and phosphorylation of RAF by Lck has been reported by several groups [110–112]. Despite the findings that C-RAF is an intracellular substrate for the CD4/Lck complex in normal human T-lymphocytes [111] and that activation of C-RAF by Lck occurs through phosphorylation of C-RAF at the conserved residues Y340/Y341 [112–115], the exact mechanism of this direct regulation

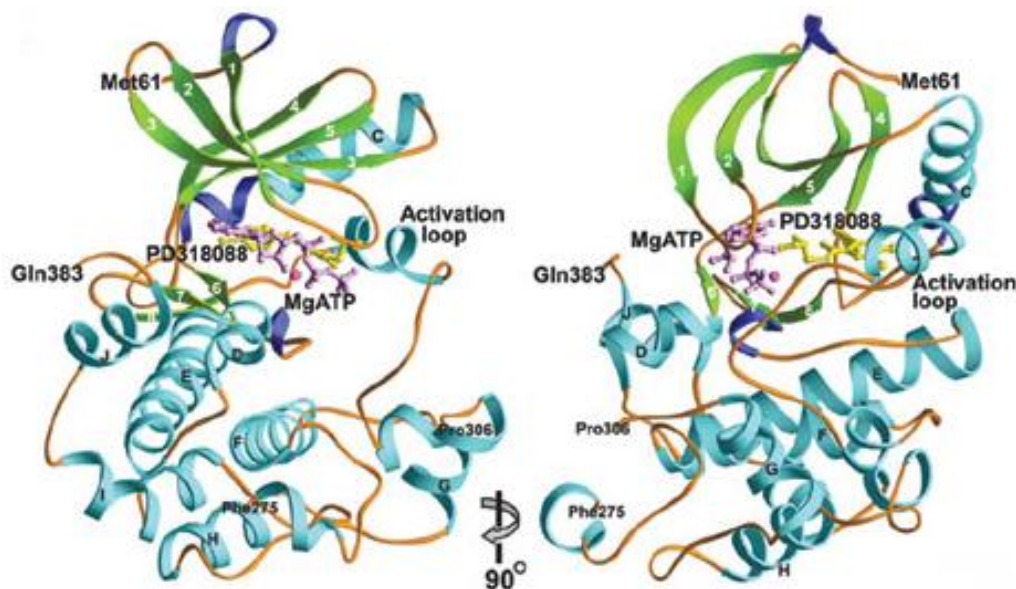
of RAF by Lck has not been completely elucidated so far.

### 3.2.4. MEK

MEK proteins are the primary downstream targets of RAF. They constitute an evolutionarily conserved group of three highly homologous (~85%) mammalian isoforms [116–118]. These isoforms are the 45-kDa MEK1, its alternatively spliced variant MEK1b (43 kDa) that is thought to be inactive, and the 46-kDa MEK2. This family of dual specific kinases has both, serine/threonine and tyrosine activity. MEK proteins are composed of a catalytic kinase domain, which is surrounded by a negative regulatory N-terminal domain, and a shorter C-terminal MAP kinase binding domain, which is required for binding and activation of ERKs. Deletion of the regulatory domain results in constitutive MEK and ERK activation [119]. Crystal structures of human MEK1 and MEK2, which have been published by Ohren *et al.* [120] (see also **Fig. 8**), revealed a conserved homodimer interface. Furthermore, the results of analytical ultracentrifugation have shown that, *in vitro*, MEK1 and MEK2 self-associate to form stable dimers [120]. However, the *in vivo* evidence for dimerization of MEKs is not available so far.

MEKs are activated by phosphorylation of two serine residues in their activation loop (S217 and S221 in MEK1) located within the S-X-A-X-S/T motif [121,122], which is typical to all MAP2Ks. These two residues are phosphorylated by RAF kinases [121]. Additionally, the activity of MEKs is regulated by a proline-rich insert in the C-terminal

domain of the catalytic core that is not present in any other known MEK family members. This insert contains phosphorylation sites for proline-directed and other protein kinases, and is phosphorylated in intact cells. *In vitro*, MEK1 is phosphorylated in this insert by ERKs, Cdk2, PAK1 and others. For instance, phosphorylation of S386 and S289 in MEK1 by ERKs [123] can either inhibit ERKs activity [124] or, under other conditions, facilitate the activation by enhancing the binding of MEK1 to the scaffold Grb10 [125]. Phosphorylation of S298 in MEK1 by PAK1 plays an accessory role in MEKs' activation [126,127], a process that can be inhibited by a feedback phosphorylation on T292 of MEK1 by ERKs [128]. The down-regulation of MEKs involves a rapid dephosphorylation of pS218 and pS222 within the activation loop, mainly by the protein S/T-phosphatase PP2A [129], but possibly also by other phosphatases. Upon activation, MEKs phosphorylate the regulatory tyrosine and threonine residues of ERKs at the next tier of the cascade, thereby causing their activation [130]. Importantly, ERKs seem to be the only physiological substrates of MEKs [119].



*Ohren et al. [120]*

**FIGURE 8: Crystal structure of an N-terminally truncated form of human MEK1 bound to MgATP and an analog of PD184352.** Two views of the MEK1 protein kinase structure with the N-terminal lobe on top, the C-terminal lobe at the bottom, the kinase active site occupied by MgATP and the inhibitor located in the hinge region. The  $\alpha$ -helical regions of the protein are cyan, the  $\beta$ -sheet regions are green, the ATP co-factor is pink, the magnesium atom is magenta and PD318088 is gold [120].

Association of RAF with its substrate MEK requires two elements in the C-terminal domain of RAF. The binding sites are located within the RAF fragments 325–349 and 350–648. These two independent sites cooperate on the single molecular context to confer RAF a high affinity binding to MEK in response to TPA [131]. Moreover, interaction between RAF and MEK is phosphorylation-dependent. Zhu *et al.* [132] reported that phosphorylation of the highly conserved S471 in C-RAF is essential for binding to MEK. Similar results were also obtained for B-RAF. Importantly, the naturally occurring, cancer-associated activating

mutation V600E in B-RAF eliminates the need for an activating phosphorylation at S579 within the MEK-binding segment [132]. Furthermore, phosphorylation of S338 or Y341 in C-RAF as well as integrity of the RAF ATP-binding site facilitate an optimal conformation of RAF, allowing maximal binding and phosphorylation of MEK1 [131].

The MAPK pathways function as an integral step in the formation, progression and survival of tumors. In light of the experimental evidence, the MAPK signaling pathway represents an attractive target for the pharmacological intervention in proliferative diseases. Although numerous small molecules that inhibit different molecular targets at the different levels of the MAPK pathway have been discovered, MEK inhibitors represent the first selective inhibitors of MAPK pathway activation to enter the clinic. The first pharmacological reagent that has been described to inhibit the MEK signaling was PD098059. Unfortunately, this inhibitor is neither sufficiently soluble nor sufficiently bioavailable to be admitted into clinical testing. Due to this limitation, PD098059 has been mostly used in cell systems to study MEK inhibition, in order to further delineate the role of the MAPK pathway in carcinogenesis. Similarly, U0126, a second MEK inhibitor with more potency than PD098059, has been mostly used as an *in vitro* laboratory reagent. These particular inhibitors are non-competitive with ATP and ERK. They bind in an allosteric binding pocket that is adjacent to but not overlapping with the MgATP-binding site (**Fig. 8**). Thus, the mechanism of action of these inhibitors is to bind and stabilize a naturally occurring inactive conformation of MEK. In 1999 PD184352 (CI-1040) was identified as a highly selective, potent and non-competitive inhibitor of MEK1 and MEK2, which is able to prevent tumor growth *in vivo*. Although CI-1040 was generally well tolerated, its antitumor activity, metabolic stability and bioavailability were considered insufficient, and the development of CI-1040 was terminated in favor of developing a more potent and biopharmaceutically superior compounds, such as PD0325901 and ARRY-142886 (AZD6244) that are currently under study in clinical trials [133].

### 3.2.5. ERK

ERK proteins are the evolutionary conserved products of the two genes, *erk1* and *erk2* [4,5,134]. Beside two main protein products, the 44-kDa ERK1 and the 42-kDa ERK2, several other alternatively spliced variants have been identified [135-137]. All ERK isoforms are composed of a catalytic kinase domain wrapped by regulatory stretches and contain a unique insert sequence within their kinase domain (**Fig. 9**) [5]. As already mentioned, the ERKs are all activated by dual phosphorylation on their regulatory tyrosine and threonine residues located within the T-X-Y motif [119]. In the case of ERK2, these are T183 and Y185. ERK2 achieves maximal activity only when both residues are phosphorylated. This unique phosphorylation seems to be mediated solely by MEKs [119].

Interaction of ERK with MEK requires a region located at the C-terminus of ERK (amino acids 312–320 in ERK2) [138,139]. This region is also important for ERK interaction with many other proteins and therefore termed common docking (CD) domain [140]. The most important interacting residues in this region are three acidic amino acids (D316,

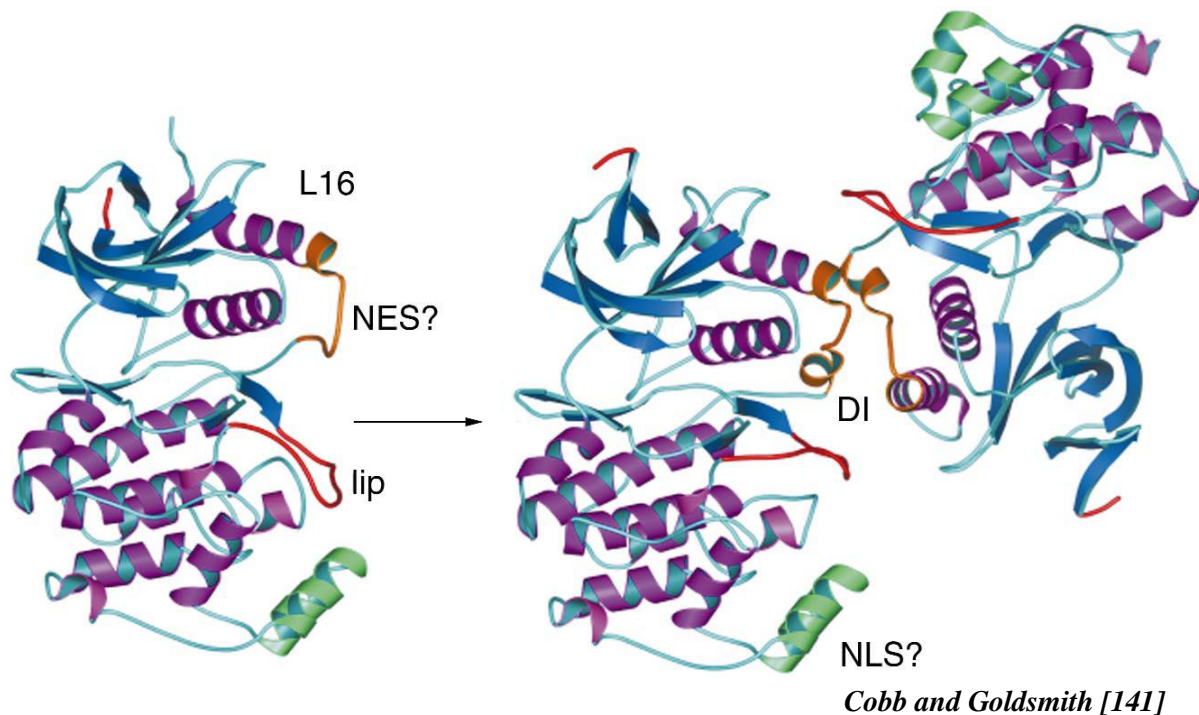


**FIGURE 9: Structures of unphosphorylated and phosphorylated ERK2.** Low-activity ERK2 monomer (*left*) and phosphorylated ERK2 dimer (*right*). Helices are purple, strands are dark blue, MAPK insertion is green, the phosphorylation lip (activation loop) and N-terminus are red, and the dimer interface in L16 is orange. Location of dimer interface (DI) in phosphorylated ERK2 and putative nuclear export and nuclear localization sequences (NES and NLS, respectively) are marked [141].

D319 and E320 in ERK2) as well as a few hydrophobic residues. This region was shown to interact with three basic and two hydrophobic residues in the N-terminus of MEKs termed the D-domain. Crystallization studies have revealed that binding of the D-domain of MEKs to the CD-domain of ERKs induces a conformational change that exposes the regulatory threonine and tyrosine residues to the environment, and thereby allows the attached MEKs to phosphorylate them [119]. The regulatory threonine and tyrosine are part of the activation loop (also known as L12 or “lip”), which is positioned between protein kinase subdomains VII and VIII (**Fig. 9**). In the inactive conformation, peptide-binding site is blocked by Y185. Upon activation, the “lip” is refolded, bringing the phosphothreonine and phosphotyrosine into alignment with the surface of the arginine-rich binding sites. This induces a rotation and depression in the surface of the catalytic pocket of ERKs to form a pocket that allows the binding of the ERKs' substrates [14,142]. These changes allow a full catalytic activity of the ERK2, which is 5–6 orders of magnitude higher than its basal activity [142,143].

ERKs phosphorylate substrates on serines and threonines within the consensus site, which is in most cases P-X-S/T-P [144]. However, the shorter sequence S/T-P alone is sometime sufficient to direct ERKs' phosphorylation [145]. In addition, many of the substrates can interact with ERK via specialized docking domains [146,147]. Upon stimulation, ERKs phosphorylate a large number of substrates. Some of these substrates are localized in the cytoplasm, whereas others are phosphorylated in the nucleus by ERK molecules that are



translocated into this organelle upon stimulation. Of note, ERKs phosphorylate and activate a series of transcription factors, such as Elk1, c-Fos, p53, Ets1/2 and c-Jun, which are involved in the initiation and regulation of cell proliferation and oncogenic transformation [119].

Beside its activating potency, phosphorylation of two residues within the activation loop enables ERK to dimerize [148]. By comparing the structures of unphosphorylated and phosphorylated ERK2 (ERK2-2p) Cobb and Goldsmith [141] proposed a mechanism how phosphorylation promotes dimerization. Residues in the two most flexible parts of ERK2, the activation loop and the C-terminal extension called L16 (P309 to R358), change conformation in ERK2-2p, so that tight interactions can then be formed between them (**Fig. 9**). The two ERK2-2p molecules are locked together by a hydrophobic zipper and two ion pairs, one at each end of the zipper [141].

As mentioned already, activated ERKs can enter the nucleus to control gene expression by phosphorylating transcription factors. The mechanism of the nuclear translocation of ERKs is not completely understood. It has been shown that ERKs translocate to the nucleus using either a non-regulated (diffusion) or a facilitated mechanisms. The facilitated mechanism was proposed to require homodimerization of ERKs that occur upon activation. However, other studies revealed that mutation of the dimerization sites does not significantly influence the stimulated translocation, and therefore the importance of dimerization is still controversial [119]. Recently, it was suggested that the cytonuclear shift might occur by a direct interaction with several nuclear pore proteins (NUPs). Furthermore, Cobb and Goldsmith [141] proposed that nuclear localization of ERK might be regulated by putative NLS (nuclear localization sequence) and NES (nuclear export sequence, **Fig. 9**). However, the experimental studies supporting this assumption are still missing. Numerous studies support the opinion that the localization of ERKs, both before and after stimulation, is largely dependent on their interaction with various regulatory proteins, such as PEA-15 (phosphoprotein enriched in astrocytes). It is a widely expressed 15-kDa protein with a death effector domain. In the cytoplasm, PEA-15 binds ERKs but not any other component of the ERK cascade. This binding prevents ERKs' nuclear translocation without inhibiting their kinase activity, therefore causing a reduction in the nuclear activity of ERKs without much effect on the cytoplasmic activity. The mechanism by which PEA-15 prevents nuclear translocation of ERKs is still unclear, but may involve PEA-15-dependent interference with ERKs' binding to NUPs [119].

The inactivation of ERKs is mainly mediated by removal of the phosphates from either one or both of the regulatory threonine and tyrosine residues of ERKs. This process is mediated by either protein serine/threonine phosphatases (PPs), such as PP2A [149], by protein tyrosine phosphatases, such as PTP-SL [150], or by dual specificity phosphatases, generally termed MAPK phosphatases (MKPs) [151]. Apart from the downregulation by phosphatases, ERKs seem to participate in multiple feedback loops that are important for the reduction of their activity at later stages after stimulation. These include inhibitory phosphorylation of the upstream exchange factor SOS [145], RAFs [152-154] and MEKs [127].

### 3.2.6. Scaffolds

The importance of scaffold proteins lies mainly in their ability to recruit proteins belonging to a specific signal transduction event and bring them to a close proximity to each other. Additionally, scaffold proteins can provide better stability to some of the cascade components to determine the threshold of signaling. Finally, scaffolds can determine the localization of the cascade components or protect signaling components from phosphatases, thereby regulating their activity. To date more than 50 scaffolding and anchoring proteins have been described for the ERK cascade [119,155].

One of the best-studied scaffolds of the ERK cascade is the KSR1 (kinase suppressor of Ras-1), initially identified as a key component in the ERK signaling in *D. melanogaster* [156] and *C. elegans* [157]. KSR1 displays high homology to RAF kinases, but its kinase domain has mutations of key residues that are essential for catalytic activity in other protein kinases. Thus, it is still controversial whether it can phosphorylate any substrate involved in ERK signaling. Nevertheless, all available data support a kinase-independent function of KSR1, which appears to serve as a scaffold protein [119,158,159].

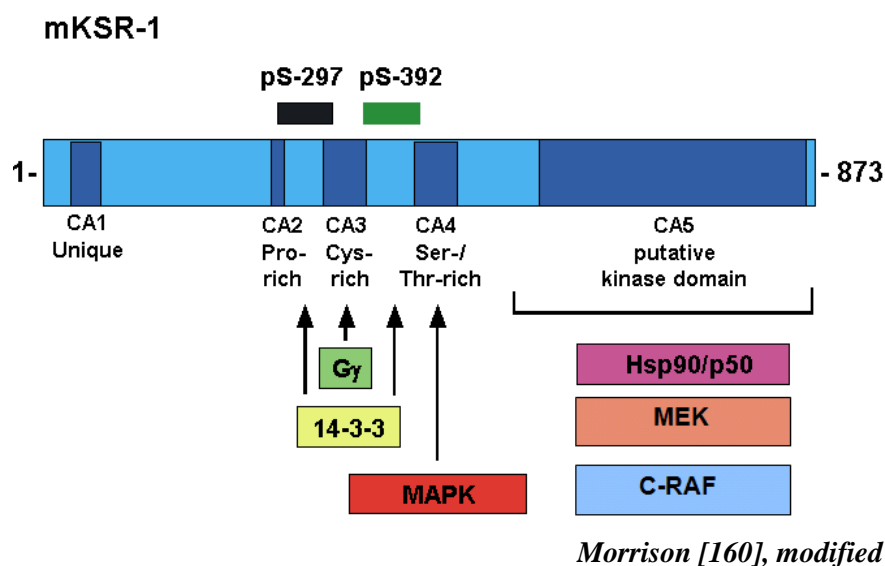
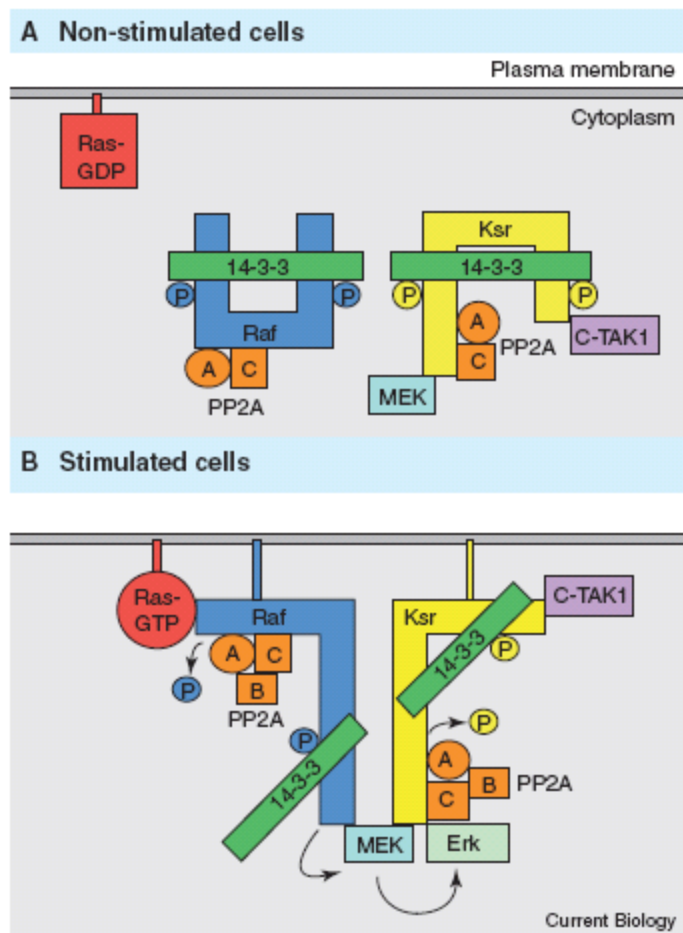


**FIGURE 10: Schematic presentation of KSR domains and interaction partners.** KSR consists of five conserved domains: CA1, which is unique to KSR1 and lacking in KSR2; CA2, a proline-rich sequence; CA3, a cysteine-rich domain that mediates interactions with membrane lipids; CA4, a serine/threonine-rich region that binds ERK/MAPK; and CA5, the putative kinase domain. Binding sites for some interacting proteins are indicated. For more details, see text.

In quiescent cells, KSR1 is found in the cytoplasm where it interacts with MEK and, like the inactive RAF protein, with 14-3-3 proteins. The 14-3-3 proteins form dimers that bind to motifs containing phosphoserines 297 and 392 (**Fig. 10**). These residues are constitutively phosphorylated by Cdc25C-associated kinase C-TAK1, which is associated with KSR in resting cells as well [161]. In addition, KSR associates with inactive PP2A and with the inhibitory E3 ubiquitin ligase (IMP1), which assists in maintaining the cytosolic localization



*Raabe and Rapp [159]*

**FIGURE 11: Model for the regulation of RAF and KSR by protein phosphatase 2A (PP2A).** For details, see text.

of the multiprotein complex. Treatment of cells with growth factors results in dephosphorylation of KSR specifically at S392, thereby releasing 14-3-3 from this site. S297 and S392 flank the cysteine-rich C1 domain (CA3, **Fig. 10**), which is essential for translocation and accumulation of KSR at the membrane. Release of 14-3-3 causes a conformational change, allowing the C1 domain of KSR to contact with yet unknown membrane-bound ligands. In parallel, IMP1 is recruited by GTP-loaded Ras. This leads to polyubiquitination and subsequent degradation of the IMP1. These two processes together allow the rest of the KSR1 complex to translocate to and interact with the plasma membrane, where it associates with activated RAF kinase. Subsequently, RAF promotes phosphorylation of MEK. Simultaneously, ERK is recruited to the activated complex, and this facilitates its phosphorylation and activation, which are followed by the release of ERK from the complex (see also **Fig. 11**)

[119,159]. Interaction of MEK with KSR1 is direct and occurs through the CA5 domain of KSR1. MEK is stably associated with KSR1 in quiescent as well as in growth factor-treated cells, whereas ERK binding to KSR1 is not constitutive but is induced upon Ras activation. The direct interaction of ERK with KSR1 is mediated by an F-X-FP motif found in the CA4 domain of KSR1. The interaction between KSR1 and RAF kinase is less clearly defined and may vary in different organisms. Several other proteins, such as G-protein- $\beta\gamma$ , Hsp70, Hsp90 and CDC37 have been reported to interact with KSR as well (**Fig. 10**) [155].

Other scaffolds, such as connector enhancer of KSR (CNK) and suppressor of Ras-8 (SUR-8) have been shown to interact also with RAF kinase [162]. In contrast, no interaction with MEK or ERK has been reported for either of these molecules, indicating that their potential scaffolding functions are likely to be quite different from those of KSR. CNK has no catalytic motifs, but it does have several protein interaction domains including SH3-binding sites, indicating a function as a multivalent adaptor protein. CNK might play a crucial role in facilitating the assembly of signaling complexes at the plasma membrane, thereby leading to efficient RAF activation [163]. The SUR-8 protein has been found to complex with Ras and

RAF in mammalian cells, and it has been proposed that SUR-8 may enhance the signaling strength of Ras by promoting the Ras-RAF interaction [155,158,164].

Another protein that has been demonstrated to have ERK scaffolding properties is MEK-partner 1 (MP1), a small protein that selectively promotes signaling from MEK1 to ERK1, but not from MEK2 and not to ERK2 [165]. Association of MEK1 with MP1 is mediated by the proline-rich sequence (PRS), which is located between kinase subdomains IX and X of MEK1 (residues 270–307) and is essential for binding to MP1. In recent studies, MP1 has been found to localize specifically to late endosomes through its interaction with the adaptor protein p14. Binding of MP1 to p14 is constitutive and is both, necessary and sufficient to localize MP1 to late endosomes [166,167]. Moreover, these studies have demonstrated that the endosomal localization of the MP1/p14 complex appears to be required for full ERK1 activation and signaling in response to EGF stimulation, suggesting that MP1 plays a specialized role in ERK1 activation at late endosomes [155]. MAPK organizer-1 (MORG1), a recently isolated MP1-interaction partner, also associates with RAF, MEK and ERK. MP1 and MORG1 seem to be modules of larger ERK/MAPK pathway complexes that are built from nested scaffolds [164]. ERK and MEK can interact with an additional anchoring protein termed Sef1, which directs MEK/ERK complex to the Golgi apparatus, prevents nuclear translocation of ERK and may regulate cell cycle [119].

Another scaffold protein that attracts portions of the MEK and ERK molecules is  $\beta$ -arrestin. Initially,  $\beta$ -arrestin has been implicated into desensitization and termination of G-protein-coupled receptor (GPCR) signaling [168]. Following agonist binding and phosphorylation of GPCR by specialized GPCR kinases (GRK),  $\beta$ -arrestins translocate from the cytoplasm and interact directly with the phosphorylated GPCR at the cell surface. This leads to uncoupling of the receptor from heterotrimeric G-proteins and targeting it for endocytosis. A growing body of evidence disclosed an additional function of  $\beta$ -arrestin as GPCR signal transducers and MAPK scaffolds. All three cascade components (RAF, MEK and ERK) have been observed in the GPCR/ $\beta$ -arrestin complexes. Irreversible association of this multiprotein complex results in the retention of active ERK in the cytoplasm and a diminished transcriptional response to signaling stimuli. Thus, the  $\beta$ -arrestin scaffold targets specifically the ERK activity to a pool of cytoplasmic substrates [119,155,168].

The further scaffold protein that directs ERKs' signal to cytoplasmic targets is paxillin. Paxillin is a member of the focal adhesion protein family that plays a central role in focal adhesion assembly and is essential for cell spreading and migration. Similar to KSR1, paxillin associates constitutively with MEKs, whereas ERKs and RAFs are recruited to the complex only upon activation. However, in contrast to KSR1, paxillin interaction partially prevents the nuclear translocation of ERKs [119].

### 3.2.7. RAF kinases

The serine/threonine-specific protein kinase RAF (named for rapidly accelerated fibrosarcoma) is a key modulator of the classical MAP kinase cascade (**Figs. 1 and 2**). It was

originally discovered in 1983 by Ulf R. Rapp and co-workers as a retroviral oncogene *v-RAF*, which was isolated from the genome of 3611 murine sarcoma virus, an acutely transforming retrovirus [169]. Using *v-RAF* sequence as reference, *v-RAF*-related genes were soon identified in avian carcinoma virus MH2 (*v-MIL*) [170,171] as well as in several multicellular eukaryotes as diverse as *Arabidopsis* (*CTR1*) [172], *Caenorhabditis elegans* (*LIN-45*) [173], *Drosophila* (*D-RAF*) [174] and man [175]. Unlike lower eukaryotes, which express only one *RAF* gene, vertebrates inherit at least three members of the *RAF* family of proto-oncogenes, *C-RAF*, *A-RAF* and *B-RAF* [175-178]. Historically, the best characterized mammalian *RAF* isoform is the *C-RAF* (*RAF-1*), which is expressed in a wide range of tissues [179]. The second prominent member of the *RAF* family, *B-RAF*, is likely to be the original *RAF* kinase in the evolution of vertebrates. In its nucleotide sequence, *B-RAF* is more closely related to all other eukaryotic *RAF* homologues than either *A-* or *C-RAF*. *B-RAF* isoform plays also an important role in cancer progression. This is underlined by the fact that in several cancer types, like melanoma and colorectal cancer, a single amino acid exchange in *B-RAF* (V600E, formerly V599E) is one of the most commonly found mutations. In contrast, comparatively little is known about the third member of *RAF* family, *A-RAF*, whose significance for cell survival as well as for complex functioning of whole organism has not been understood to its full extent to date.

So far, the genes coding for the *RAF* kinases have been found in multicellular organisms only. This suggests that the evolution of *RAF* kinases is closely associated with the evolution of multicellularity. Metazoans as well as multicellular plants contain *RAF* as a MAP kinase regulator. *RAF*-related kinase from plants and metazoan *RAF* are similar at their kinase domain, but significantly divergent at their non-catalytic sequences. An extended phylogenetic analysis of the kinase domains revealed that *RAF* kinases together with animal receptor kinases, animal receptor tyrosine kinases (RTKs) and plant receptor-like kinases (RLKs) form a well-supported group, sharing a common origin within the superfamily of serine/threonine/tyrosine kinases (see also **Fig. 12B**) [180]. Plant genomes contain no *RAS* genes at all. Accordingly, *RAF*-like kinases from plants contain no Ras binding domain, the attribute that is common for all *RAF* kinases from animals. In plants, *RAF*-like kinases are a key regulator of the ethylene signaling and are under the control of the ethylene receptor histidine kinase *ETR1*. Therefore, it is conceivable that animals and plants diverged prior to the occurrence of the *RAS* signaling module. Invention of *RAS* at the level of development of opisthokonts/amoebzoa lineage led to gain of an RBD by the pre-existing *RAF*-like kinase(s) through domain shuffling and to the appearance of receptor tyrosine kinase signaling in conjunction with multicellularity in metazoans. This enabled *RAF* to become the primary messenger of *RAS*-mediated signals from receptor tyrosine kinases to the MEK–ERK pathway in animals (see also **Fig. 12A**) [12]. The data from the few animal genomes that have been sequenced to date reveal that the three *RAF* isoforms are present only in vertebrates. This suggests that the divergence of the *RAF* isoforms occurred at the level of development of vertebrates. Invention of which vertebrates-specific properties led to the divergent evolution of duplicated *RAF* genes is still unknown.

Mammalian *RAF* isoforms show remarkable differences with respect to basal and growth factor-induced activity. *B-RAF* displays extraordinarily high basal activity compared with *C-RAF*, is weakly responsive to oncogenic Ras and is not stimulated at all by activated

Src [113]. In contrast, C-RAF possesses low activity in non-stimulated cells, but can be readily activated by oncogenic Ras and Src [113,114,181,182]. Although A-RAF has also been shown to be activated by Ras and Src, the level of A-RAF activity obtained under these conditions is only ~20% of that for C-RAF and is considerably lower compared with B-RAF [113].

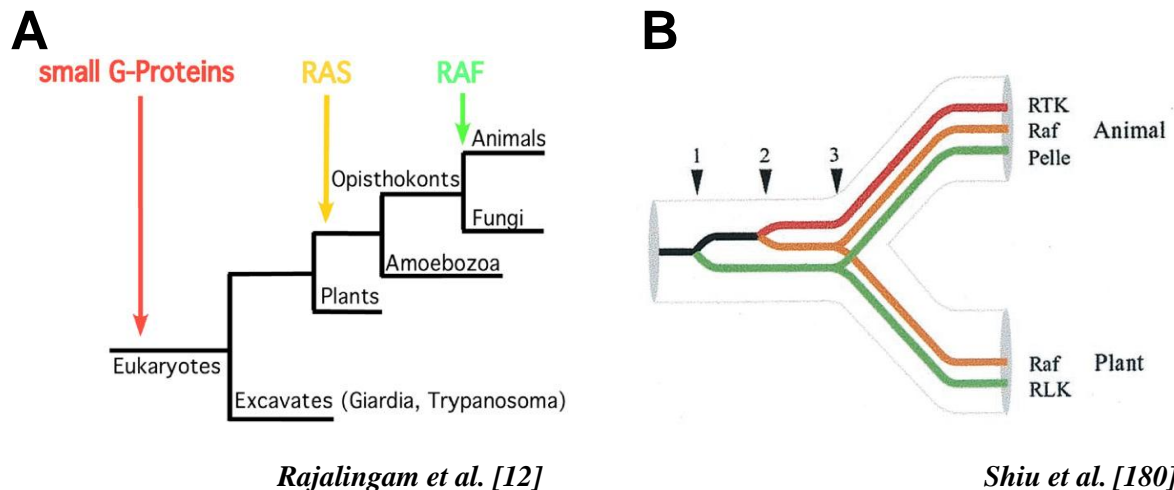


**FIGURE 12: Evolution of RAF kinases.** (A) Major steps in the evolution of RAS and RAF signaling. (I) The compartmentalization of eukaryotic cells into membrane-enclosed organelles was accompanied by gene duplication and functional diversification of small G-proteins. (II) Genomic evidence puts the appearance of RAS to a common ancestor of opisthokonts and slime molds. (III) RAF kinases linking RAS and MAPK signaling accompanied the development of multicellularity in animals [12]. (B) The proposed evolutionary relationships between receptor kinase family members are as follows: (I) an ancient duplication event, leading to the divergence of RLK/Pelle from RTK/RAF; (II) a more recent gene duplication, leading to the divergence of RTK from RAF; (III) the divergence of plant and animal lineages, resulting in the ancestral sequences that gave rise to the extant receptors and related kinases [180].

### 3.2.7.1. Structure of RAF proteins

All RAF isoforms share three conserved regions (CR1, CR2 and CR3) and can be divided in two functional parts, the N-terminal regulatory domain and the C-terminal kinase domain. The regulatory part includes CR1 and CR2 that in the case of C-RAF span residues 51–194 (CR1) and 254–269 (CR2). CR3 represents the kinase domain extending in C-RAF from residues 347 to 613. The conserved regions are embedded in variable sequences that are conserved within one isoforms from different species but not between the three RAF isoforms of the same species, suggesting that they have isozyme-specific functions (see also **Fig. 13**) [76].

CR1 includes two domains, the Ras binding domain (RBD) followed by cysteine rich domain (CRD) [183]. The latter forms a zinc-finger motif of the type C-X<sub>2</sub>-C-X<sub>9</sub>-C-X<sub>2</sub>-C related to the C1 domain of protein kinase C (PKC) family proteins [184]. Both RBD and CRD are known to be involved in binding of active GTP-bound Ras and recruitment of RAF

to the plasma membrane for further activation [185,186]. Recent studies, analyzing the mechanism of RAF membrane localization, have indicated a binding site for phospholipids – specifically for phosphatidylserine – within the zinc-finger domain of the human C-RAF kinase [11,187]. Based on these findings, a new function of zinc-finger domain in activation of human C-RAF is discussed by Kerkhoff and Rapp [188] – phosphatidylserine associated zinc-finger domain of C-RAF might recruit the kinase to the plasma membrane, where the interaction with activated Ras is facilitated.

The role of the serine/threonine-rich CR2 domain is less well defined. Phosphorylation of this region and various protein-protein interactions via CR2 might affect the localization and activation of RAF isoforms [189,190].

The C-terminal CR3 is the catalytic kinase domain of RAF proteins and is also subject to regulation by phosphorylation of certain conserved residues. Besides catalytic activity, the kinase domain of RAF can bind to phospholipids, such as phosphatidic acid (PA) [11,191,192]. The precise function of this phospholipids/kinase domain interaction has not been fully understood. However, two distinct functions might be proposed: (I) localization of RAF kinase to membrane, as it has been already discussed for the CR1 domain, and (II) regulation of kinase activity.

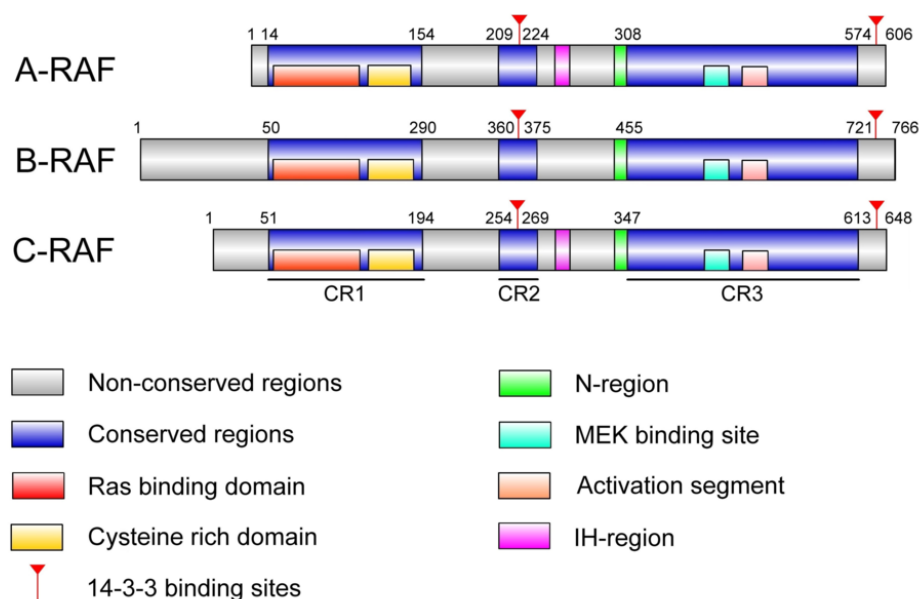
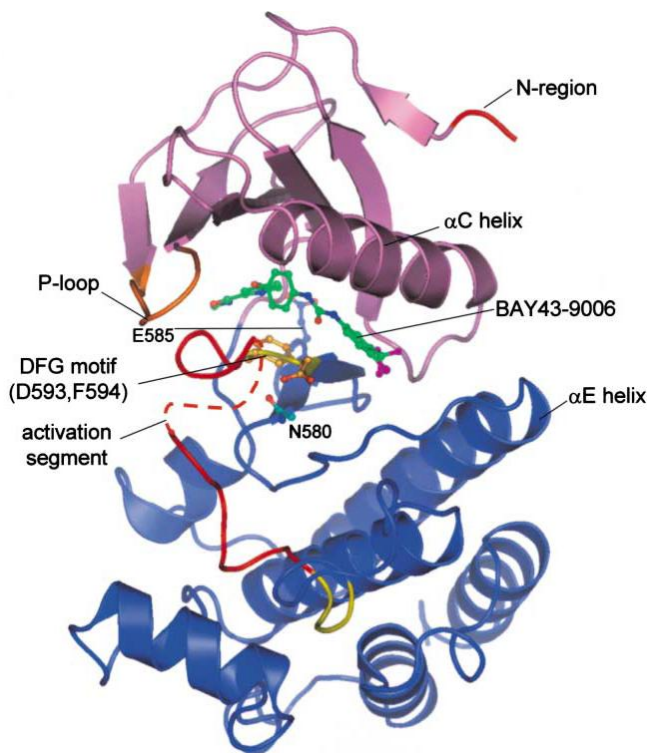


**FIGURE 13: Schematic presentation of human A-, B- and C-RAF kinases with their regulatory domains.** For details, see text.

The N-terminal part of the protein is the regulator of the C-terminal kinase domain, since deletion of the entire amino-terminal half results in constitutively activated RAF kinase [169,184]. The high degree of sequence similarity between the RAF isoforms suggests that all RAF proteins adopt a similar conformation in the inactive state – the N-terminal regulatory half of RAF is proposed to interact with its own C-terminal kinase domain. Consequently, activation of RAF kinase requires displacement of the regulatory domain from the kinase domain, which occurs as a result of preceded phosphorylation/dephosphorylation events

and/or interactions with other regulatory factors [76,176]. Unfortunately, the three-dimensional structure has been solved only for the isolated catalytic domain of B-RAF (**Fig. 14**) [193]. The crystallization of the full-length RAF proteins is failed so far, partially due to the heterogeneity of the purified RAF proteins caused by phosphorylations at numerous regulatory sites [194]. Thus, the spacial structure of the full-length protein is still matter of speculation.



*Wan et al. [193]*

**FIGURE 14: Ribbons diagram of wild type B-RAF kinase domain in complex with BAY43-9006.** Activation segment and the N-region are in red. N-lobe is in magenta, C-lobe in marine and P-loop in orange. Residues 600–611 of the activation loop are disordered (dashed lines) [193].

frees the activation segment and allows the kinase to fold into the active conformation [195]. Presumably, phosphorylation of the corresponding sites in C-RAF and A-RAF would regulate these kinases through similar mechanisms.

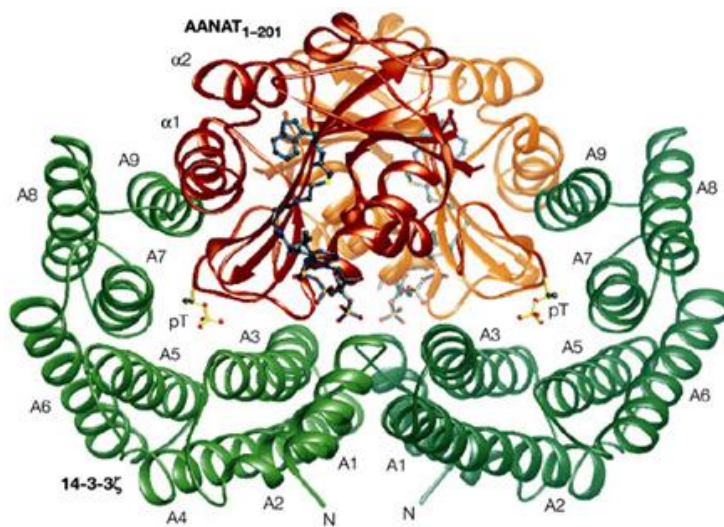
Nevertheless, the crystal structure of the kinase domain of B-RAF provides an insight into how the catalytic activity of RAF proteins is regulated. In general, the kinase domain of B-RAF adopts the bilobal architecture characteristic of other members of the protein kinase family. However, there is an atypical intramolecular interaction between the activation segment (a sequence within the activation loop) and the glycine-rich P-loop (see also **Fig. 14**) [193]. This interaction traps B-RAF in an inactive conformation. Phosphorylation of activation segment at T599 (T452 in A-RAF and T491 in C-RAF) is predicted to disrupt the interaction between the glycine-rich loop and the activation segment and allow the formation of the active conformation. This would explain why substitution of T599 to isoleucine, which has been found to occur in human cancer, renders B-RAF strongly active. Obviously, introduction of the bulky side chain of the isoleucine into this position disrupts the interaction between the glycine-rich loop and the activation segment, which

### 3.2.7.2. Regulation of RAF activity by 14-3-3 proteins

The family of 14-3-3 proteins is a highly conserved during evolution and ubiquitously expressed. In mammals, there are at least seven isoforms ( $\beta$ ,  $\gamma$ ,  $\epsilon$ ,  $\sigma$ ,  $\zeta$ ,  $\tau$  and  $\eta$ ),



each encoded by a distinct gene [196]. The members of 14-3-3 family are acidic proteins with molecular masses of approximately 30 kDa. All 14-3-3 proteins share a similar tertiary structure, as revealed by the crystal structures of the seven different human isoforms [197]. They consist of nine  $\alpha$ -helices and form the biologically functional homo- and heterodimers, resembling a U-shaped structure (see **Fig. 15**). Four amino-terminal  $\alpha$ -helices mediate dimerization and form a platform to which the five carboxy-terminal helices have a rectangular orientation, representing the walls of the U-shaped dimer [198]. Most of the conserved amino acids are found on the interior side of the amphipathic groove that is formed inside the 14-3-3 dimer (A3, A5, A7 and A9 in **Fig. 15**), whereas the variant chains point towards the outside.



*Obsil et al. [198]*

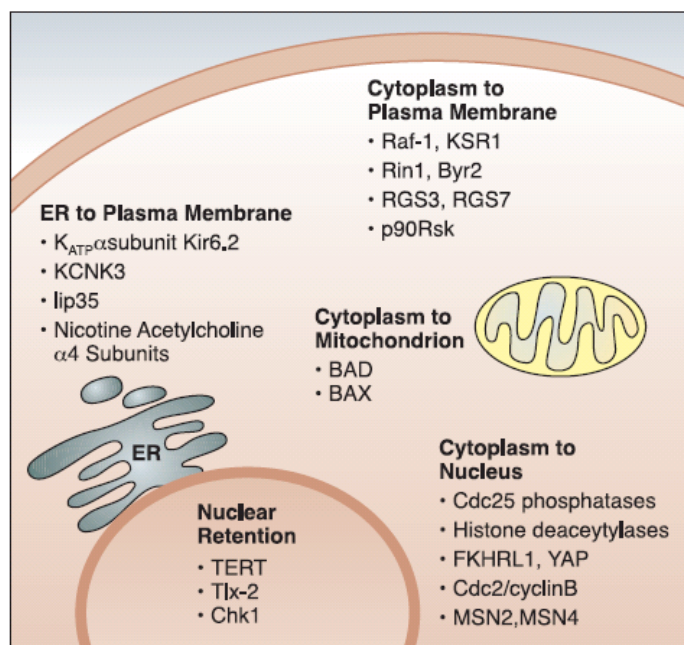
**FIGURE 15: Structure of two serotonin-*N*-acetyltransferase (AANAT) molecules bound to one 14-3-3 dimer.** The AANAT/14-3-3 $\zeta$  interaction is dependent on AANAT being phosphorylated on its 14-3-3 binding motif. AANAT molecules bind to the two amphipathic grooves of the 14-3-3 dimer, but also contact other parts of the central channel.

amino acids that form a basic pocket and belong to the four amino-terminal helices (K49, R56, R127, and Y128). These residues form a basic pocket in an otherwise acidic molecule, explaining the ability of substrate phosphorylation to act as a molecular switch, controlling ligand binding (**Fig. 15**) [196,198]. Despite of their conserved sequence and structure, not all isotypes of 14-3-3 bind equivalently to particular ligands.

14-3-3 proteins accomplish a wide range of functions in the cell. They have been shown to participate in the regulation of such crucial cellular processes as metabolism, signal transduction, cell cycle control, apoptosis, protein trafficking, transcription, stress responses and malignant transformation. The regulation of cellular processes by 14-3-3 occurs through several different mechanisms: modulating enzymatic activity, altering protein localization, preventing dephosphorylation, promoting protein stability, inhibiting protein interactions and

14-3-3 proteins can interact with a wide variety of cellular proteins. The binding of 14-3-3 to client proteins occurs through defined high affinity peptide motifs, two of which (RS-X-pS-X-P and R-XXX-pS-X-P) are highly conserved and recognized by all 14-3-3 isoforms. In most cases, binding occurs only if a specific serine within the motif is phosphorylated, but some 14-3-3 interactions are independent of phosphorylation [196]. Co-crystallization of 14-3-3 proteins with ligand phosphopeptides has shown that the interactions between them are mediated by specific amino acids that are located within both, the amino- and carboxy-terminal helices. The phosphorylated serine/threonine residue of the ligand contacts

mediating protein interactions [199]. In the case of 14-3-3-mediated modulation of protein localization, 14-3-3 binding sequesters the target protein in a particular subcellular compartment, and the release of 14-3-3 then allows the target to relocate. This relocation is due to the exposure of an intrinsic subcellular targeting sequence that was masked by the 14-3-3 dimer. This mechanism of regulation contributes to the nuclear retention of proteins, such as human telomerase reverse transcriptase (TERT), and plays a crucial role in the cytoplasm-mitochondrion shuttling of BAD and BAX, and in the cytoplasm-nucleus shuttling of proteins, including Cdc25 and histone deacetylase. It has become apparent that this regulatory mechanism also applies to proteins that shuttle from the cytoplasm to the plasma membrane, particularly proteins that are involved in Ras signaling (see also **Fig. 16**) [199].



*Dougherty and Morrison [199]*

**FIGURE 16: Proteins whose subcellular localization is regulated by 14-3-3 binding.**

There is a great deal of evidence confirming the regulation of RAF kinases by 14-3-3 family members, but the process of RAF regulation by 14-3-3, best analyzed for C-RAF, is so far not completely understood. It is already established that C-RAF contains at least two high-affinity phosphoserine sites (S259 in CR2 domain and S621 at the C-terminal end of CR3 kinase domain) that mediate binding to a 14-3-3 dimer. These 14-3-3 binding sites are highly conserved in all three RAF isoforms. In A-RAF, they correspond to S214 and S582, respectively, whereas in B-RAF these are S365 and S729. However, while the C-terminal 14-3-3 protein binding motif of RAF kinases is highly conserved, the sequence surrounding serine 365 in B-RAF differs from the corresponding 14-3-3 binding motif in A- and C-RAF. Therefore, it is possible that the 14-3-3 proteins bind with different affinity to the position pS365 in B-RAF compared to the corresponding sites in A- and C-RAF. An additional 14-3-3 binding site in C-RAF, surrounding S233, has also been characterized [200]. It is questionable, however, whether the corresponding domains in A- and B-RAF serve as a 14-3-3 binding domain as well, since the basic residue in position -3 is not present in these isoforms. Finally, an atypical 14-3-3 binding site positioned at the C-terminal part of C-RAF-CRD and close to RBD (comprising the residues RKT in position 143–145) has been described [201]. Near this 14-3-3 binding site at the CRD a contact domain for farnesyl residue of Ras proteins has been identified, which is located in the hydrophobic region LAF (149–151). Therefore, it is possible that the interaction of the farnesyl residue with this domain is necessary to remove sterical hindrances caused by 14-3-3 proteins.

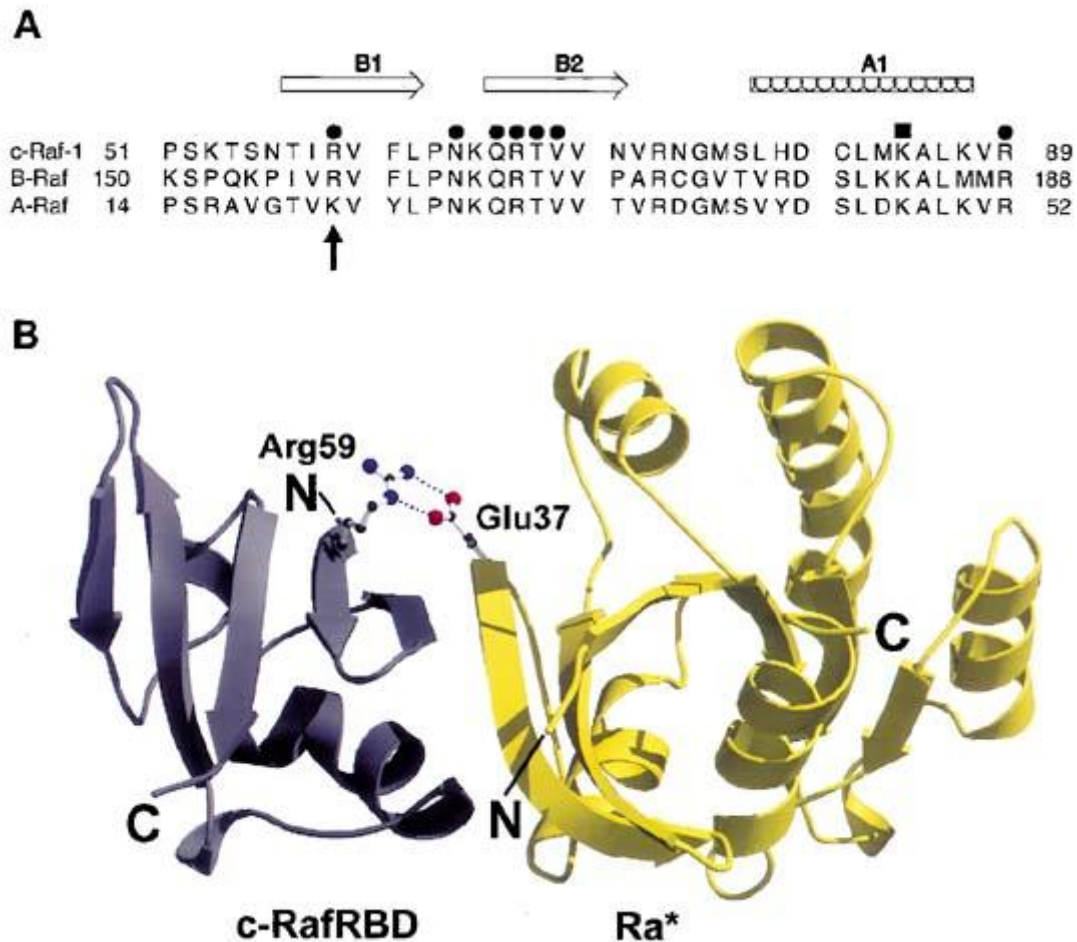
Recently, Hekman *et al.* [202] investigated 14-3-3 interaction with purified full-length RAF kinases and found that RAF isozymes differ in their 14-3-3 association rates. In addition, they showed that the C-terminal 14-3-3 binding site (pS621) represents the high-affinity binding site, whereas the pS259 epitope mediates lower affinity binding. Of importance, they visualized for the first time the dynamic changes of the essential C-RAF phosphorylation events, including 14-3-3 binding, in response to growth factor stimulation [202].

Based on available information, which is unfortunately insufficient for designing an unchallengeable regulation model, Hagemann and Rapp [76] suggest a hypothetical model, in which 14-3-3 proteins are necessary for stability of the inactive as well as the fully active conformation of RAF. In this model, 14-3-3 dimer binds to the conserved phosphoserine sites to keep RAF in a closed inactive conformation. Binding of activating protein, such as Ras-GTP to the RBD and the cysteine-rich region of RAF might displace the 14-3-3 from the phosphoserine site in the CR2 domain. This leads to conformational rearrangement, which subsequently, causes a basal activation of RAF. Additional factors might reinforce the RAF activity. Finally, binding of 14-3-3 dimers again might stabilize the fully active RAF conformation [76]. Studies, which are more recent, provide some additional details to this regulation model. It has been shown that dephosphorylation of serine in CR2 domain is necessary as a prerequisite for RAF activation in growth factor-stimulated cells [203]. Furthermore, there also appears to be a competition between Ras and 14-3-3 for binding to RAF kinase [204], hence the additional function of 14-3-3 dimer might be to mask regions on RAF that are required for translocation and subsequent activation of this kinase by Ras. In addition, our group [205] has recently shown that 14-3-3 dimer can be replaced from the internal binding site of C-RAF by the scaffold prohibitin (PHB) during the activation process (see also **Fig. 18**).

Although the discussed regulation mechanism was conceptualized on the basis of interactions between 14-3-3 and C-RAF, the highly conserved 14-3-3 binding sites presented in A-RAF suggest that this mechanism can be generalized for RAF kinases including A-RAF. In the case of A-RAF, isolation of the 14-3-3 isoforms  $\beta$ ,  $\epsilon$ ,  $\zeta$ ,  $\tau$  and  $\eta$  in a two-hybrid screen using A-RAF as a bait [206] as well as co-immunoprecipitation of overexpressed 14-3-3 with A-RAF [207] reinforce the assumption that A-RAF, just like C-RAF, might be regulated by 14-3-3 proteins. Moreover, in direct two-hybrid tests with A-RAF deletion mutants, it has been confirmed that the predicted 14-3-3 binding sites S214 and S582 of A-RAF are indeed necessary for interaction with 14-3-3 [207]. Recently, our group has shown that A-RAF associates *in vivo* with at least two 14-3-3 isoforms, epsilon and tau [205].

### 3.2.7.3. Mechanism of Ras–RAF coupling

Although Ras proteins play a crucial role in the activation of C-RAF, the exact mechanism of Ras–RAF coupling is not completely understood. The RBD of C-RAF comprises the residues 51–131 and binds directly to the switch-I region of active Ras-GTP [208]. In addition to the RBD, the CRD domain of C-RAF, encompassing residues 139–184,



Weber et al. [209]

**FIGURE 17: Ras–RAF interacting residues.** (A) Sequence alignment of the Ras binding domains (RBD) of A-RAF, B-RAF and C-RAF. Elements of the secondary structure are represented on the top with strands as open arrows (B1 and B2) and helices as hatched boxes. Amino acid residues involved in the interaction of the individual RBDs with Rap or Ras are indicated by solid circles, with K84 responsible for the specificity between Ras and Rap1 is marked by a solid box. The arrow indicates the difference of the interacting residues of B-RAF and C-RAF compared with those of A-RAF. (B) Structure of the C-RAF-RBD/Ra\* complex. Ra\* represents the Rap1-E30D-K31E double mutant, a protein with a crystallographic structure similar to Ras with an identical core effector region [210]. Amino acid R59 in RAF-RBD and its interaction partner E37 in Ra\* are highlighted and the side chain interactions are indicated [209].

appears to play an important role in Ras–RAF coupling and activation of RAF. Whereas the Ras–RBD interaction is understood in detail, a number of reports have provided conflicting data regarding the role of CRD. Initial studies [211,212] demonstrated a considerably decreased interaction of Ras with the N-terminal part of C-RAF, when some of the zinc binding cysteines were mutated to serine. These findings have been confirmed with full-length C-RAF expressed in mammalian cells [213,214]. The possibility that the farnesyl residue of Ras may interact directly with the hydrophobic surface of CRD has been shown as well [191,201]. However, as demonstrated previously [215], the Ras–CRD interaction was

essentially independent of the guanine nucleotide state of Ras. Besides the ability to interact with processed Ras, CRD was reported to possess binding sites for 14-3-3 proteins and phosphatidylserine. Thus, CRD reveals a multifunctional role with respect to regulation of C-RAF activation. Together, these findings supported a dual role for Ras: (I) tight coupling of Ras-GTP to C-RAF-RBD with high affinity constants and (II) weaker coupling of farnesyl-Ras to the CRD, a process that seems to be necessary for induction of C-RAF activation.

Concerning the role of palmitoyl residues attached to H- and N-Ras, Rocks *et al.* [90] reported recently that the de-/repalmitoylation of H-Ras plays an crucial role in the subcellular distribution, driving rapid exchange of Ras between plasma membrane and Golgi apparatus. Furthermore, Fischer *et al.* [216] reported recently that, contrary to the isolated RBD fragment, the full-length C-RAF associates preferentially with farnesylated Ras. The significantly weaker interaction of C-RAF with the GDP-form of farnesylated Ras may account for the proposed precoupled state between Ras and RAF that may exist prior to the cell stimulation by external agents [11]. B-RAF, on the other hand, exhibits profoundly different binding properties with regard to Ras coupling, when compared with C-RAF. It has been found that B-RAF binds with similar affinities both, farnesylated and non-farnesylated H-Ras in solution (mimicking the cytosolic environment). This observation implicates that B-RAF does not necessarily need recruitment to the plasma membrane in order to associate with Ras.

The first crystal structure of the complex between a Ras-related protein (Rap1A) and the Ras-binding domain of C-RAF has been reported by the group of A. Wittinghofer [208]. Surprisingly, the crystal structure revealed that RBD possesses the ubiquitin superfold (see **Fig. 17**) and that the structure of Rap1A is very similar to that of Ras. The interaction between Rap1A and C-RAF-RBD is mediated mostly by hydrogen bonds and polar interactions between charged residues, from both main-chain and side-chain polar groups [209]. The RBD of the three different RAF kinases (A-, B- and C-RAF) display high homology but also differences in their amino acid sequences (see **Fig. 17**). Therefore, the question of Ras binding specificity to these different RBDs arose soon after the finding that Ras regulates RAF activity. The dissociation constants ( $K_{DS}$ ) for the complex formation between Ras-GTP and RBDs of A-, B- and C-RAF monitored by two different experimental techniques revealed that Ras indeed shows high diversity with respect of this interaction [209,216]. Both contributions show consistently that Ras binds with considerably lower affinity to the A-RAF-RBD. On the other hand, Ras bound with high affinity to RBDs of B- and C-RAF, yielding  $K_D$  values in the range between 10 and 30 nM. Similar observations have been made by use of full-length C- and A-RAF kinases. Weber *et al.* [209] demonstrated that the transient transfection of oncogenic H-Ras (H-Ras12V) leads to a preferential activation of endogenous C-RAF in HEK293 cells as opposed to A-RAF. Noticeably, the Ras-binding interface of C-RAF differs from A-RAF by a conservative arginine to lysine exchange at residue 59 or 22, respectively (see **Fig. 17**). Mutational analysis revealed that this residue represents a point of isozyme discrimination: C-RAF-R59K mutant bound H-Ras weaker than the wild type; likewise, A-RAF-K22R increased its affinity to H-Ras *in vivo* and *in vitro*. Thus, these data introduced a new level of isoform discrimination in Ras/RAF signaling as a functional consequence of a conservative amino acid exchange in the Ras binding domains. Based on crystallographic data presented by Nassar *et al.* [208], Weber *et al.* [209] suggested a model for A-RAF-RBD

interaction with Ras. As illustrated in **Fig. 17**, R59 in C-RAF forms a salt bridge with E37 in H-Ras. Since lysine can only form a single side chain contact, it is likely that the reduced contribution of K22 in A-RAF is responsible for the observed reduction of binding affinity of A-RAF to H-Ras.

#### 3.2.7.4. Current mechanism of RAF activation

The molecular mechanism, by which RAF activity is regulated, is highly complex and, despite intensive investigations over the past 25 years, not completely elucidated. Although experimental support is missing, it has been generally accepted that in quiescent cells C-RAF exists in an inactive conformation maintained by autoinhibitory interactions occurring between the N-terminal regulatory and the C-terminal catalytic domains [10,176]. This inactive conformation is stabilized by the binding of 14-3-3 dimer to the conserved phosphoserines within the internal and the C-terminal 14-3-3 binding sites of RAF. The binding of 14-3-3 dimer acts like a clothespin, folding the RAF polypeptide into a closed configuration (see **Fig. 18**). In the inactive conformation of RAF, the catalytic domain is presumably blocked by the RAF zinc finger, which obstructs access to the ATP binding site. There is evidence that a fraction of RAF molecules exists as membrane-prebound, being targeted to the plasma membrane primarily by association with cholesterol and ceramides (raft microdomains) [11]. Additionally, the association of RAF with the membrane may be facilitated through the binding of the RAF catalytic domain to phosphatidic acid (PA). The PA binding segment of C-RAF is located between residues 389 and 423 that are highly conserved between all mammalian RAF isoforms [191,217]. Thus, this model implicates that RAF association with plasma membrane lipids represents the initial step in RAF activation.

Ligand activation of a receptor tyrosine kinase promotes formation of Ras-GTP, which creates a high affinity binding to RBD of RAF. Furthermore, the farnesyl residue at the carboxy-terminus of Ras has been shown to be necessary for binding and activation of C-RAF, but dispensable for association with B-RAF [216]. Association of RAF with membrane lipids and with Ras-GTP displaces 14-3-3 from RAF. Removal of 14-3-3 proteins allows access to phosphatases. Recently, it has been found that prohibitin (PHB), a membrane chaperone, influences RAF activation in a positive manner [218]. The interaction of membrane-bound PHB with RAF in the proximity of the N-region is suggested to induce the kinase activity of RAF by displacement of 14-3-3 from the internal binding domain, allowing access to phosphatases (see also **Fig. 18**). The subsequent dephosphorylation of the internal 14-3-3 binding site initiates the activation of RAF kinase. The fate of the 14-3-3 half-dimer displaced from the internal 14-3-3 binding site is still unclear. Some groups suggest that RAF undergoes phosphorylation at an unidentified site in the catalytic domain, distinct from the N-region, which creates a new binding site for the 14-3-3 half-dimer. The binding of 14-3-3 to this putative site would stabilize an open, active conformation of RAF, enabling its release from Ras-GTP into cytosol in a stably active state [219,220]. Other groups suppose that the 14-3-3 half-dimer may bind to phosphorylated site of KSR cross-linking the RAF/KSR

complex and delivering KSR-bound MEK to RAF (see also **Fig. 18**) [221,222]. However, at present, only indirect data regarding this issue are available.

A tentative model has been proposed for the subsequent steps with respect to C-RAF activation that includes Ras-driven B- and C-RAF hetero-oligomerization [154,216,223,224]. As reported by our group [223], mutation of the serine 621 to alanine in the C-terminal 14-3-3 binding motif of C-RAF reduced considerably the extent of the heterodimer formation, indicating that 14-3-3 proteins regulate this process.

Other important elements of RAF activation process are caveolin, a scaffolding protein, which may sequester inactive RAF [225], the scaffolds CNK and SUR-8 [162], and lots of protein kinases that facilitate RAF activation through phosphorylation at several regulatory sites [115,226-228].

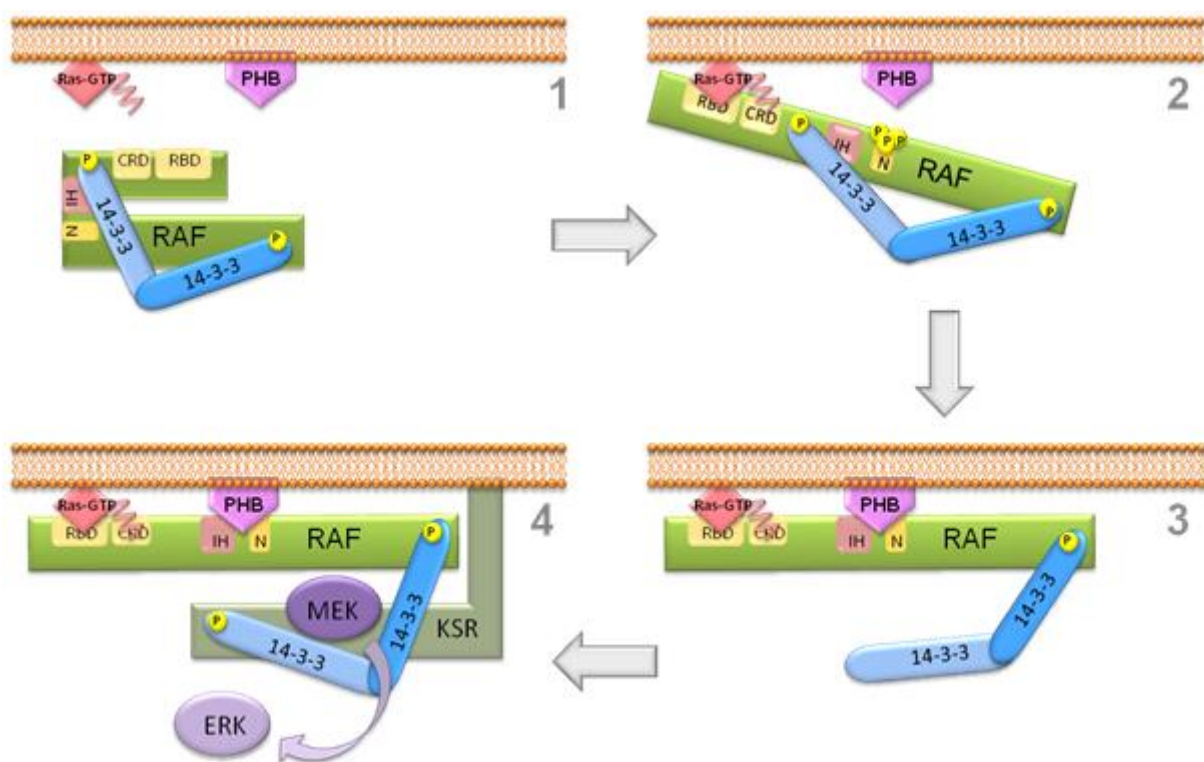


**FIGURE 18: Current model for activation mechanism of RAF kinases.** Association of RAF with Ras-GTP and membrane lipids (not shown) results in translocation of the inactive cytosolic RAF/14-3-3 complex to the plasma membrane (*panels 1 and 2*) [11]. Targeting of RAF to membranes and binding to activated Ras reorients RAF molecules and induces structural modifications that allow phosphorylation/dephosphorylation events and assembly of a RAF signalosome, containing different adaptor/scaffold proteins and RAF substrate MEK (*panel 4*). Interaction of membrane-bound scaffold protein prohibitin (PHB) with RAF induces its kinase activity by displacement of 14-3-3 from the internal binding site (*panel 3*), allowing access to phosphatases. The subsequent dephosphorylation of the internal 14-3-3 binding site contributes to maintenance of the activity [202]. KSR coordinates the assembly of a multiprotein complex containing MEK and ERK and facilitates signal transmission from RAF to MEK and ERK [229]. The cross-linking of KSR and RAF by 14-3-3 proteins may stabilize this protein complex. The multiprotein complex formation of RAF with heat shock proteins and additional scaffold proteins such as CNK and SUR-8 as well as dimerization of RAF molecules have not been considered in this presentation.

### 3.2.7.5. Regulation of RAF activity by phosphorylation

Phosphorylation of RAF kinases is of particular importance in RAF regulation, as it plays a crucial role in the activation/inactivation process. In C- and B-RAF, both stimulatory and inhibitory sites have been reported. Although several phosphorylation sites are well established, RAF phosphorylation remains one of the most controversial aspects of RAF research since the discovery of growth factor-induced tyrosine phosphorylation of C-RAF [230]. In C-RAF, the most prominent basal phosphorylation sites have been identified as serines 43, 259 and 621. These sites have been shown to be phosphorylated in growth factor-stimulated as well as in resting cells [231]. Phosphorylation of serines in positions 259 and 621 is necessary for association with 14-3-3 proteins [232]. Phosphorylation of the internal 14-3-3 binding site S259 has been reported to suppress C-RAF kinase activity [189,233-235], whereas regulation of C-RAF kinase activity by S621 phosphorylation is controversially discussed. On the one hand, there is strong evidence that S621 is essential for catalytic activity [236], on the other hand, it has been suggested that it serves as a phosphorylation site that confers negative regulation [237]. Furthermore, Dumaz *et al.* [238] reported that in addition to S259, cAMP dependent phosphorylation of serines 43 and 233 by protein kinase A results in negative regulation of C-RAF function. Recently, serine 471 in C-RAF and corresponding residue in B-RAF (S579) were identified as *in vivo* phosphorylation sites that are critical for RAF activity and serve as a docking site for MEK [132].

The highly conserved motif DFGLATVKS<sub>R</sub>, which is a part of the activation segment, is also subject to regulation by phosphorylation of conserved residues, threonine 491 and serine 494 in the case of C-RAF. They are homologous to T452 and T455 of A-RAF as well as to T599 and S602 of B-RAF. This segment lies within the activation loop of the kinase domain and is likely to be necessary for kinase activity of RAF, since in B-RAF, mutation of these amino acids to alanine results in loss of activity induced by activated Ras, whereas substitution of these sites by phosphomimetic residues (acidic residues) results in a constitutive B-RAF activity [239]. Similarly, mutation of the corresponding residues in C-RAF influences kinase activity of this isoform, however, to lower degree compared to B-RAF [240]. The importance of these conserved residues for A-RAF activation remains to be investigated.

Treatment of cells with growth factors induces phosphorylation of C-RAF at multiple sites located within the regulatory part of the protein. These are threonines 268/269, serines 289/296/301, serines 338/339 and tyrosines 340/341. Threonine 268 within the CR2 domain in C-RAF and the homologous residue T372 in B-RAF represent an autophosphorylation site [231,241], whereas threonine 269 of C-RAF has been proposed to serve as a target for phosphorylation by KSR [242]. Recently, novel phosphorylation sites at three SP motifs of C-RAF (serines 289, 296 and 301) were identified [152,153,194]. They are located within the variable sequence stretch that connects CR2 with kinase domain. Although the interpretation of the results is still controversial, the published data document that these sites regulate C-RAF by direct ERK-mediated feedback phosphorylation [152,153].

Furthermore, a short conserved sequence in front of the kinase domain, also called N-region (the name is derived from Negative-charge regulatory region), has been reported to be necessary for the basal activity and growth factor-induced activation of RAF kinases. This



region contains one highly conserved serine, which is present in all three RAF isoforms (S299 in A-RAF, S338 in C-RAF and S446 in B-RAF) and two conserved tyrosines (Y301/Y302 in A-RAF and Y340/Y341 in C-RAF) at positions where in B-RAF aspartates are located (D448/D449). Stimulation-dependent phosphorylation of these sites regulates positively the kinase activity of C- and B-RAF [113,181,182]. In the case of A-RAF, a stimulating role of tyrosines 301/302, corresponding to tyrosines 340/341 in C-RAF, has been demonstrated [113], whereas involvement of serine 299 in regulation of A-RAF kinase activity has not been investigated.

Regarding regulation of B-RAF activity by phosphorylation, there are similarities but also essential differences compared to C-RAF. Phosphorylation of serines 365 and 729, which are equivalent to serines 259 and 621 of C-RAF, has been shown to mediate 14-3-3 binding to B-RAF and regulate its activity in the similar way as reported for C-RAF [202,243]. On the other hand, the N-region-mediated regulation is quite different in B- and C-RAF, because the tyrosine residues of C-RAF (Y340 and Y341) are occupied by aspartic acids in B-RAF (D448 and D449). This leads to constitutive phosphorylation of the serine 446 in B-RAF [195]. Thus, due to the accumulated negative charge at the N-region the B-RAF kinase exhibits unusual high basal kinase activity [11,182]. In addition, our group recently reported that the prolonged N-terminal part of B-RAF and the facilitated binding of non-lipidated Ras proteins also contribute to elevated basal B-RAF activity [216]. Together, these findings indicate that the mechanisms for regulation of RAF activation differ considerably for each RAF isoform. With some exceptions, little is known about the role of phosphorylation in the activation process of A-RAF.

### **3.3. Isoform-specific properties of A-RAF**

#### **3.3.1. A-RAF gene**

##### **3.3.1.1. Localization of A-RAF gene**

*A-RAF* cDNA was originally isolated from a mouse spleen cDNA library by homology to a *v-RAF* oncogene probe [177]. This murine cDNA (*mA-RAF*) was subsequently used to isolate a related human *A-RAF* cDNA (*hA-RAF*). On screening both mouse and human cDNA libraries was found that there is only one *A-RAF* gene in mouse (*mA-RAF*), whereas the human genome includes two *A-RAF* genes (*hA-RAF-1* and *hA-RAF-2*). *hA-RAF-2* maps to the human chromosome 7, specifically to region 7p11.4-7q21 and is likely to be a pseudogene, since no transcriptional activity of this locus has been observed. In contrast, *hA-RAF-1*, which is translated, is located within the proximal short arm of the human X chromosome [244]. Accordingly, the murine *A-RAF* is mapped to the centromeric region of the mouse X chromosome [244,245]. Mapping and genetic linkage analysis in mouse and man have demonstrated that *A-RAF* is situated in a highly conserved gene cluster at Xp11.2 [244] with genes for the neuron-specific phosphoprotein synapsin I (*SYN1*), the tissue inhibitor of

metaloproteinases (TIMP) and the serum glycoprotein properdin (PFC) [245]. These genes lie within 70 kb of each other in the order of (5')*A-RAF*(3')–*SYNI*(3')–*TIMP-SYNI*(5')–(3')*PFC*(5') [245-248]. One of the interesting features of this gene cluster is the conserved arrangement of the *SYNI* gene and the *A-RAF* gene. These genes lie immediately adjacent to each other in the 3'-end-to-3'-end manner and are transcribed from opposite strands [245,247,248]. Moreover, Lee *et al.* [249] do not exclude a possibility that both, *A-RAF* and *SYNI* might overlap in their 3'-termini, since the 3'-ends of either genes map to the same restriction site. However, the functional importance of this association remains obscure.

### 3.3.1.2. Molecular organization of *A-RAF* gene

The human *A-RAF-1* gene is composed of 16 exons that span 10.8 kb and appears to be the smallest of the *RAF* gene family. All sequences of the intron/exon boundaries conformed to consensus splice junctions, except for the exon 13 splice acceptor site that contains GG as the last two nucleotides instead of the consensus AG [249]. hA-*RAF-1* gene is expressed as a 2.6-kb (including poly(A) sequence) transcript, coding for a 68-kDa protein [184,250]. The 3'-end of the hA-*RAF-1* gene is not firmly established, due to the absence of a consensus polyadenylation sequence AAUAAA [249]. However, a variant sequence CAUAAA was identified at position nucleotide 10.891 and is suggested by Lee *et al.* [249] to be the putative non-consensus polyadenylation site of hA-*RAF-1* mRNA. The hA-*RAF-1* minimal promoter, which is located between nucleotides –59 and +93, has a low G + C content similar to some tissue-specific gene promoters and unlike the GC-rich human *C-RAF-1* promoter region [249]. Furthermore, the hA-*RAF-1* promoter lacks consensus CAAT, TATA and Inr sequence motifs, but shows sequence similarity (5/6 nucleotide identities) at position –1 to the consensus E-box (CACGTG), which is known to interact with USF and TFII-I transcription factors [249]. The 5'-flanking region of the hA-*RAF-1* gene contains DNA sequences of potential regulatory significance, including multiple glucocorticoid and thyroid hormone response elements (GRE and TRE, respectively) and putative Sp1 binding sites [249]. The importance of some of the identified regulatory elements was emphasized by comparison of the nucleotide sequences in 5'-flanking region of both, mouse and human *A-RAF* genes. The sequence alignment performed by Lee *et al.* [251] revealed that sequence block between –59 and –4 is conserved between mouse and man and contains two highly conserved putative GRE motifs at positions –18 and –34 with 5/6 and 6/6 nucleotide sequence identities, respectively. Furthermore, DNA binding studies undertaken by the same group using purified glucocorticoid receptor DNA binding domain (DBD) demonstrated that the glucocorticoid receptor forms multiple protein/DNA complexes with conserved hormone response elements GRE1, GRE2 and GRE3 at positions –17, –34 and –168, respectively, within the *A-RAF* promoter region [251].

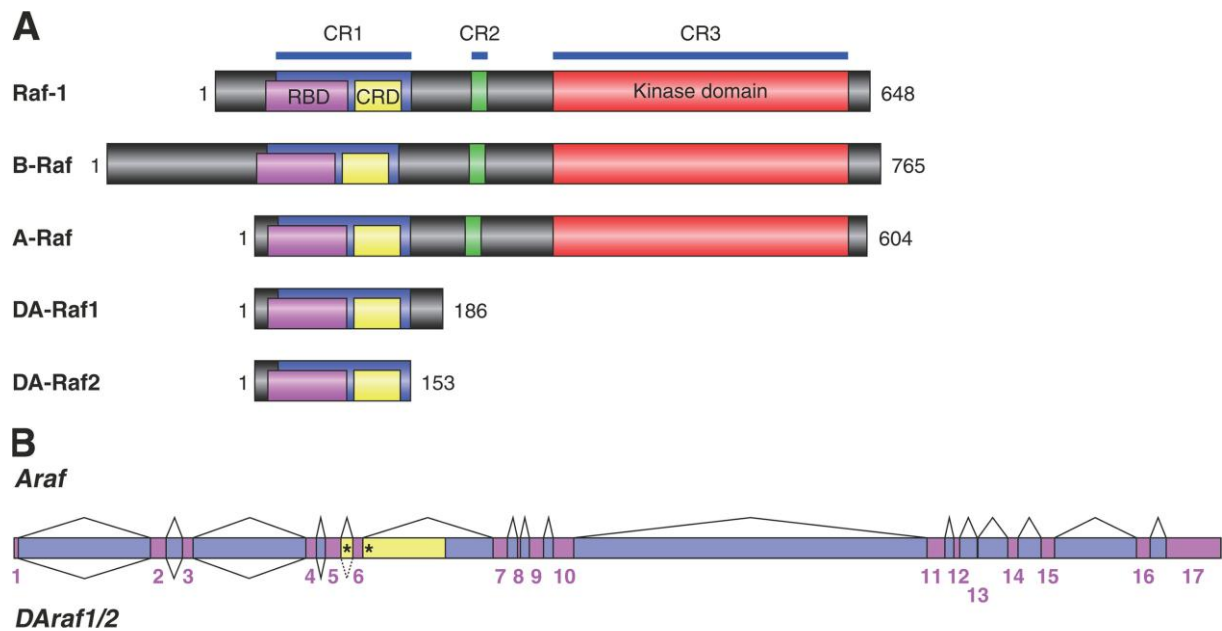
### 3.3.2. A-RAF protein

#### 3.3.2.1. Splicing variants of A-RAF

The first evidence for an alternative splicing of *A-RAF* transcripts came from Wadewitz *et al.* [250], who observed an additional transcript of 4.3 kb in Northern blot analysis of RNA isolated from mouse testis using *A-RAF* specific riboprobes, but a sequence of this transcript and the existence of corresponding protein have not been clearly defined. Recently, Yokoyama *et al.* [252] isolated two *A-RAF* splicing variants referred to as DA-RAF1 and DA-RAF2 that are generated by alternative splicing of *A-RAF* pre-mRNA. The DA-RAF1 variant corresponds exactly to the N-terminal 186 amino acids of A-RAF, which contains CR1 but lacks CR2 and CR3, whereas DA-RAF2 is somewhat shorter than DA-RAF1. The *DA-RAF2* mRNA encodes a protein, consisting of the N-terminal 153 amino acids of A-RAF, which also includes RBD and CRD. *DA-RAF1* cDNA retains intron 6–7 linked to exon 6 and consequently gives rise to the termination codon TAG, starting from the second nucleotide of intron 6–7. Poly(A) tail is added 12 bases downstream of the putative poly(A) addition signal AATAAA. In contrast, *DA-RAF2* mRNA contains intron 5–6 between exons 5 and 6. The retention of intron 5–6 generates the termination codon TGA, starting from the second nucleotide of intron 5–6 (see also **Fig. 19**) [252].

#### 3.3.2.2. Expression of *A-RAF*

*A-RAF* expression patterns are determined in a variety of mouse tissues collected from male and female adults as well as from mouse embryos and fetuses. The *A-RAF* activity is found in all examined tissues. However, the levels of *A-RAF* expression vary considerably among different tissues and between different developmental stages. Although results of examination of *A-RAF* expression patterns in adult mice reported by several groups are controversial, in some cases there is one common feature. High levels of *A-RAF* expression have been observed in several tissues of the male and female urogenital systems, whereas barely detectable levels of *A-RAF* expression have been present in brain, spinal cord, skeletal muscle, and skin [177,179,250,253]. The observed *A-RAF* expression pattern is consistent with the predicted control mechanism of *A-RAF* promoter activity. Steroid hormone dependent activation of the *A-RAF* promoter reported by Lee *et al.* [251] correlates with preferential expression of *A-RAF* in several tissues of the urogenital system, most of which are known to be steroid hormone responsive. Moreover, *A-RAF* expression studies in castrate and hemicastrate mice have indicated that serum androgens as well as unknown additional testicular factors are required for the highly segment-specific pattern of *A-RAF* expression in the caput region of mice epididymis [254]. On the other hand, the low constitutive level of *A-RAF* expression observed in all other mouse tissues might be the result of a low basal *A-RAF* promoter activity in the absence of steroids, as discussed by Lee *et al.* [251].

Yokoyama *et al.* [252]

**FIGURE 19: Domain structure of DA-RAF1/2 and splicing patterns of A-RAF/DA-RAF pre-mRNA.** (A) Functional domains of RAF proteins and DA-RAF1/2. The numbers indicate amino acid residues of mouse proteins. (B) Alternative splicing of A-RAF/DA-RAF pre-mRNA generating A-RAF and DA-RAF1/2 mRNAs. Pink boxes, exons; purple boxes, introns; yellow boxes, introns retained in DA-RAF1/2 mRNAs but not in A-RAF mRNA; asterisks, termination codons for DA-RAF2 (in intron 5–6) and DA-RAF1 (in intron 6–7) [252].

In mouse fetuses and embryos, *A-RAF* expression demonstrates a somewhat different pattern than in adult animals. As in adults, *A-RAF* is expressed in most tissues at low levels at each developmental stage. However, in E9.5 and E11.5 embryos prominent levels of *A-RAF* mRNA are detected in the heart, whereas at stage E16, *A-RAF* is expressed at high levels in intestine and placenta. The lowest level of the fetal *A-RAF* expression was observed in brain [179,253]. Thus, *A-RAF* expression seems to be developmentally regulated in certain tissues.

Based on cross-section analysis of adult urogenital tissues, Luckett *et al.* [253] suggested that high *A-RAF* expression activity is likely to be restricted to the epithelial cell layers that require a high level of metabolic activity to practice their endogenous functions, such as ciliary action of ciliated epithelial cells or active transport of salts by epithelial cells in the kidney cortex. Furthermore, elevated expression of *A-RAF* was observed during differentiation of preadipocyte fibroblasts into adipocytes, which are known to metabolize glucose by the glycolytic pathway for the synthesis of triacylglycerols and hence to be highly metabolic active [255].

Transcripts of *A-RAF* have been also found in lymphocytes from peripheral blood of bovine with chronic lymphocytic leukemia at the peak of their proliferative activity in primary culture [256]. Furthermore, expression of *A-RAF* gene has been observed in several human hematopoietic cell lines such as TF-1, K562, HL60, U937 and Jurkat cells [257].

Recently, *A-RAF* expression pattern in human adult and fetal tissues has been published. Although both, mouse and man belong to mammals, the expression of *A-RAF* in

these organisms is not in all cases coincident. Similar to *A-RAF* expression in mouse, the lowest level of *A-RAF* mRNA has been observed in human neuronal tissues. However, in contrast to mouse tissues that display high *A-RAF* expression in urogenital tract, in human tissues the highest *A-RAF* expression has been observed in skeletal muscle, pancreas, liver and placenta [258]. For want of information at the moment, it is difficult to propose whether the discrepancy between *A-RAF* expression patterns in mouse and man is a result of evolutionary divergence or a measurement artifact.

In contrast to *A-RAF*, which has more limited tissue distribution, *DA-RAF1* and *DA-RAF2* are ubiquitously expressed in a variety of mouse tissues with a highest expression levels in the brain and heart [252].

### 3.3.2.3. Localization of A-RAF protein

As a signal transduction module of the MAP kinase pathway, A-RAF similar to C- and B-RAF is suggested to change its cellular localization in order to transmit the signal from the activated receptor of the cell membrane to the cytosolic downstream protein kinases. The cytosolic inactive form of A-RAF is proposed to translocate or be translocated to the cellular membrane, where it subsequently would be activated by its interaction with the members of Ras protein family or with other membrane receptor activated factors. Co-segregation of A-RAF to caveolae-specialized plasma membrane microdomains that play an important role in the modulation of cell signal transduction reinforces the proposed translocalization of A-RAF to the cell membrane [259].

Furthermore, Yuryev *et al.* [260] provided evidence for a potential mitochondrial localization of A-RAF. The first clue came from a two-hybrid screen of a HeLa cells' cDNA library. Specific interactions between A-RAF and the mitochondrial protein transport system proteins hTOM and hTIM44 were observed in this experiment, suggesting that A-RAF might be localized in mitochondria [261]. Subsequent isolation of mitochondria from rat liver and Western analysis of the mitochondrial fraction confirmed this hypothesis. Investigations using preparations of mitoplasts (mitochondria stripped of outer membranes and intermembrane components) and immunogold labeling with anti-A-RAF antibodies revealed that a significant portion of A-RAF is present in the inner matrix as well as in the intermembrane space of the mitochondria. However, a portion of A-RAF was also found in cytosolic fraction, suggesting that A-RAF may be partitioned both, in mitochondria and in the cytoplasm [260]. The domain of A-RAF sufficient for interaction with hTOM and hTIM44 was mapped to the region, containing the zinc finger domain CRD of the regulatory part of A-RAF protein [260]. However, the results published by Yuryev *et al.* [260] have not been reproduced so far. Moreover, according to data of Galmiche *et al.* [262], C-RAF but not A- or B-RAF, has been localized at the mitochondria. Thus, the localization of A-RAF at and within the mitochondria is still controversially discussed.

### 3.3.2.4. Physiological role of A-RAF

#### *Mice with a loss-of-function mutation in the A-RAF gene*

The phenotype of A-RAF-deficient mice has been described by Pritchard *et al.* [263] as follows: the knockout mice display neurological and intestinal abnormalities and die between 7 and 21 days postpartum. Although the knockout mice appear normal at birth, they display delayed growth relative to control animals in the following days. The few animals that survived to P21 appear to suffer from a wasting syndrome. Due to a pronounced ataxia, the animals suckle poorly and are incapable of feeding once weaned. The neurological abnormal phenotype of the A-RAF-deficient mice includes abnormal movement and proprioception. They display athetotic movements and have difficulty maintaining an upright position [263,264]. Histopathological investigations performed on A-RAF-deficient mice and reported by the same group [263] have shown that apart from a gross distention of the colon, all organs appear normal in architecture and morphology. Moreover, all tissues of the colon as well as blood supply to the colon and colon innervation are likely to be normal and did not provide any clues for possible explanation of the abnormal distention of colon. Similarly, with regard to the neurological abnormalities of A-RAF-deficient mice, it is also and perhaps more remarkable that the gross anatomy and architecture of the brain and spinal cord appear normal, as well as the expression pattern of neurospecific proteins [263]. Furthermore, Western blot of lysates of A-RAF knockout mouse brains with an antibodies that detect synapsin protein has confirmed that homologous targeting of the *A-RAF* gene has not accidentally disrupted expression of *SYN1* gene, which is located close to *A-RAF* gene, as described above. Thus, the abnormal physiological and neurological appearance of the A-RAF-deficient mice cannot be related to the overt changes in morphological, histological or genetic characteristics. Rather, subtle biochemical defects in functioning of A-RAF-deficient cells might be responsible for the altered phenotype of the whole organism.

#### *A-RAF in differentiation of muscle cells*

Recently, DA-RAF1, the short splicing variant of A-RAF, was described as a positive regulator of myogenic differentiation. As reported by Yokoyama *et al.* [252], expression of DA-RAF1 is almost absent in myoblasts but prominently induced during differentiation. DA-RAF1, which consists of RBD and CRD, and lacks CR2 and kinase domain, binds to active H-Ras and M-Ras and antagonizes the Ras-ERK pathway. The binding to active H-Ras and M-Ras *in vivo* was confirmed by the findings that DA-RAF1 was translocated to the cellular membranes to colocalize with H-Ras and M-Ras activated by mitogenic signals. The inhibition of Ras-ERK cascade by DA-RAF1 has several consequences, including cell cycle arrest, the expression of myogenin and other muscle-specific proteins, and myotube formation [252].

*A-RAF in endocytosis*

Using high-throughput RNA interference and automated image analysis Pelkmans *et al.* [265] identified A-RAF kinase as a regulator of caveolae/raft-mediated endocytosis. Because the silencing of A-RAF resulted in diffuse CAV1-GFP staining that was laterally mobile, the authors concluded that A-RAF regulates coat stability and dynamics of caveolae on the cell surface [265,266]. These findings were confirmed and extended by Nekhoroshkova *et al.* (*PLoS ONE*, in revision), who have shown a specific localization of A-RAF to endocytic compartments in yeast and human cells. Furthermore, they demonstrated that multiple domains co-determine the localization pattern of A-RAF and that A-RAF participates in regulation of endocytic trafficking, functioning upstream of ARF6. Of importance, an N-terminal fragment of A-RAF (AR149) that corresponds to the short splicing variant DA-RAF1 has been shown to act as a dominant negative regulator of endosomal trafficking (Nekhoroshkova *et al.*, *PLoS ONE*, in revision).

**3.3.2.5. Interaction partners of A-RAF**

Unlike B-RAF and C-RAF, there are only few reports about interaction partners of A-RAF. A-RAF binding proteins can be divided in two groups: the first one includes proteins that bind specifically only to A-RAF, whereas members of the second group have been shown to interact with B-RAF and C-RAF as well. The most known A-RAF interaction partners were initially identified in yeast two-hybrid screens. Some of these protein-protein interactions were confirmed by results of additional experiments such as co-immunoprecipitation and kinase assay (see **Table 1**).

**Table 1: Interaction partners of A-RAF kinase.**

<http://www.thebiogrid.org/SearchResults/summary/106864> (modified).

| Name   | Aliases  | Description   | Evidence Code(s)    | Role     | Source(s) |
|--------|--|---|---------------------|----------|-----------|
| TH1L   | <i>HSPC130</i><br><i>NELF-C</i><br><i>NELF-D</i><br><i>EG51497</i> | TH1 drosophila homolog / TH1-like protein / negative elongation factor proteins C and D; TH1-like ( <i>Drosophila</i> )                                   | <i>In vitro</i>     | hit      | [267]     |
|        |  |   | <i>In vivo</i>      | hit      | [267]     |
|        |  |   | Two-hybrid          | hit      | [267]     |
|        |  |   | Affinity Capture-MS | hit      | [261]     |
| TIMM44 | <i>DKFZ-p686H...</i><br><i>TIM44</i><br><i>EG10469</i>             | Mitochondrial inner membrane translocase / translocase of inner mitochondrial membrane 44; translocase of inner mitochondrial membrane 44 homolog (yeast) | <i>In vitro</i>     | bait     | [260]     |
|        |  |   | Two-hybrid          | bait     | [260]     |
|        |  |   | Affinity Capture-MS | hit      | [261]     |
|        |  |   | Affinity Capture-MS | bait/hit | [268]     |

|                 |  |   |                     |             |                |
|-----------------|--|---|---------------------|-------------|----------------|
| <b>MAP2K2</b>   | <i>MAPKK2</i><br><i>MEK2</i><br><i>MKK2</i><br><i>EG5605</i>     | CFC syndrome / ERK activator kinase 2 / MAP kinase kinase 2 / MAPK/ERK kinase 2 / dual specificity mitogen-activated protein kinase kinase 2 / mitogen-activated protein kinase kinase 2, p45; mitogen-activated protein kinase kinase 2  | <i>In vitro</i>     | bait        | [267]          |
|                 |  |   | Two-hybrid          | bait        | [267]          |
|                 |  |   | Affinity Capture-MS | hit         | [268]          |
| <b>C20orf14</b> | <i>ANT-1</i><br><i>TOM</i><br><i>PRPF6</i><br><i>EG24148</i>     | PRP6 pre-mRNA processing factor 6 homolog /U5 snRNP-associated 102 kDa protein / androgen receptor N-terminal domain transactivating protein-1 / p102 U5 small nuclear ribonucleoprotein particle-binding protein / putative mitochondrial outer membrane protein import receptor; PRP6 pre-mRNA processing factor 6 homolog ( <i>S. cerevisiae</i> ) | <i>In vitro</i>     | bait        | [260]          |
|                 |  |   | Two-hybrid          | bait<br>hit | [260]<br>[261] |
| <b>RRAS</b>     | <i>EG6237</i>  | Related RAS viral (r-ras) oncogene homolog; oncogene RRAS   | <i>In vitro</i>     | bait        | [260]          |
|                 |  |   | Two-hybrid          | bait<br>hit | [260]<br>[261] |
| <b>PBK</b>      | <i>FLJ14385</i><br><i>Nori-3</i><br><i>SPK</i><br><i>EG55872</i> | MAPKK-like protein kinase / PDZ-binding kinase / T-LAK cell-originated protein kinase / serine/threonine protein kinase / spermatogenesis-related protein kinase; PDZ binding kinase  | Affinity Capture-MS | hit         | [268]          |
|                 |  |   | Two-hybrid          | hit         | [261]          |
| <b>COPS3</b>    | <i>SGN3</i><br><i>EG8533</i>                                     | COP9 complex subunit 3 / COP9 constitutive photomorphogenic homolog subunit 3 / JAB1-containing signalosome subunit 3; COP9 constitutive photomorphogenic homolog subunit 3 ( <i>Arabidopsis</i> )  | Two-hybrid          | hit         | [261]          |
|                 |  |   | Affinity Capture-MS | hit         | [268]          |
| <b>ASS</b>      | <i>ASS1</i><br><i>CTLN1</i><br><i>EG445</i>                      | Argininosuccinate synthetase 1; citrulline-aspartate ligase   | Two-hybrid          | hit         | [261]          |
|                 |  |   | Affinity Capture-MS | hit         | [268]          |
| <b>CSNK2B</b>   | <i>CK2B</i><br><i>CK2N</i><br><i>CSK2B</i><br><i>EG1460</i>      | Casein kinase II beta subunit / alternative name: G5a, phosvitin / phosvitin; casein kinase 2, beta polypeptide   | <i>In vitro</i>     | hit         | [269]          |
|                 |  |   | Two-hybrid          | hit         | [269]          |
| <b>EFEMP1</b>   | <i>DHRD</i><br><i>DRAD</i><br><i>FBLN3</i><br><i>EG2202</i>      | EGF-containing fibulin-like extracellular matrix protein 1; fibrillin-like / fibulin 3  | Two-hybrid          | bait/hit    | [261]          |
|                 |  |   | Affinity Capture-MS | hit         | [268]          |



|                |  |  |                     |          |       |
|----------------|--|--|---------------------|----------|-------|
| <b>RABGGTB</b> | <i>GGTB</i><br><i>RP4-682C2...</i>                               | Rab geranylgeranyltransferase, beta subunit  | Two-hybrid          | hit      | [261] |
| <b>SFN</b>     | <i>YWHAS</i><br><i>EG2810</i>                                    | 14-3-3 sigma; stratifin  | Affinity Capture-MS | bait     | [270] |
| <b>YWHAG</b>   | <i>14-3-3-GAMMA</i><br><i>EG7532</i>                             | Tyrosine 3-monooxygenase /tryptophan 5-monooxygenase activation protein, gamma polypeptide; 14-3-3 gamma   | Affinity Capture-MS | bait     | [271] |
| <b>PIK3R1</b>  | <i>GRB1</i><br><i>p85-ALPHA</i><br><i>EG5295</i>                 | Phosphatidylinositol 3-kinase, regulatory subunit, polypeptide 1 (p85 alpha) / phosphatidylinositol 3-kinase, regulatory, 1 / phosphatidylinositol 3-kinase-associated p-85 alpha / phosphoinositide-3-kinase, regulatory subunit, polypeptide 1 / phosphoinositide-3-kinase, regulatory subunit, polypeptide 1 (p85 alpha); phosphoinositide-3-kinase, regulatory subunit 1 (p85 alpha) | <i>In vivo</i>      | hit      | [272] |
| <b>KLHL12</b>  | <i>C3IP1</i><br><i>DKIR</i><br><i>FLJ27152</i><br><i>EG59349</i> | Kelch-like 12 / kelch-like protein C3IP1; kelch-like 12 ( <i>Drosophila</i> )  | Two-hybrid          | bait/hit | [268] |

## **4. AIM OF THE PROJECT**

Phosphorylation of RAF kinases is of particular importance in RAF regulation, as it plays a crucial role not only in the activation process but is also a prerequisite for docking of interacting partners, such as 14-3-3 proteins and MEK. Although several phosphorylation sites are well established, RAF phosphorylation remains one of the most controversial aspects of RAF research since the discovery of growth factor-induced tyrosine phosphorylation of C-RAF. In B- and C-RAF, numerous stimulatory and inhibitory phosphorylation sites have been reported. In contrast, little is known about the regulatory phosphorylation of A-RAF kinase.

The main focus of this study was to identify regulatory phosphorylation sites of A-RAF and to characterize their role in the activation process of this kinase. In order to address this aim a systematic analysis of the potential phosphorylation sites in A-RAF was performed. Recently, our group undertook a quantitative analysis of C-RAF phosphorylation by use of mass spectrometry that resulted in identification of several new phosphorylation sites in C-RAF. The same approach was applied to A-RAF in this work. The role of identified phosphorylation sites in the regulation of A-RAF was established by substitution analysis. To this end, the regulatory serines and threonines were replaced by alanine, thus preventing phosphorylation at these positions. Kinase activity, phosphorylation pattern and subcellular localization of A-RAF mutants were examined by use of *in vitro* kinase assay, immunoblotting with phosphospecific antibodies and cell fractionation technique. Structural consequences of A-RAF phosphorylation were established by tools of molecular modeling.

## 5. MATERIALS AND METHODS

The methods described in this section are all based upon today's standard molecular and cellular biology techniques.

### 5.1. Materials

#### 5.1.1. Instruments

##### Hardware

Bacterial incubator  
Bacterial incubator shaker  
BIAcore-X or BIAcore-J system  
Bruker APEX II FT-ICR mass spectrometer  
Cell culture hood  
Cell culture incubator  
Centrifuges  
  
DNA Sequencer  
Electrophoresis power supply  
Film developing machine  
Horizontal gel system  
LTQ XL mass analyzer  
Magnetic stirrer  
PCR machine  
pH meter  
Qstar Elite mass analyzer  
Semi dry blotting system  
  
Shakers  
  
Thermoshaker for microfuge tubes  
UV/Visible Spectrophotometer  
Vertical gel system  
  
Vortex

##### Manufacturer

Heraeus B 6200  
Innova 4330, New Brunswick Scientific  
Biacore AB, Uppsala, Sweden  
Bruker Daltonic GmbH, Bremen  
LaminAir, Heraeus Instrument  
Heraeus Instrument  
Biofuge Fresco, Heraeus Instrument;  
Megafuge 1.0R, Heraeus Instrument  
ABI PRISM 373, ABI  
EV202, Peqlab  
CP1000, AGFA-GEVAERT N. V.  
PerfectBlue Maxi Gel System M, Peqlab  
Thermo Scientific, Dreieich  
MMS 3000, A. Hartenstein Laborbedarf  
Primus 96, Peqlab  
InoLab, A. Hartenstein Laborbedarf  
Applied Biosystems, Darmstadt  
PerfectBlue Semi-Dry Electro Blotter,  
Peqlab  
Tetramax 101, Heidolph  
Mini Rocker MR1, A. Hartenstein  
Laborbedarf  
Thermomixer comfort, Eppendorf  
Ultrospec 3000, Pharmacia Biotech  
PerfectBlue Dual Gel System Twin S,  
Peqlab  
VTX-3000C, A. Hartenstein Laborbedarf

### 5.1.2. Chemical reagents and general materials

| <b><u>Reagent</u></b>   | <b><u>Purchased from</u></b> |
|---|------------------------------|
| Acrylamide (30%)/Bisacrylamide (0.8%)   | Roth                         |
| Adenosin-5'-triphosphate (ATP)  | Sigma                        |
| Agarose (ultra pure)  | Roth                         |
| Ammonium peroxydisulfate (APS)  | Roth                         |
| Ampicillin  | Roth                         |
| Antipain  | AppliChem                    |
| Aprotinin   | Roth                         |
| $\beta$ -Glycerophosphate   | Roth                         |
| $\beta$ -Mercaptoethanol  | Roth                         |
| Bovine serum albumin (BSA)  | Roth                         |
| Bromphenol Blue   | Roth                         |
| 1-Butanol   | Roth                         |
| C18 ZipTip  | Millipore                    |
| Calcium chloride dihydrate ( $\text{CaCl}_2 \times 2\text{H}_2\text{O}$ )         | Roth                         |
| Coomassie Protein Assay Reagent   | Pierce                       |
| Coumaric acid   | Sigma                        |
| dNTP Mix (2mM)  | Fermentas                    |
| Dimethyl sulfoxide (DMSO)   | Roth                         |
| Dithiothreitol (DTT)  | Sigma                        |
| EDTA (Ethylenediaminetetraacetic acid-disodium salt)                              | Roth                         |
| EGTA (Ethylene glycol-bis-( $\beta$ -aminoethylether)-N,N,N',N'-tetraacetic acid) | AppliChem                    |
| Empigen BB  | Calbiochem                   |
| Ethanol (p. A.)   | AppliChem                    |
| Ethanol (denaturated with 1% MEK)   | AppliChem                    |
| Ethidium bromide  | Roth                         |
| Glutathione   | Sigma                        |
| Glutathione Sepharose   | Pharmacia                    |
| Glycerol  | Roth                         |
| Glycine   | Roth                         |
| HEPES   | Roth                         |
| Hydrochloride (HCl)   | AppliChem                    |
| Hydrogen peroxide   | Sigma                        |
| Isopropanol   | Roth                         |
| Lambda DNA/Eco91I Marker, 15  | Fermentas                    |
| LB-Agar   | Roth                         |
| Leupeptin   | AppliChem                    |
| Luminol   | Biomol                       |
| Magnesium chloride hexahydrate ( $\text{MgCl}_2 \times 6\text{H}_2\text{O}$ )     | Roth                         |

|   |                             |
|---|-----------------------------|
| Magnesium sulfate heptahydrate (MgSO <sub>4</sub> ×7H <sub>2</sub> O)       | Roth                        |
| Manganese (II) chloride tetrahydrate (MnCl <sub>2</sub> ×4H <sub>2</sub> O) | Roth                        |
| MEK inhibitor U0126   | Promega                     |
| Milk powder (nonfat)  | AppliChem                   |
| Nitrocellulose membrane   | A. Hartenstein Laborbedarf  |
| Nonidet P40 (NP-40)   | AppliChem                   |
| Pepstatin   | Roth                        |
| PIPES   | Sigma                       |
| PMSF (Phenylmethylsulfonylfluorid)  | Roth                        |
| Potassium chloride (KCl)  | Roth                        |
| Prestained Protein Ladder   | PageRuler, Fermentas        |
| Protein G-Agarose   | Roche                       |
| CENTRI-SEP columns  | Princeton Separations, Inc. |
| Sucrose   | Roth                        |
| SDS (ultra pure)  | Roth                        |
| Sodium chloride (NaCl)  | Roth                        |
| Sodium fluoride (NaF)   | Roth                        |
| Sodium hydroxide (NaOH)   | Roth                        |
| Sodium orthovanadate (Na <sub>3</sub> VO <sub>4</sub> )                     | Sigma                       |
| Sodium pyrophosphate (Na <sub>4</sub> P <sub>2</sub> O <sub>7</sub> )       | Roth                        |
| TEMED (N,N,N',N'-Tetramethylethylenediamine)                                | Roth                        |
| Tris (Tris-(hydroxymethyl)-aminomethan)                                     | Roth                        |
| Tween 20  | Roth                        |
| Whatman 3MM Paper   | Schleicher & Schüll         |
| X-ray film  | Pierce                      |
| Xylene cyanol   | Roth                        |

### **5.1.3. Software**

**Software**

QUANTA2006

**Manufacturer**

Accelrys Inc, San Diego, USA

### **5.1.4. Cell culture materials**

**Reagent**

Dulbecco's Modified Eagle Medium (D-MEM)  
Epidermal growth factor (EGF)  
Fetal calf serum (FCS)  
jetPEI and 150 mM NaCl

**Source**

Invitrogen  
Invitrogen  
Invitrogen  
Biomol

|                                 |            |
|---------------------------------|------------|
| L-Glutamine                     | Invitrogen |
| Neutral Red                     | Invitrogen |
| Phosphate buffered saline (PBS) | Invitrogen |
| Penicillin/streptomycin         | Invitrogen |
| TC-100 medium                   | Invitrogen |
| Trypsin-EDTA                    | Invitrogen |
| Trypan Blue                     | Sigma      |

### 5.1.5. Antibodies used for Western blotting and immunoprecipitation

| <u>Antibody</u>   | <u>Source</u>             |
|---|---------------------------|
| <i>Anti-Rabbit IgG</i> , goat, peroxidase-conjugated  | Dianova                   |
| <i>Anti-Mouse IgG</i> , goat, peroxidase-conjugated   | Dianova                   |
| <i>Anti-Actin</i> , goat polyclonal, against the C-terminus of human actin  | Santa Cruz                |
| <i>Anti-c-Myc</i> , mouse monoclonal, against amino acids 408–439 within the C-terminal domain of human c-Myc   | Santa Cruz                |
| <i>Anti-ERK 2</i> , rabbit polyclonal, against peptide mapping at the C-terminus of rat ERK 2   | Santa Cruz                |
| <i>Anti-Histon 3</i> , rabbit polyclonal  | Upstate                   |
| <i>Anti-KDEL</i> , mouse monoclonal   | Stressgene                |
| <i>Anti-Lck</i> , mouse monoclonal, against a recombinant protein corresponding to amino acids 54–222 of human Lck p56                                      | Santa Cruz                |
| <i>Anti-PARP</i> , rabbit polyclonal  | Biomol                    |
| <i>Anti-M2PK</i> , mouse monoclonal   | ScheBo Biotech            |
| <i>Anti-p-C-RAF (Ser338)</i> , rabbit monoclonal, against phosphopeptide corresponding to residues surrounding serine 338                                   | Cell Signaling            |
| <i>Anti-p-ERK</i> , mouse monoclonal, against phosphorylated tyrosine 204 of human ERK  | Santa Cruz                |
| <i>Anti-p-RAF (Ser259)</i> , rabbit polyclonal, against synthetic phosphoserine 259 peptide corresponding to residues surrounding serine 259 of human C-RAF | Cell Signaling            |
| <i>Anti-p-RAF (Ser621)</i> , mouse monoclonal, against synthetic phosphoserine 621 peptide (KINRSApSEPSLHRA)  | MSZ                       |
| <i>Anti-p-Tyrosine</i> , mouse monoclonal   | MSZ                       |
| <i>Anti-Ras</i> , mouse monoclonal  | Transduction Laboratories |
| <i>Anti-Vimentin</i> , mouse monoclonal   | Dako                      |

### 5.1.6. Enzymes

#### Items

*Phusion* high fidelity DNA polymerase  
*Not I* restriction enzyme  
*Sac II* restriction enzyme  
 T4 DNA ligase  
*PfuTurbo* DNA polymerase  
*Dpn I* restriction enzyme

#### Source

Finnzymes  
 New England BioLabs  
 New England BioLabs  
 New England BioLabs  
 Stratagene  
 Stratagene

### 5.1.7. Kits

#### Items

*ProteoExtract* subcellular proteome extraction kit  
*QIAquick* gel extraction kit  
*QIAquick* PCR purification kit  
*QIAprep* spin miniprep kit  
*QIAGEN* plasmid midi kit

#### Source

Calbiochem  
 Qiagen  
 Qiagen  
 Qiagen  
 Qiagen

### 5.1.8. Plasmids

#### Plasmids

##### *Basic vectors*

pcDNA3.1/*myc*-His B (mammalian expression vector)  
 pGEX2T (*E. coli* expression vector)

Invitrogen  
 Pharmacia

##### *Source for human A-RAF cDNA*

pPC86-hA-RAF(WT)

MSZ

##### *Source for human C-RAF cDNA*

pcDNA3-His-hC-RAF(WT)

MSZ

##### *Expression plasmid for H-Ras12V cDNA*

pcDNA3-hH-Ras12V

MSZ

##### *Expression plasmid for Lck cDNA*

K-RSPA-hLck

MSZ

*Expression plasmids for human A-RAF cDNAs*

|  |                        |
|--|------------------------|
| pcDNA3.1/myc-His-hA-RAF(WT)                      | A. Baljuls             |
| pcDNA3.1/myc-His-hA-RAF(G300S)                   | A. Baljuls             |
| pcDNA3.1/myc-His-hA-RAF(Y296R)                   | A. Baljuls             |
| pcDNA3.1/myc-His-hA-RAF(Y296R/G300S)             | A. Baljuls             |
| pcDNA3.1/myc-His-hA-RAF(Y301D/Y301D)             | A. Baljuls             |
| pcDNA3.1/myc-His-hA-RAF(Y296R/G300S/Y301D/Y302D) | A. Baljuls             |
| pcDNA3.1/myc-His-hA-RAF(S214A)                   | A. Baljuls             |
| pcDNA3.1/myc-His-hA-RAF(S582A)                   | A. Baljuls             |
| pcDNA3.1/myc-His-hA-RAF(S250A)                   | A. Baljuls             |
| pcDNA3.1/myc-His-hA-RAF(T253A)                   | A. Baljuls             |
| pcDNA3.1/myc-His-hA-RAF(S257A)                   | A. Baljuls             |
| pcDNA3.1/myc-His-hA-RAF(S259A)                   | A. Baljuls             |
| pcDNA3.1/myc-His-hA-RAF(S262A)                   | A. Baljuls             |
| pcDNA3.1/myc-His-hA-RAF(S264A)                   | A. Baljuls             |
| pcDNA3.1/myc-His-hA-RAF(S265A)                   | A. Baljuls             |
| pcDNA3.1/myc-His-hA-RAF(S262A/Y301D/Y302D)       | A. Baljuls             |
| pcDNA3.1/myc-His-hA-RAF(T452A)                   | A. Baljuls             |
| pcDNA3.1/myc-His-hA-RAF(T455A)                   | A. Baljuls             |
| pcDNA3.1/myc-His-hA-RAF(S432A)                   | A. Baljuls             |
| pcDNA3.1/myc-His-hA-RAF(T442A)                   | A. Baljuls             |
| pcDNA3.1/myc-His-hA-RAF(R359A)                   | A. Baljuls             |
| pcDNA3.1/myc-His-hA-RAF(K360A)                   | A. Baljuls             |
| pERG- <i>Srf1</i> -GST-hA-RAF(WT)                | E. Nekhoroschkowa, MSZ |

*Expression plasmids for human C-RAF cDNAs*

|                                      |            |
|--------------------------------------|------------|
| pcDNA3.1/myc-His-hC-RAF(WT)          | A. Baljuls |
| pcDNA3.1/myc-His-hC-RAF(S339G)       | A. Baljuls |
| pcDNA3.1/myc-His-hC-RAF(Q335Y)       | A. Baljuls |
| pcDNA3.1/myc-His-hC-RAF(Q335Y/S339G) | A. Baljuls |
| pcDNA3.1/myc-His-hC-RAF(Q335R)       | A. Baljuls |
| pcDNA3.1/myc-His-hC-RAF(D337A)       | A. Baljuls |
| pcDNA3.1/myc-His-hC-RAF(S339A)       | A. Baljuls |
| pcDNA3.1/myc-His-hC-RAF(R398A)       | A. Baljuls |
| pcDNA3.1/myc-His-hC-RAF(K399A)       | A. Baljuls |

**5.1.9. Oligonucleotides****Primer name****Sequence***Cloning primers for constructs*

ARAFFWNotI

5'-aaggaaaaaagcggccgcatggagccaccacggggc-3'



|                                 |  |
|---------------------------------|--|
| ARAFREVSacII                    | 5'-tccccgcggaggcacaaggcgggctgc-3'                      |
| CRAFNotIFW                      | 5'-aaggaaaaaagcggccgcgccaccatggagcacatacaggggagc-3'    |
| CRAFSacII                       | 5'-ttccccgcgggaagacaggcagcctcgg-3'                     |
| <i>Mutagenesis primers</i>      |  |
| Mut-Koz-5_FW                    | 5'-cagcacagtggcggcaccatggagccaccacg-3'                 |
| Mut-Koz-3_RV                    | 5'-cgtggtggctccatggtgccgactgtgctg-3'                   |
| ARAF_G300S_FW                   | 5'-cctggggtaccgggactcaagctattactgg-3'                  |
| ARAF_G300S_RV                   | 5'-ccagtaatagcttgagtcccgggtacccagg-3'                  |
| ARAF_Y296R_FW                   | 5'-gtgaagaacctgggggagacgggactcaggctattactgg-3'         |
| ARAF_Y296R_RV                   | 5'-ccagtaatagcctgagtcccgtctcccagggttcttcac-3'          |
| ARAF_Y296R/G300S_FW             | 5'-gtgaagaacctgggggagacgggactcaagctattactgggagg-3'     |
| ARAF_Y296R/G300S_RV             | 5'-cctcccagtaatagcttgagtcccgtctcccagggttcttcac-3'      |
| ARAF_Y301D/Y302D_FW             | 5'-cgggactcaggcgatgactgggaggtacc-3'                    |
| ARAF_Y301D/Y302D_RV             | 5'-ggtacctcccagtcacgcctgagtcgg-3'                      |
| ARAF_Y296R/G300S/Y301D/Y302D_FW | 5'-gtgaagaacctgggggagacgggactcaagcgatgactgggaggtacc-3' |
| ARAF_Y296R/G300S/Y301D/Y302D_RV | 5'-ggtacctcccagtcacgcctgagtcgggtctcccagggttcttcac-3'   |
| A-RAF(S250A)_FW                 | 5'-ggtagtagaggaggtgctgatggaaccccc-3'                   |
| A-RAF(S250A)_RV                 | 5'-gggggggtccatcagcacctccttactacc-3'                   |
| A-RAF(T253A)_FW                 | 5'-gtagtatggagccccgggggag-3'                           |
| A-RAF(T253A)_RV                 | 5'-ctccccggggggctccatcactac-3'                         |
| A-RAF(S257A)_FW                 | 5'-cccccggggggccccagcccagc-3'                          |
| A-RAF(S257A)_RV                 | 5'-gctgggctgggggcccccgggggg-3'                         |
| A-RAF(S259A)_FW                 | 5'-ggggagccccgccccagccagcgtg-3'                        |
| A-RAF(S259A)_RV                 | 5'-cacgctggctggggcgggctcccc-3'                         |
| A-RAF(S262A)_FW                 | 5'-ccagcccagccgctgtcctcggg-3'                          |
| A-RAF(S262A)_RV                 | 5'-cccgaggacacggcggctgggctgg-3'                        |
| A-RAF(S264A)_FW                 | 5'-cagccagcgtggcctcggggaggaag-3'                       |
| A-RAF(S264A)_RV                 | 5'-cttctccccgagccacgctggctg-3'                         |
| A-RAF(S265A)_FW                 | 5'-ccagcgtgtccgcggggaggaagtc-3'                        |
| A-RAF(S265A)_RV                 | 5'-gacttctccccgcggacacgctgg-3'                         |
| A-RAF(S432A)_FW                 | 5'-ccaccgagatctcaaggctaacaacatcttctac-3'               |
| A-RAF(S432A)_RV                 | 5'-gtaggaagatggttagccttgagatctcggtgg-3'                |
| A-RAF(T442A)_FW                 | 5'-catgaggggctcgggtgaagatcgg-3'                        |
| A-RAF(T442A)_RV                 | 5'-ccgatctcaccgcgagcccctcatg-3'                        |
| A-RAF(T452A)_FW                 | 5'-ctttggcttgccgcagtgaagactcgtg-3'                     |
| A-RAF(T452A)_RV                 | 5'-catcgagtcttactcggccaagccaaag-3'                     |
| A-RAF(T455A)_FW                 | 5'-gccacagtgaaggctcgtgagcgg-3'                         |
| A-RAF(T455A)_RV                 | 5'-ccgctccatcagccttactgtggc-3'                         |
| A-RAF(R359A)_FW                 | 5'-gatgcaggtgctcgcgaagacgcgacatgc-3'                   |
| A-RAF(R359A)_RV                 | 5'-gacatgtcgcgtcttcgcgagcacctgcatc-3'                  |

|                 |  |
|-----------------|--|
| A-RAF(K360A)_FW | 5'-gatgcaggtgctcagggcgacgcgacatgtc-3'              |
| A-RAF(K360A)_RV | 5'-gacatgtcgcgtcgccctgagcacctgcatc-3'              |
| CRAFS339GFW     | 5'-cgtggacagagagattcaggctattattgggaaatag-3'        |
| CRAFS339GRV     | 5'-ctatttccaataatagcctgaatctctctgtccacg-3'         |
| CRAFQ335YFW     | 5'-caaaattaggcctcgtggatacagagattcaagctattattggg-3' |
| CRAFQ335YRV     | 5'-ccaataatagcctgaatctctgtatccacgaggcctaattttg-3'  |
| CRAFQ335RFW     | 5'-ggcctcgtggacggagagattcaagctattattggg-3'         |
| CRAFQ335RRV     | 5'-ccaataatagcctgaatctctcctccacgaggcc-3'           |
| CRAF339G335YFW  | 5'-caaaattaggcctcgtggatacagagattcaggctattattggg-3' |
| CRAF339G335YRV  | 5'-ccaataatagcctgaatctctgtatccacgaggcctaattttg-3'  |
| C-RAF(S339A)_FW | 5'-cctcgtggacagagagattcagcctattattgggaaatag-3'     |
| C-RAF(S339A)_RV | 5'-ctatttccaataataggctgaatctctctgtccacgagg-3'      |
| C-RAF(D337A)_FW | 5'-cgtggacagagagcttcaagctattattgggaaatag-3'        |
| C-RAF(D337A)_RV | 5'-ctatttccaataatagcctgaagctctctgtccacg-3'         |
| C-RAF(R398A)_FW | 5'-gaggtggctgttctggccaaaacacggcatgtg-3'            |
| C-RAF(R398A)_RV | 5'-cacatgccgtgtttggccagaacagccac-3'                |
| C-RAF(K399A)_FW | 5'-gtggctgttctgcgcgcaacacggcatgtg-3'               |
| C-RAF(K399A)_RV | 5'-cacatgccgtgttgcgcgcaacagccac-3'                 |

*Sequencing primers*

|                     |                                      |
|---------------------|--------------------------------------|
| A-RAF5, 5' human    | 5'-ccaggattgtccggaggctccagacagc-3'   |
| A-RAFSa11, 5' human | 5'-ctatctgtccccggacctcagcaaaatctc-3' |
| A-RAFA1a3, 3' human | 5'-gctcctcccgtggaacttgaggcagtcag-3'  |
| A-RAFSac5, 3' human | 5'-cacggcagccaatgtggctgtaag-3'       |
| C-RAF218for         | 5'-cgagagtctgtttccaggatgcctgtt-3'    |
| C-RAF298for         | 5'-aacaatctgagcccaacaggctgg-3'       |
| C-RAF397for         | 5'-cgcaaaacacggcatgtgaacatt-3'       |
| C-RAF 478 for       | 5'-gaaggcttaacagtgaaattggagat-3'     |
| C-RAF 612 for       | 5'-atcctgtcttcattgagctgctc-3'        |
| BGH pA 3'           | 5'-acctactctgacaatgcgatg-3'          |
| T7 5'               | 5'-taatacgaactcactatag-3'            |
| CMV 5'              | 5'-agagctctctggctaactag-3'           |

**5.1.10. Cell lines and bacterial strains**

| <u>Cell lines</u> | <u>Source</u> |
|-------------------|---------------|
| HEK293            | MSZ           |
| COS7              | MSZ           |
| Sf9               | MSZ           |

**Bacterial strains**

*Escherichia coli* (*E. coli*) DH5a

**Source**

Bethesda Research Laboratories. Optimized for DNA transformation and replication

## 5.2. Solutions and buffers

***LB-medium (Luria/Miller)***

The ready-to-use LB-medium powder was obtained from Roth.

10 g/l Bacto-tryptone

5 g/l Yeast extract

10 g/l NaCl

pH 7.0

Disperse 25 g of ready-to-use powder in 1 L of deionized water. Swirl to mix and sterilize by autoclaving at 121 °C for 15 min. Cool to ca. 47 °C and add filter sterilized antibiotic if required.

***LB-agar (Luria Bertani)***

The ready-to-use LB-agar powder was obtained from Roth.

10 g/l Bacto-tryptone

5 g/l Yeast extract

10 g/l NaCl

15 g/l Agar

pH 7.0

Disperse 40 g of ready-to-use powder in 1 L of deionized water. Swirl to mix and sterilize by autoclaving at 121 °C for 15 min. Cool to ca. 47 °C and add filter sterilized antibiotic if required. Pour into Petri dishes, allow to set and dry the surface prior to inoculation.

***SOB medium***

|                | <u>for 1 L solution</u> | <u>final concentration</u> |
|----------------|-------------------------|----------------------------|
| Bacto-tryptone | 20 g                    | 2%                         |
| Yeast extract  | 5 g                     | 0.5%                       |
| NaCl           | 0.6 g                   | 10 mM                      |
| KCl            | 0.2 g                   | 2.5 mM                     |

Adjust pH to 7.5 with NaOH and sterilize by autoclaving at 121 °C for 15 min. Before use, add 10 ml MgCl<sub>2</sub> (1 M stock solution; 10 mM, final concentration) and 10 ml MgSO<sub>4</sub> (1 M stock solution; 10 mM, final concentration). Sterilize the MgCl<sub>2</sub> and MgSO<sub>4</sub> stock solutions before use by filtering through 0.45 µm membrane filter.

***TB-buffer***

|                   | <u>for 250 ml solution</u> | <u>final concentration</u> |
|-------------------|----------------------------|----------------------------|
| PIPES             | 0.8 g                      | 10 mM                      |
| CaCl <sub>2</sub> | 0.6 g                      | 15 mM                      |
| KCl               | 4.7 g                      | 250 mM                     |

Adjust pH to 6.7 with KOH and add 2.7 g MnCl<sub>2</sub> (55 mM, final concentration). Sterilize the solution by filtering through 0.45 µm membrane filter and store at 4 °C.

***5 × HF-buffer***

The 5 × HF-buffer was obtained together with *Phusion* DNA polymerase from Finnzymes. It contains 7.5 mM MgCl<sub>2</sub>, which supplies 1.5 mM MgCl<sub>2</sub> in final reaction conditions.

***10 × TBE-buffer***

The *Rotiphorese* ready-to-use 10 × TBE-buffer was obtained from Roth. It contains 1 M Tris-Borat (pH 8.3) and 20 mM EDTA in deionized water.

***6 × DNA gel loading buffer***

|                 | <u>final concentration</u> |
|-----------------|----------------------------|
| Sucrose         | 40% (w/v)                  |
| Bromphenol Blue | 0.25% (w/v)                |
| Xylene cyanol   | 0.25% (w/v)                |

***10 × T4 DNA ligase buffer***

The buffer was obtained together with T4 DNA ligase enzyme from New England BioLabs.  
 500 mM Tris-HCl, pH 7.5  
 100 mM MgCl<sub>2</sub>  
 100 mM DTT  
 10 mM ATP  
 250 µg/ml BSA

***10 × PfuTurbo DNA polymerase reaction buffer***

The buffer was obtained together with *PfuTurbo* DNA polymerase from Stratagene.  
 200 mM Tris-HCl (pH 8.8)  
 20 mM MgSO<sub>4</sub>  
 100 mM KCl  
 100 mM (NH<sub>4</sub>)<sub>2</sub>SO<sub>4</sub>  
 1% Triton X-100  
 1 mg/ml nuclease-free BSA

***1 × AC lysis buffer***

|                      | <u>for 1 L</u> | <u>final concentration</u> |
|----------------------|----------------|----------------------------|
| Tris-HCl, pH 8.0     | 6.1 g          | 50 mM                      |
| NaCl                 | 8 g            | 137 mM                     |
| Sodium pyrophosphate | 4.5 g          | 10 mM                      |
| β-Glycerophosphate   | 5.4 g          | 25 mM                      |
| EDTA                 | 0.74 g         | 2 mM                       |
| EGTA (200 mM)        | 10 ml          | 2 mM                       |
| Glycerol             | 100 ml         | 10% (v/v)                  |
| β-Mercaptoethanol    | 1 ml           | 0.1% (v/v)                 |
| NaF                  | 1 g            | 25 mM                      |

The buffer was aliquoted in 50 ml samples and stored at –20 °C. Following reagents were added before use:

|                               | <u>final concentration</u> |
|-------------------------------|----------------------------|
| Sodium orthovanadate (100 mM) | 1 mM                       |
| Antipain (5 mg/ml)            | 10 µg/ml                   |
| Aprotinin (1 mg/ml)           | 10 µg/ml                   |
| Leupeptin (0.5 mg/ml)         | 1 µg/ml                    |
| Pepstatin (0.7 mg/ml)         | 1.4 µg/ml                  |
| PMSF (100 mg/ml)              | 200 µg/ml                  |
| NP-40                         | desired concentration      |

***1 × IC lysis buffer***

|                      | <u>final concentration</u> |
|----------------------|----------------------------|
| Tris-HCl, pH 7.6     | 25 mM                      |
| NaCl                 | 150 mM                     |
| Sodium pyrophosphate | 10 mM                      |
| β-Glycerophosphate   | 25 mM                      |
| NaF                  | 25 mM                      |
| Glycerol             | 10%                        |

Following reagents were added before use:

|                               | <u>final concentration</u> |
|-------------------------------|----------------------------|
| Sodium orthovanadate (100 mM) | 1 mM                       |
| Antipain (5 mg/ml)            | 10 µg/ml                   |
| Aprotinin (1 mg/ml)           | 10 µg/ml                   |
| Leupeptin (0.5 mg/ml)         | 1 µg/ml                    |
| Pepstatin (0.7 mg/ml)         | 1.4 µg/ml                  |
| PMSF (100 mg/ml)              | 200 µg/ml                  |
| NP-40                         | desired concentration      |

***1 × PBS buffer***

The 10 × PBS Ready-Mixed Powder was obtained from BioAtlas. Ready-mixed phosphate buffered saline powder should be dissolved in 1 L of distilled water. On dilution, the resultant 1 × PBS will have final concentration:

137 mM NaCl  
10 mM Phosphate, pH 7.4  
2.7 mM KCl

***5 × SDS-loading buffer***

|                        | <u>for 20 ml</u> | <u>final concentration</u> |
|------------------------|------------------|----------------------------|
| Tris-HCl, pH 6.8 (1 M) | 1.4 ml           | 70 mM                      |
| β-Mercaptoethanol      | 1 ml             | 5% (v/v)                   |
| Glycerol (87%)         | 9.2 ml           | 40% (v/v)                  |
| SDS (20%)              | 3 ml             | 3% (w/v)                   |
| Bromphenol Blue        | 0.01 g           | 0.05% (w/v)                |

***1 × SDS-PAGE buffer***

The ready-to-use *Rotiphorese* 10 × SDS-PAGE buffer was obtained from Roth. It contains 1.92 M glycine, 0.25 M Tris and 1% (w/v) SDS.

***Anode buffer I***

|               | <u>for 1 L</u> | <u>final concentration</u> |
|---------------|----------------|----------------------------|
| Tris, pH 10.4 | 36 g           | 300 mM                     |
| Methanol      | 100 ml         | 10% (v/v)                  |

***Anode buffer II***

|               | <u>for 1 L</u> | <u>final concentration</u> |
|---------------|----------------|----------------------------|
| Tris, pH 10.4 | 3 g            | 25 mM                      |
| Methanol      | 100 ml         | 10% (v/v)                  |

***Cathode buffer***

|              | <u>for 1 L</u> | <u>final concentration</u> |
|--------------|----------------|----------------------------|
| Tris, pH 9.4 | 3 g            | 25 mM                      |
| Glycine      | 3 g            | 40 mM                      |
| Methanol     | 100 ml         | 10% (v/v)                  |

***10 × TBS buffer***

|                  | <u>for 1 L</u> | <u>final concentration</u> |
|------------------|----------------|----------------------------|
| Tris-HCl, pH 7.6 | 48.5 g         | 400 mM                     |
| NaCl             | 160.7 g        | 2.75 M                     |

***ECL solution I***

|                               | <u><i>for 100 ml</i></u> |
|-------------------------------|--------------------------|
| Tris-HCl (1 M), pH 8.5        | 10 ml                    |
| Luminol (250 mM in DMSO)      | 1 ml                     |
| Coumaric acid (90 mM in DMSO) | 440 µl                   |
| ddH <sub>2</sub> O            | 90 ml                    |

***ECL solution II***

|                         | <u><i>for 100 ml</i></u> |
|-------------------------|--------------------------|
| Tris-HCl (1 M), pH 8.5  | 10 ml                    |
| Hydrogen peroxide (35%) | 55 µl                    |
| ddH <sub>2</sub> O      | 90 ml                    |

***Stripping buffer***

|                  | <u><i>for 1 L</i></u> | <u><i>final concentration</i></u> |
|------------------|-----------------------|-----------------------------------|
| Tris-HCl, pH 6.7 | 7.6 g                 | 62.5 mM                           |
| SDS (20%)        | 100 ml                | 2%                                |

Before use, add 345 µl β-mercaptoethanol per 50 ml buffer.

***10 × Kinase buffer***

|                    | <u><i>for 100 ml</i></u> | <u><i>final concentration</i></u> |
|--------------------|--------------------------|-----------------------------------|
| HEPES, pH 7.4      | 6 g                      | 250 mM                            |
| NaCl               | 8.8 g                    | 1.5 M                             |
| β-Glycerophosphate | 5.4 g                    | 250 mM                            |

***GST elution buffer***

25 mM Tris-HCl, pH 7.6  
 10% Glycerol  
 20 mM Glutathione

***IC transfection buffer***

25 mM HEPES, pH 7.1  
 140 mM NaCl  
 125 mM CaCl<sub>2</sub>  
 (filter sterilized)

***Biosensor buffer***

10 mM HEPES, pH 7.4  
 150 mM NaCl  
 0.01% NP-40

## 5.3. Methods

### 5.3.1. Bacterial manipulation

Plasmid transformed bacteria were selected on LB-agar plates with the appropriate antibiotic for 24 h. For overnight mini-cultures, single colonies were picked and inoculated in LB-medium (ca. 3–5 ml) with antibiotic and shaken overnight at 37 °C (180 rpm). This pre-culture could be used for preparing frozen glycerol stock cultures or plasmid DNA. For storage of bacteria, a glycerol stock culture was prepared by growing bacteria to an OD of 0.8 at a wavelength of 600 nm in culture medium. 500 µl bacterial culture was taken and added to 500 µl 80%-glycerol and then mixed thoroughly in a 1.5 ml microfuge tube. This stock solution was subsequently frozen at –80 °C. To inoculate an overnight culture again, bacteria were taken out and held at RT until surface was thawed. A small amount of cells was picked and mixed into 3–5 ml culture medium and left to grow for several hours at 37 °C in a bacterial culture shaker. The frozen stock should be immediately returned to the –80 °C.

#### 5.3.1.1. Preparation of chemocompetent cells (CaCl<sub>2</sub> method)

On the first day, 10–12 colonies were picked from a prestreaked plate (from glycerol stock), inoculated in 250 ml SOB-medium (2 L Erlmeyer flask), and left to grow at 18 °C and shaking to aerate (180 rpm) until OD of 0.6 at wavelength of 600 nm was reached. Then the culture was cooled down on ice for at least 10 min. (The following procedures were carried out at 4 °C in pre-cooled sterile tubes). The cells were transferred into 50 ml tubes and harvested in a centrifuge (*Megafuge 1.0R*) at 3000 rpm for 10 min. The supernatant was discarded. The bacterial pellets were resuspended thoroughly in 80 ml ice cold TB-buffer and incubated on ice for 10 min. Then the cells were harvested as before and the bacterial pellets were resuspended carefully in 20 ml ice cold TB-buffer. The bacteria suspension was supplemented with 1.4 ml DMSO (7%, finale concentration) and left on ice for 10 min. The suspension was aliquoted in 100 to 200 µl samples, shock-frozen, and stored at –80 °C.

#### 5.3.1.2. Transformation of chemocompetent bacteria

The competent bacteria from a desired origin were thawed on ice for ca. 10 min. A maximum of 20 ng ligated DNA or purified plasmid DNA were added to 100 µl chemocompetent cells in a cold 1.5 ml microfuge tube. The bacteria were mixed carefully and kept on ice for 30 min. Then the bacteria were heat-shocked at 42 °C for 90 sec and 1 ml antibiotic-free LB-medium was added. The cells were aerate at 37 °C for 45 min. Selection of transformed bacteria was done by plating 100 µl of the bacterial suspension on antibiotic containing LB-agar plates. Only bacteria that have taken up the desired plasmids, which



contain antibiotic resistance cassette, can grow on the LB-agar plates. Single colonies were then expanded in LB- medium and used for DNA preparation.

### **5.3.2. Methods of molecular biology**

#### **5.3.2.1. Amplification of DNA fragments by PCR**

The polymerase chain reaction (PCR) is a method for oligonucleotide primer directed enzymatic amplification of a specific DNA sequence of interest. This technique is capable of amplifying a sequence up to 10<sup>6</sup>-fold from ng amounts of template DNA within a large background of irrelevant sequences (e.g. from total genomic DNA). A prerequisite for amplifying a sequence using PCR is to have known unique sequences flanking the segment of DNA to be amplified, so that specific oligonucleotides can be obtained. It is not necessary to know anything about the intervening sequence between the primers. The PCR product is amplified from the DNA template using a heat-stable DNA polymerase and using an automated thermal cycler to put the reaction through 30 or more cycles of denaturation, annealing of primers and polymerization.

#### *Recommendations for choosing oligonucleotide primers*

The aim is to choose oligonucleotide primers complementary to relatively unique sequences flanking the segment to be amplified. Primers for PCR are generally 20–30 bp long and are chosen to be complementary to one strand (5' to 3') upstream and complementary to the opposite strand (5' to 3') downstream from the sequence to be amplified. The 5'-ends of the primers define the ends of the amplified PCR product. Primers should ideally contain relatively balanced GC vs. AT content (e.g. 45–55% GC) and no long stretches of any one base. Caution should also be taken that the two primers of the primer pair do not contain complementary structures >2 bp to avoid “primer dimer” formation resulting from annealing of the two primers (especially at their 3'-ends). The melting temperature (T<sub>m</sub>) of flanking primers should not differ by more than 5 °C, so the GC content and length must be chosen accordingly. It can be calculated using the following formula:

$$T_m = 69.3 + 41 \times (n_C + n_G) / S - 650 / S$$

n<sub>C</sub>, number of cytosine nucleotides in the primer

n<sub>G</sub>, number of guanine nucleotides in the primer

S, number of all nucleotides in the primer

#### *Procedure for polymerase chain reaction*

The PCR reaction was performed in volume of 50 µl. The following components were mixed on ice:

|  | <u>for 50 <math>\mu</math>l reaction volume</u> | <u>finale concentrations</u> |
|--|---|------------------------------|
| Sterile ddH <sub>2</sub> O                                   | 29 $\mu$ l                                      |                              |
| Reaction buffer of the DNA polymerase (5 $\times$ HF-buffer) | 10 $\mu$ l                                      | 1 $\times$                   |
| dNTPs (2 mM)   | 5 $\mu$ l                                       | 200 $\mu$ M                  |
| Primer 1 (10 pmol/ $\mu$ l)                                  | 2.5 $\mu$ l                                     | 0.5 $\mu$ M                  |
| Primer 2 (10 pmol/ $\mu$ l)                                  | 2.5 $\mu$ l                                     | 0.5 $\mu$ M                  |
| Plasmid DNA (10 ng/ $\mu$ l)                                 | 0.5 $\mu$ l                                     | 0.1 ng/ $\mu$ l              |
| <i>Phusion</i> DNA polymerase (2 U/ $\mu$ l)                 | 0.5 $\mu$ l                                     | 0.02 U/ $\mu$ l              |

### *Cycling conditions*

The PCR machine must be programmed for the specific reaction conditions desired. Each cycle in the polymerase chain reaction involves three steps (denaturation, primer annealing, polymerization), and the products are amplified by performing many cycles one after the other with the help of the automated thermal cycler.

*Initial denaturation step:* the initial denaturation was performed over an interval of 30 sec at 98 °C.

*Denaturation step:* denaturation was done at 98 °C for 10 sec.

*Primer annealing step:* primers longer than 20 nucleotides were annealed for 30 sec at a  $T_m + 3$  °C. For primers shorter than 20 nucleotides an annealing temperature equal to the  $T_m$  was used. If nonspecific PCR products were obtained, the first 5 cycles were performed at the annealing temperature equal to the  $T_m$  or  $T_m + 3$  °C, whereas the remaining cycles were done at the temperature of 68 °C.

*Extending step:* the extending step was performed at 72 °C. The extension time of 15 sec per 1 kb was used.

*Number of cycles:* the number of PCR cycles depends on the amount of template DNA in the reaction mix and on the expected yield of the PCR product. As the initial quantity of template DNA used in this work was high, 30 cycles were sufficient.

*Final extending step:* after the last cycle, the samples were incubated at 72 °C for 7 min to fill-in the protruding ends of newly synthesized PCR products.

After amplification, the products were separated accordingly to size by agarose gel electrophoresis and were directly visualized after staining with ethidium bromide.

### **5.3.2.2. Agarose gel electrophoresis of DNA**

Agarose gel electrophoresis is a method for separating and visualizing DNA fragments. The fragments are separated by charge and size by forcing them to move through an agarose gel matrix, which is subjected to an electric field. The electric field is generated by applying potential (voltage) across an electrolytic solution (buffer). Agarose is a marine

colloid purified from algae. When boiled in an aqueous buffer it dissolves and then upon cooling solidifies to a gel.

To pour a gel, 1 g agarose powder was mixed with 100 ml electrophoresis buffer (1 × TBE-buffer) to obtain a final concentration of 1% and heated in a microwave oven until completely melted. After cooling the solution to about 60 °C, ethidium bromide was added (0.5 µg/ml, final concentration) to facilitate visualization of DNA after electrophoresis. Then the solution was poured into a casting tray containing a sample comb and allowed to solidify at room temperature. After the gel has solidified, the comb was removed. The gel, still in its plastic tray, was inserted horizontally into the electrophoresis chamber and covered with 1 × TBE-buffer. Samples, containing DNA mixed with 6 × DNA gel loading buffer, were then filled into the sample wells. DNA electrophoresis was performed at 120 V until adequate separation of DNA fragments has occurred. The DNA fragments were visualized under UV-light.

#### **5.3.2.3. Isolation of DNA fragments from agarose gel**

DNA fragments were isolated from agarose gel using the *QIAquick* gel extraction kit according to the manufacturer's protocol.

#### **5.3.2.4. Purification of DNA fragments**

DNA fragments were purified using *QIAquick* PCR purification kit according to the manufacturer's protocol.

#### **5.3.2.5. Digestion of DNA with restriction endonucleases**

Restriction endonucleases recognize specific palindromic sequences and cleave a phosphodiester bond on each strand at that sequence. Each restriction enzyme requires specific reaction conditions for optimum activity. One of the most important reaction conditions, which vary between different restriction enzymes, is the salt (usually NaCl) concentration. Enzyme buffers are specifically formulated to provide the salt concentration for optimal enzyme activity. It is important, therefore, that the correct buffer solution is used for a particular restriction enzyme. After digestion with a restriction endonuclease, the resulting DNA fragments can be separated by agarose gel electrophoresis.

The preparative and analytical digestion reactions were performed in a total volume of 20 µl. If concentration of DNA in the stock solution was too low, the total volume of digestion reaction was increased to 50 µl. The following components were mixed in a 1.5 ml microfuge tube on ice:

|   | <i>for 20 <math>\mu</math>l</i> |
|---|---------------------------------|
| Nuclease-free ddH <sub>2</sub> O                      | 16 $\mu$ l                      |
| 10 $\times$ Recommended buffer for restriction enzyme | 2 $\mu$ l                       |
| Substrate DNA (in ddH <sub>2</sub> O)                 | 1 $\mu$ l (~ 1 $\mu$ g)         |
| Restriction enzyme                                    | 0.2–0.5 $\mu$ l (2–5 U)         |

The restriction reaction was incubated at the optimum temperature for 1–16 h. After digestion, the products were separated accordingly to size by agarose gel electrophoresis and were directly visualized after staining with ethidium bromide. In the case of preparative digestion, DNA fragments were isolated from the agarose gel, purified and used for ligation reaction.

### 5.3.2.6. DNA ligation

DNA ligation is the process of joining two ends of DNA molecule (either from the same or different molecules). Specifically, it involves creating a phosphodiester bond between the 3'-hydroxyl of one nucleotide and the 5'-phosphate of another. This reaction is usually catalyzed by a DNA ligase enzyme. The enzyme ligates DNA fragments having blunt or overhanging, complementary, “sticky” ends. Typically, it is easier to ligate molecules with complementary “sticky” ends than blunt ends. T4 DNA ligase is the most commonly used DNA ligase for molecular biology techniques and can ligate “sticky” or blunt ends. The two components of the DNA in the ligation reaction should be equimolar and around 100  $\mu$ g/ml. Most commonly, one wants to ligate an insert DNA molecule into a plasmid ready for bacterial transformation. Typically, DNA and plasmid vector are individually cut to yield complementary ends, then both are added to a ligation reaction to be circularized by DNA ligase. If the ratio of the plasmid backbone to the insert DNA is too high, then excess of “empty” mono- and polymeric plasmids will be generated. If the ratio is too low, then the result may be an excess of linear and circular homo- and heteropolymers.

#### *Cohesive end ligation*

The ligation reaction was performed in a total volume of 20  $\mu$ l. The plasmid DNA and/or DNA fragment were prepared by cutting it with suitable restriction enzymes, which was followed by purification. To ligate an insert DNA molecule into a plasmid a 3:1 molar ratio of insert to vector was used. Following components were mixed in a 1.5 ml microfuge tube on ice:

|  | <i>for 20 <math>\mu</math>l</i>            |
|--|--|
| Nuclease-free ddH <sub>2</sub> O                   | (16 – Volume of vector and insert) $\mu$ l |
| 10 $\times$ T4 DNA ligase buffer                   | 2 $\mu$ l                                  |
| Purified linearized vector (in ddH <sub>2</sub> O) | 25 ng                                      |
| Purified linearized insert (in ddH <sub>2</sub> O) | 75 ng                                      |
| T4 DNA ligase (400 U/ $\mu$ l)                     | 2 $\mu$ l (800 U)                          |

The reaction was incubated at RT for 2 h or at 16 °C overnight. To inactivate the enzyme the mixture was heated at 65 °C for 10 min.

#### **5.3.2.7. Mini-preparation of plasmid DNA**

Mini-preparation of plasmid DNA was performed by use of the *QIAprep* spin miniprep kit according to the manufacturer's protocol.

#### **5.3.2.8. Midi-preparation of plasmid DNA**

Midi-preparation of plasmid DNA was performed by use of the *QIAGEN* plasmid midi kit according to the manufacturer's protocol.

#### **5.3.2.9. Determination of DNA concentration and quality**

DNA can be quantified in an agarose gel by comparing the intensity of the fluorescence emitted by an ethidium bromide-stained DNA sample relative to a dilution series of a DNA standard of known concentration. If the sample is pure, which means it is essentially free of contaminations, such as RNA, proteins, phenol and agarose, a spectrophotometric method based on measuring the amount of UV irradiation, which is absorbed by the bases, is accurate and straightforward. The ratio  $OD_{260}/OD_{280}$  can be determined in order to assess the purity of the sample. If this ratio is 1.8–2.0, the absorption is probably due to nucleic acids. A ratio less than 1.8 indicates that there may be proteins and/or other UV absorbers in the sample. In these cases, it is advisable to reprecipitate the DNA. A ratio higher than 2.0 indicates that the sample may be contaminated with chloroform or phenol and should be reprecipitated with ethanol. DNA concentration is estimated from the 260 nm readings. The values are in OD (optical density units) where 1 OD = 50 µg/ml. Final concentration of DNA can be calculated by use of the formula:

$$c (\mu\text{g/ml}) = OD_{260} \times 50 \mu\text{g/ml} \times \text{dilution factor}$$

For spectrometric measurement of DNA concentration, 96 µl deionized water was mixed with 4 µl stock solution of purified DNA giving a dilution factor of 25.

### 5.3.2.10. DNA sequencing (Sanger's Dideoxynucleotide Synthetic Method)

DNA can be sequenced by generating fragments through the controlled interruption of enzymatic replication. DNA polymerase I is used to copy a particular sequence of a single-stranded DNA. The synthesis is primed by complementary fragment, which may be obtained from a restriction enzyme digestion or synthesized chemically. In addition to the four deoxyribonucleoside triphosphates (dNTP), the incubation mixture contains a 2',3'-dideoxy analogue of one of them. The incorporation of this analogue blocks further growth of the new chain, because it lacks the 3'-hydroxyl terminus needed to form the next phosphodiester bond. A fluorescent tag is attached to the oligonucleotide primer, a differently colored one in each of the four chain-terminating reaction mixtures. The reaction mixtures are combined and separated by electrophoresis together. The separated bands of DNA are then detected by their fluorescence as they pass out the bottom of the tube, and the sequence of their colors directly yields the base sequence.

#### *Sequencing reaction*

The "Taq cycle sequencing" was performed using *PRISM Ready Reaction DyeDeoxy Terminator Cycle Sequencing Kit*. The following reagents were mixed in a 0.6 ml double-snap-cap microfuge tube:

|                     |                    |
|---------------------|--------------------|
| Terminator premix * | 9.5 $\mu$ l        |
| DNA template        | 100 ng–1.0 $\mu$ g |
| Primer              | 10 pmol            |

The final reaction volume was adjusted to 20  $\mu$ l with ddH<sub>2</sub>O.

- \* A-Dye Terminator labeled with dichloro[R6G]
- C-Dye Terminator labeled with dichloro[TAMRA]
- G-Dye Terminator labeled with dichloro[R110]
- T-Dye Terminator labeled with dichloro[ROX]

The tubes were placed in a thermal cycler preheated to 96 °C, which was followed by 25 cycles of thermal cycling steps: 96 °C for 15 sec; 48 °C for 15 sec; 60 °C for 4 min; and keep at 4 °C after the reaction.

#### *Removal of the excess dye terminators by using CENTRI-SEP columns*

*CENTRI-SEP* columns are designed for the fast and efficient purification of large molecules from small molecules. The *CENTRI-SEP* columns were prepared according to the standard procedures. The *DyeDeoxy* terminator reaction mixture was transferred to the top of the gel. The sample was carefully dispensed onto the centre of the gel bed at the top of the column without disturbing the gel surface. The column was placed into the sample collection tube and both were placed into the rotor. Proper column orientation was maintained. The column and collection tube were spun at 750 g for 2 min. The purified sample was collected

in the bottom of the sample collection tube. Finally, the sample was dried in a vacuum centrifuge.

*Preparation and loading of the samples*

The pellet was resuspended in 4  $\mu$ l of the following reagent mixture containing 5  $\mu$ l deionized formamide and 1  $\mu$ l 25 mM EDTA with blue dextran (50 mg/ml). The solution was centrifuged to collect all the liquid at the bottom of the tube. The samples were denatured at 95 °C for 2 min and transferred immediately on ice. The samples were then separated on polyacrylamide gel on the *ABI PRISM 373 DNA Sequencer* with the appropriate run module, DT [dR Set Any-Primer] mobility file and matrix file.

### **5.3.2.11. Site-directed mutagenesis**

The site-directed mutagenesis protocol is used to make point mutations, switch amino acids and delete or insert single or multiple amino acids. This method is performed using *PfuTurbo* DNA polymerase and a thermal temperature cycler. *PfuTurbo* DNA polymerase replicates both plasmid strands with high fidelity and without displacing the mutant oligonucleotide primers. The basic procedure utilizes a supercoiled double-stranded DNA (dsDNA) vector with an insert of interest and two synthetic oligonucleotide primers containing the desired mutation. The oligonucleotide primers, each complementary to opposite strands of the vector, are extended during temperature cycling by use of *PfuTurbo* DNA polymerase. Incorporation of the oligonucleotide primers generates a mutated plasmid containing staggered nicks. Following temperature cycling, the product is treated with *Dpn* I. The *Dpn* I endonuclease (target sequence: 5'-Gm6ATC-3') is specific for methylated and hemimethylated DNA and is used to digest the parental DNA template and to select for mutation-containing synthesized DNA. DNA isolated from almost all *E. coli* strains is methylated and therefore susceptible to *Dpn* I digestion. The nicked vector DNA incorporating the desired mutations is then transformed into competent bacterial cells. The small amount of starting DNA template is required to perform this method. The high fidelity of the *PfuTurbo* DNA polymerase and the low number of thermal cycles all contribute to the high mutation efficiency and decreased potential for random mutations.

*Primer design guidelines*

The mutagenic oligonucleotide primers for use with this protocol must be designed individually according to the desired mutation. The following considerations should be made for designing mutagenic primers:

- 1) Both mutagenic primers must contain the desired mutation and anneal to the same sequence on opposite strands of the plasmid.

- 2) Primers should be between 25 and 45 bases in length, with a melting temperature (T<sub>m</sub>) of ≥78 °C. Primers longer than 45 bases may be used, but using longer primers increases the likelihood of secondary structure formation, which may affect the efficiency of the mutagenesis reaction.
- 3) The following formula is commonly used for estimating the T<sub>m</sub> of primers:

$$T_m = 81.5 + 0.41 \times (\%GC) - 675/N - \% \text{ mismatch},$$

where N is the primer length in bases, %GC percentage of guanine and cytosine nucleotides in the primer, and values for %GC and % mismatch are whole numbers.

- 4) For calculating T<sub>m</sub> for primers intended to introduce insertions or deletions, use this modified version of the above formula:

$$T_m = 81.5 + 0.41 \times (\%GC) - 675/N,$$

where N does not include the bases, which are being inserted or deleted.

- 5) The desired mutation (deletion or insertion) should be in the middle of the primer with ~10–15 bases of correct sequence on both sides.
- 6) The primers optimally should have a minimum GC content of 40% and should terminate in one or more C or G bases.

*Procedure for site directed mutagenesis*

The mutagenesis PCR reaction was performed in a total volume of 50 µl. The sample was prepared on ice as indicated below:

|   | <u>for 50 µl</u> |
|---|------------------|
| ddH <sub>2</sub> O                                  | 35 µl            |
| 10 × <i>PfuTurbo</i> DNA polymerase reaction buffer | 5 µl             |
| dsDNA template (25 ng/ml)                           | 1 µl             |
| Oligonucleotide primer 1 (10 pmol/µl)               | 1.5 µl           |
| Oligonucleotide primer 2 (10 pmol/µl)               | 1.5 µl           |
| dNTP mix (2 mM)                                     | 5 µl             |
| <i>PfuTurbo</i> DNA polymerase (2.5 U/µl)           | 1 µl             |

The mutagenesis sample was cycled using the cycling parameters outlined below:

| <u>Step</u>          | <u>Temperature</u> | <u>Time</u>                |
|----------------------|--------------------|----------------------------|
| Initial denaturation | 95 °C              | 3 min                      |
| Denaturation         | 95 °C              | 30 sec                     |
| Primer annealing     | 55 °C              | 1 min                      |
| Extension            | 68 °C              | 1 min/kb of plasmid length |

18 PCR cycles were used for site-directed mutagenesis.



Following temperature cycling, the reaction tube was placed on ice for 2 min to cool the reactions to  $\leq 37$  °C. 1  $\mu$ l of the *Dpn* I restriction enzyme (10 U/ $\mu$ l) was added directly to the amplification reaction. The reaction mixture was gently and thoroughly mixed by pipetting the solution up and down several times. The reaction mixture was spun down in a microcentrifuge for 1 min, then the reaction was immediately incubated at 37 °C for 1 h to digest the parental (non-mutated) supercoiled dsDNA. 100  $\mu$ l chemocompetent *E. coli* bacterial cells were transformed with 10  $\mu$ l *Dpn* I treated DNA as described in section 5.3.1.2. The whole transformation reaction was plated on LB-agar plates containing appropriate antibiotic for the plasmid vector and incubated at 37 °C for >16 h. Following mini-preparation of the mutated plasmid DNA, the fidelity of mutagenesis was confirmed by DNA sequencing.

### **5.3.3. Biochemical methods**

#### **5.3.3.1. Preparation of cell lysates**

Preparation of cell lysates was performed on ice.

##### *Lysis of adherent mammalian cells (HEK293 and COS7)*

For the experiments requiring lysis of adherent cells, mammalian cells were first washed twice with 1  $\times$  PBS buffer (5 ml for 10 cm diameter Petri dish), scraped off in ice cold AC lysis buffer (1 ml for 10 cm diameter Petri dish) containing 1% NP-40, transferred into a microtube and lysed by rotating at 4 °C for 45 min. The cell lysate was then clarified by centrifugation at 10,000 rpm (*Biofuge Fresco*) for 15 min at 4 °C. The supernatant was transferred into a clean microtube and the pellet containing cell nuclei and membranes was discarded. The lysate was used for Western blotting and immunoprecipitation.

##### *Lysis of suspension insect cells (Sf9)*

Baculovirus-infected Sf9 cells were transferred into 15 ml tubes, pelleted at 1100 rpm (*Megafuge 1.0R*) for 2 min and washed with 3 ml 1  $\times$  PBS buffer. The pelleted cells were resuspended in 1 ml 1  $\times$  PBS and transferred into 1.5 ml microfuge tube. The cell suspension was centrifuged at 1100 rpm (*Biofuge Fresco*) for 3 min and the supernatant was discarded. The cell pellet was resuspended in 1 ml IC lysis buffer containing 0.75% NP-40 and incubated at 4 °C for 45 min with gentle rotation. Every 5 min, the cell suspension was mixed by vortexing for few seconds. The cell lysate was then clarified by centrifuging at 14,000 rpm (*Biofuge Fresco*) for 10 min at 4 °C. The supernatant was transferred into a clean microfuge tube, and the pellet containing cell nuclei and membranes was discarded. The lysate was used for Western blotting, protein purification, immunoprecipitation and RAF kinase assay.

### 5.3.3.2. Determination of protein concentration (Bradford Assay)

Use of Coomassie G-250 dye in a colorimetric reagent for the detection and quantitation of total protein was first described by M. Bradford in 1976 [273]. In the acidic environment of the reagent, protein binds to the Coomassie dye. This results in a spectral shift from the reddish/brown form of the dye (absorbance maximum at 465 nm) to the blue form of the dye (absorbance maximum at 610 nm). The difference between the two forms of the dye is greatest at 595 nm, which, therefore, is the optimal wavelength to measure the blue color from the Coomassie dye/protein complex.

1 ml of the Bradford reagent (ready-to-use Coomassie Blue G-250 based reagent, Pierce) was mixed with 10  $\mu$ l of the protein solution (cell lysate). After 5 min of incubation, the extinction was measured at 595 nm versus respective controls in a photometer. Absolute values were determined by correlation to known amounts of BSA.

### 5.3.3.3. Sodium dodecyl sulfate polyacrylamide gel electrophoresis (SDS-PAGE)

Proteins can be easily separated on the basis of mass by electrophoresis in a polyacrylamide gel under denaturing conditions. 5  $\times$  SDS-loading buffer is used to denature proteins in lysate, eluate or immunoprecipitate samples, and then heated at 95  $^{\circ}$ C for 5 min. SDS is an anionic detergent that disrupts nearly all non-covalent interactions in native proteins.  $\beta$ -Mercaptoethanol is also included in the sample buffer to reduce disulfide bonds. The SDS complexes with the denatured proteins are then electrophoresed on a polyacrylamide gel in the form of a thin vertical slab. Vertical gels are set in between two glass plates with an internal thickness of 1.5 mm between the two plates. In this chamber, the acrylamide mix is poured and left to polymerize for at least 30 min at RT. The gels are composed of two layers: a 6–15% separating gel (pH 8.8) that separates the proteins according to size and a lower percentage (5%) stacking gel (pH 6.8) that insures the proteins simultaneous entry into the separating gel at the same height.

|                        | <i>for 50 ml separating gel</i> | <i>for 10 ml stacking gel</i> |
|------------------------|---------------------------------|-------------------------------|
| ddH <sub>2</sub> O     | 26.5–11.4 ml                    | 6.8 ml                        |
| 30% Acrylamide mix     | 10–25 ml                        | 1.7 ml                        |
| 1.5 M Tris-HCl, pH 8.8 | 12.5 ml                         | 1.25 ml                       |
| 10% SDS                | 0.5 ml                          | 0.1 ml                        |
| 10% APS                | 0.5 ml                          | 0.1 ml                        |
| TEMED                  | 0.04–0.02 ml                    | 0.01 ml                       |

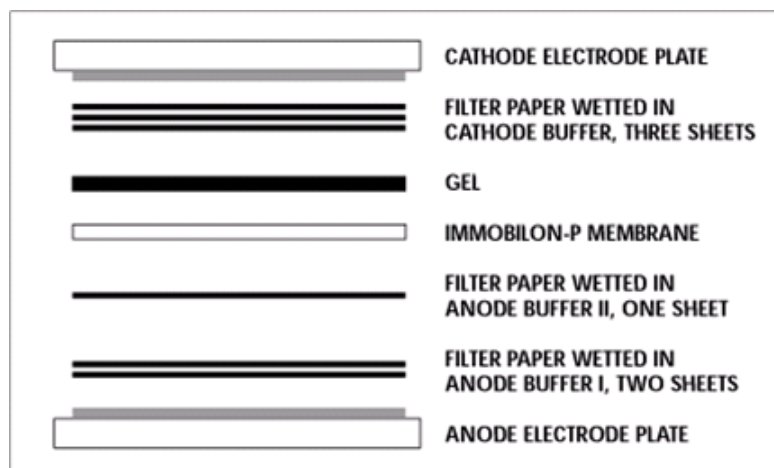
The separating gel was poured in between two glass plates, leaving a space of about 1cm plus the length of the teeth of the comb. 1-Butanol was added to the surface of the gel to exclude air. After the separating gel was polymerized, the 1-butanol was removed. The stacking gel was poured on top of the separating gel, the comb inserted and allowed to polymerize. The samples were loaded into the wells of the gel and electrophoresis buffer

(1 × SDS-PAGE buffer) was added to the chamber. A cover was then placed over the gel chamber and 160 V were applied. The negatively charged SDS-protein complexes migrate in the direction of the anode at the bottom of the gel. Small proteins move rapidly through the gel, whereas large ones migrate slower. Proteins that differ in mass by about 2% can be separated with this method. The electrophoretic mobility of many proteins in SDS-polyacrylamide gels is proportional to the logarithm of their mass.

#### **5.3.3.4. Immunoblotting**

The immunoblotting (alternately, Western blotting) is a method to detect a specific protein in a given sample of tissue homogenate or extract. It uses gel electrophoresis to separate native or denatured proteins by the length of the polypeptide (denaturing conditions) or by the 3-D structure of the protein (native/non-denaturing conditions). The proteins are then transferred to a membrane (typically nitrocellulose or PVDF), where they are probed (detected) using antibodies specific to the target protein.

The proteins of the sample were separated using gel electrophoresis under denaturing conditions. In order to make the proteins accessible to antibody detection, they were moved from within the gel onto a membrane made of nitrocellulose using semidry electroblotter. The gel was removed from its glass cassette and any stacking gel was trimmed away. The gel was immersed in cathode buffer for 15 min. Six pieces of filter paper were soaked in anode buffer I for at least 30 sec. Three pieces of filter paper were soaked in anode buffer II for at least 30 sec. Six pieces of filter paper were soaked in cathode buffer for at least 30 sec. The nitrocellulose membrane was equilibrated in anode buffer II for at least 5 min. The six pieces of filter paper soaked in anode buffer I were placed in the center of the anode electrode plate. The three pieces of filter paper soaked in anode buffer II were placed on top of the first six sheets. Nitrocellulose membrane was placed on top of the filter papers. The gel was placed on top of the membrane. The six pieces of filter paper soaked in cathode buffer were placed on top of the membrane. To ensure an even transfer, air bubbles between layers were removed by carefully rolling a pipette or stirring rod over the surface of each layer in the stack. The complete transfer stack looked like this:



The protein transfer was performed at 2.5 mA/cm<sup>2</sup> for 2 h. For immunodetection, the membrane was incubated in 1 × TBS buffer containing 0.1% Tween 20 and 5% milk or BSA for 1 h at RT or overnight at 4 °C on a shaker (*Mini Rocker MRI*). Then the membrane was washed three times with 1 × TBS buffer containing 0.1% Tween 20 by vigorous shaking (*Tetramax 101*), each time for 10 min. The first antibody was diluted in 1 × TBS buffer containing 0.02% Tween 20 (unless otherwise indicated) and added to the membrane. The membrane was incubated with the first antibody overnight at RT on a shaker (*Mini Rocker MRI*). After incubation the membrane was washed again three times with the 1 × TBS buffer containing 0.1% Tween 20 by vigorous shaking, each time for 10 min. The appropriate peroxidase-conjugated secondary antibody was dilute in 1 × TBS buffer containing 0.02% Tween 20 and 3% milk (or according to manufacturers' instructions) and added to the membrane. The membrane was incubated with the secondary antibody at RT for 1 h and washed three times with the 1 × TBS buffer containing 0.1% Tween 20 by vigorous shaking, each time for 10 min. This step was followed by the standard enhanced chemiluminescence reaction (ECL system).The membrane was incubated in a 1:1 mixture of ECL solutions I and II. This reaction is based on a peroxidase-catalyzed oxidation of luminol, which leads to the emission of light photons that can be detected on X-ray film. Thus, the peroxidase conjugated secondary antibodies bound to the primary antibody detect the protein of interest.

#### **5.3.3.5. Immunoblot stripping**

The removal of primary and secondary antibodies from a membrane is possible, so that it can be reprobbed with alternative antibodies. After the enhanced chemiluminescence reaction, the membrane was washed with 1 × TBS buffer containing 0.1% Tween 20 for 5 min by vigorous shaking and subsequently incubated in stripping buffer for 1 h at 60 °C. Every 20 min the membrane was vigorously shaken for 5 sec. Then the membrane was washed three times with 1 × TBS buffer containing 0.1% Tween 20 by vigorous shaking, each time for 10 min. The membrane was then reprobbed as described above.

#### **5.3.3.6. Immunoprecipitation**

Immunoprecipitation (IP) is highly specific and effective technique for analytical separations of target antigen from the cell or tissue homogenate. In the IP method, the protein is precipitated in an appropriate lysis buffer by means of an immune complex, which includes the antigen (protein), primary antibody and Protein A-, G- or L-agarose conjugate or a secondary antibody-agarose conjugate. The choice of agarose conjugate depends on the species origin and isotype of the primary antibody. The methods described are comparable and the choice of method depends on the specific antigen-antibody system.

For isolation of Myc-tagged proteins, cell lysates were incubated with mouse monoclonal anti-Myc antibody (1 µl antibody for 100 µl cell lysate) at 4 °C for 1 h, followed

by addition of Protein G-agarose beads (10  $\mu$ l 50% suspension for 1  $\mu$ l antibody) and further incubation for 2 h at 4 °C. During the incubation, the samples were gently rotated. After two washes in lysis buffer containing 0.2% NP-40 (25  $\mu$ l buffer per 1  $\mu$ l pellet) and one wash in 1  $\times$  kinase buffer (20  $\mu$ l buffer per 1  $\mu$ l pellet) the immunoprecipitated proteins were either used for *in vitro* kinase assay or boiled in 5  $\times$  SDS-loading buffer and subjected to SDS-PAGE.

### **5.3.3.7. RAF *in vitro* kinase assay**

RAF kinase activity can be assayed by the ability of the RAF enzyme to phosphorylate recombinant MEK kinase. To amplify the phosphorylation signal, a coupled kinase assay can be used, in which activated MEK phosphorylates its unique substrate ERK. This assay system allows to measure activity of the purified or immunoprecipitated RAF kinase, as well as the RAF activity in crude cellular extracts.

The kinase reaction was performed in a total volume of 50  $\mu$ l. The reaction mixture for the RAF kinase assay was prepared on ice as indicated below:

|  | <i>for 50 <math>\mu</math>l</i>          |
|--|--|
| ddH <sub>2</sub> O                       | (34 – Volume of RAF preparation) $\mu$ l |
| 10 x kinase buffer                       | 5 $\mu$ l                                |
| MgCl <sub>2</sub> (1 M)                  | 0.5 $\mu$ l                              |
| DTT (100 mM)                             | 5 $\mu$ l                                |
| ATP (10 mM)                              | 5 $\mu$ l                                |
| Purified recombinant MEK                 | 3 $\mu$ l                                |
| Purified recombinant ERK2                | 2 $\mu$ l                                |
| Na <sub>3</sub> VO <sub>4</sub> (100 mM) | 0.5 $\mu$ l                              |
| RAF preparation or cell lysate           | 1–10 $\mu$ l                             |

The appropriate amount of the reaction mixture was added to the RAF preparation, still on ice, mixed well and transferred to the thermoshaker for microfuge tubes. The reaction mixture was incubated at 30 °C for 30 min at 700 rpm. The assay was terminated by adding 20  $\mu$ l 5  $\times$  SDS-loading buffer. The kinase reaction was monitored by Western blotting analysis with a monoclonal anti-phospho-ERK1/2 antibody that recognizes only protein phosphorylated at position Y204 of ERK1 and at corresponding position of ERK2, the sites of ERK1/2 phosphorylation by MEK.

#### 5.3.3.8. Purification of GST-fusion RAF proteins from Sf9 and COS7 cell lysates

The glutathione S-transferase (GST) family of enzymes comprises a long list of cytosolic, mitochondrial and microsomal proteins that are capable of multiple reactions with a multitude of substrates. GSTs catalyze the conjugation of reduced glutathione via the sulfhydryl group to electrophilic centers on a wide variety of substrates. Frequently, glutathione S-transferase is used to create the so-called “GST gene fusion system”. Here, GST is used to purify and detect proteins of interest. In a GST gene fusion system, the GST sequence is incorporated into an expression vector alongside the gene sequence encoding the protein of interest. Induction of protein expression from the multiple cloning sites of the vector results in expression of a fusion protein – the protein of interest fused to the GST protein. This GST-fusion protein can then be purified from cells via its high affinity for glutathione. Adding free glutathione to beads that bind purified GST-proteins will release the GST-protein in solution.

To purify GST-tagged RAF proteins, clarified Sf9 and COS7 cell lysates were incubated with 0.5 ml glutathione-sepharose beads (50% suspension) for 2 h at 4 °C with rotation. After incubation, the beads were washed three times with IC lysis buffer containing 0.2% NP-40. RAF proteins bound to the beads were eluted with 0.5 ml of GST elution buffer. The purity of RAF kinases was documented by SDS–PAGE (10% gels) and staining with Coomassie Blue.

#### 5.3.3.9. Purification of GST-fusion 14-3-3 proteins from *E. coli*

All of the seven mammalian 14-3-3 isoforms were expressed in *E. coli* as glutathione GST-fusion proteins using pGEX2T vector and purified by glutathione-sepharose affinity chromatography as described above for RAF proteins. Purified 14-3-3 proteins were dialyzed against 20 mM Tris-HCl (pH 7.6) and 150 mM NaCl and concentrated to 5 mg/ml. Purification of 14-3-3 proteins was performed by A. Fischer (MSZ, Würzburg).

#### 5.3.3.10. Purification of His-tagged RAF proteins from Sf9 cell lysates

A polyhistidine tag is an amino acid motif in proteins that consists of at least six histidine residues at the N- or C-terminus of the protein. It is also known as hexahistidine tag (6×His-tag) and by the trademarked name His-tag. The polyhistidine-tag binds with micromolar affinity to media containing bound metal ions, either nickel or cobalt.

The purification procedure for His-tagged RAF kinases (A-, B- and C-RAF) was similar as described above with the exception that the Sf9 cell lysates (12 ml) were incubated with 0.5 ml of Ni-NTA-Agarose. The bound proteins were then eluted with imidazole containing buffer using a step gradient. To remove 14-3-3 proteins associated with RAF, some purification procedures were carried out in the presence of 1.0% Empigen BB.

### **5.3.3.11. Subcellular fractionation**

Cell fractions were isolated using the *ProteoExtract* subcellular proteome extraction kit. This system takes advantage of the differential solubility of certain subcellular compartments in specific reagent mixtures preserving the structural integrity of the subcellular structures before and during the extraction. The extraction procedure provides four subproteomes of decreased complexity. With extraction buffer I cytosolic proteins are released (fraction 1). Subsequently, membranes and membrane organelles are solubilized with extraction buffer II, without impairing the integrity of nucleus and cytoskeleton (fraction 2). Next, nucleic proteins are enriched with extraction buffer III (fraction 3). Components of the cytoskeleton are finally solubilized with extraction buffer IV (fraction 4).

For subcellular fractionation of adherent tissue culture cells, the cells were grown on the 10 cm Petri dishes. The cell monolayer was washed with 2 ml ice cold wash buffer by gentle agitation of plate at 4 °C for 5 min. The wash step was repeated to remove contaminating media components. 1 ml extraction buffer supplemented with 5 µl protease inhibitor cocktail was added to the cell monolayer. The plate was carefully rotated until all cells were covered with buffer. The Petri dish was incubated at 4 °C for 10 min with gentle agitation. The supernatant (fraction 1) was transferred to a clean microcentrifuge tube without disrupting the cell monolayer. 1 ml extraction buffer II supplemented with 5 µl protease inhibitor cocktail was added to the cells without disrupting the cell monolayer. The plate was carefully rotated until all cells were covered with buffer and incubated at 4 °C for 30 min with gentle agitation. The supernatant (fraction 2) was transferred to a clean microcentrifuge tube without disrupting the cell monolayer. 500 µl extraction buffer III were mixed with 5 µl protease inhibitor cocktail and 1.5 µl *Benzonase* nuclease and added to the plate. The plate was carefully rotated until all cells were covered with buffer and incubated at 4 °C for 10 min with gentle agitation. The supernatant (fraction 3) was transferred to a clean microcentrifuge tube without disrupting the cell monolayer. Sometimes, the cells detached during the third incubation step. In this case, cell suspension was transferred to a microcentrifuge tube and the insoluble material was pelleted by centrifuging at 6,800 rpm (*Biofuge Fresco*) for 10 min at 4 °C. The supernatant was then transferred to the clean microcentrifuge tube. Finally, 500 µl extraction buffer IV were mixed with 5 µl protease inhibitor cocktail and added to the Petri dish. The plate was carefully rotated until all cells were covered with buffer. The remaining cell structures detached upon treatment with extraction buffer IV, so that after complete solubilization of the residual material, the extract (fraction 4) was transferred to a clean microcentrifuge tube. In the case of the pelleted cell structures, the residual particles were resuspended in 500 µl extraction buffer IV containing protease inhibitors by pipetting up and down (fraction 4). The samples were stored at -20 °C. The selectivity of subcellular extraction was documented by immunoblotting against marker proteins (M2PK for cytosolic fraction, KDEL for membranes, histon 3 and PARP for nuclear fraction, and vimentin for cytoskeletal fraction).

### 5.3.3.12. Mass spectrometry measurements

Mass spectrometers can be divided into three fundamental parts, namely the ionization source, the analyzer and the detector. The sample has to be introduced into the ionization source of the instrument. Once inside the ionization source, the sample molecules are ionized, because ions are easier to manipulate than neutral molecules. These ions are extracted into the analyzer region of the mass spectrometer where they are separated according to their mass(*m*)-to-charge(*z*) ratios (*m/z*). The separated ions are detected and this signal sent to a data system where the *m/z* ratios are stored together with their relative abundance for presentation in the format of a *m/z* spectrum. The analyzer and detector of the mass spectrometer, and often the ionization source too, are maintained under high vacuum to give the ions a reasonable chance of travelling from one end of the instrument to the other without any hindrance from air molecules. The ionization methods used for the majority of biochemical analyses are Electrospray Ionization (ESI) and Matrix Assisted Laser Desorption Ionization (MALDI).

ESI is one of the Atmospheric Pressure Ionization (API) techniques and is well suited to the analysis of polar molecules ranging from less than 100 Da to more than 1000,000 Da in molecular mass. During standard electrospray ionization, the sample is dissolved in a polar, volatile solvent and pumped through a narrow, stainless steel capillary (75–150  $\mu\text{m}$  i.d.) at a flow rate of between 1  $\mu\text{l}/\text{min}$  and 1  $\text{ml}/\text{min}$ . A high voltage of 3 or 4 kV is applied to the tip of the capillary, which is situated within the ionization source of the mass spectrometer. As a consequence of this strong electric field, the sample emerging from the tip is dispersed into an aerosol of highly charged droplets, a process that is aided by a coaxially introduced nebulizing gas flowing around the outside of the capillary. This gas, usually nitrogen, helps to direct the spray emerging from the capillary tip towards the mass spectrometer. The charged droplets diminish in size by solvent evaporation, assisted by a warm flow of nitrogen known as the drying gas, which passes across the front of the ionization source. Eventually charged sample ions, free from solvent, are released from the droplets, some of which pass through a sampling cone or orifice into an intermediate vacuum region and from there through a small aperture into the analyzer of the mass spectrometer, which is held under high vacuum. The lens voltages are optimized individually for each sample [274].

For mass spectrometrical analysis, the purified GST-tagged A-RAF samples (about 10 pmol of each) were applied to SDS-PAGE. Proteins were visualized by Coomassie Blue staining applying the method of Neuhoff *et al.* [275]. In-gel reduction, acetamidation and tryptic digestion were done according to Wilm *et al.* [276]. After elution of the peptides, solutions were desalted using C18 ZipTip according to the manufacturer's instructions. ESI-MS was performed on a Bruker APEX II FT-ICR mass spectrometer equipped with an Apollo-Nano-ESI ion source in positive ion mode.

To determine the exact positions of phosphates within the peptides the nano-LC-MS/MS analysis was carried out as follows: A-RAF samples were separated by SDS-PAGE, protein bands were excised, washed, digested and generated peptides were extracted as described by Reinders *et al.* [277]. Nano-LC-MS/MS analyses and transformation of raw data into MGF format were conducted as described by Zahedi *et al.* [278] on a Qstar Elite and an LTQ XL mass analyzer in multistage mode, respectively. Generated peak lists were searched



using *Mascot* 2.2 against a SGD protein database with the concatenated A-RAF protein sequence (a total of 6,318 sequences) using the following criteria: trypsin with a maximum of 2 missed cleavage sites, carbamidomethylation of cysteine residues as fixed and phosphorylation of serine, threonine and tyrosine residues as variable modifications. For the *Qstar Elite*, mass tolerances were set to 0.1 Da for MS and MS/MS, whereas for the *LTQ XL*, mass tolerances were set to 0.3 Da for MS as well as 2.0 for MS/MS. Additionally, the  $^{13}\text{C}$  option was set to 1 to account for the potentially inaccurate assignment of monoisotopic peaks. All phosphopeptide MS/MS spectra were validated manually as described by Zahedi *et al.* [278]. Peptides represented in **Table 3** were identified reproducibly, whereas a number of further potential phosphopeptides generated MS/MS spectra of inferior quality and therefore were omitted.

Mass spectrometric analysis was done by Dr. Werner Schmitz (Institute for Physiological Chemistry II, University of Würzburg) and Dr. René Zahedi (Rudolf Virchow Center/DFG Research Center for Experimental Biomedicine, University of Würzburg).

### **5.3.3.13. BIAcore's SPR technology**

BIAcore's SPR technology has been designed to investigate the functional nature of binding events. By use of this method protein-protein interaction and binding affinities of interacting partners can be quantitatively determined. The technology is based on surface plasmon resonance (SPR), an optical phenomenon that enables detection of unlabeled interactants in real time.

The underlying physical principles of SPR are complex. SPR-based instruments use an optical method to measure the refractive index (within ~300 nm) near a sensor surface. In the BIAcore this surface forms the floor of a small flow cell, 20–60 nl in volume, through which an aqueous solution (henceforth called the running buffer) passes under continuous flow (1–100  $\mu\text{l}/\text{min}$ ). In order to detect an interaction between two molecules, one interacting partner (the ligand) is immobilized onto the sensor surface. Its binding partner (the analyte) is injected in aqueous solution (sample buffer) through the flow cell, also under continuous flow. As the analyte binds to the ligand, the accumulation of protein on the surface results in an increase in the refractive index. This change in refractive index is measured in real time, and the result plotted as response units (RUs) versus time (a sensorgram). One RU represents the binding of approximately 1 pg protein/ $\text{mm}^2$ . Importantly, a background response will also be generated, if there is a difference in the refractive indices of the running and sample buffers. This background response must be subtracted from the sensorgram to obtain the actual binding response. The background response is recorded by injecting the analyte through a control or reference flow cell, which has no ligand or an irrelevant ligand immobilized to the sensor surface.

BIA sensor measurements presented in this work were carried out either on a BIAcore-X or BIAcore-J system at 25 °C. For that purpose, the biosensor chip CM5 was first loaded with anti-GST antibody using covalent derivatization. Purified and GST-tagged 14-3-3 proteins were injected in BIA sensor buffer (10 mM HEPES, pH 7.4, 150 mM NaCl, and

0.01% NP-40) at a flow rate of 10  $\mu$ l/min, which resulted in a deposition of approx. 1200 RU. Next, the purified His-tagged RAF proteins were injected at increasing concentrations as indicated. The values for unspecific binding measured in the reference cell were subtracted. In some assays, unspecific binding of His-RAF to the GST group was observed (approx. 10% of the maximal RAF binding). Addition of BSA (0.2 mg/ml) reduced significantly the unspecific binding. To measure the competition between RAF and 14-3-3 using synthetic peptides GST-14-3-3 $\zeta$  was first captured to the anti-GST antibody. Next, RAF proteins were injected in the absence and presence of increasing concentrations of the peptides and the competition between RAF and peptides of interest for 14-3-3 binding was monitored.

### **5.3.4. Cell culture methods**

#### **5.3.4.1. Cultivation and passaging of eukaryotic cells**

##### *Cultivation and passaging of mammalian adherent cells*

Experimental work with mammalian cells was done in a sterile laboratory hood, using standard tissue culture techniques. Cells were cultured in polystyrol-plastic vessels (T-flasks and dishes 10 or 15 cm sizes) in 5% carbon dioxide at 37 °C and 95% humidity in a cell culture incubator.

For passaging, cells were washed once with 1  $\times$  PBS after removing the medium and 2 ml trypsin/EDTA solution was added. After an incubation of maximal 5 min at 37 °C cells were detached from culture plates via throbbing and trypsin was inactivated by addition of serum-containing media. An appropriate volume of cell suspension was then aliquoted into freshly prepared T-flasks with media.

##### *Cultivation and passaging of insect cells*

Sf9 insect cells grow well in suspension or monolayer culture, with a convenient doubling time of approximately 20 h at 27 °C. They require 10% FCS in an appropriate medium and constant temperature but do not require CO<sub>2</sub>, since their growth media are buffered at a pH approximately 6.2. As Sf9 cells adhere relatively loosely to tissue culture vessels, they can be conveniently subcultured without the use of trypsin. Sf9 cells of monolayer culture are normally subcultured two or three times per week, by diluting resuspended cells 4- to 8-fold in fresh medium. The insect cells do not become contact-inhibited, and so should be subcultured at 90% confluency or below.

For RAF protein expression, Sf9 cells were grown in suspension. The cells were seeded at density of approximately  $2.5 \times 10^5$  cells per ml in to a total volume of 250 ml of complete medium in a 1000 ml spinner flask. The cells were incubated at 27 °C with constant stirring at 50–60 rpm until the cell density reaches approximately  $2 \times 10^6$  cells/ml. Then the

cells were subcultured by removing 200 ml of the suspension and replacing it with 200 ml of fresh complete medium, giving the cell density of approximately  $0.4 \times 10^6$  cells/ml.

#### **5.3.4.2. Cell counting**

Trypsinized cells were counted by use of a hemocytometer (Neubauer's cell counting chamber). A hemocytometer is a specialized glass slide that has a grid pattern etched upon it. The volume of a given grid is known. Each of the large squares represents a specific area. Since the well has a specific depth, each square also represents an equivalent volume. Using a microscope, the number of cells can be counted to get a measure of the concentration of cells in the suspension. Often, dye is used in cell counting procedures as an indication of cell viability. The most commonly used dye is Trypan Blue. Trypan Blue is excluded from viable cells, so the blue cells are dead ones, and the whiter colored cells are alive.

A small amount of cell suspension was diluted 1:1 with Trypan Blue and incubated for 5 min. 10  $\mu$ l of the mixture were loaded into the both wells of hemocytometer. After being covered by a cover slip, the cells spread out due to capillary action. Five squares were counted. Only viable cells were counted. It is important to adopt a rule for counting cells that fall on the lines to eliminate duplicate counts. For example, cells that fall on a left or top line that bound a square are counted as part of a square, but not those that fall on the bottom or right lines.

Each square of the hemocytometer (with cover slip in place) has surface area of 1  $\text{mm}^2$  and represents a depth of 0.1 mm, giving a total volume of 0.1  $\text{mm}^3$  or  $10^{-4} \text{ cm}^3$ . Since 1  $\text{cm}^3$  is equivalent to 1 ml, the subsequent cell concentration per ml (and the total number of cells) was determined using the following calculations:

*Average number of cells:*

$$\frac{\text{total number of cells}}{5 \text{ squares} \times 0.1 \text{ mm}^3} = \frac{\text{total number of cells}}{5 \text{ squares} \times 10^{-4} \text{ cm}^3} = \frac{\text{total number of cells}}{5 \text{ squares} \times 10^{-4} \text{ ml}} = \text{cells/ml},$$

where  $0.1 \text{ mm}^3 = \text{volume of 1 square} = 10^{-4} \text{ cm}^3 = 10^{-4} \text{ ml}$

*Dilution factor:*

$$\frac{\text{volume of Trypan Blue} + \text{volume of cell suspension}}{\text{volume of chamber aliquot}}$$

*Average number of cells per milliliter:*

$$\text{average number of cells (cells/ml)} \times \text{dilution factor} = \text{cells/ml}$$

#### 5.3.4.3. Freezing, long-term storage and thawing of cells

For long-term storage, eukaryotic cells were frozen down in their appropriate medium containing 10% DMSO and 20% serum. Trypsinized cells were harvested by centrifuging at ca.  $200 \times g$  (1100 rpm, *Megafuge 1.0R*) for 10 min at RT. The cell pellet was resuspended in the freeze medium to give a final concentration of between  $2$  and  $4 \times 10^6$  cells/ml and 1 ml cell suspension was aliquoted into each cryovial. The cells were frozen gradually. Before transferring into liquid nitrogen, the cells were at first incubated at  $-20^\circ\text{C}$  for 2 h followed by incubation at  $-80^\circ\text{C}$  overnight.

For thawing, cells were hand warmed or placed in a  $37^\circ\text{C}$  water bath, until all ice clusters were melted. Then 1 ml serum was added to the cryovial and the cell suspension was transferred into the 15 ml tube. The cells were pelleted at ca.  $200 \times g$  (1100 rpm, *Megafuge 1.0R*) for 10 min at RT. After removal of supernatant cells were carefully resuspended in their appropriate medium and taken into general tissue culture.

#### 5.3.4.4. Transfection of mammalian adherent cells

Mammalian adherent cells (HEK293 and COS7) were transfected by use of *jetPEI* cationic polymer transfection reagent. *jetPEI* reagent compacts DNA into positively charged particles capable of interacting with anionic proteoglycans at the cell surface and entering cells by endocytosis. It possesses the property of acting as a “proton sponge” that buffers the endosomal pH and protects DNA from degradation. The continuous proton influx also induces endosome osmotic swelling and rupture, which provides an escape mechanism for DNA particles to the cytoplasm.

For optimal transfection with *jetPEI*, the cells were seeded into 10 cm Petri dishes 24 h before transfection. At the time of transfection the cells were 50–60% confluent. The DNA/transfection reagent complex was prepared as follows: for each 10 cm Petri dish 500  $\mu\text{l}$  *jetPEI* reagent solution (16  $\mu\text{l}$  *jetPEI* were diluted into 500  $\mu\text{l}$  150 mM NaCl) were added to the 500  $\mu\text{l}$  DNA solution (8  $\mu\text{g}$  plasmid DNA were diluted into 500  $\mu\text{l}$  of 150 mM NaCl) all at once and vortex-mixed immediately. The transfection mixture was incubated for 30 min at RT. Then the 1 ml *jetPEI*/DNA mixture was added drop-wise onto the 4 ml fresh medium in each dish and the mixture was homogenized by gently swirling the plate. Transfection experiments were performed either in serum containing medium (20% FCS) or at starvation conditions (0.03% FCS) and were stopped either after 24 h or 48 h.

#### 5.3.4.5. Infection of insect cells

Baculoviruses are insect-pathogenic and insect-specific viruses, belonging to the group of nuclear polyhedrosis viruses. The most prominent member of this group is *Autographa californica* nuclear polyhedrosis virus (AcNPV). This virus infects more than 30

different species of insects of the *lepidoptera* family. The genome of baculovirus is a circular closed double-stranded DNA with a length of 80–200 kb. Free viruses consist of a viral capsid that is surrounded by a lipid-containing membrane. Several nucleocapsids can aggregate to form superstructures. Following productive infection of susceptible insect cells (for example, *Spodoptera frugiperda*) one observes free extracellular virus particles and intracellular forms of the virus that are easily distinguished microscopically as dense viral inclusion bodies surrounded by proteins. The infection cycle of baculovirus is biphasic. Initially infectious virus particles infect gut cells of an insect. It migrates to the cell nucleus and sheds its protein coat. After approx. 6 h one observes first signs of viral DNA replication. After approx. 12 h new infectious viruses are released by budding. Viruses are taken up by other cells either by endocytosis or by fusion. The production of extracellular virus particles reaches its maximum approx. 36–48 h post infection. Approx. 18–24 h post infection inclusion bodies with up to 100 embedded virus particles are formed in the nuclei of infected cells. These bodies consist of polyhedrin, a virus-encoded protein of 29 kDa. Inclusion bodies accumulate until the cell lyses 4–5 days post infection. Viral inclusion bodies are an important component of the infection cycle. Polyhedrin crystals are relatively inert and resistant against environmental influences. They are released into the environment after the death of an infected insect and are then taken up by other insects with their food. Inclusion bodies lyse in the alkaline milieu of the insect gut and then release their infectious virus particles, thus closing the infection cycle. As the polyhedrin gene is neither required for virus infectivity nor intracellular multiplication, it has been used to design vectors allowing the expression of heterologous proteins in infected insect cells. Polyhedrin has been shown to accumulate in virus-infected cells. As it can make up 20 % of the total protein content of a cell, yields are on the order of 1 gram of foreign protein per liter of infected cell cultures. (1 mg of protein per  $1-2 \times 10^6$  of infected cells). Cloning vectors exploit the extraordinary strength of the polyhedrin gene promoter and are constructed in a way allowing the foreign gene to be expressed at high levels under the control of the polyhedrin gene promoter. Due to its size, the virus genome itself cannot be used as a cloning vector. Instead, a so-called intermediate or transfer vector is used, which allows all cloning operations to be carried out in bacteria. The foreign gene to be expressed in insect cells is inserted between 5' and 3' sequences of the polyhedrin gene, which is located on the transfer vector. Infectious recombinant baculoviruses are usually obtained by recombination *in vivo*, following simultaneous infection of insect cells with wild type viruses and the engineered cloning vector carrying the foreign gene. One particular advantage of the use of baculovirus vectors in insect cell systems is the fact that insect cells can perform correct posttranslational modification of heterologous proteins. The foreign proteins have antigenic and other immunological properties resembling those of genuine proteins produced in their native cell systems. This is a distinct advantage over heterologous gene expression in bacteria, which cannot process eukaryotic proteins correctly [279-281].

#### *Transfection of insect cells with baculovirus DNA using calcium phosphate*

Approximately  $1 \times 10^6$  Sf9 cells were seeded (from a long-phase culture) per 35 mm tissue culture dish in 2 ml of complete medium and allowed to attach to the surface for 1 h at 27 °C. The medium was aspirated and replaced with 1 ml fresh medium. 1ml of the IC

transfection buffer was mixed with 200 ng linearized baculovirus DNA and 2 µg recombinant transfer vector in a sterile 1.5 ml microcentrifuge tube. The mixture then was added drop-wise while swirling to the medium in the dish. The plate was incubated 5 h at 27 °C without shaking. After incubation, the medium was aspirated and the cells were washed with 2 ml of complete medium. Finally, 2 ml of complete medium were added to the cells and the cells were incubated at 27 °C for 4–5 days without shaking. After the last incubation, the medium from the plate was transferred to a sterile centrifuge tube and centrifuged at 1000 g for 5 min to clarify the virus-containing supernatant fluid. The resultant virus stock was stored at 4 °C prior to plaque assay or amplification.

### *Plaque assay*

A suspension culture of Sf9 cells was grown to a density of less than  $3 \times 10^6$ . This culture was then diluted to a density of 5 to  $6 \times 10^5$ . 2 ml of this cell suspension were transferred to each well of a 6-well culture dish. The cells were left to settle to bottom of the plate for 1 h at RT. Following incubation of the plates, the monolayers were observed under the inverted microscope to confirm cell attachment and 50% confluence. Meanwhile, an eight-log serial dilution of the harvested viral supernatant was produced by sequentially diluting 0.5 ml of the previous dilution in 4.5 ml of complete medium in 12-ml disposable. Eight tubes containing each of a  $10^{-1}$  to  $10^{-8}$  dilution of the original virus stock were prepared. The supernatant from each well was removed and discarded, and immediately replaced with 1 ml of the respective virus dilution to each well. The plate was then incubated for 1 h at RT. 30 ml of the complete medium (incubated at 40 °C in water bath before use) and 10 ml of the 4% liquid agarose gel (incubated at 70 °C in water bath before use) were quickly dispensed to the empty bottle and mixed gently. The bottle of plaquing overlay was then returned to the 40 °C water bath until use. The virus liquid was removed from the wells and replaced with 2 ml of the diluted agarose. The plates were incubated at RT for 10 to 20 min before moving to allow gel to harden. Then the plates were incubated at 27 °C in a humidified incubator for 4 to 10 days. Recombinant virus produces milky/gray plaques of slight contrast visible without staining or other detection methods. The plates were monitored daily until the number of plaques counted did not change for two consecutive days. To determine the titer of the inoculum employed, an optimal range to count is 3 to 20 plaques per well of a 6-well plate. To stain the plates, an overlay agarose solution was prepared: 1/100 volume of the 1% Neutral Red solution was added to the molten agarose (e.g. 100 µl Neutral Red to 10 ml agarose). 1 ml of the overlay agarose was then added to each well and the plate was incubated at 27 °C for at least 4 h. The titer (pfu<sup>\*</sup>/ml) was calculated by the following formula:

$$\text{Pfu/ml (of original stock)} = \text{number of plaques per ml of inoculum} \times (\text{dilution factor})^{-1}$$

\* plaque forming unit

*Preparation of clonal virus stocks*

In wells containing just a few plaques, well-isolated ones were marked by circling with a pen on the underside of the plate. About 10 of the marked plaques were picked by pushing a sterile Pasteur pipette through the agarose into the plaque, and gently sucking an agarose plug in to the pipette tip. Each plug was transferred into 1 ml of complete medium in a separate microcentrifuge tube. The medium was vortexed gently and left overnight at 4 °C to elute the virus particle from the agarose. 35 mm wells were seeded with  $5 \times 10^5$  Sf9 cells in 2 ml of complete medium. The cells were incubated for 1 h at 27 °C to allow the cells to settle and attach. After incubation, the medium was aspirated and 100 µl eluted virus suspension was added to the middle of the dish. The cells were left for 1 h at RT, then 1 ml of complete medium was added. The cells were incubated at 27 °C for 3–4 days, then the medium was transferred to the sterile centrifuge tube and centrifuged at 1000 rpm for 5 min to clarify the virus containing supernatant fluid. The resultant virus stock was stored at 4 °C prior to plaque assay or amplification. Expression of the desired recombinant protein was confirmed by Western blotting analysis of the cell lysate.

*Estimation of viral titre by cell-lysis assay*

Sf9 cells were harvested from exponentially growing culture, sedimented at 1000 g for 5 min at RT and resuspended gently at a density of  $0.25 \times 10^6$  cells/ml in complete medium. A sample of viral stock was serially diluted, making dilutions (200 µl volume) in complete medium from  $10^{-1}$  to  $10^{-10}$  in sterile cryovials. One volume of cell suspension was added to each virus dilution and mixed gently. Triplicate 10 µl aliquots of each mixture were added to wells in each row of a *Nunc HLA* plate. This should be resulted in approx. 50% confluency after setting. If it was not a case, the cell resuspension density was adjusted. To maintain humidity within the plate, medium was added to the empty wells or a drop (100 µl) in each corner. The lid of the plate was replaced and the plate was placed in a sealed humid box inside of a 27 °C incubator. The cells were incubated at 27 °C for 6 days to observe the extent of cell lysis. The cells were observed each day until no further increase in cell lysis was observed. At the end of the experiment the viral titre was approximated using the following approach: Consider the situation where there is lysis in all wells of dilution  $10^{-(x-1)}$ , but not in all of  $10^{-x}$ . For this to occur, on average, there must be less than 1 virus particle in 10 µl of the  $10^{-x}$  dilution, but more than 0.1 particles. Correspondingly, there must be less than  $1 \times 10^x$  virions in 10 µl of the mixture of original virus stock plus cell suspension, but more than  $1 \times 10^{(x-1)}$ . It follows, therefore, that there are less than  $2 \times 10^x$  particles in 10 µl of the original virus stock, and more than  $2 \times 10^{(x-1)}$ . Thus, the titre lies between  $2 \times 10^{(x+1)}$  and  $2 \times 10^{(x+2)}$  virus particles/ml.

*Amplification and storage of recombinant baculovirus*

Virus containing supernatant fluid was transferred to a sterile tube. The fluid was clarified by centrifugation at 1000 g for 5 min at RT. The clarified medium was transferred to

fresh tubes and the titre was determined. To amplify the virus, a monolayer exponential culture of Sf9 cells was infected at an MOI\* 0.01–0.1. The virus was harvested after 72–120 h. This resulted in at least a 100-fold amplification that normally yielded virion at a high enough concentration for assaying protein expression. If a larger stock was required, larger Sf9 culture was infected. The virus was stored at 4 °C in the dark.

\*MOI = the ratio of infective virion to Sf9 cells. To estimate the viral inoculum required the following formula was used:

Inoculum required (ml) = (total number of cells) × (MOI in pfu/ml) / (viral titer of inoculum in pfu/ml)

For the production of recombinant A-RAF proteins, 10<sup>7</sup> Sf9 cells were infected with the desired baculoviruses at a multiplicity of infection (MOI) of 5 and incubated for 48 h at 27 °C. The cells were then washed with PBS-buffer and pelleted as described in 5.3.3.1.

## **5.3.5. Bioinformatic methods**

### **5.3.5.1. Modeling of the N-region interactions with the catalytic part of RAF kinases**

The structure models for the kinase domain of A-RAF and C-RAF were obtained by homology modeling, using the crystal structure of B-RAF catalytic domain as a template. The amino acid sequences of all three homologs were aligned using *ClustalW*, and the differing amino acid residues of B-RAF with respect to A- and C-RAF were exchanged using the software *QUANTA2005*. Side chain orientations of the substituted residues were first optimized by the tool *X-Build* in *Quanta2005* to yield side chain orientations that are most common for the particular amino acid type unless the side chain orientation resulted in a steric clash with neighboring residues. The N-terminal extension, which is not present in the crystal structure of the B-RAF template (residues G295 to G300 in A-RAF and residues G334 to S339 in C-RAF), was first build with an extended  $\beta$ -strand conformation for the backbone atoms. Backbone and side chain atoms of the N-terminal extension were then optimized by energy minimization using 500 steps of *AdoptedRaphson Newton* algorithm and the *CHARMM22* force field employing only geometrical energy terms and no electrostatics. As the final step, a full energy term minimization was performed for the N-terminal extension, and all other residues were kept fixed, employing a distance-dependent dielectric treatment for the electrostatics.

### **5.3.5.2. Modeling of the three-dimensional structure of the IH-segment in A-RAF**

The structure models for the IH-segment of A-RAF comprising residues S246 to E277 were obtained by *de novo* modeling using the software *QUANTA2006*. Briefly, the peptide sequence was built using the *Sequence Builder* in the *ProteinDesign* tool of



*QUANTA2006* with the peptide adopting an extended conformation. The sequence of the phosphopeptide was built in the identical manner using phosphoserines and -threonine for residues S250, T253, S257, S259, S262, S264 and S265. Secondary structure prediction using the software *ProteinPredict* [282], *JPred* [283] and *AGSSP* (<http://imtech.res.in/raghava/apssp/>) was performed to test whether the IH-segment of A-RAF might adopt a defined secondary structure. However, none of the programs predicted defined secondary structure elements independent whether this or longer stretches covering the region of interest were used in the prediction. Thus, molecular dynamics simulation was used to determine possible differences due to the phosphorylation. First, shorter simulations starting with an extended peptide were performed *in vacuo* using the *CHARMM22* force field including electrostatic terms but with a constant dielectric with the dielectric constant  $\epsilon$  set to 78 as in water. Simulations of 200 ps were performed causing the extended peptide to collapse to a more globular structure. These globular structures were put into explicit solvent by immersing the peptide structures in water using a water shell of 10Å around the peptide. After energy minimization using 1000 steps of conjugate gradient minimization, molecular dynamics simulations of 500 ps length were performed employing the *CHARM22* force field. Several runs were conducted to determine the probabilities of defined structure elements obtained in these simulations. No defined structures could be obtained by these simulations, which is consistent with the secondary structure predictions. Calculation of the electrostatic potential maps of the phosphorylated and non-phosphorylated peptide was carried out using the software *ABPS* [284]. The charge force field of *AMBER7.0* was used. Charges for phosphoserine and -threonine were obtained from Homeyer *et al.* [285]. Potential maps were calculated using an ionic strength of 0 mM, however using physiological salt concentrations of 150 mM did not alter the maps other than scaling the potentials to the higher salt. Charge distribution was identical at different salt concentrations.

Molecular modeling was done by Prof. Dr. Thomas Müller (Julius-von-Sachs Institute for Biosciences, University of Würzburg).

## 6. RESULTS

### 6.1. MS analysis of A-RAF phosphorylation

Most of the phosphorylation sites in C- and B-RAF are well established. In contrast, phosphorylation of A-RAF is incompletely investigated. Recently our group performed a quantitative analysis of C-RAF phosphorylation by use of mass spectrometry that resulted in identification of several new phosphorylation sites [194]. To obtain a more comprehensive map of potential phosphorylation sites in A-RAF, the mass spectrometry technique was used here again. For that purpose, A-RAF proteins were expressed in Sf9 and mammalian cells in the presence and absence of H-Ras12V and Lck. After trypsin and/or GluC digestion of purified protein and desalting procedures, the selective detection of the phosphopeptides has been performed by ESI-MS. To determine the exact positions of phosphates within the fragments the nano-LC-MS/MS analysis was carried out. Three independent measurements provided 84% coverage of the entire protein sequence. The combined results obtained for A-RAF phosphorylation are summarized in **Tables 2** and **3**, and **Fig. 20**, revealing a number of novel phosphorylation sites in A-RAF. To compare the mass spectrometry results obtained for A-RAF with the known phosphorylation sites in B- and C-RAF, the amino acid sequences of RAF isoforms were aligned as shown in **Fig. 20**.

#### 6.1.1. Phosphorylation sites within the kinase domain of A-RAF

Most of the identified phosphorylation sites within the kinase domain of A-RAF are conserved, suggesting that regulation by these sites is similar for all RAF isoforms. The peptides corresponding to A-RAF 432–444 and 445–456 could be ascribed to the MEK binding domain and activation segment, respectively, due to homology with B- and C-RAF [132,239,240]. Furthermore, a number of putative phosphorylation sites within the A-RAF kinase domain, whose function has not previously been elucidated for any RAF kinase, were detected. A-RAF peptide 315–326 carrying three phosphate residues at T318, S320 and T323; peptide 401–423 carrying two phosphates at T413 and Y419; peptide 457–476 carrying three phosphorylated serines at positions 458, 467 and 469; and peptide 573–579 containing one phosphate at S573 cover the sequences that are highly conserved in all three RAF isoforms (see also **Fig. 20**). Because the number of phosphates within these three peptides corresponds to the number of phosphorylation possibilities, we propose that all these positions represent putative phosphorylation sites of RAF proteins. Similarly, the number of the detected phosphates in the partially conserved peptides 305–314, 340–354, 534–544 and 545–554 correlates with the available phosphorylation sites, suggesting that S308, S341, T344, S535, S536 and S547 may fulfill an isoform specific regulatory role in A-RAF function (**Fig. 20** and **Table 2**). In contrast, the exact position of the phosphates within the peptides 355–386 and 525–533 has not been specified despite the fragmentation analysis.

|       |     |  |     |
|-------|-----|--|-----|
| A-RAF | 1   | -----  | 1   |
| B-RAF | 1   | MAALSGGGGGGAEPGQALFNGDMEPEAGAGAGAAASSAADPAIPEEVVNIKQMIKLTQEH       | 60  |
| C-RAF | 1   | -----  | 1   |
|       |     |  |     |
| A-RAF | 1   | -----  | 1   |
| B-RAF | 61  | IEALLDKFGGEHNPPSIYLEAYEYTSKLDALQQREQQLLES LGNGTDFSVSSSASMDTV       | 120 |
| C-RAF | 1   | -----MEHIQGAWKTI SNGFGF-----KDAV                                   | 21  |
|       |     |  |     |
| A-RAF | 1   | -----MEP-----PRGPPANG--AEP SRAVGVTKVYLPNKQRTVVIVRDGMSVYDS          | 44  |
| B-RAF | 121 | TSSSSSSLSVLPSSLSVFNPTDVARSNPKSPQKPIVRVFLPNKQRTVVVPCRCVTVRDS        | 180 |
| C-RAF | 22  | FDGSSCISPTIVQQFGYQRRASDDGKLTDPKSTNTIRVFLPNKQRTVVVNRNGMSLHDC        | 81  |
|       |     | MW 2718 (1P) MW 1687 (1P) MW 1448 (2P) MW 813 (1P) MW 2453 (3P)    |     |
| A-RAF | 45  | LDKALKVRGLNQDCCVVRRLI---KGRKTVTAWDTAATAPLDGEE LIVEVLEDVPLIMHNF     | 101 |
| B-RAF | 181 | LKKALMMRGLIPECCAVYRIQ---DGEKKPIGWDTDISWLTGEE LHVEVLENVPLTTHNF      | 237 |
| C-RAF | 82  | LMKALKVRGLQPECCAVFRLLLHEHKGKKARLDWNTDAASLIGEELQVDFLDHVLPTTHNF      | 141 |
|       |     | MW 2300 (1P) MW 2648 (2P)  |     |
| A-RAF | 102 | VRKFFSLAFCD FCLKFLFHGFRCCGKFKHQHCSKVPTVCVDMSTNRQQF-----            | 155 |
| B-RAF | 238 | VRKTFFTLAFCD FCRKLLFQGFRCQTCGYKFKHQRCS TEVPLMCVNYDQLDLLFVSKFFEH    | 297 |
| C-RAF | 142 | ARKTFLKLAFCDCIQKFLNNGFRQC TCYKFEHCSTKVPTMCVDWSNIRQLLL-----         | 195 |
|       |     | MW 1996 (3P) MW 1787 (1P)  |     |
| A-RAF | 156 | ----H VQDLS-GGSRQHEAPSNRPLNELLIPQGP PR QHCDPEHFPP-----PAPANAP      | 206 |
| B-RAF | 298 | HPIPQEEASLAETALTS GSSSPSAPASDSIGPQILTSPSPSKSIPI PQPFRPADEDHRNQF    | 357 |
| C-RAF | 195 | ----FPNSTIGDSGVPALPSLTMRRMRESVSRMPVSSQHYRSTPHAFTFNTSSPSSEGLS       | 251 |
|       |     | MW 2518 (1P) MW 2035 (2P) MW 2510 (1P)                             |     |
| A-RAF | 207 | LQRIRSTSTPNVHMVSTTAP-MDSNLIQLIGQSFSDAAGSRGSDGTPRGSPSPASVSS         | 265 |
| B-RAF | 358 | GQRDRSSAPNVHINTIEPVNIDDLIRDQGFGRDGGSTTGLSATP-----PASLPGSLT         | 411 |
| C-RAF | 252 | SQRQRSTSTPNVHMVSTTLP-VDSRMIEDAIRSHSESASPSALSS-----SPNNLSP-T        | 303 |
|       |     | MW 2112 (2P) MW 2024 (1P) MW 2375 (7P) MW 2072 (4P)                |     |
| A-RAF | 266 | GRKSPH K K PAE-QRERK LADDKKKVNKLG YRDSG Y WEVPPSEVQLLKRIGTSGFTV    | 324 |
| B-RAF | 412 | NVKALQKSPGPQRERKSSSSSEDRNRMKT LGRDSSDDWEIPDGOITVQGRIGSGSFGTV       | 471 |
| C-RAF | 304 | GWSQPKTPVPAQRERAPVSGTQEKNKIRPRGQDRDSSYYWEIEASEVMLSTRIGSGSFGTV      | 363 |
|       |     | MW 1667 (2P) MW 728 (1P) MW 1189 (1P) MW 1537 (3P)                 |     |
| A-RAF | 325 | FRGRWHGDVAVKVLKVSQP IAEQAQAFKNEMQVLRKTRHVNILLFMGFMIRPGFAI I I QW   | 384 |
| B-RAF | 472 | YKGWKHGDVAVKMLNVTAPT PQQLQAFKNEVGVL RKRTRHVNILLFMGYSTKPQLAIVTQW    | 531 |
| C-RAF | 364 | YKGWKHGDVAVKILKVVDPTPEQFQAFRNEVAVLRKTRHVNILLFMGYMTKDNLAIVTQW       | 423 |
|       |     | MW 1807 (2P) MW 4005 (1P)  |     |
| A-RAF | 385 | CEGSSLYHHLHVADTRFDMVQLIDVARQTAQGM DY LHAKNI IHRDLKSNNI FLHEGLTVK   | 444 |
| B-RAF | 532 | CEGSSLYHHLHI IETKFEMIKLID IARQTAQGM DY LHAKSI IHRDLKSNNI FLHEDLTVK | 591 |
| C-RAF | 424 | CEGSSLYKHLHVQETK FQMFQLID IARQTAQGM DY LHAKNI IHRDMKSNNI FLHEGLTVK | 483 |
|       |     | MW 2842 (2P) MW 1551 (1P)  |     |
| A-RAF | 445 | IGDFGLATV KTRW GAQPLEQPSG SVLWMAAEVIRMQDPNPYSFQSDVYAYGVVLYELMT     | 504 |
| B-RAF | 592 | IGDFGLATV KSRW S GSHQFEQLSGSILWMAPEVIRMQDKNPYSFQSDVYAFGIVLYELMT    | 651 |
| C-RAF | 484 | IGDFGLATV KSRW S GQQVEQPTGSVLWMAPEVIRMQDNNPYSFQSDVYSYGIVLYELMT     | 543 |
|       |     | MW 1436 (2P) MW 2383 (3P)  |     |
| A-RAF | 505 | GSLPYSHIGCRDQII FMVGRGYLSPDL SKI SSNCPKAMRRLI S DCLKFQREERPLFPQIL  | 564 |
| B-RAF | 652 | GQLPYSNINNRDQII FMVGRGYLSPDL SKVRSNCPKAMKRLMAECLKKRDRERPLFPQIL     | 711 |
| C-RAF | 544 | GELPYSHINNRDQII FMVGRGYLSPDL SKLYKNCPKAMKRLVADCVKVKKEERPLFPQIL     | 603 |
|       |     | MW 1691 (1P) MW 1059 (1P) MW 1479 (2P) MW 1302 (1P)                |     |
| A-RAF | 565 | ATIPELLQR L PKIERSASEPSLHR-TQADELPACL I SAARLVP-----               | 606 |
| B-RAF | 712 | ASIELLARSLPKIHRSAEPLNRAGFQTEDFSLYACASPKTPIQAGGYGAFPVH              | 766 |
| C-RAF | 604 | SSIELLOHSLPKINRSASEPSLHRAAHTEDINACTLITSPRLPVF-----                 | 648 |
|       |     | MW 1142 (2P) MW 922 (1P) MW 2446 (3P) MW 2028 (2P)                 |     |

**FIGURE 20: Sequence alignment of human A-, B- and C-RAF depicting representative tryptic phosphopeptides of A-RAF obtained by mass spectrometry analysis.** For the detailed list of all the identified phosphopeptides, see **Table 2**. The conserved regions CR1, CR2 and CR3 are highlighted in salmon pink. The sequences of tryptic phosphopeptides of A-RAF are underlined in green. The molecular weight (*MW*) of the tryptic fragments and the number of the phosphate residues (*P*) are indicated. The phosphorylation sites of A-RAF are highlighted in red (specified) and green (non-specified), and their positions within the sequence are indicated by numbers. The corresponding conserved sites in B- and C-RAF are highlighted in grey.

Furthermore, phosphorylation of three peptides at the very C-terminus of A-RAF protein has been detected (**Fig. 20** and **Table 2**). One of them (580–588) carrying one or two phosphates corresponds to the highly conserved fragment that has been reported to function as the 14-3-3 binding domain in B- and C-RAF [202,232,243]. Using fragmentation analysis serines 582 and 585 were determined as the proper A-RAF phosphorylation sites (**Fig. 20** and **Table 3**). The second peptide (589–606) carrying two phosphates cover the sequence that is non-conserved and contains two A-RAF specific phosphorylation sites, T589 and S600. The third peptide (584–603) containing three phosphate residues covers part of the 14-3-3 binding domain (pS585) and the very C-terminal sequence (pS589 and pS600).

### 6.1.2. Phosphorylation sites within the regulatory part of A-RAF

In contrast to the kinase domain, most of the identified phosphorylation sites within the regulatory part of the protein are A-RAF specific. Phosphorylation at five peptides, partially localized within the CR1 domain, that contain four putative phosphorylation sites S15, T20 and Y24 has been found (see **Fig. 20** and **Table 2**). Because the number of phosphates within these peptides corresponds to the number of phosphorylation possibilities, we propose that all these positions represent putative phosphorylation sites of A-RAF. Phosphorylation of the Y24 was confirmed additionally by nano-LC-MS/MS (see **Table 3**). Whereas S15 is conserved through all three RAF isoforms, T20 is present only in A- and C-RAF, Y62 in A- and B-RAF, and Y24 appears to be A-RAF specific site. Remarkably, the Y24 homolog in B- and C-RAF and the Y62 homolog in C-RAF are replaced by phenylalanine, the amino acid that possesses a similar aromatic structure, but cannot be phosphorylated (see **Fig. 20**). Furthermore, three peptides that were only partially phosphorylated have been detected within the CR1 domain (31–50, 93–113 and 125–139, see also **Fig. 20** and **Table 2**). Despite the fragmentation analysis, the exact positions of the phosphorylated residues within these peptides have not been specified.

The most exiting finding was the identification of numerous phosphorylation sites within the non-conserved regions of RAF. Four phosphopeptides corresponding to the sequence of the non-conserved stretch between CR1 and CR2 reveal one conserved (S186 in A-RAF) and three A-RAF specific phosphorylation sites (Y155, S157 and T189, see also **Fig. 20** and **Table 2**). Phosphorylation of the Y155, S157 and S186 was confirmed additionally by tandem mass spectrometry (**Table 3**). Furthermore, several peptides covering the segment

between residues 248–288 located within the non-conserved region between CR2 and CR3 were identified (**Fig. 20** and **Table 2**). This sequence stretch bears up to ten putative phosphorylation sites that are only partially conserved. Of importance, phosphorylation status of S257, S262, S264, S272 and S274 within this region was confirmed by nano-LC-MS/MS (**Table 3**). Two of these phosphorylation sites S257 and S262 are homologous to the serines 296 and 301 of C-RAF that were identified as feed-back regulatory sites [152,153,194]. The role of the remaining phosphorylation sites has not previously been elucidated for any RAF kinase. In addition, two phosphorylated peptides (229–247 and 298–315) were found in front of and shortly after the highly phosphorylated 248–288 region (**Fig. 20** and **Table 2**). Unfortunately, the exact positions of the phosphate residues within these peptides could not be identified even by fragmentation analysis. Nevertheless, in the case of the peptide 298–315, phosphorylation events might be ascribed to S299 and Y301/Y302, due to the findings that the homologous residues in C-RAF (S338 and Y340/Y341) are phosphorylated upon stimulation with growth factors [113,114,181,182].

To investigate the functional role of the phosphorylation sites detected by MS technique, particularly with respect to regulation of A-RAF activation, A-RAF proteins were cloned, in which serine/threonine residues were substituted by alanine at positions that appear to be of importance for the activation process.

**TABLE 2: A-RAF phosphopeptides obtained by trypsin (T) and/or GluC (G) digestion.** The putative phosphorylation sites (P-sites) and the number of the phosphates (P-number) detected in each of the peptides by mass spectrometry are indicated. The phosphorylation sites of A-RAF are highlighted in red (specified) and green (non-specified).

| Peptides   | Enzyme | P-number | P-sites                    |
|--|--------|----------|----------------------------|
| 1-16 MEPPRGPPANGAEP <b>SR</b>  | T      | 1p       | <b>S15</b>                 |
| 6-22 GPPANGAEP <b>S</b> RAV <b>G</b> TVK   | T      | 1p       | S15, T20                   |
| 17-28 AV <b>G</b> T <b>V</b> K <b>V</b> Y <b>L</b> PNK   | T      | 2p       | <b>T20, Y24</b>            |
| 17-28 AV <b>G</b> T <b>V</b> K <b>V</b> Y <b>L</b> PNK   | T      | 1p       | T20, Y24                   |
| 17-30 AV <b>G</b> T <b>V</b> K <b>V</b> Y <b>L</b> PNK <b>QR</b>   | T      | 1p       | T20, Y24                   |
| 23-28 <b>V</b> Y <b>L</b> PNK  | T      | 1p       | <b>Y24</b>                 |
| 29-47 Q <b>R</b> T <b>V</b> V <b>T</b> VRD <b>G</b> M <b>S</b> V <b>Y</b> D <b>S</b> LDK                                     | T      | 1p       | T31, T34, S40,<br>Y42, S44 |
| 31-47 <b>T</b> V <b>V</b> T <b>V</b> VRD <b>G</b> M <b>S</b> V <b>Y</b> D <b>S</b> LDK                                       | T      | 2p       | T31, T34, S40,<br>Y42, S44 |
| 31-50 <b>T</b> V <b>V</b> T <b>V</b> VRD <b>G</b> M <b>S</b> V <b>Y</b> D <b>S</b> LDK <b>ALK</b>                            | T      | 3p       | T31, T34, S40,<br>Y42, S44 |
| 37-63 D <b>G</b> M <b>S</b> V <b>Y</b> D <b>S</b> LDK <b>ALK</b> VRGLNQDCC <b>V</b> Y <b>R</b>                               | T      | 2p       | S40, Y42, S44, Y62         |
| 51-69 VRGLNQDCC <b>V</b> Y <b>R</b> LIKGRK   | T      | 1p       | <b>Y62</b>                 |
| 93-113 DV <b>P</b> L <b>T</b> M <b>H</b> N <b>F</b> V <b>R</b> K <b>T</b> <b>F</b> <b>F</b> <b>S</b> L <b>A</b> F <b>C</b> D | G      | 2p       | T97, T105, S108            |
| 125-131 C <b>Q</b> T <b>C</b> G <b>Y</b> K   | T      | 1p       | T127, Y130                 |

|         |                                       |     |    |  |
|---------|---------------------------------------|-----|----|--|
| 125-139 | CQTCGYKFHQHCSSK                       | T   | 3p | T127, Y130, S137, S138   |
| 152-166 | QQFYHVSVDLGGSR                        | T   | 1p | Y155, S157, S162, S165   |
| 167-188 | QHEAPSNRPLNELLTPQGSPR                 | T   | 1p | S172, T181, S186   |
| 179-195 | LLTPQGPSPRTQHCDPE                     | G   | 1p | T181, S186, T189   |
| 179-195 | LLTPQGPSPRTQHCDPE                     | G   | 2p | T181, S186, T189   |
| 189-209 | TQHCDPEHFPPAPANAPLQR                  | T   | 1p | T189   |
| 212-247 | STSTPNVHVMVSTTAPMDSNLIQLTGQSFSTDAAGSR | T   | 1p | S212, T213, S214, T215, S222, T223, T224, S229, T235, S238, S240, T241, S246 |
| 212-247 | STSTPNVHVMVSTTAPMDSNLIQLTGQSFSTDAAGSR | T   | 2p | S212, T213, S214, T215, S222, T223, T224, S229, T235, S238, S240, T241, S246 |
| 229-247 | SNLIQLTGQSFSTDAAGSR                   | T/G | 2p | S229, T235, S238, S240, T241, S246   |
| 248-268 | GGSDGTPRGSPSPASVSSGRK                 | T   | 1p | S250, T253, S257, S259, S262, S264, S265                                     |
| 248-267 | GGSDGTPRGSPSPASVSSGR                  | T   | 7p | S250, T253, S257, S259, S262, S264, S265                                     |
| 256-267 | GSPSPASVSSGR                          | T   | 1p | S257, S259, S262, S264, S265   |
| 256-267 | GSPSPASVSSGR                          | T   | 2p | S257, S259, S262, S264, S265   |
| 256-273 | GSPSPASVSSGRKSPHSK                    | T   | 4p | S257, S259, S262, S264, S265, S269, S272                                     |
| 256-279 | GSPSPASVSSGRKSPHSKSPAEQR              | T   | 2p | S257, S259, S262, S264, S265, S269, S272, S274                               |
| 268-288 | KSPHSKSPAEQRERKSLADDK                 | T   | 2p | S269, S272, S274, S283   |
| 268-281 | KSPHSKSPAEQRER                        | T   | 1p | S269, S272, S274   |
| 269-281 | SPHSKSPAEQRER                         | T   | 2p | S269, S272, S274   |
| 282-287 | KSLADD                                | T/G | 1p | S283   |
| 298-315 | DSGYYWEVPPSEVQLLKR                    | T   | 3p | S299, Y301, Y302, S308   |
| 305-314 | VPPSEVQLLK                            | T/G | 1p | S308   |

|         |   |     |    |                                    |
|---------|---|-----|----|------------------------------------|
| 315-326 | RIG <b>T</b> S <b>F</b> GT <b>V</b> FR  | T   | 3p | T318, S320, T323                   |
| 316-326 | IG <b>T</b> G <b>S</b> FG <b>T</b> VFR  | T   | 1p | T318, S320, T323                   |
| 337-360 | VLKV <b>S</b> Q <b>P</b> TAEQAQAFKNEMQVLRK  | T   | 2p | S341, T344                         |
| 340-359 | V <b>S</b> Q <b>P</b> TAEQAQAFKNEMQVLR  | T   | 1p | S341, T344                         |
| 340-354 | V <b>S</b> Q <b>P</b> TAEQAQAFKNE   | T/G | 2p | S341, T344                         |
| 340-360 | V <b>S</b> Q <b>P</b> TAEQAQAFKNEMQVLRK   | T   | 1p | S341, T344                         |
| 355-386 | MQVLRK <b>T</b> RHVNILLFMGF <b>M</b> TRPGFAI <b>T</b> QWCE  | G   | 1p | T361, T374, T382                   |
| 401-423 | FDMVQLIDVARQ <b>T</b> AQGMD <b>Y</b> LHAK   | T   | 2p | T413, Y419                         |
| 401-428 | FDMVQLIDVARQ <b>T</b> AQGMD <b>Y</b> LHAKNIIHRD   | T   | 2p | T413, Y419                         |
| 403-423 | MVQLIDVARQ <b>T</b> AQGMD <b>Y</b> LHAK   | T/G | 1p | T413, Y419                         |
| 403-423 | MVQLIDVARQ <b>T</b> AQGMD <b>Y</b> LHAK   | T/G | 2p | T413, Y419                         |
| 409-429 | VARQ <b>T</b> AQGMD <b>Y</b> LHAKNIIHRD   | G   | 2p | T413, Y419                         |
| 412-428 | Q <b>T</b> AQGMD <b>Y</b> LHAKNIIHR   | T   | 2p | T413, Y419                         |
| 432-444 | <b>S</b> NNIFLHEGL <b>T</b> VK  | T   | 1p | S432, T442                         |
| 445-456 | IGDFGLAT <b>V</b> K <b>T</b> R  | T   | 1p | T452, T455                         |
| 445-456 | IGDFGLAT <b>V</b> K <b>T</b> R  | T   | 2p | T452, T455                         |
| 457-476 | W <b>S</b> GAQPLEQ <b>P</b> <b>S</b> <b>G</b> S <b>V</b> LWMAAE   | T/G | 3p | S458, S467, S469                   |
| 516-548 | DQIIFMVGRG <b>Y</b> L <b>S</b> PD <b>L</b> <b>S</b> K <b>I</b> <b>S</b> S <b>N</b> CPKAMR <b>R</b> <b>L</b> <b>L</b> <b>S</b> D   | T/G | 1p | Y526, S528, S532, S535, S536, S547 |
| 517-548 | QIIFMVGRG <b>Y</b> L <b>S</b> PD <b>L</b> <b>S</b> K <b>I</b> <b>S</b> S <b>N</b> CPKAMR <b>R</b> <b>L</b> <b>L</b> <b>S</b> D  | G   | 2p | Y526, S528, S532, S535, S536, S547 |
| 517-530 | QIIFMVGRG <b>Y</b> L <b>S</b> PD  | G   | 1p | Y526, S528                         |
| 525-533 | G <b>Y</b> L <b>S</b> PD <b>L</b> <b>S</b> K  | T   | 1p | Y526, S528, S532                   |
| 525-540 | G <b>Y</b> L <b>S</b> PD <b>L</b> <b>S</b> K <b>I</b> <b>S</b> S <b>N</b> CPK   | T   | 1p | Y526, S528, S532, S535, S536       |
| 525-544 | G <b>Y</b> L <b>S</b> PD <b>L</b> <b>S</b> K <b>I</b> <b>S</b> S <b>N</b> CPKAM <b>R</b> R  | T   | 2p | Y526, S528, S532, S535, S536       |
| 534-544 | <b>I</b> <b>S</b> S <b>N</b> CPKAM <b>R</b> R   | T   | 2p | S535, S536                         |
| 534-543 | <b>I</b> <b>S</b> S <b>N</b> CPKAM <b>R</b>   | T   | 1p | S535, S536                         |
| 541-556 | AMR <b>R</b> <b>L</b> <b>L</b> <b>S</b> D <b>C</b> L <b>K</b> FQ <b>R</b> E <b>E</b>  | T/G | 1p | S547                               |
| 544-551 | R <b>L</b> <b>L</b> <b>S</b> D <b>C</b> L <b>K</b>  | T   | 1p | S547                               |
| 545-554 | L <b>L</b> <b>S</b> D <b>C</b> L <b>K</b> F <b>Q</b> R  | T   | 1p | S547                               |
| 569-578 | L <b>L</b> <b>Q</b> <b>R</b> <b>S</b> <b>L</b> <b>P</b> <b>K</b> <b>I</b> <b>E</b>  | G   | 1p | S573                               |
| 573-592 | <b>S</b> L <b>P</b> <b>K</b> <b>I</b> <b>E</b> <b>R</b> <b>S</b> <b>A</b> <b>S</b> <b>E</b> <b>P</b> <b>S</b> <b>L</b> <b>H</b> <b>R</b> <b>T</b> <b>Q</b> <b>A</b> <b>D</b>        | T/G | 3p | S573, S580, S582, S585, T589       |
| 573-579 | <b>S</b> L <b>P</b> <b>K</b> <b>I</b> <b>E</b> <b>R</b>   | T   | 1p | S573                               |
| 577-588 | <b>I</b> <b>E</b> <b>R</b> <b>S</b> <b>A</b> <b>S</b> <b>E</b> <b>P</b> <b>S</b> <b>L</b> <b>H</b> <b>R</b>   | T   | 1p | S580, S582, S585                   |
| 580-588 | <b>S</b> <b>A</b> <b>S</b> <b>E</b> <b>P</b> <b>S</b> <b>L</b> <b>H</b> <b>R</b>  | T   | 1p | S580, S582, S585                   |
| 580-588 | <b>S</b> <b>A</b> <b>S</b> <b>E</b> <b>P</b> <b>S</b> <b>L</b> <b>H</b> <b>R</b>  | T   | 2p | S580, S582, S585                   |
| 584-603 | <b>P</b> <b>S</b> <b>L</b> <b>H</b> <b>R</b> <b>T</b> <b>Q</b> <b>A</b> <b>D</b> <b>E</b> <b>L</b> <b>P</b> <b>A</b> <b>C</b> <b>L</b> <b>L</b> <b>S</b> <b>A</b> <b>A</b> <b>R</b> | T/G | 3p | S585, T589, S600                   |
| 589-606 | <b>T</b> <b>Q</b> <b>A</b> <b>D</b> <b>E</b> <b>L</b> <b>P</b> <b>A</b> <b>C</b> <b>L</b> <b>L</b> <b>S</b> <b>A</b> <b>A</b> <b>R</b> <b>L</b> <b>V</b> <b>P</b>                   | T   | 2p | T589, S600                         |

**TABLE 3: Phosphorylation sites specified by fragmentation analysis using nano-LC-MS/MS approach.** P-site, phosphorylation site; z, precursor charge; m/z, mass-to-charge ratio; Mr(expt), experimental mass; Mr(calc), theoretical mass; Delta, mass deviance Mr(expt)-Mr(calc). All *Mascot*<sup>TM</sup> results pages of the manually validated phosphopeptide spectra from this table are attached in the appendix part.

| Position | Peptide sequence         | P-site     | m/z    | z | Mr(expt) | Mr(calc) | Delta | Mass analyzer |
|----------|--------------------------|------------|--------|---|----------|----------|-------|---------------|
| 17-28    | AVGTVKVPYLPNK            | Y24        | 685,00 | 2 | 1367,98  | 1367,72  | 0,26  | LTQ XL        |
| 152-166  | QQFpYHSVQDLSSGSR         | Y155       | 597,21 | 3 | 1788,62  | 1787,76  | 0,85  | LTQ XL        |
| 152-166  | QQFYHpSVQDLSSGSR         | S157       | 596,93 | 3 | 1787,76  | 1787,76  | 0,00  | QstarElite    |
| 167-188  | QHEAPSNRPLNELLTP-QGPpSPR | S186       | 840,48 | 3 | 2518,42  | 2517,21  | 1,21  | LTQ XL        |
| 256-267  | GpSPSPASVSSGR            | S257       | 584,75 | 2 | 1167,49  | 1167,49  | 0,00  | QstarElite    |
| 256-267  | GpSPSPApSVSSGR           | S257, S262 | 624,83 | 2 | 1247,64  | 1247,46  | 0,19  | LTQ XL        |
| 256-267  | GpSPSPASVpSSGR           | S257, S264 | 625,35 | 2 | 1248,68  | 1247,46  | 1,22  | LTQ XL        |
| 269-281  | SPHpSKpSPAQRER           | S272, S274 | 556,92 | 3 | 1667,72  | 1667,68  | 0,04  | LTQ XL        |
| 316-326  | IGpTGSFGTVFR             | T318       | 611,29 | 2 | 1220,56  | 1220,56  | 0,00  | QstarElite    |
| 445-456  | IGDFGLApTVKpTR           | T452, T455 | 719,21 | 2 | 1436,40  | 1436,65  | -0,25 | LTQ XL        |
| 544-551  | RLLpSDCLK                | S547       | 502,78 | 2 | 1003,55  | 1003,55  | 0,00  | QstarElite    |
| 580-588  | SAPpSEPSLHR              | S582       | 532,23 | 2 | 1062,44  | 1062,45  | -0,01 | QstarElite    |
| 580-588  | SAPpSEPpSLHR             | S582, S585 | 572,20 | 2 | 1142,40  | 1142,40  | -0,02 | QstarElite    |

## 6.2. A-RAF kinase activity is regulated by 14-3-3 proteins

14-3-3 proteins have been found to support RAF activation [219]. On the other hand, it has also been reported that 14-3-3 are not essential for RAF function [286]. All three RAF kinases possess two typical 14-3-3 binding sites surrounding serines 621/259, 729/365 and 582/214 in C-, B- and A-RAF, respectively. However, while the C-terminal 14-3-3 protein binding motif (RSAPSEP) of RAF kinases is highly conserved, the sequence surrounding serine 365 in B-RAF (RSSpSAP) differs significantly from the corresponding 14-3-3 binding motifs in A- and C-RAF (RSTpSTP) (see also **Figs. 20** and **24C**).

Association of 14-3-3 proteins with B- and C-RAF has been documented [202,243,287]. In contrast, although A-RAF contains the typical 14-3-3 binding domains, little is known about the binding and regulation of A-RAF kinase activity by 14-3-3 proteins. MS analysis of A-RAF phosphorylation yielded several phosphopeptides corresponding to the A-RAF 580–588 segment and comprising the C-terminal 14-3-3 binding domain (**Fig. 20** and **Table 2**). Fragmentation analysis revealed phosphorylations at the serines 582 and 585. In addition, the phosphospecific antibody 6B4 directed against the homologous C-terminal 14-3-3 binding site of C-RAF (pS621) identified A-RAF wild type, but not the A-RAF-



S582A mutant (**Figs. 21A and 22**). Regarding the internal 14-3-3 binding domain of A-RAF surrounding serine 214, a phosphopeptide corresponding to this region has not been detected. Nevertheless, using phosphospecific antibody directed against internal 14-3-3 binding domain of C-RAF surrounding the S259, that reveals high homology to the internal 14-3-3 binding domain of A-RAF, it is shown here that A-RAF is phosphorylated at S214. Both, non-activated A-RAF and A-RAF co-expressed with Ras12V and Lck were detectable by use of anti-pS259 antibody (**Figs. 21A and 22**). Replacement of S214 by alanine completely abolished the phosphate detection by anti-pS259 antibody.

### 6.2.1. Regulation of A-RAF activity by 14-3-3 in Sf9 cells

The presence of the serines 621 and 729 in C- and B-RAF, respectively, has been shown to be necessary for the effective activation of these kinases [202,243]. This raised the question whether phosphorylation of the corresponding serine 582 in A-RAF exhibits similar effects. To answer this question, the extent of kinase activity of A-RAF WT and A-RAF mutants (A-RAF-S214A and A-RAF-S582A) was examined in the basal state and upon co-expression with Ras12V and Lck. To this end, A-RAF proteins were expressed in Sf9 cell in the presence and absence of H-Ras12V and Lck. Cells were lysed and the *in vitro* kinase assay using MEK and ERK as coupled substrates was carried out. The samples were separated by SDS-PAGE, the proteins were blotted to the nitrocellulose membrane and probed with an appropriate antibody. Results shown in **Fig. 21** document that the presence of the intact C-terminal 14-3-3 binding domain was partially required for effective kinase stimulation by Ras12V and Lck, because the degree of Ras/Lck-induced activation of A-RAF-S582A was lower than that of A-RAF WT. Moreover, the basal activity of A-RAF-S582A was completely abolished upon substitution of S582 by alanine. Regarding the second (internal) 14-3-3 binding site, it has been reported that substitution of S365 by alanine in B-RAF led to a strong increase of kinase activity, indicating that the phosphorylation of this site acts highly inhibitory [243]. Similar observations have been also obtained for C-RAF; however, the stimulatory effects were lower compared to B-RAF [288]. In the case of A-RAF, we found that both, the basal and the inducible kinase activities of the A-RAF-S214A mutant were considerably elevated compared to the wild type, resulting in an active form of A-RAF (**Fig. 21**). These results suggest that A-RAF activation is strongly influenced by both 14-3-3 binding domains.

### 6.2.2. Regulation of A-RAF activity by 14-3-3 in COS7 cells

To test whether results obtained from the heterogeneous cell system (Sf9 insect cells) possessing only two 14-3-3 isoforms could be applied to the mammalian cells expressing seven 14-3-3 isoforms [289], we analyzed the kinase activity and phosphorylation

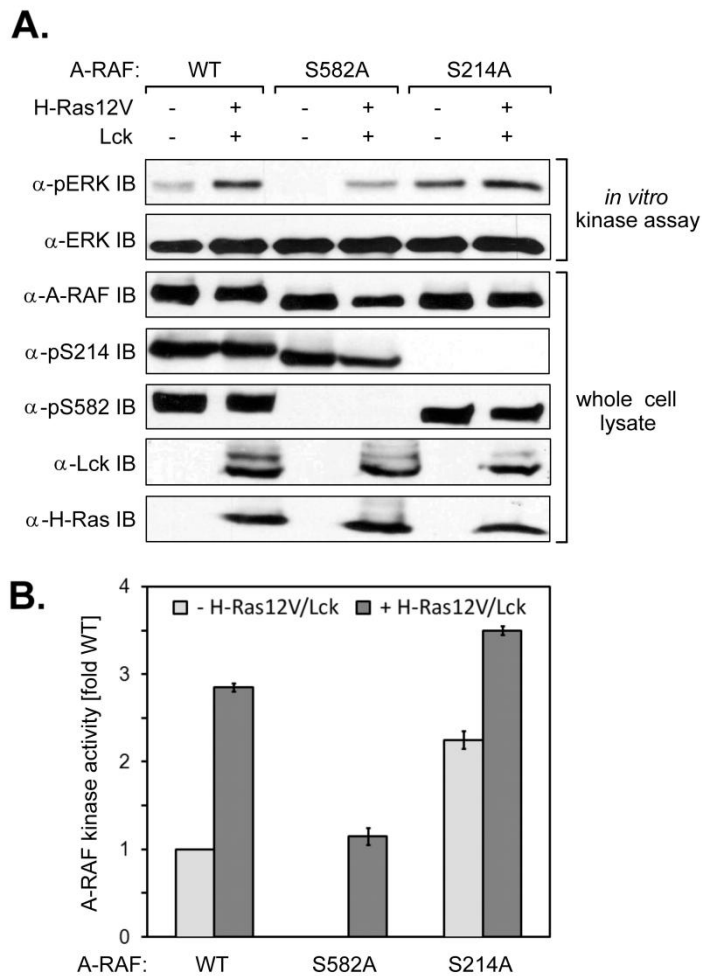


**FIGURE 21: A-RAF activity is regulated by phosphorylation of both, internal and C-terminal 14-3-3 binding sites.** (A) Western blot analysis of A-RAF kinase activity and phosphorylation degree of 14-3-3 binding sites. A-RAF wild type (WT) and A-RAF substitution mutants modified at the C-terminal (S582A) and internal (S214A) 14-3-3 binding sites were expressed in Sf9 insect cells in the presence and absence of Ras12V and Lck. The cells were lysed using detergent containing buffer. Subsequently, coupled kinase assay using recombinant MEK and ERK as substrates has been carried out, and the extents of kinase activities were monitored by anti-pERK antibody. To monitor the phosphorylation degree of A-RAF in the positions S214 and S582, the C-RAF phosphospecific antibodies anti-pS259 and anti-pS621 (see also Hekman *et al.* [202]) were used. Due to the homology of the corresponding epitopes, these antibodies detect both RAF isoforms with comparable affinity. (B) Quantification of A-RAF kinase activity. Representative blots from A were

quantified by optical densitometry. The quantification results are expressed in terms of fold activation, where 1-fold activity represents the amount of activity determined for A-RAF wild type under non-stimulating conditions. Average values derived from the data of three independent experiments were used for quantification. Expression efficiency of H-Ras12V and Lck was determined using anti-H-Ras and anti-Lck antibodies, respectively. *IB*, immunoblot.

status of A-RAF wild type and 14-3-3 binding mutants expressed in and isolated from COS7 cells. Furthermore, we extended this experiment by inclusion of A-RAF-S214A/S582A double mutant and by stimulation of the cells with EGF for 5 minutes. Similar to insect cell system, wild type A-RAF expressed in COS7 cells is phosphorylated on S214 and S582 in both activated and non-activated samples (**Fig. 22**). Substitution of serines in these positions by alanine completely abolished the phosphate detection by anti-pS259 and anti-pS621 antibody. Differently to the situation in the Sf9 cells, the replacement of S214 in A-RAF by alanine led to a strong reduction of S582 phosphorylation in non-stimulated cells and samples treated with EGF, indicating interdependence between these two 14-3-3 binding sites in COS7 cells. In the case of maximal activation by co-expression with Ras12V/Lck, phosphorylation of S582 did not depend on a presence of phosphoserine in position 214 (**Fig. 22**). Several differences between the two cell systems were also observed regarding the kinase activity of A-RAF 14-3-3 binding mutants. We found that in contrast to Sf9 cells, the kinase activity of

A-RAF-S214A mutant in COS7 cells was highly reduced even in the presence of Ras and Lck (see **Figs. 21** and **22**). These results indicate that activation of A-RAF is regulated positively by S214 in COS7 cells. A possible explanation for these effect may be the finding that A-RAF-S214A mutant was not phosphorylated at the position S582 (see **Fig. 22**), thus, making impossible any association with 14-3-3 proteins. Similar consideration may be also applied to inhibited activation of the double mutant A-RAF-S214A/S582A. In the case of A-RAF-S582A mutant isolated from the non-stimulated cells, we did not observe any differences in kinase activity compared to wild type. In contrast, the kinase activity of A-RAF-S582A mutant was slightly reduced relative to A-RAF WT in EGF-activated cells and strongly reduced in cells co-transfected with Ras12V/Lck (see **Fig. 22**). In conclusion, we propose that behavior of A-RAF 14-3-3 binding mutants depends strongly on the cell system, probably due to the differences in the number and properties of 14-3-3 proteins present in these cells.

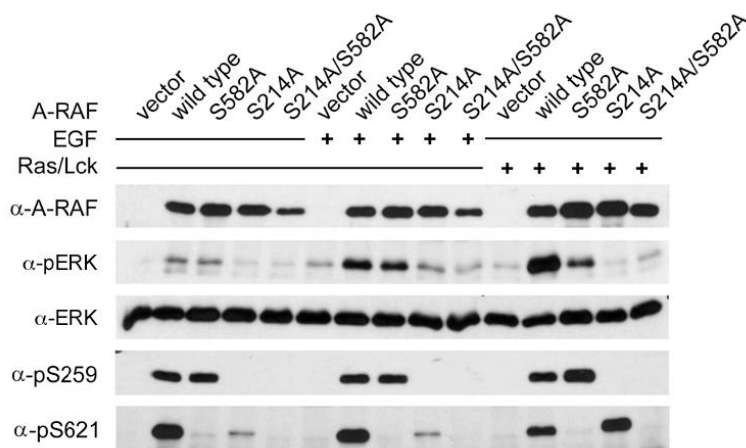


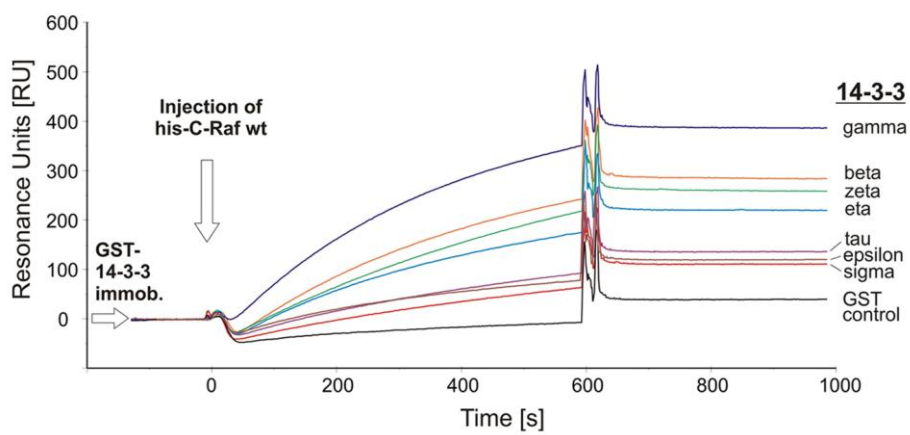
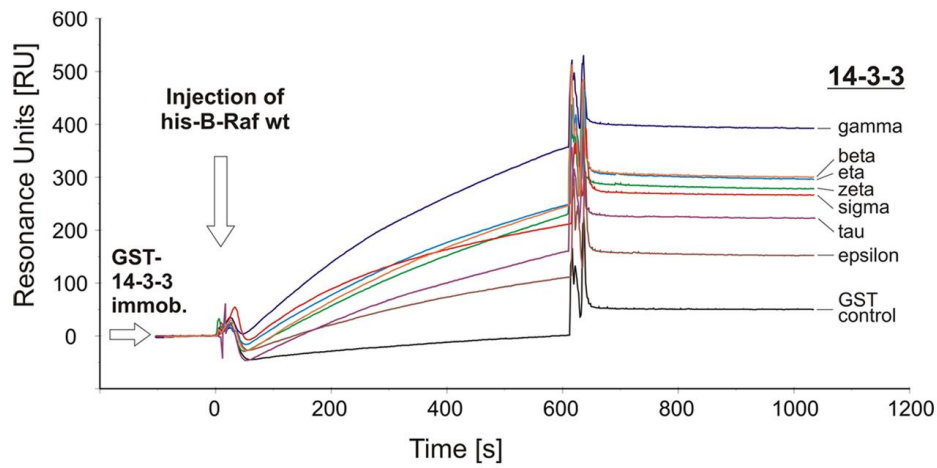
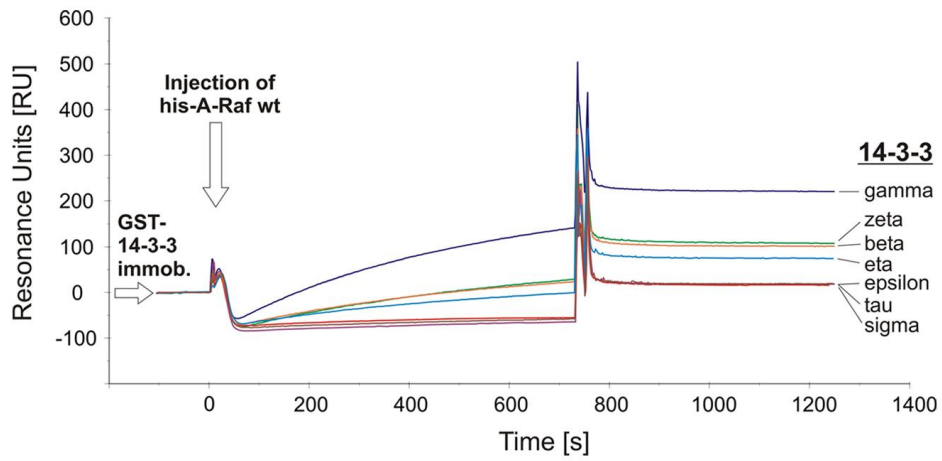
**FIGURE 22: Analysis of the phosphorylation state of 14-3-3 binding sites in A-RAF and changes of kinase activities caused by mutations within the 14-3-3 binding domains.** To determine the extents of phosphorylation at the 14-3-3 binding sites, the phosphospecific antibodies directed against pS259 and pS621 of C-RAF have been used for A-RAF, as these antibodies cross-link with adequate positions in this isoform. A-RAF WT (Myc-tagged) and indicated A-RAF mutants

impaired in 14-3-3 binding were immunoprecipitated from COS7 cell lysates by an anti-Myc antibody. The kinase activity measurements were performed directly using immunoprecipitated material attached to protein G-agarose. Stimulation of A-RAF was performed either with EGF (100 ng/ml) for 5 minutes or by co-expression with Ras12V and Lck.

### 6.2.3. Mammalian 14-3-3 proteins associate with RAF kinases in isoform-specific manner

As already mentioned in the introduction section, mammalian RAF isoforms show remarkable differences with respect to basal and growth factor-induced activity. Whereas the kinase activity of B-RAF is extraordinary high, C- and particularly A-RAF possess considerably lower enzymatic activity [113,114,181,182]. Because binding to 14-3-3 proteins plays a crucial role in the regulation of RAF activation, we assumed that potential differences in association with 14-3-3 proteins may in part determine the degree of activity of RAF isoforms. The use of purified recombinant 14-3-3 proteins and RAF kinases allows the assessment of specificity and affinity of the single mammalian 14-3-3 proteins regarding its

A



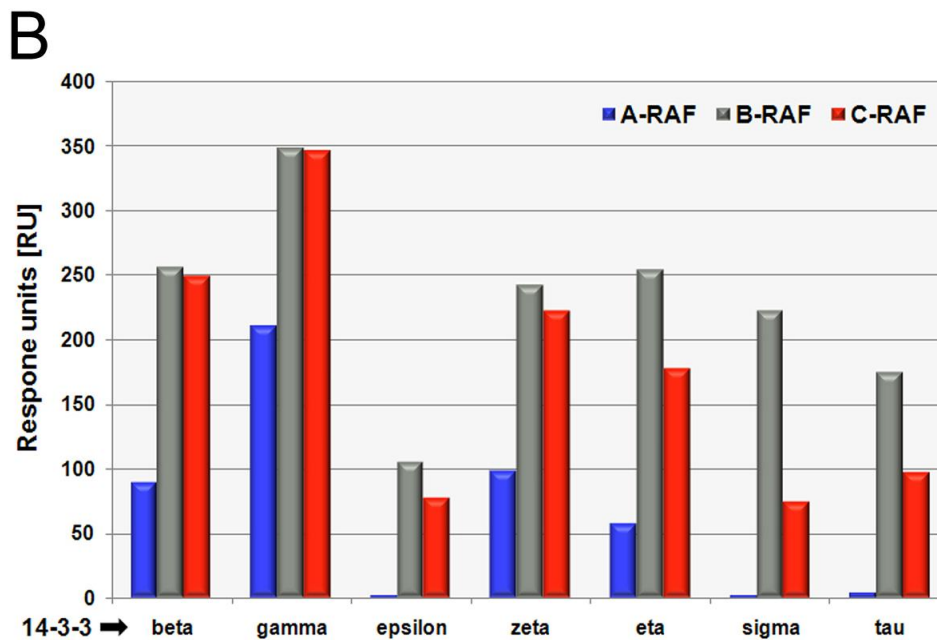


**FIGURE 23: Mammalian 14-3-3 proteins associate *in vitro* with A-, B- and C-RAF in an isoform-specific manner.** (A) Biosensor analysis of 14-3-3 binding to purified A-, B- and C-RAF. Purified and GST-tagged mammalian 14-3-3 proteins were captured by immobilized anti-GST antibody as indicated. Approximately 1100 resonance units (RU) were bound for each binding assay. In the next step His-tagged A-, B- and C-RAF were injected and the association–dissociation curves were detected. (B) Quantification of binding of 14-3-3 proteins to A-, B- and C-RAF. Biosensor analysis of 14-3-3 binding to C-RAF was performed by A. Fischer (MSZ).

binding to RAF isoforms. To address this issue we performed detailed binding studies with purified components using SPR technique. Thus, here we extended our investigations described previously in Hekman *et al.* [202] and measured binding of A-, B- and C-RAF kinases to all of the seven known mammalian 14-3-3 protein isoforms ( $\beta$ ,  $\gamma$ ,  $\epsilon$ ,  $\sigma$ ,  $\zeta$ ,  $\tau$  and  $\eta$ ) (association of 14-3-3 proteins with C-RAF was measured by A. Fischer, MSZ). For that purpose, GST-tagged 14-3-3 isoforms were immobilized to the biosensor chip that has been loaded covalently with an anti-GST antibody. Next, the purified and His-tagged RAF proteins were injected. In order to remove the endogenous 14-3-3 attached to RAF, we used in this binding assay RAF proteins that have been purified in the presence of Empigen. Under these conditions, no 14-3-3 protein remained associated with RAF (data not shown). Association–dissociation curves obtained for the interactions between the recombinant 14-3-3 proteins and RAF kinases document significant differences in binding of 14-3-3 isoforms to A-, B- and C-RAF (**Fig. 23**). While B- and C-RAF exhibited binding to all of the seven 14-3-3 isoforms, A-RAF revealed no binding affinities to epsilon, tau and sigma 14-3-3. The association rates of 14-3-3 binding to B- and C-RAF are comparable; in contrast, the  $k_{on}$  for A-RAF binding was lower. The common feature for all of the RAF isoforms was the finding that 14-3-3 gamma bound with highest affinity and 14-3-3 epsilon (in the case of B- and C-RAF) with lowest affinity among the seven 14-3-3 isoforms. In addition, we observed that 14-3-3 sigma revealed much higher affinity for B-RAF compared to A- and C-RAF (**Fig. 23**). Thus, we

show here that mammalian 14-3-3 proteins associate with RAF in a pronounced isoform-specific manner.

The findings that A-RAF associates slower and only with four 14-3-3 isoforms may explain the low abundance of 14-3-3 in purified A-RAF samples. In contrast, B-RAF purified by our group from mammalian or Sf9 cells contained almost equimolar amounts of 14-3-3 proteins, indicating highest affinity for 14-3-3 proteins among RAF isoforms. The amount of C-RAF associated 14-3-3 was only moderate compared to B-RAF [205]. Thus, the affinities of RAF isoforms to 14-3-3 proteins are consistent with their kinase activities, suggesting that the low kinase activity of A-RAF may be a consequence of insufficient binding to 14-3-3 proteins.

#### 6.2.4. 14-3-3 binding sites of RAF kinases differ in their binding affinities

Results presented in **Fig. 23** document that mammalian 14-3-3 isoforms bind differentially to RAF isoforms. However, these data did not provide information about the binding strength of 14-3-3 to the individual binding domains in A-, B- and C-RAF. To assess the binding affinities of 14-3-3 for the C-terminal and internal binding domains in RAF we developed an indirect competition assay, in which we used purified full-length protein components (RAF and 14-3-3 proteins) and synthetic phosphopeptides serving as competitive inhibitors for the RAF/14-3-3 interaction. The phosphopeptides were derived from the corresponding C-terminal and internal 14-3-3 binding domains of A-, B- and C-RAF. The purified and His-tagged RAF preparations used here were rid of 14-3-3 proteins. The 14-3-3/C-RAF association was monitored by SPR technique. Because 14-3-3 zeta isoform has been found to interact with similar affinities with all three RAF isoforms, we used this 14-3-3 isoform for competition studies presented here. For that purpose, GST-14-3-3 zeta protein was first captured by immobilized anti-GST antibody and RAF association was monitored in the absence of synthetic peptides similar to experiments depicted in **Fig. 23**. This value has been defined as 100 % binding. Next, phosphopeptides derived from 14-3-3 binding domains over a range of concentration between  $10^{-4}$  and  $10^{-9}$  M were mixed with RAF proteins and the degree of RAF/14-3-3 inhibition was detected. As demonstrated in **Fig. 24A**, peptides corresponding to the C-terminal 14-3-3 binding sites of A-, B- and C-RAF revealed considerably higher inhibitory potential than peptides derived from the internal binding sites competing with an  $IC_{50}$  value of approximately 50–100 nM. Thus, data presented in **Fig. 24** suggest that the C-terminal 14-3-3 binding domain in RAF represents the high affinity-binding site and probably the major binding epitope. These data are in accordance with previously published findings [202]. Among C-terminal peptides, no significant differences were monitored regarding inhibition of the RAF/14-3-3 binding. In contrast, peptides corresponding to the internal binding sites exhibited differential inhibitory potential. As illustrated in **Fig. 24B**, the peptide corresponding to the B-RAF internal binding site revealed highest affinity for the 14-3-3 zeta isoform following by C- and A-RAF peptides. These results suggest that B-RAF may bind 14-3-3 with highest binding capacity, indicating that the complex strength to 14-3-3 may be higher in the case of B-RAF compared to C- and A-RAF.

These observations are in accordance with the data presented in the section 6.2.3. and suggest that differences in the affinity of 14-3-3 proteins to RAF isoforms are determined *inter alia* by the internal 14-3-3 binding site.

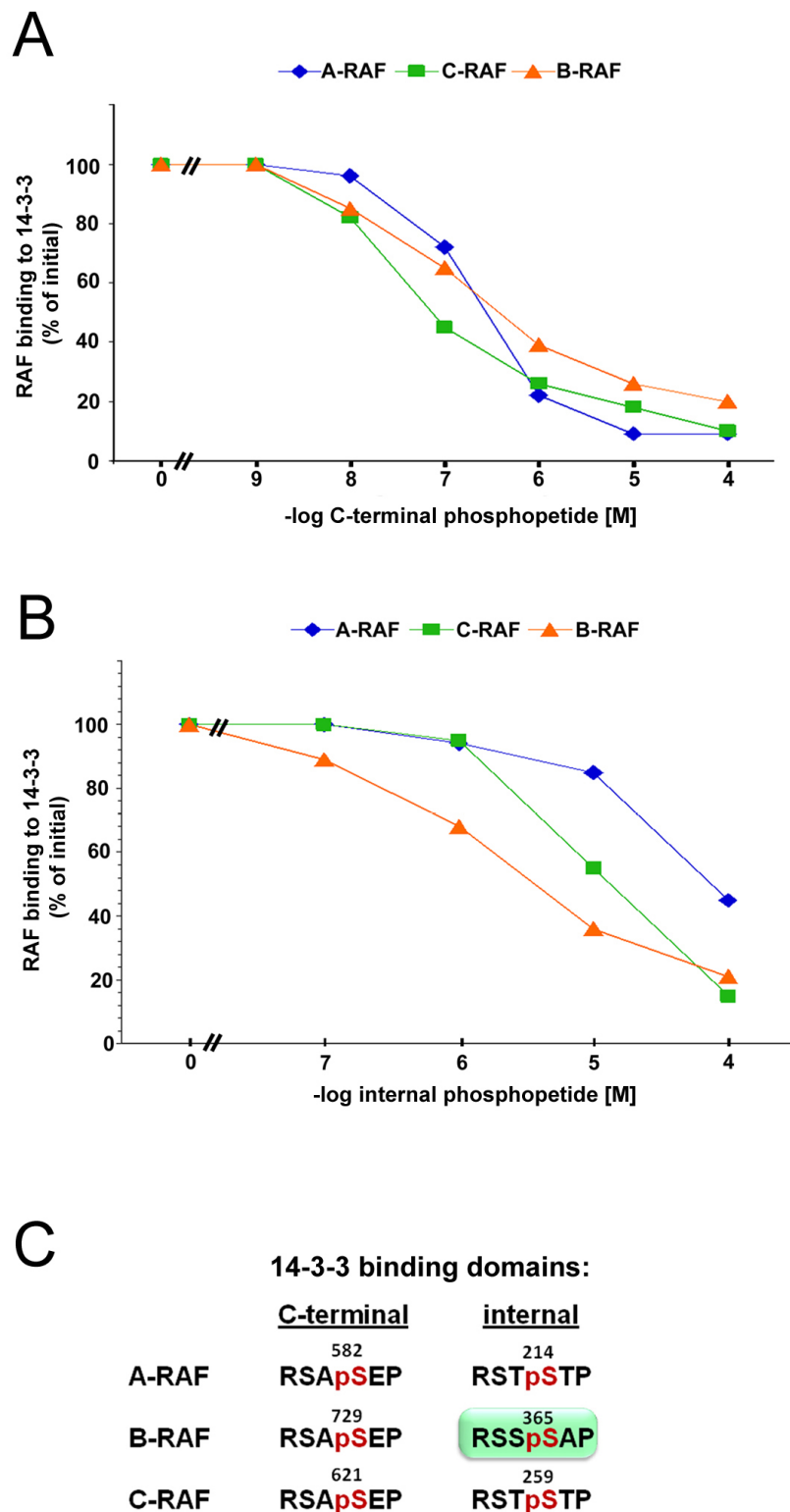


**FIGURE 24: Inhibition of RAF binding to 14-3-3 zeta by phosphopeptides derived from the C-terminal and internal 14-3-3 binding domains of A-, B- and C-RAF.** Purified and GST-tagged 14-3-3 zeta was captured by immobilized anti-GST antibody. Approximately 900 RU of 14-3-3 were

bound for each measurement. In the next step, purified C-RAF (10 pmol) was injected in the presence and absence of phosphopeptides corresponding either to the C-terminal 14-3-3 binding domains of A-, B- and C-RAF (**A**) or internal 14-3-3 binding domains (**B**). Phosphopeptides were mixed with RAF samples over a range of concentration between  $10^{-4}$  and  $10^{-9}$  M and injected without incubation. The core sequences of the internal and C-terminal 14-3-3 binding domains of A-, B- and C-RAF are depicted in **C**.

### 6.3. Phosphorylation of MEK binding sites is critical for A-RAF kinase activity

As presented in **Fig. 20** and **Table 2** a tryptic peptide with the molecular weight of 1551 Da carrying one phosphate was detected among others. This peptide has been ascribed to the highly conserved region of RAF kinases located between residues 432 and 444 in A-RAF having the following amino acid sequence: SNNIFLHEGLTVK. Zhu *et al.* [132] showed previously that the corresponding sites in C- and B-RAF (S471 and S578, respectively) located within this conserved region are critical for kinase activity and for interaction with MEK. The A-RAF fragment 432–444 possesses two putative phosphorylation

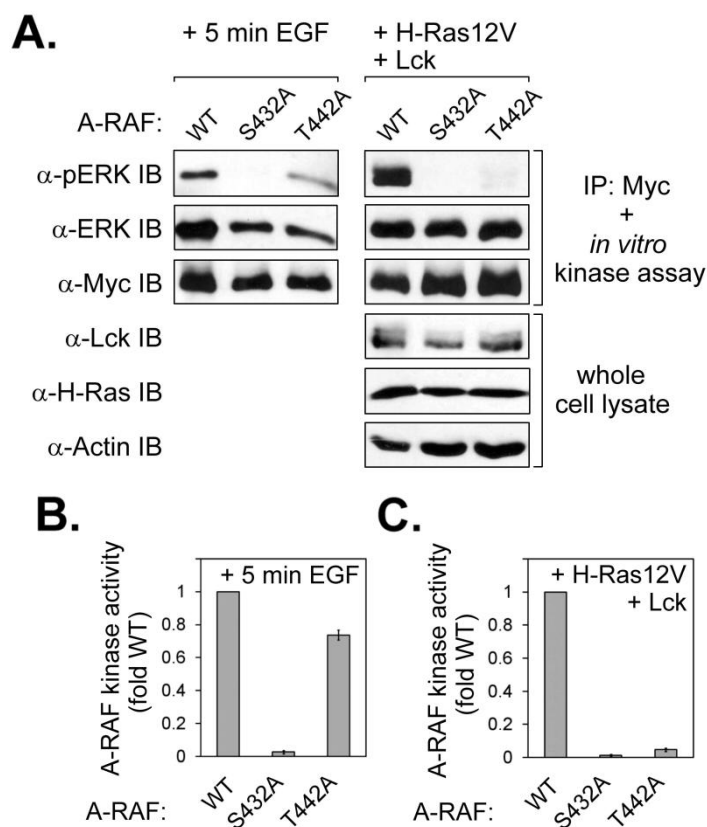


**FIGURE 25: Serine 432 is critical for catalytic activity of A-RAF *in vivo*.** (**A**) Western blot analysis of A-RAF kinase activity. C-terminal Myc-tagged A-RAF wild type (WT) and substitution mutants (S432A and T442A) were expressed in COS7 cells. Stimulation was performed either by treatment of the cells with EGF (100 ng/ml) for 5 minutes or by co-expression with H-Ras12V and Lck. Cells were lysed and A-RAF proteins were immunoprecipitated (IP) by use of an anti-Myc antibody. Subsequently, kinase activity was determined in the presence of recombinant MEK and ERK as substrates. ERK phosphorylation was detected by phosphospecific anti-ERK antibody. (**B and C**) Quantification of A-RAF kinase activity upon activation with EGF or co-expression with Ras12V/Lck, respectively. Representative blots from the **A** were quantified by optical densitometry. The quantification results are expressed in terms of fold activation, where 1-fold activity

represents the amount of activity determined for A-RAF wild type. Average values derived from the data of three independent experiments were used for quantification. Expression efficiency of H-Ras12V and Lck was determined using anti-H-Ras and anti-Lck antibodies, respectively. Actin immunodetection was used as a loading control. *IB*, immunoblot.



sites, S432 and T442. However, even the analysis by nano-LC-MS/MS did not provide information, which of these sites is being phosphorylated. To specify the functional significance of these novel phosphorylation sites in A-RAF the effects of mutations at these sites on A-RAF stimulation were examined. To this end, both A-RAF point mutants (A-RAF-S432A and A-RAF-T442A) were prepared using site-directed mutagenesis. To study the kinase activity, A-RAF WT and the A-RAF mutants were transfected into COS7 cells. Following EGF stimulation of the cells and immunoprecipitation of A-RAF proteins, kinase activities of the A-RAF mutants were compared with that of A-RAF WT. In order to achieve maximal activation, A-RAF WT and mutants were alternatively stimulated by co-expression with Ras12V and Lck. As demonstrated in **Fig. 25A** and **B**, in the case of EGF stimulation the exchange of S432 by alanine resulted in a complete abolishment of A-RAF activity, whereas A-RAF-T442A variant exhibited only a moderate reduction of kinase activity compared to A-RAF WT. These data indicate that the A-RAF residue S432, in contrast to T442, is critical for EGF-mediated A-RAF signaling, similar to the findings of Zhu *et al.* [132]. Notably, in the case of maximal activation by co-expression with Ras12V and Lck, the substitution of both residues, S432 and T442, led to marked decrease of kinase activity (**Fig. 25A** and **C**), indicating an additional aspect in the mechanism of A-RAF activation, which could not be identified by activation with EGF alone.

#### **6.4. Phosphorylation of the activation segment is necessary for maximal activation of A-RAF**

Phosphorylation of amino acids within the kinase activation loop has been reported to be necessary for activation of several protein kinases including MEK [121] and ERK [290]. The kinase activation loop is highly conserved in all RAF family kinases and lies between the kinase subdomains VII and VIII (amino acids 447–476 in A-RAF, see also **Fig. 20**). Phosphorylation of the activation segment in B- and C-RAF occurs at the conserved threonine and serine residues: in B-RAF, these are T599 and S602, and the corresponding residues in C-RAF are T491 and S494. Although phosphorylation of T599/S602 in B-RAF is sufficient to generate a highly active state of this kinase [239], the corresponding sites in C-RAF require support by additional phosphorylation [240]. Notably, no data are available regarding phosphorylation of A-RAF within its activation segment. Therefore, we searched for the phosphorylated fragment in the mass spectrometry data, corresponding to the putative A-RAF activation segment. As shown in **Fig. 20** and **Table 2**, we detected an A-RAF fragment (IGDFGLATVKTR) corresponding to the activation segment. Both of the putative phosphorylation sites (T452 and T455) within this peptide were phosphorylated, as revealed by fragmentation analysis (**Table 3**). This finding indicates that both of these threonines may play a regulatory role in A-RAF activation. To test this assumption, we prepared A-RAF point mutants in which the threonines 452 and 455 were substituted by alanines. COS7 cells were used for expression of A-RAF WT, A-RAF-T452A and A-RAF-T455A mutants. Following EGF stimulation or co-expression with Ras12V and Lck and subsequent immunoprecipitation

of the A-RAF proteins, the levels of kinase activities were detected by means of the coupled kinase assay using recombinant MEK and ERK. As shown in **Fig. 26A** and **B**, we did not observe any significant differences in the magnitude of kinase activity for A-RAF-T452A and A-RAF-T455A variants compared to A-RAF WT following EGF stimulation. Surprisingly, the Ras12V/Lck-mediated activation of A-RAF was strongly reduced by substitution of T452 or T455 with alanine (**Fig. 26A** and **C**). These results indicate that phosphorylation of A-RAF activation segment does not play a crucial role in the course of EGF-mediated activation; however, it is necessary for maximal A-RAF activation.

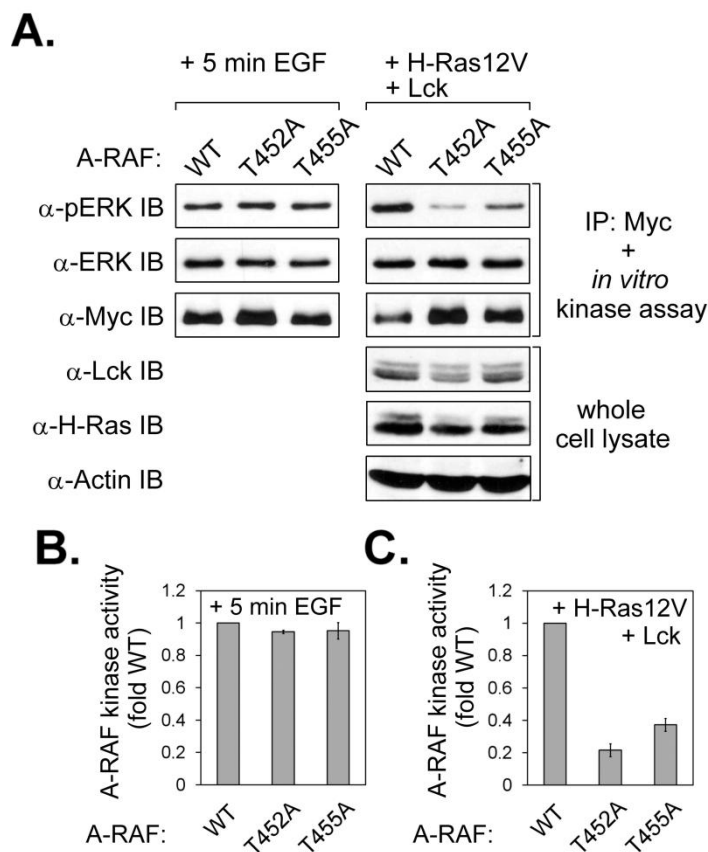


**FIGURE 26: Threonines 452 and 455 located within the activation segment are not involved in the EGF-mediated stimulation of A-RAF.** (A) Western blot analysis of A-RAF kinase activity. C-terminal Myc-tagged A-RAF wild type (WT) and substitution mutants (T452A and T455A) were expressed in COS7 cells. Stimulation was performed either by treatment of the cells with EGF (100 ng/ml) for 5 minutes or by co-expression with H-Ras12V and Lck. Cells were lysed and A-RAF proteins were immunoprecipitated (IP) by use of an anti-Myc antibody. Subsequently, coupled kinase assay using recombinant MEK and ERK as substrates has been carried out and the extents of kinase activities were monitored by anti-pERK antibody. (B and C) Quantification of A-RAF kinase activity upon activation with EGF or co-expression with H-Ras12V/Lck, respectively. Representative blots from the A were quantified by optical densitometry. The quantification

results are expressed in terms of fold activation, where 1-fold activity represents the amount of activity determined for A-RAF wild type. Average values derived from the data of three independent experiments were used for quantification. Expression efficiency of H-Ras12V and Lck was determined using anti-H-Ras and anti-Lck antibodies, respectively. Actin immunodetection was used as a loading control. *IB*, immunoblot.

## 6.5. N-region determines low basal activity and limited inducibility of A-RAF kinase

A short conserved sequence in front of the kinase domain, also called N-region (the name is derived from Negative-charge regulatory region), has been reported to be necessary for the basal activity and growth factor-induced activation of RAF kinases. This region

contains one highly conserved serine, which is present in all three RAF isoforms (S299 in A-RAF, S338 in C-RAF and S446 in B-RAF) and two conserved tyrosines (Y301/Y302 in A-RAF and Y340/Y341 in C-RAF) at positions where in B-RAF aspartates are located (D448/D449) (**Fig. 27A**). Stimulation-dependent phosphorylation of these sites positively regulates kinase activity of C- and B-RAF [113,114,181,182]. In the case of A-RAF, a stimulating role of tyrosines 301/302, corresponding to tyrosines 340/341 in C-RAF, has been demonstrated [113], whereas involvement of serine 299 in regulation of A-RAF kinase activity has not been investigated.

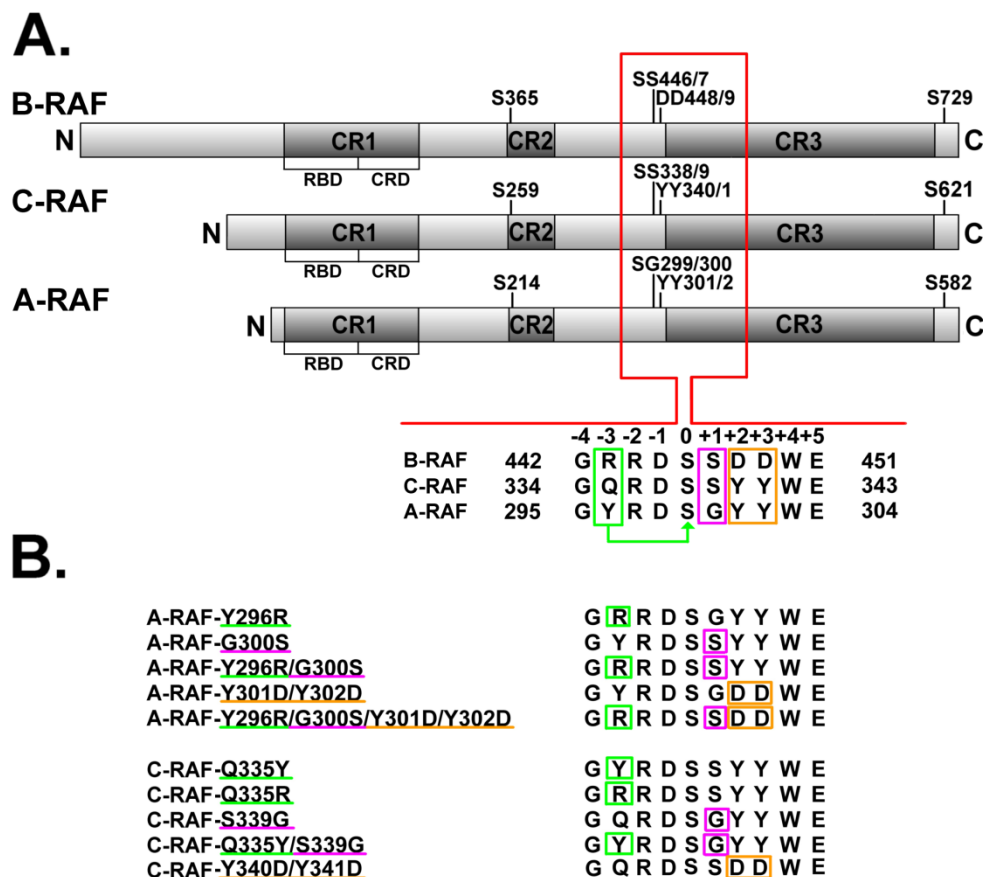


**FIGURE 27: Schematic presentation of A-, B- and C-RAF proteins and sequences of the N-region of wild type proteins and of the A- and C-RAF substitution mutants investigated in this work.** (A) *Upper panel*, schematic presentation of A-, B- and C-RAF kinases with conserved regulatory phosphorylation sites within N-region and within 14-3-3 protein binding sites. *Light shaded boxes*, non-conserved parts of the sequence; *dark shaded boxes*, conserved regions. CR1 consists of the Ras binding domain (RBD) and the cysteine rich domain (CRD). CR2 is the serine-threonine rich domain and CR3 is the kinase domain. Phosphorylation sites within the N-region are indicated by a *red rectangle*. *Lower panel*, alignment of the N-region sequences of three RAF isoforms. The variable amino acids are indicated by *colored rectangles*. (B) Alignment of the N-region sequences of A- and C-RAF substitution mutants investigated in this work. *Green rectangles*, substitutions at position -3 to conserved phosphoserine; *purple rectangles*, substitutions at position +1 to conserved phosphoserine; *orange rectangles*, substitutions at positions +2 and +3 to conserved phosphoserine.

### 6.5.1. Substitution of serine 299 to alanine in A-RAF abrogates its activation

As already reported and shown in **Fig. 20** and **Table 2**, a tryptic peptide (298–315) carrying three phosphates and corresponding to the sequence of the N-region of A-RAF was detected by MS. This A-RAF fragment contains four putative phosphorylation sites: S299, Y301, Y302 and S308. However, fragmentation analysis did not determine the exact phosphorylation positions. To determine whether phosphorylation of serine 299 is essential for A-RAF activation as shown for serine 338 in C-RAF [181], we generated the A-RAF-S299A mutant. Wild type and mutant A-RAF expressed in Sf9 cells alone or in combination with H-Ras12V and/or Lck were tested for kinase activity and the level of tyrosine phosphorylation at position 301/302. As shown in **Fig. 28**, we observed enhanced tyrosine phosphorylation in the presence of Lck in both, A-RAF wild type and A-RAF-S299A mutant, suggesting that S299A substitution did not prevent the tyrosine phosphorylation in A-RAF-S299A. However, this substitution almost completely abrogated activation of A-RAF kinase (see **Fig. 28**). Thus, our data suggest that the residue serine 299 is essential for A-RAF kinase activity, and substitution of this residue with alanine prevents activation of A-RAF by both, oncogenic Ras and Lck. Moreover, our experimental results demonstrate that tyrosine phosphorylation does not compensate the serine 299 to alanine mutation with respect to kinase activity of A-RAF.

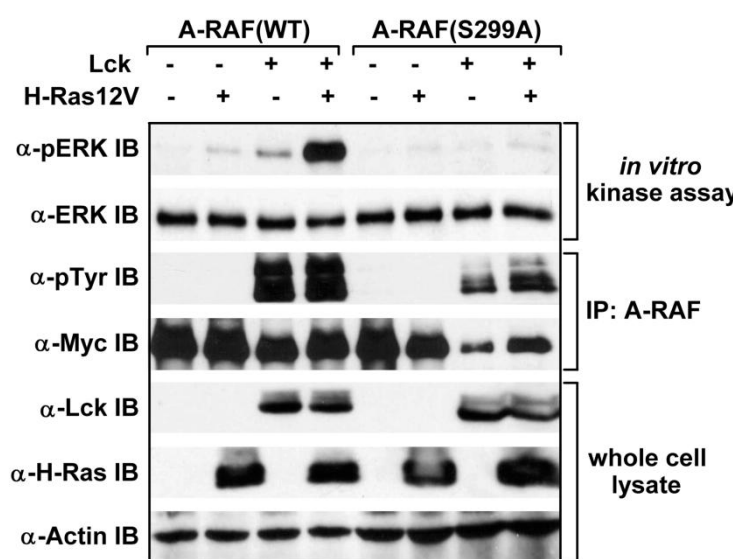


**FIGURE 28: Substitution of serine 299 to alanine in A-RAF does not prevent tyrosine phosphorylation, but almost completely abrogates activation of A-RAF kinase.** Sf9 insect cells were infected with desired baculovirus constructs as indicated. After the cells were lysed A-RAF wild type (WT) and A-RAF-S299A proteins were immunoprecipitated (IP) by anti-A-RAF antibody. Subsequently, coupled kinase assay using MEK and ERK as substrates has been carried out and the extents of kinase activities were monitored by anti-pERK antibody. Tyrosine phosphorylation was monitored by use of anti-phosphotyrosine antibody 4G10. Expression efficiency of H-Ras12V and Lck was

determined using an anti H-Ras and an anti-Lck antibody, respectively. Actin immunodetection was used as a loading control. *IB*, immunoblot.

### 6.5.2. Phosphorylation of the conserved serine in the N-region is predicted to depend on amino acid at position –3

Because it has been observed that the level of A-RAF activity following growth factor stimulation is considerably lower compared to C- and B-RAF [113] and because there are major differences in the sequence of the regulatory N-region, we decided to explore the role of non-conserved amino acids of this region. We noticed that serine 339 of C-RAF (the homologous residue in B-RAF is S447), which is next to the strongly conserved serine 338, is substituted by glycine in the case of A-RAF (G300) (**Fig. 27A**). Additionally, the amino acid in position 296 in A-RAF (Y296), which is analogous to glutamine 335 in C-RAF and to arginine 443 in B-RAF, is variable for all of three isoforms. *In silico* analysis of the phosphorylation efficiency by using the *NetPhos 2.0* algorithm [291] revealed that the phosphorylation efficiency of the conserved serine 299 (A-RAF), 338 (C-RAF) and 446 (B-RAF) differed enormously between RAF isoforms. According to the prediction, phosphorylation efficiency of serine 338 in C-RAF and serine 446 in B-RAF is 98.1% and 99.8%, respectively, while the phosphorylation probability of the homologous serine (S299) in A-RAF is strongly reduced to 15.3%. Moreover, phosphorylation efficiency of the conserved serine 299 in A-RAF is predicted to depend largely on the nature of the amino acid at position –3 (**Fig. 27A**). Thus, the phosphorylation probability of serine 299 in A-RAF increases up to 76.7%, if tyrosine at position –3 is substituted by glutamine (corresponding to C-RAF) and further increases to 99.1%, if the residue in position –3 is an arginine (as in B-RAF). In the case of C-RAF, the effect of the amino acid at the position –3 on phosphorylation efficiency of the conserved serine 338 is moderate. Substitution of glutamine 335 by tyrosine (mimicking A-RAF) is predicted to decrease the phosphorylation efficiency of serine 338 to 80.7%. In contrast, the degree of phosphorylation of the conserved serine 446 in B-RAF does not seem to be affected by amino acid in the position –3 relative to phosphorylation site. However, if the aspartates 448 and 449 are substituted by tyrosines (thus, mimicking A- and C-RAF), the phosphorylation efficiency of the serine 446 in B-RAF becomes highly dependent on the nature of the amino acid in position –3, suggesting that aspartates in positions +2 and +3 may abolish the dependence of serine 446 phosphorylation on amino acid in position –3. On the other hand, the variable amino acid G300 in A-RAF, S339 in C-RAF and S447 in B-RAF at the position +1 relative to the implicated serine residue was predicted to have no significant effect on the phosphorylation of conserved serine in all three RAF isoforms. According to the prediction by *NetPhos 2.0*, serine 339 in C-RAF and the homologous serine 447 in B-RAF represent likely phosphorylation sites (99.5% and 98.8% phosphorylation probability, respectively). However, at present quantitative data regarding phosphorylation of these residues in C- and B-RAF are not available and *in vivo* phosphorylation of these sites was reported to have no effect on RAF activation [182]. Notably, this conserved phosphorylation site is absent in A-RAF, since there is a glycine (G300) instead of a serine (**Fig. 27A**). Following the results of *NetPhos 2.0* analysis, we speculated that the amino acid at position –3 relative to the conserved serine may critically influence phosphorylation of this serine and thus may contribute to regulation of RAF kinase activity.

### 6.5.3. Mutation in the N-region leads to a constitutively active form of A-RAF kinase

Considering the prediction data and the reports that phosphorylation of the conserved serine 338 in C-RAF and serine 446 in B-RAF is one of the most important events in the process of kinase activation, we hypothesized that the predicted moderate degree of phosphorylation of homologous serine 299 in A-RAF (possibly caused by the presence of tyrosine in the position 296) may be responsible for the weak kinase activity of this isoform. To examine this possibility, we generated an A-RAF substitution mutant in which tyrosine 296 was replaced by arginine (A-RAF-Y296R, **Fig. 27B**). In addition, because *NetPhos 2.0* did not provide further information on the involvement of the glycine residue at position 300 in phosphorylation of serine 299 in A-RAF, we decided to test the contribution of G300 to A-RAF kinase activation by mutagenesis. For this purpose we generated A-RAF substitution mutants A-RAF-G300S and A-RAF-Y296R/G300S, the latter partially resembling the N-region sequence of B-RAF. We also prepared A-RAF mutants where the tyrosines 301 and 302 were substituted by aspartates (A-RAF-Y301D/Y302D and A-RAF-Y296R/G300S/Y301D/Y302D, designated as A-RAF-DD and A-RAF-Y296R/G300S/DD, respectively) to investigate an N-region structure, completely homologous to B-RAF (**Fig. 27B**). All mutants carried a C-terminal Myc-tag. Because A-RAF appeared not to be responsive to EGF stimulation alone in HEK293 cells (data not shown), we decided to use the combination of H-Ras12V and Lck, which has been reported to be a potent stimulus for activation of A-RAF kinase [113]. Upon transfection of each A-RAF construct into HEK293 cells either alone or together with H-Ras12V/Lck, A-RAF proteins were immunoprecipitated by means of an anti-Myc antibody and subjected to *in vitro* coupled kinase assay. The extent of A-RAF kinase activity was monitored by anti-phospho-ERK antibody.

As shown in **Fig. 29**, A-RAF wild type as well as A-RAF substitution mutants A-RAF-Y296R, A-RAF-G300S and A-RAF-Y296R/G300S are highly responsive to stimulation by oncogenic Ras and Lck. Although wild type A-RAF isolated from starved HEK293 cells was completely inactive, cotransfection with H-Ras12V and Lck resulted in elevated kinase activity. The same effect was also observed with the A-RAF-G300S mutant. Substitution of A-RAF tyrosine 296 by arginine (A-RAF-Y296R variant) led to elevated kinase activity even in the absence of any stimulatory agents, demonstrating that this mutant is constitutively active (**Fig. 29**). Even more strikingly, the elevated basal activity of the A-RAF-Y296R mutant was almost completely abrogated by the additional introduction of a serine residue instead of glycine at position 300 in the A-RAF-Y296R/G300S double mutant (**Fig. 29**), suggesting that serine at this position may act in an inhibitory fashion with respect to basal A-RAF kinase activity. Because substitution of tyrosines 301 and 302 by aspartates in A-RAF generates a kinase that can be activated by oncogenic Ras, but not by Lck [113], we stimulated the A-RAF-Y296R/G300S/DD mutant with H-Ras12V only. **Fig. 29** shows that this mutant had an elevated basal level of activity and was still responsive to stimulation by oncogenic Ras, indicating that the inhibitory effects of G300S substitution did not significantly impair the activating potential of Y301D/Y302D substitution.

Because we did not observe significant differences in kinase activity of A-RAF mutants following co-transfection with H-Ras12V/Lck (see **Fig. 29**), we attempted to improve

discrimination by activating with H-Ras12V only. To exclude differences in kinase activity of A-RAF constructs as a consequence of transfection variability, the HEK293 cells were first transfected with Ras12V. 48 hours after transfection, the cells were transfected again with plasmids expressing each A-RAF construct. 12 hours after the second transfection, the cells were starved for an additional 12 hours. A-RAF activity was subsequently monitored using anti-Myc A-RAF immunoprecipitation and MEK/ERK-coupled kinase assay.

Following activation by oncogenic Ras, the A-RAF-Y296R mutant revealed considerably higher kinase activity compared with A-RAF WT (**Fig. 30A and B**). This observation is in line with the results obtained with the same mutant under non-activating conditions (see **Fig. 29**). Surprisingly, the G300S substitution, mimicking B- and C-RAF in this position, completely abrogated the activation by Ras12V resulting in an inactive kinase (**Fig. 30A and B**). A similar effect was also observed with the A-RAF-Y296R/G300S mutant, indicating that serine in position 300 of A-RAF indeed acts inhibitory under stimulating (see **Fig. 30A and B**) as well as non-stimulating (see **Fig. 29**) conditions. Furthermore, kinase activity of the A-RAF-Y296R/G300S/DD mutant was slightly lower than that of the A-RAF-DD variant, suggesting a dominant role of serine at position 300 over the otherwise activating tyrosine 296 to arginine exchange (**Fig. 30 A and B**). In agreement with the *NetPhos 2.0* prediction, activation of A-RAF mutants was associated with phosphorylation of serine 299 (C-RAF S338 homolog), as judged by reactivity with the anti-C-RAF-pS338 antibody. The antibody recognizes the RDSS motif in both, C- and B-RAF as well as in A-RAF mutants carrying the G300S substitution (**Fig. 30A and C**). Whereas the A-RAF-Y296R/G300S double mutant was slightly phosphorylated, the single A-RAF-G300S mutant was not

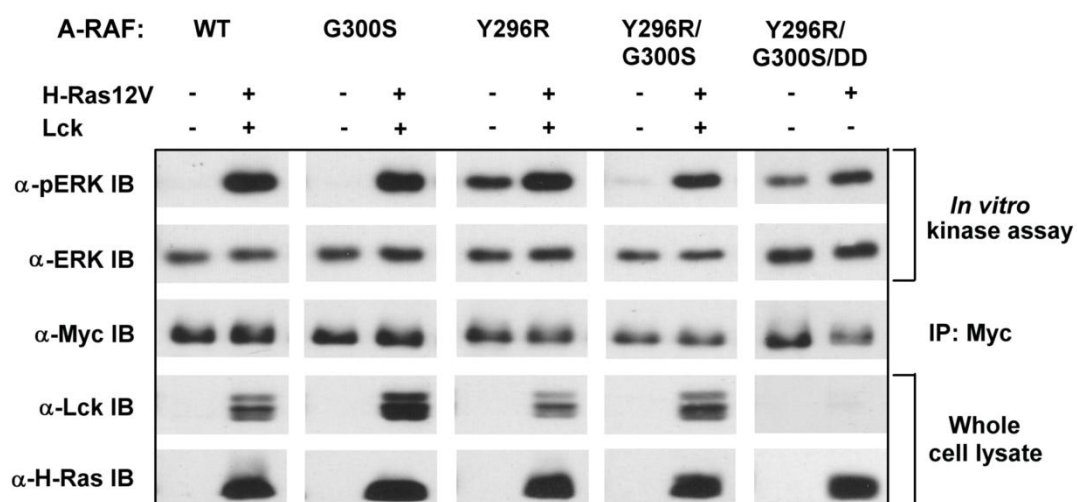


**FIGURE 29: A-RAF-Y296R mutant is constitutively active in starved cells.** C-terminally Myc-tagged A-RAF wild type (WT) and A-RAF substitution mutants (G300S, Y296R, Y296R/G300S and Y296R/G300S/DD) were expressed in HEK293 cells in the presence and absence of H-Ras12V and Lck. The cells were serum-starved for the last 12 hours of incubation and lysed using detergent containing buffer. Levels of A-RAF in each sample were determined and balanced against each other, so that equivalent amounts of A-RAF were immunoprecipitated (IP) by anti-Myc antibody. Subsequently, coupled kinase assay using MEK and ERK as substrates has been carried out, and the extents of kinase activities were monitored by anti-pERK antibody. Expression efficiency of H-Ras12V and Lck was determined using anti-H-Ras and anti-Lck antibodies, respectively. IB, immunoblot.

phosphorylated at all (see **Fig. 30A** and **C**). Unfortunately, the anti-pS338 antibody directed against the N-region of C-RAF could not be used for detection of phosphorylation at position 299 of A-RAF WT and A-RAF mutants containing glycine at position 300, such as A-RAF-Y296R, presumably because of the differences in the structure of the recognition sequence. On the other hand, we conclude that elevated activity of the constitutively active A-RAF-Y296R mutant was not caused by phosphorylation of tyrosines 301/302, because we did not detect any tyrosine phosphorylation using anti-phosphotyrosine antibody 4G10 in the basal state or following stimulation with H-Ras12V in A-RAF wild type as well as in A-RAF-Y296R, A-RAF-G300S and A-RAF-Y296R/G300S mutants. In contrast, in the presence of Ras12V and Lck considerable tyrosine phosphorylation was detected in all A-RAF mutants (**Fig. 30D**).

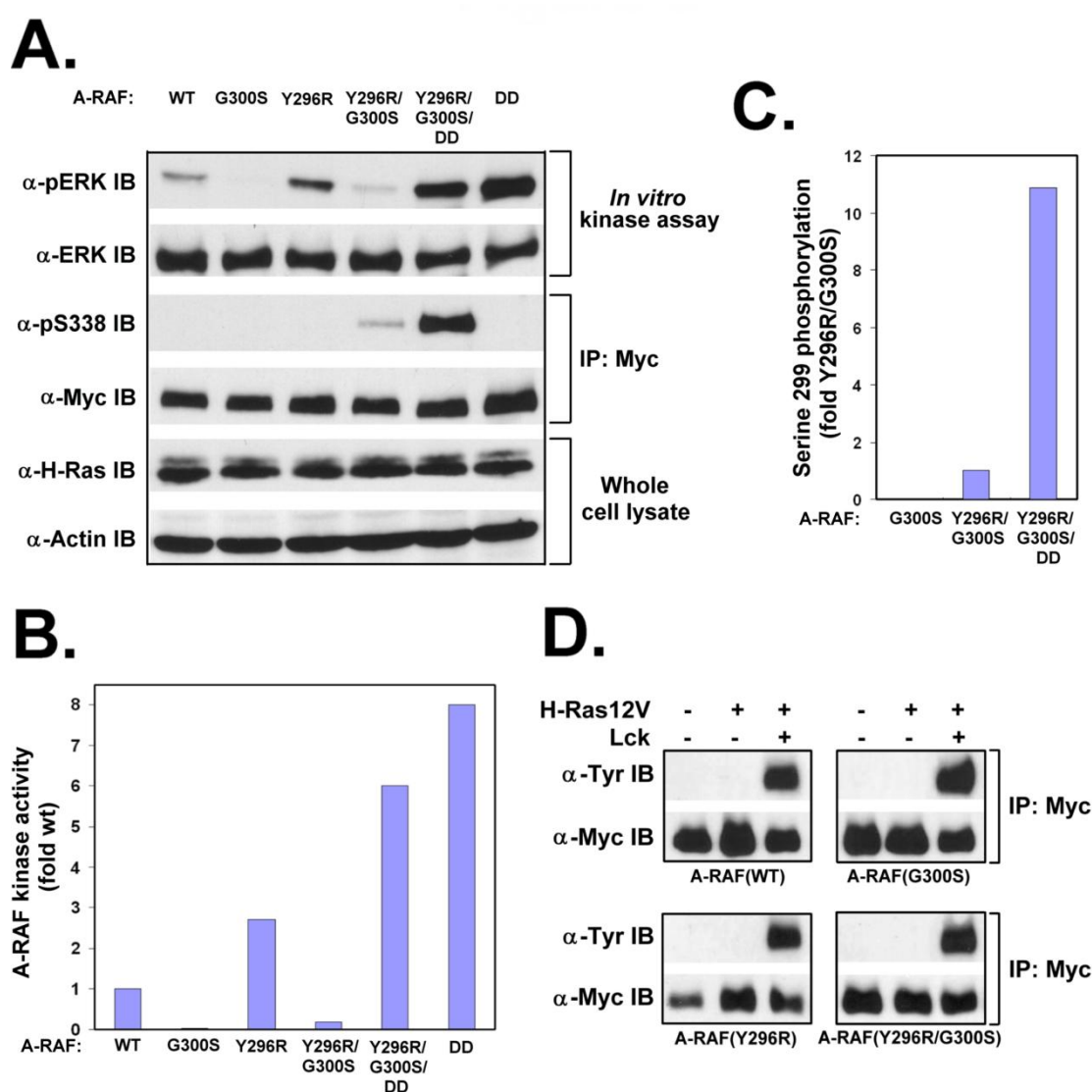


**FIGURE 30: Y296R and G300S substitutions affect A-RAF activation by H-Ras12V.** (A) Western blot analysis of A-RAF kinase activity and serine 299 phosphorylation. HEK293 cells were first transfected with H-Ras12V only, then divided and secondary transfected with A-RAF wild type (WT) or with A-RAF substitution mutants (G300S, Y296R, Y296R/G300S, Y296R/G300S/DD and DD) carrying C-terminal Myc-tag. After the cells have been lysed, levels of A-RAF in each sample were determined and balanced against each other, so that equivalent amounts of A-RAF were



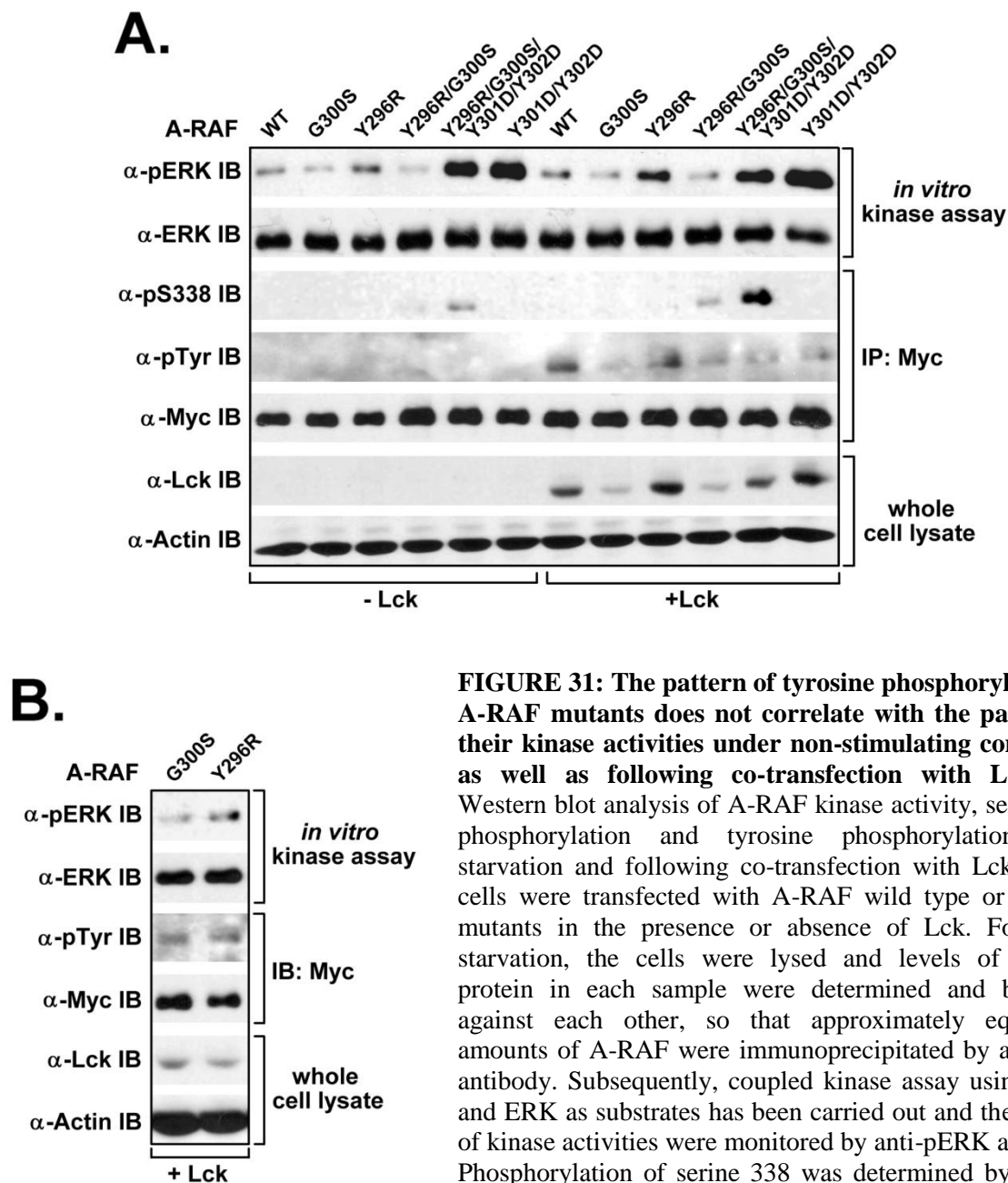
immunoprecipitated (*IP*) by anti-Myc antibody. Subsequently, coupled kinase assay using MEK and ERK as substrates has been carried out, and the extents of kinase activities were monitored by anti-pERK antibody. Expression efficiency of H-Ras12V was determined using an anti-H-Ras antibody. Actin immunodetection was used as a loading control. *IB*, immunoblot. **(B)** Quantification of A-RAF kinase activity. Representative blots from the **A** were quantified by optical densitometry. The quantification results are expressed in terms of fold activation, where 1-fold of activity represents the amount of activity determined for A-RAF wild type. **(C)** Quantification of A-RAF phosphorylation on serine 299 by use of anti-C-RAF-pS338 antibody. Representative blots from the **A** were quantified by optical densitometry. The quantification results are expressed in terms of fold phosphorylation, where 1-fold of phosphorylation represents the amount of phosphate incorporation determined for A-RAF-Y296R/G300S mutant. **(D)** Tyrosine phosphorylation of A-RAF wild type and A-RAF mutants. HEK293 cells were transfected with C-terminally Myc-tagged A-RAF wild type or with the same A-RAF substitution mutants as shown in **A** in the presence and absence of H-Ras12V or in the presence of both, H-Ras12V and Lck. The cells were serum-starved for the last 12 hours of incubation and lysed using detergent-containing buffer. A-RAF proteins were immunoprecipitated by anti-Myc antibody, and the extent of tyrosine phosphorylation was monitored by use of the anti-phosphotyrosine antibody 4G10. A-RAF-DD and A-RAF-Y296R-G300S-DD mutants are not shown, because they revealed only marginal tyrosine phosphorylation because of the substitution of Y301 and Y302 by aspartates.

To address the question, whether the extent of kinase activity of A-RAF mutants compared with A-RAF wild type might correlate with the phosphorylation of tyrosines upon stimulation by Src family kinases alone, we transfected the cells with A-RAF constructs in the presence or absence of Lck. As shown in **Fig. 31**, the pattern and the extent of kinase activities of A-RAF mutants were comparable under both, non-stimulating conditions and upon co-transfection with Lck (the slight increase in kinase activity of some samples in the presence of Lck is because of the higher amounts of A-RAF proteins). In both cases the level of kinase activity of the A-RAF-Y296R mutant was elevated, whereas kinase activity of A-RAF mutants carrying G300S substitution was diminished compared with wild type (see **Fig. 31A**). Importantly, the pattern of tyrosine phosphorylation did not correlate with the pattern of kinase activity of A-RAF mutants. Consistent with the **Fig. 30D**, we did not observe any tyrosine phosphorylation in the absence of Lck. On the other hand, upon co-transfection with Lck, a moderate tyrosine phosphorylation was detectable, whereby the levels of tyrosine phosphorylation were comparable for all A-RAF mutants. We conclude that the observed differences in tyrosine phosphorylation are because of the variations in Lck expression, since in the case of equal Lck expression we did not detect differences in tyrosine phosphorylation (compare **Fig. 31A** and **B**).

The results presented here confirm the predictions from *NetPhos 2.0*, suggesting that amino acid at position -3 relative to the conserved serine 299 in the N-region determines the phosphorylation efficiency of this serine and consequently regulates the kinase activity of A-RAF. Furthermore, as shown in **Fig. 30A**, substitution of tyrosines at positions 301/302 to aspartates acts stimulatory toward serine 299 phosphorylation in A-RAF upon transfection with oncogenic Ras, because phosphorylation of this serine in A-RAF-Y296R/G300S/DD was about 11-fold higher than that in A-RAF-Y296R/G300S mutant.

Taken together, these results demonstrate that amino acid variations in the short N-region change profoundly the kinase properties of A-RAF protein. In particular, we show here

that the substitution of glycine 300 with serine acts in an inhibitory manner preventing Ras-dependent activation, whereas replacement of tyrosine 296 by arginine, mimicking the situation in B-RAF, leads to a constitutively active A-RAF kinase possessing elevated activity even in the absence of any activating agents. These observations indicate that the poor basal activity of A-RAF compared with B-RAF can be ascribed not only to the tyrosines at positions 301/302 but also to the tyrosine at position 296 in A-RAF.



#### 6.5.4. C-RAF behaves similar to A-RAF: mutations at the positions 335 and 339 in the N-region of C-RAF modulate its kinase activity

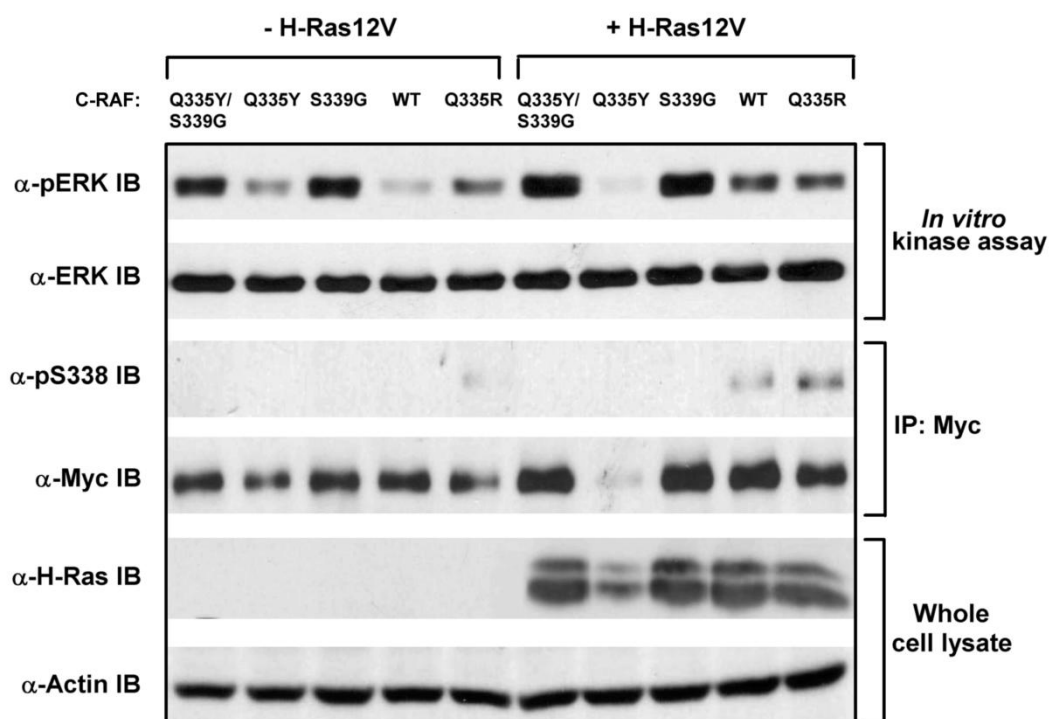
To address the question whether substitution of amino acids at the analogous positions within the N-region of C-RAF (Q335 and S339) would also lead to changes in serine 338 phosphorylation and consequently to changes in the activation process, we next generated C-RAF mutants mimicking N-region sequences of A- or B-RAF. To this end, we first replaced glutamine 335 in C-RAF by either tyrosine (as present in A-RAF) or arginine mimicking B-RAF (see **Fig. 27B**). Additionally, following our observations that the introduction of serine instead of glycine at position 300 in A-RAF (analogous to position 339 in C-RAF) led to inhibition of the activation process, we also exchanged the serine 339 in C-RAF by glycine, to examine whether this substitution might affect C-RAF activity. Furthermore, a double mutant of C-RAF (C-RAF-Q335Y/S339G) was generated in which both residues were replaced by amino acids that are normally present in A-RAF wild type, thus resembling the N-region of A-RAF (**Fig. 27B**).

First, we investigated differences of serine 338 phosphorylation and kinase activity of C-RAF constructs under non-stimulating conditions and by co-transfecting COS7 cells with H-Ras12V. For this purpose, the cells were transfected either with expression vectors for C-terminally Myc-tagged C-RAF WT and C-RAF substitution mutants alone or together with oncogenic Ras. The C-RAF proteins were immunoprecipitated and subjected to the coupled kinase assay. As shown in **Figs. 32** and **33**, the basal kinase activities (without any stimulation of the cells) exhibited already remarkable differences. Although C-RAF WT and C-RAF-Q335Y mutant displayed very low basal activities, substitution of Q335 by arginine (C-RAF-Q335R) resulted in an increase of basal activity. In parallel, phosphorylation of serine 338 in the C-RAF-Q335R mutant was strongly elevated compared with C-RAF WT, indicating that arginine in this position promotes phosphorylation of serine 338 (**Fig. 32** and **Fig. 33B** and **D**). More strikingly, the introduction of glycine in the position 339 instead of serine (C-RAF-S339G mutant) led to a constitutively active C-RAF kinase having almost 20-fold higher basal activity compared with C-RAF WT (**Fig. 32** and **Fig. 33A–C**). These results demonstrate clearly that the introduction of glycine in the position +1 relative to S338 is stimulatory with respect to C-RAF kinase activity. On the other hand, the reverse substitution of glycine by serine in the analogous position in A-RAF (G300S) led to an inactive kinase (**Fig. 30A**). Interestingly, the double mutant of C-RAF (C-RAF-Q335Y/S339G) also revealed elevated basal activity (**Fig. 32** and **Fig. 33A–C**), indicating that the inhibitory effect of the Q335Y substitution can be compensated by the S339G mutation.

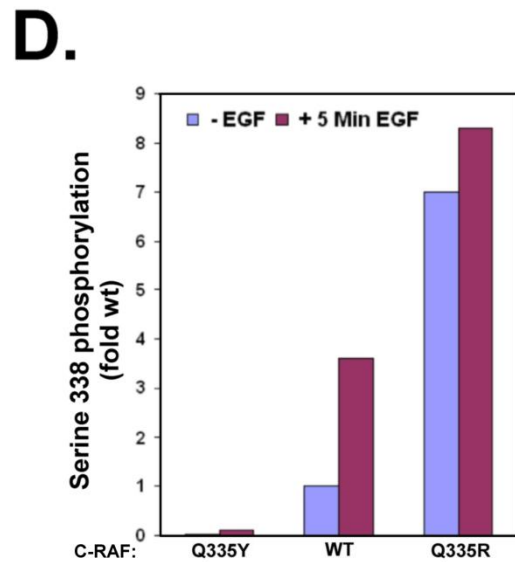
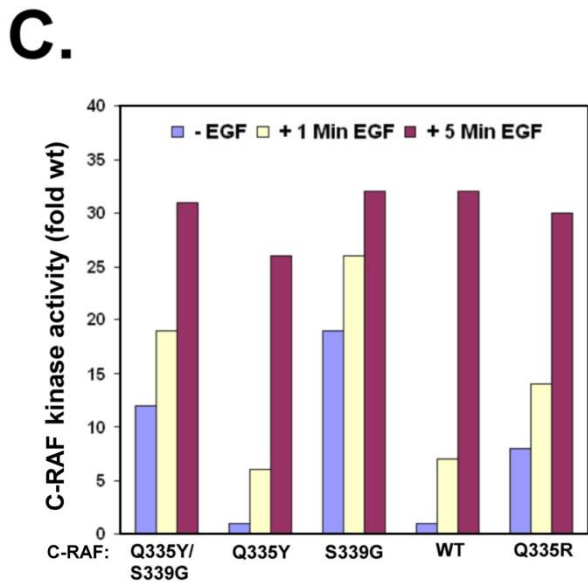
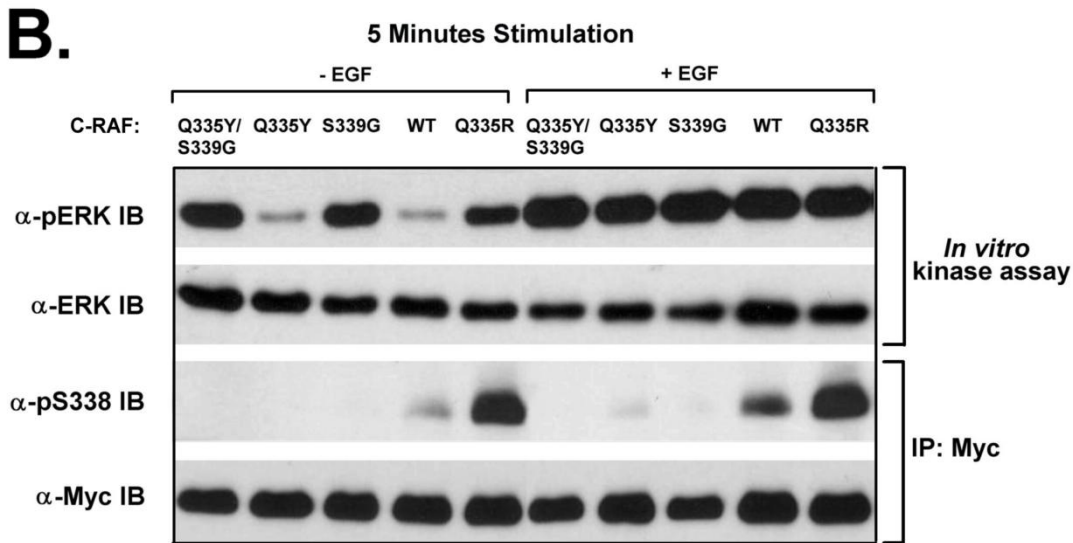
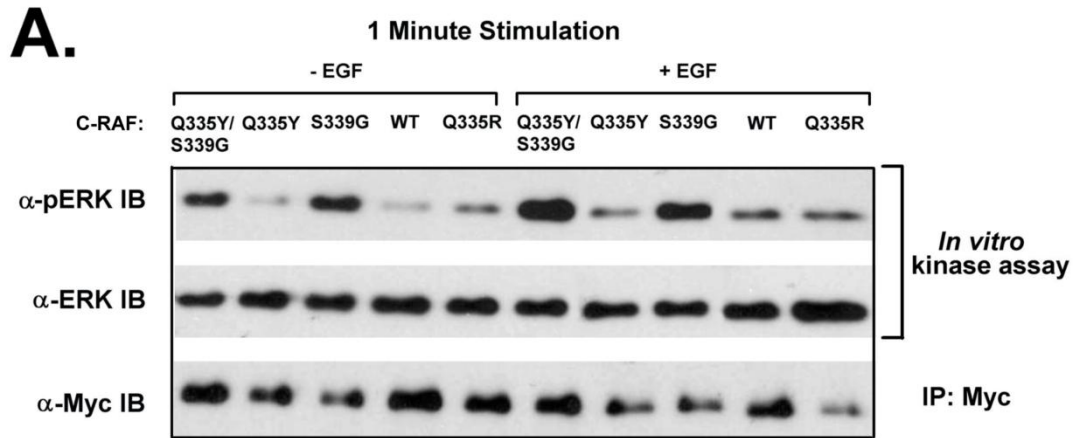
Unfortunately, the degree of phosphorylation of serine 338 in C-RAF mutants S339G and Q335Y/S339G could not be determined by anti-pS338 antibody, because the structure of recognition sequence seems to be disrupted by introduction of glycine instead of serine. Furthermore, as demonstrated in **Fig. 32**, cotransfection with oncogenic Ras did not significantly change the serine 338 phosphorylation and the kinase activity pattern of C-RAF mutants. However, the levels of kinase activity of each C-RAF mutant as well as degrees of phosphorylation of C-RAF WT and C-RAF-Q335R mutant were increased upon transfection with H-Ras12V (**Fig. 32**), indicating that despite their increased basal activity all C-RAF mutants tested are still sensitive to stimulation by oncogenic Ras. Similar results were also

observed with HEK293 cells (data not shown), suggesting that differences in activation and serine 338 phosphorylation of C-RAF mutants are not cell line-specific.

To test the susceptibility to activation of C-RAF substitution mutants compared with C-RAF WT under physiological conditions, we performed short- and long-term stimulation of cells by EGF. Here we chose COS7 cells, because of the fact that this cell line has been reported to be more sensitive to EGF activation than HEK293 cells [292]. Because EGF stimulation of C-RAF is a rapid process reaching a maximum already after 30–60 s [202,293], we stimulated the cells for 1 and 5 minutes. Immediately after stimulation with EGF, the cells were lysed and C-RAF kinase activities were determined. As shown in **Fig. 33A** and **C**, stimulation of COS7 cells with EGF for 1 minute resulted in a similar pattern of kinase activity for C-RAF WT and C-RAF mutants, as has already been observed with non-stimulated cells and with cells co-transfected with oncogenic Ras. In contrast, after 5 minutes of EGF stimulation, all C-RAF proteins showed similar levels of maximal kinase activity (**Fig. 33B** and **C**), suggesting that the mutations within the N-region of C-RAF are relevant for the basal activity as well as for the initial steps of the activation process; however, they do



**FIGURE 32: Substitution of serine 339 by glycine in the N-region of C-RAF leads to constitutively active kinase.** C-terminally Myc-tagged C-RAF wild type (WT) and C-RAF substitution mutants (Q335Y, Q335R, S339G and Q335Y/S339G) were expressed in COS7 cells in the presence (*right panel*) and absence (*left panel*) of H-Ras12V. After 12 h of serum starvation, cells were lysed using detergent-containing buffer. Cell lysates were subjected to immunoprecipitation (IP) with anti-Myc antibody. Subsequently, coupled kinase assay using MEK and ERK as substrates has been carried out, and extents of ERK phosphorylation were monitored by anti-pERK antibody. Phosphorylation of serine 338 was examined by use of anti-C-RAF-pS338 antibody. Expression efficiency of H-Ras12V was determined using anti-H-Ras antibody. Actin immunodetection was used as a loading control. Notice that expression degree of the sample containing C-RAF-Q335Y and H-Ras12V was lower compared with other samples. *IB*, immunoblot.



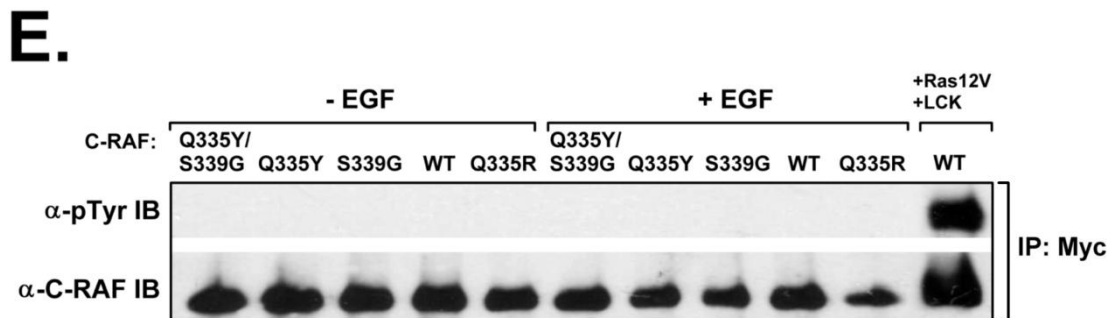


**FIGURE 33: Phosphorylation of conserved serine 338 does not completely correlate with the extent of kinase activity of C-RAF upon long-term activation with EGF.** COS7 cells were transfected with C-RAF wild type or C-RAF mutants as indicated. Following starvation for 24 hours, the cells were stimulated by EGF for 1 and 5 minutes. Levels of C-RAF in each sample were determined and balanced against each other, so that equivalent amounts of C-RAF were immunoprecipitated (*IP*) by anti-Myc antibody. Subsequently, kinase activities were measured using a coupled kinase assay in the presence of recombinant MEK and ERK proteins. ERK phosphorylation was detected by phosphospecific anti-ERK antibody. Phosphorylation of serine 338 was determined by anti-C-RAF-pS338 antibody. **(A)** Analysis of C-RAF kinase activity under non-stimulating conditions (*left panel*) and upon short-term stimulation (1 minute) with EGF (*right panel*). *IB*, immunoblot. **(B)** Analysis of C-RAF kinase activity and serine 338 phosphorylation under non-stimulating conditions (*left panel*) and upon long-term stimulation (5 minutes) with EGF (*right panel*). **(C)** Quantification of C-RAF kinase activity. Average values derived from the data of five independent experiments were used for quantification. Quantification results are expressed in terms of fold activation, where 1-fold of activity represents the amount of activity determined for C-RAF wild type under non-stimulating conditions. **(D)** Quantification of serine 338 phosphorylation. Representative blots from the **B** were quantified by optical densitometry. The quantification results are expressed in terms of fold phosphorylation, where 1-fold of phosphorylation represents the amount of phosphorylation determined for C-RAF wild type under non-stimulating conditions. **(E)** Tyrosine phosphorylation of C-RAF wild type and C-RAF mutants under non-activating conditions and following stimulation with EGF. C-RAF wild type, which was expressed in the presence of oncogenic Ras and Lck and has been shown to be highly phosphorylated on tyrosines [182], was used as a positive control for the reactivity of anti-tyrosine antibody 4G10.

not seem to be relevant for the maximal activation. Although the levels of kinase activity of C-RAF WT, C-RAF-Q335Y and C-RAF-Q335R did not significantly differ upon long term stimulation (5 minutes) with EGF, we observed significant differences of serine 338 phosphorylation in these C-RAF mutants (**Fig. 33B–D**). These discrepancies indicate that phosphorylation on serine 338 regulates kinase activity of C-RAF under starvation conditions and at the initial steps of EGF stimulation, whereas additional regulatory events promote the activating process upon prolonged stimulation. Moreover, because our results shown in **Figs. 32** and **33** indicate that continuous expression of oncogenic Ras did not lead to compensation of differences in kinase activity of C-RAF mutants in contrast to prolonged EGF stimulation, we suggest that C-RAF activating events initiated by EGF do not act through the H-Ras pathway alone. Interestingly, these additional activating pathways did not regulate kinase activity of C-RAF by phosphorylation of activating tyrosines in the positions 340/341, because Western blot analysis of immunoprecipitated proteins did not show any tyrosine phosphorylation following stimulation with EGF (see **Fig. 33E**).

Collectively, these results together with results obtained for A-RAF indicate that the residues in positions  $-3$  and  $+1$  relative to S338 in C-RAF and S299 in A-RAF play an important role in the activation process of these isoforms. Introduction of glycine in position  $+1$  leads to a constitutively active C-RAF kinase, whereas substitution of glutamine in position  $-3$  by arginine provided a mixed effect; although phosphorylation of serine 338 was strongly increased, elevation of the kinase activity was only moderate. These data demonstrate that serine 338 phosphorylation does not necessarily correlate with the extent of kinase activity. Obviously, other pathways are required to convert C-RAF from the inactive to the active state.

### 6.5.5. Active forms of C-RAF mutants are located preferentially at membranes

Translocation of cytosolically located RAF kinases to the plasma membrane has been initially proposed to be mediated solely by GTP-loaded Ras proteins via interactions with Ras binding domain [212,294]. We and others provided evidence that RAF kinases *per se* possess high affinities for certain membrane lipids, supporting a new model in which a small fraction of RAF molecules is already associated with the plasma membrane, where Ras-RAF interactions subsequently take place by lateral diffusion in the plane of the membrane [11,217]. To investigate whether the mutations in the N-region influence the translocation of C-RAF kinase to cell membranes, we examined the subcellular localization of C-RAF WT and C-RAF mutants listed in **Fig. 27B**. In parallel, we determined the serine 338 phosphorylation status and the kinase activity of C-RAF proteins in different cell fractions. To this end, COS7 cells were transfected with plasmids expressing Myc-tagged C-RAF wild type and C-RAF substitution mutants listed in **Fig. 27B**. In this experiment, we included C-RAF-Y340D/Y341D (C-RAF-DD) mutant, because this substitution mutant is known to be highly active as well as strongly phosphorylated at serine 338 under non-stimulating conditions, features that we also found with C-RAF-S339G and C-RAF-Q335R mutants. Following serum starvation, subcellular fractions were collected according to the protocol of the *ProteoExtract* subcellular proteome extraction kit. The extraction procedure yields four subproteome fractions as follows: cytosolic, membrane, nuclear and cytoskeletal fractions. C-RAF proteins were absent from the nuclear and cytoskeletal fractions and were exclusively detected in the cytosolic and membrane fractions (see **Fig. 34A**). However, under non-stimulating conditions more C-RAF protein accumulated in the cytosolic fraction compared with isolated membranes. Because we did not observe significant differences in distribution of C-RAF mutants between cytoplasm and membranes, we next looked at the distribution of their kinase activity. The extraction of cytosolic and membrane fractions yields C-RAF proteins in their native state including enzyme activity, because control experiments showed that RAF activity was not affected by extraction buffers (data not shown). The extent of C-RAF kinase activity in membrane and cytosolic fractions was determined by use of MEK/ERK coupled kinase assay. Because the quantities of C-RAF protein differed between fractions, the values of observed kinase activity were normalized for C-RAF content.

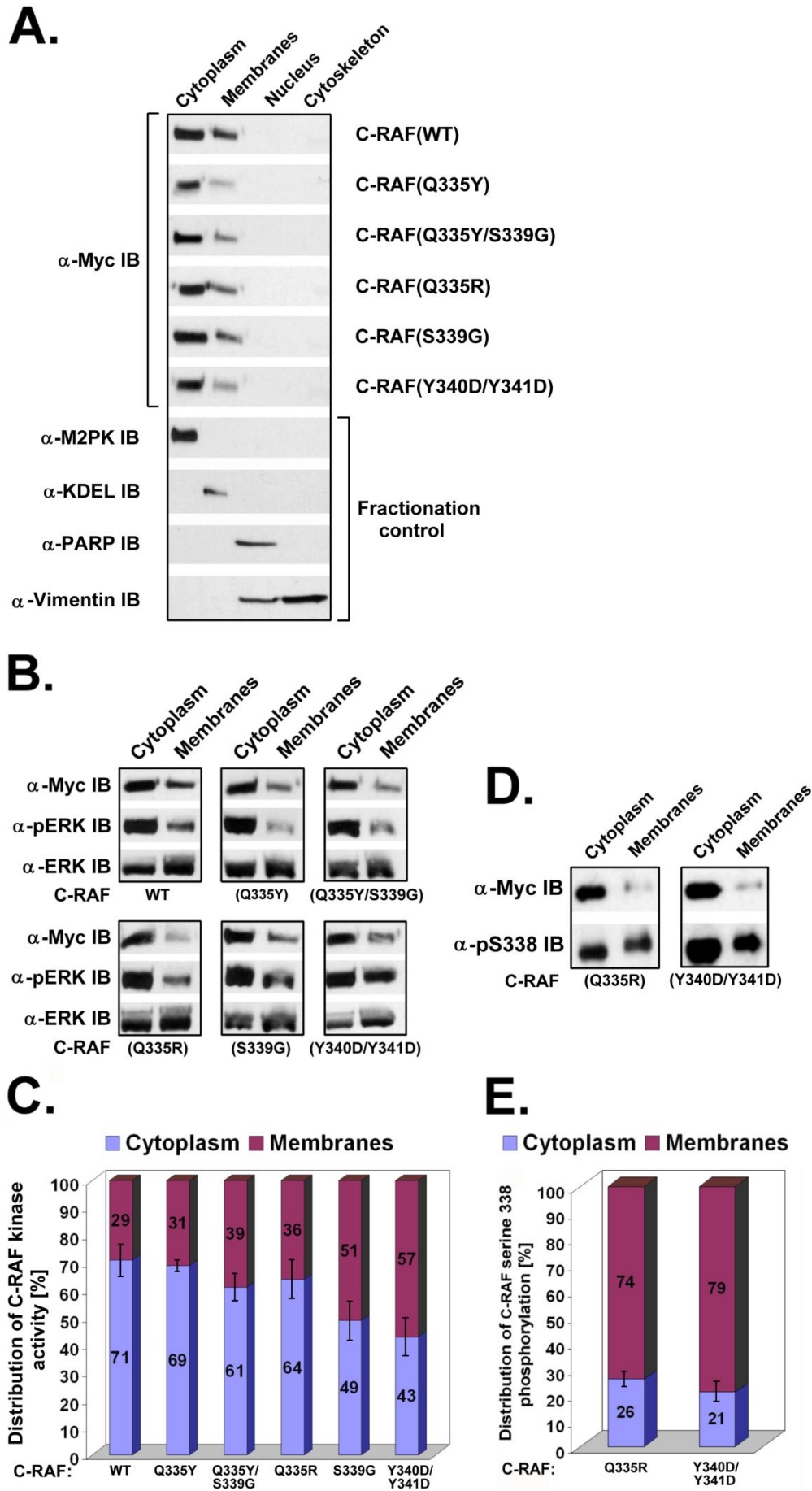




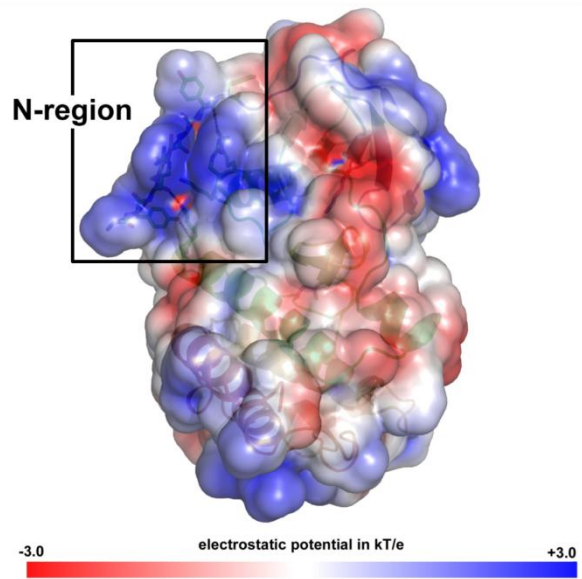
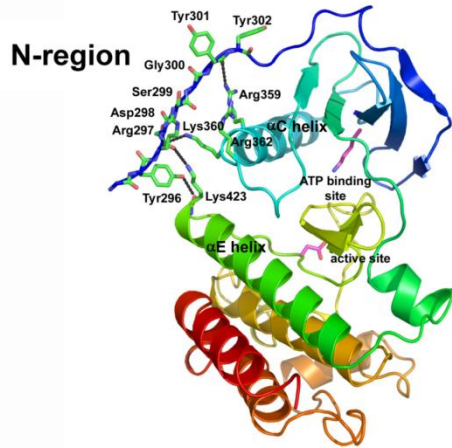
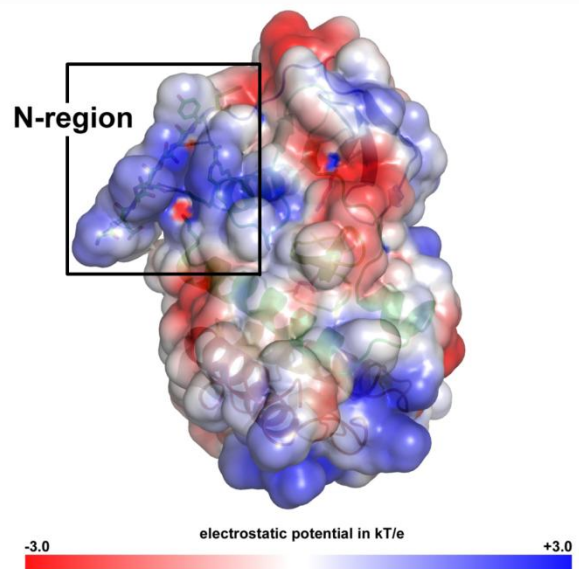
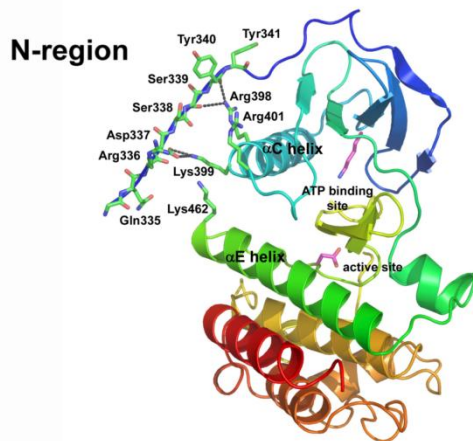
**FIGURE 34: Subcellular distribution of kinase activity and serine 338 phosphorylation of C-RAF wild type and C-RAF mutants in COS7 cells.** (A) Western blot analysis of subcellular distribution of C-RAF wild type and C-RAF mutants. COS7 cells were transfected with C-RAF wild type and C-RAF substitution mutants (as indicated) carrying C-terminal Myc tag. After 24 hours of serum starvation, cytoplasmic, membrane, nuclear and cytoskeletal fractions were collected according to the protocol of the *ProteoExtract* subcellular proteome extraction kit. *Fractionation control*: anti-M2PK immunodetection for cytosolic fraction, anti-KDEL immunodetection for membrane fraction, anti-PARP immunodetection for nuclear fraction, and anti-vimentin immunodetection for cytoskeletal fraction. *IB*, immunoblot. (B) Western blot analysis of C-RAF kinase activity in cytosolic and membrane fractions. Extent of C-RAF kinase activity was determined using MEK/ERK-coupled kinase assay and monitored by anti-phospho-ERK antibody. (C) Quantification of C-RAF kinase activity in cytosolic and membrane fractions. Data from two independent experiments were quantified by optical densitometry. Values of observed kinase activity were normalized for C-RAF content. They represent %-ratio of measured C-RAF kinase activity in each fraction relative to the total kinase activity observed in both, cytosolic and membrane fractions together. (D) Western blot analysis of C-RAF serine 338 phosphorylation in cytosolic and membrane fractions. Quantities of phosphorylated protein were determined by anti-pS338 antibody. (E) Quantification of C-RAF serine 338 phosphorylation in cytosolic and membrane fractions. Data from two independent experiments were quantified by optical densitometry. Values of observed phosphorylation were normalized for C-RAF content. They represent %-ratio of measured serine 338 phosphorylation in each fraction relative to the total phosphorylation in both, cytosolic and membrane fractions together.

As shown in **Fig. 34B** and **C**, most of the kinase activity of the C-RAF-DD mutant was associated with the membrane fraction (57%), in contrast to only 29% of the kinase activity for C-RAF WT. Importantly, C-RAF-Q335Y mutant exhibiting low basal activity behaved similarly to C-RAF WT (**Fig. 34B** and **C**). On the other hand, the degree of membrane-bound RAF activity was increased significantly in the case of C-RAF mutants with elevated basal activity (C-RAF-S339G and C-RAF-Q335R). We also examined the distribution of C-RAF serine 338 phosphorylation between cytosolic and membrane fractions. The quantities of phosphorylated protein were determined by anti-pS338 antibody, and the values of observed phosphorylation were normalized for C-RAF content. This examination could only be performed with C-RAF-Q335R and C-RAF-DD mutants, because the phosphorylation degree of C-RAF WT and C-RAF-Q335Y mutants was below the limit of detection. As shown in **Fig. 34D** and **E**, C-RAF phosphorylated on serine 338 was associated preferentially with the membrane fraction, confirming previous findings, suggesting that phosphorylation of serine 338 and tyrosine 341 contributes to Ras-independent membrane localization [181]. These results indicate that mutations in the N-region do not impair translocation of C-RAF protein to the membrane fraction. Moreover, they document again the importance of the non-conserved positions 335 and 339 in C-RAF and show that the C-RAF-S339G and C-RAF-Q335R mutants reveal similar properties, as have been reported for the constitutively active C-RAF-DD, at least with regard to membrane-associated kinase activity.

### 6.5.6. A model derived from the tertiary structure of RAF reveals a tight contact between the N-region of A-RAF and its catalytic domain

To correlate the experimental results presented in this study (see **Figs. 28–34**) with the steric constellation of the N-region and the catalytic domain, we searched for putative contact points between these two moieties by molecular modeling. For this purpose, we took advantage of the recently published three-dimensional structure of B-RAF catalytic domain [193]. The validity of this approach is supported by the high degree of homology of the catalytic domain between A-, B- and C-RAF. The C-terminal part of RAF (CR3) has 96% identity among human isoforms and 95% identity between human and mouse enzymes. In contrast, the similarity among RAF isoforms in their N-terminal portions is only 60%. As shown in **Fig. 35A**, several contact points could be identified between the catalytic domain and the N-regions in A- and C-RAF. However, there are differences in the interaction patterns between these two RAF isoforms. In both, A- and C-RAF, the highly conserved aspartate of the N-region (D337 in C-RAF and D298 in A-RAF) interacts with the spatially adjacent lysine (K399 in C-RAF and K360 in A-RAF) from the  $\alpha$ C helix of the catalytic domain. Furthermore, in both, A- and C-RAF, the oxygen of the backbone of the N-region interacts with the side chain of the conserved arginine (R398 in C-RAF and R359 in A-RAF) from the  $\alpha$ C helix. However, in the case of C-RAF, the arginine 398 of the catalytic domain makes an additional hydrogen bond to the side chain of the serine 339 of the N-region (**Fig. 35A, lower panel**). In contrast, in A-RAF this interaction is missing, because this isoform contains glycine instead of serine in the analogous position (**Fig. 35A, upper panel**). Importantly, substitution of C-RAF serine 339 by glycine (as is the case in the C-RAF-S339G mutant) abrogates this C-RAF-specific hydrogen bond between the N-region and the catalytic domain (**Fig. 35C, right panel**), whereas introduction of serine instead of glycine 300 (as is the case in the A-RAF-G300S) generates the analogous interaction in A-RAF (**Fig. 35B, right panel**). These observations together with the experimental results of this study suggest that the presence of a hydrogen bond between the side chain of the serine in position +1 relative to the conserved serine and arginine of the catalytic domain may be inhibitory for RAF kinase activity. Disruption of this close contact between N-region and catalytic domain results in highly elevated basal activity, as has been demonstrated for C-RAF-S339G mutant (**Figs. 32 and 33**), whereas introduction of this additional hydrogen bond in A-RAF results in completely inhibited kinase, as has been shown for A-RAF-G300S (**Fig. 30A**).

Furthermore, the modeling data presented in **Fig. 35** revealed that the presence of tyrosine at position 296 confers very specific properties onto A-RAF among the RAF kinase family. As illustrated in **Fig. 35A, upper panel** and **B**, the aromatic group of tyrosine 296 interacts with the backbone of lysine 423 from the  $\alpha$ E helix of the catalytic domain. Moreover, this interaction is further strengthened by the hydrogen bond between the side chain of the lysine 423 from the  $\alpha$ E helix and the backbone oxygen from the N-region, conferring a tighter contact between N-region and catalytic domain in A-RAF compared with C-RAF, in which these two interactions are missing, because of a glutamine residue (Q335) in the analogous position (**Fig. 35A, lower panel** and **C**). Obviously, tyrosine in this position favors a spatial orientation of the N-region segment, which enables a more close fitting

**A.****A-RAF****C-RAF**

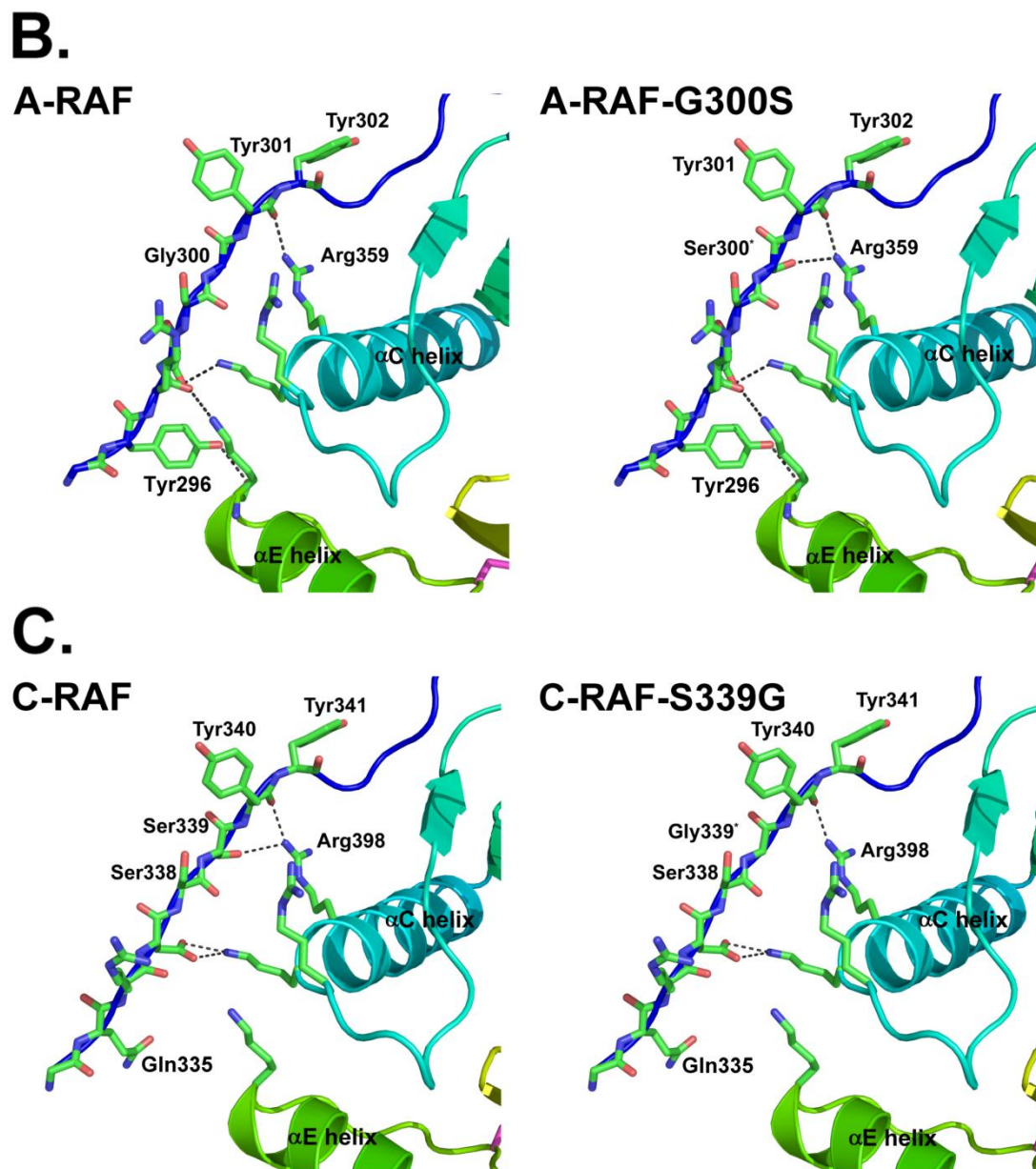


**FIGURE 35: Reconstruction of spatial orientation of the N-region relative to the catalytic domain in A- and C-RAF utilizing three-dimensional structure of the B-RAF catalytic domain as a template. (A) Ribbons diagram and Connolly surface of the reconstructed three-dimensional structure of A-RAF (*upper panel*) and C-RAF (*lower panel*). The positions of Tyr-296, Arg-297, Asp-298, Ser-299, Gly-300, Tyr-301 and Tyr-302 of the N-region and the positions of Lys-423, Arg-359, Lys-360 and Arg-362 of the catalytic domain in A-RAF, as well as the positions of the corresponding amino acids in C-RAF are indicated. ATP-binding site and active site are in *purple*;  $\alpha$ C helix is in *light blue*;  $\alpha$ E helix is in *green*. The area formed by interaction between N-region and catalytic domain within the Connolly surface presentation is indicated by *black rectangle*. (B) Alterations of hydrogen bonds between the N-region and the catalytic domain in A-RAF wild type and A-RAF-G300S mutant (close-up view). (C) Alterations of hydrogen bonds between the N-region and the catalytic domain in C-RAF wild type and C-RAF-S339G mutant (close-up view).**

contact with catalytic domain, whereas glutamine in this position partially weakens this interaction. According to this observation, we suggest that the tyrosine 296, which is unique for A-RAF kinase, contributes considerably to the low activating potency of A-RAF caused not only by significantly lower probability of the serine 299 phosphorylation but also by sterical reasons.

Finally, Connolly surface presentations (**Fig. 35A, right panels**) revealed not only the conformational differences between A- and C-RAF but also differences in the pattern of the electrostatic potential. The area formed by interaction between N-region and catalytic domain in A-RAF reveals significantly higher electrostatic potential compared with the same area in C-RAF, suggesting that this A-RAF specific feature may also contribute to the low activating potency of this isoform.

Taken together, our results, which have been obtained using reconstruction model, suggest that the tight binding between the N-region and the catalytic domain acts inhibitory with regard to the kinase activity of RAF proteins, whereas release of this interaction favors the active form of the kinase.

### **6.5.7. R398/K399 in C-RAF and analogous residues R359/K360 in A-RAF are indispensable for their activation**

As discussed in the previous section, binding of the N-region to the kinase domain is proposed to regulate the inducibility of RAF kinase activity. To test this assumption, we examined the kinase activity of C-RAF following disruption of interaction either between S339 and R398 or between D337 and K399 (see also **Fig. 35C**). To this end, we generated C-RAF mutants by substitution of D337, S339, R398 and K399 with alanine. All Myc-tagged C-RAF mutants were expressed in COS7 cells in presence or absence of H-Ras12V and isolated by anti-Myc immunoprecipitation. Subsequently, the extents of their activity were tested in the *in vitro* kinase assay. In addition, phosphorylation degree of the S338, S259 and S621 were probed with the appropriate antibodies. As shown in **Fig. 36A and B** the basal kinase activity of the C-RAF-S339A mutant was highly increased relative to C-RAF WT, whereas the Ras12V-induced activity of the mutant did not significantly differ compared to the activity of the wild type protein. Analogous situation was observed with the phosphorylation of serine 338. Substitution of serine 339 with alanine induced S338 phosphorylation in the basal state (see **Fig. 36A and C**). In contrast, S338 phosphorylation of the C-RAF-S339A mutant was comparable with the phosphorylation degree of C-RAF WT upon co-expression with Ras12V. These findings are partially in accordance with the results obtained with the C-RAF-S339G mutant (see section 6.5.4.), suggesting that not the alteration of the N-region structure caused by substitution of S339 with glycine, but rather the disruption of the interaction between the N-region and kinase domain induces an increase in the C-RAF kinase activity. This conclusion is supported by the observation that both, substitution of S339 with glycine and alanine led to elevated C-RAF kinase activity (**Figs. 32, 33, and 36**). However, whereas phosphorylation of the C-RAF-S339A mutant could be detected with anti-pS338 antibody (**Fig. 36A and C**), this phosphospecific antibody did not recognize the C-RAF-S339G mutant

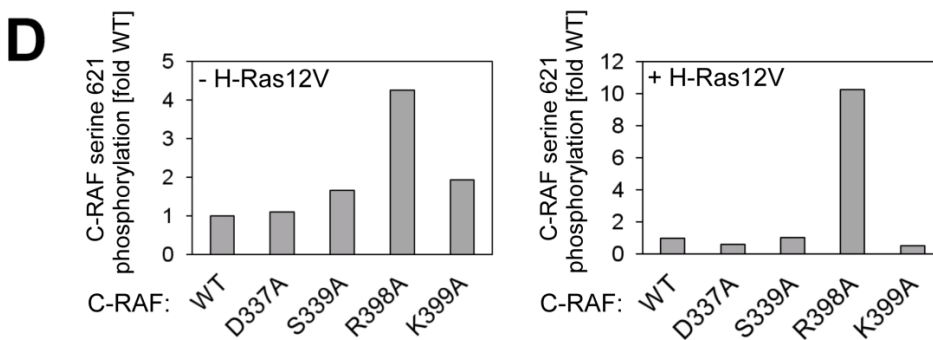
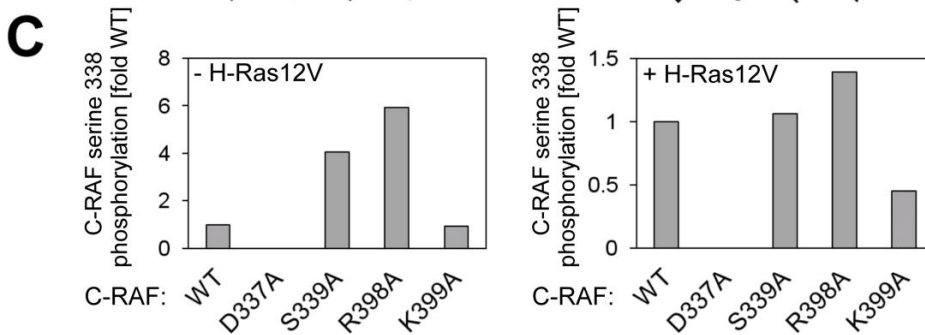
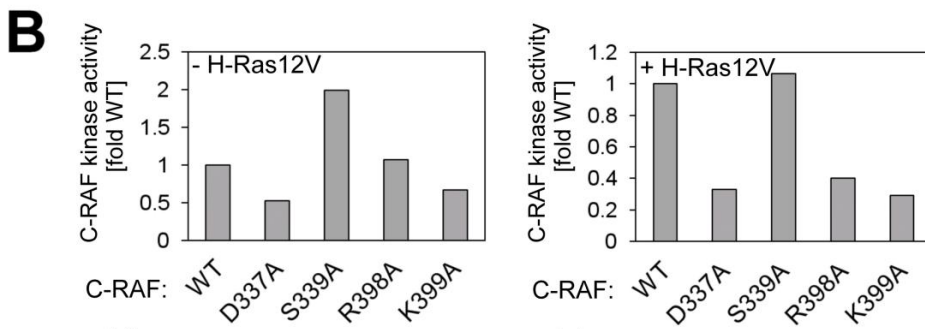
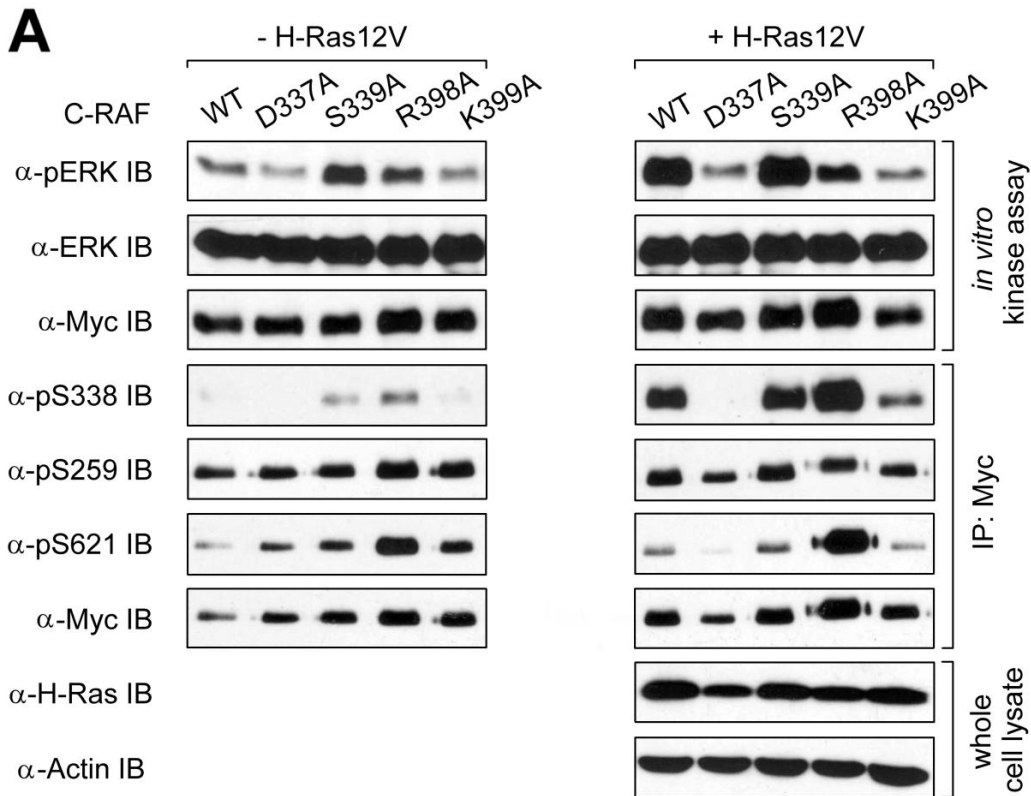


**FIGURE 36: Substitution of R398 or K399 by alanine inhibits the Ras-induced activation of C-RAF.** COS7 cells were transfected with C-RAF wild type (WT) or C-RAF substitution mutants as indicated in the presence or absence of Ras12V. Following starvation for 24h, the cells were lysed and C-RAF proteins were immunoprecipitated (IP) by use of an anti-Myc antibody. Subsequently, kinase activities were measured using recombinant MEK and ERK as substrates. ERK phosphorylation was detected by phosphospecific anti-pERK antibody. To monitor the phosphorylation degree of C-RAF in the positions S338, S259 and S621 the C-RAF phosphospecific antibodies anti-pS338, anti-pS259 and anti-pS621 (see also Hekman *et al.* [202]) were used. **(A)** Western blot analysis of C-RAF kinase activity and phosphorylation degree of S338, S259 and S621 in basal state (*left panel*) and upon co-expression with H-Ras12V (*right panel*). **(B)** Quantification of C-RAF kinase activity. The quantification results are expressed in terms of fold activation, where 1-fold activity represents the amount of activity determined for C-RAF wild type. **(C and D)** Quantification of serine 338 and serine 621 phosphorylation, respectively. The quantification results are expressed in terms of fold phosphorylation, where 1-fold of phosphorylation represents the amount of phosphorylation determined for C-RAF wild type. Expression efficiency of H-Ras12V was determined using anti-H-Ras antibodies. Actin immunodetection was used as a loading control. *IB*, immunoblot.

(**Fig. 33**), suggesting that the local structure of the N-region has been disturbed by serine to glycine substitution, but not by serine to alanine substitution. Thus, we conclude that the stimulatory effects of S339 substitution by glycine or alanine are due to the disruption of the interaction between the N-region and the kinase domain.

In contrast to the C-RAF-S339A mutant, substitution of D337 by alanine led to decrease in basal kinase activity of C-RAF as well as to inhibition of the activity induced by co-expression with Ras12V (see **Fig. 36A and B**). These results are in conflict with our prediction that disruption of the interaction between D337 of the N-region and K399 of the kinase domain would elevate the kinase activity of C-RAF. Immunoblot analysis of C-RAF-D337A mutant with the anti-pS338 antibody clarified this discrepancy. As presented in **Fig. 36A and C** substitution of aspartate in position 337 with alanine completely abrogated the basal and the induced phosphorylation of serine 338. This indicates that amino acid exchange at position 337 alters the local structure of the N-region, making the S338 of C-RAF inaccessible for appropriate kinase. Thus, the abolished phosphorylation of S338 is the most likely reason for the inhibition of kinase activity of the C-RAF-D337A mutant. Additionally, this C-RAF mutant revealed reduced phosphorylation at S621 upon stimulation with Ras12V (**Fig. 36A and D**). Because S621 of C-RAF has been proposed to function as an auto-phosphorylation site [202,295], the reduction of phosphorylation at S621 might be the result of the low kinase activity of the C-RAF-D337A mutant.

Regarding the R398, which in our model interacts with the S339 of the N-region (**Fig. 35C**), substitution of this residue with alanine resulted in slightly elevated basal kinase activity (**Fig. 36A and B, left panel**). This increase of activity can be ascribed to improved phosphorylation of S338 that was observed in the C-RAF-R398A mutant compared with the wild type protein (**Fig. 36A and C, left panel**). In contrast, Ras12V-induced activation of C-RAF-R398A was considerably inhibited, despite elevated phosphorylation of S338 in this mutant compared with C-RAF WT (**Fig. 36A–C, right panel**). Moreover, the C-RAF-R398A mutant revealed more than 4-fold higher phosphorylation of S621 in non-stimulated state and up to 10-fold higher amounts of pS621 in Ras12V-stimulated sample compared to C-RAF WT (**Fig. 36A and D**). These results argue against the autophosphorylation hypothesis of C-

RAF at S621, but prefer rather interdependence between phosphorylation of S338 and S621. In the case of K399, which in our model interacts with D337 (**Fig. 35C**) of the N-region in C-RAF, substitution of this amino acid with alanine did not reduce significantly the basal kinase activity, but strongly diminished the Ras12V induced activation of C-RAF-K399A mutant compared with wild type (**Fig. 36A and B**). The impaired activation of C-RAF-K399A can be ascribed to inhibited phosphorylation of S338 observed in this mutant (**Fig. 36A and C**). In contrast, phosphorylation of S621 in this mutant was comparable with the appropriate phosphorylation in C-RAF WT (**Fig. 36A and D**). This is an additional argument against auto-phosphorylation of C-RAF at S621. In contrast to S621, none of the substitution mutants revealed changes in phosphorylation status of S259 (**Fig. 36A**).

As the sequence surrounding R398 and K399 in C-RAF is highly conserved between RAF isoforms, we asked whether regulation of A-RAF kinase activity by these basic residues would be analogous to C-RAF. To address this issue, we substituted R359 and K360 in A-RAF by alanine and examined the Ras12V/Lck induced activation of these mutants. As presented in **Fig. 37**, both, A-RAF-R359A and A-RAF-K360A mutants, revealed strong inhibition of the Ras12V/Lck induced kinase activity compared with wild type protein. The inhibition pattern was similar to that previously observed for C-RAF (**Fig. 36A**), suggesting that regulation of RAF kinases by this domain is conserved at least between A- and C-RAF.

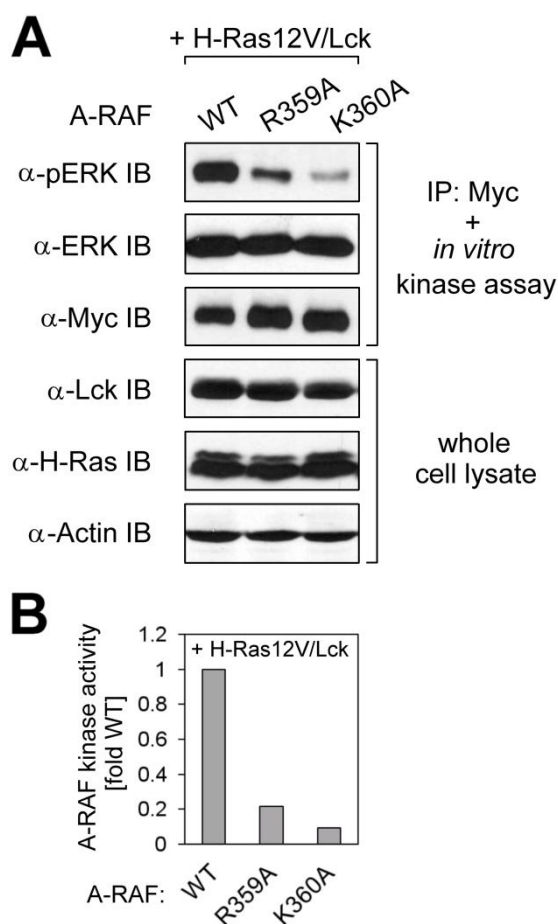


**FIGURE 37: Similar to C-RAF, substitution of R359 or K360 by alanine inhibits the Ras/Lck-induced activation of A-RAF.** COS7 cells were transfected with A-RAF wild type (WT) or A-RAF substitution mutants as indicated in the presence of Ras12V and Lck. Following starvation for 24 h, the cells were lysed and A-RAF proteins were immunoprecipitated (IP) by use of an anti-Myc antibody. Subsequently, kinase activities were measured using recombinant MEK and ERK as substrates. ERK phosphorylation was detected by phosphospecific anti-pERK antibody. **(A)** Western blot analysis of A-RAF kinase activity upon co-expression with Ras12V and Lck. **(B)** Quantification of A-RAF kinase activity. The quantification results are expressed in terms of fold activation, where 1-fold activity represents the amount of activity determined for A-RAF wild type. Expression efficiency of H-Ras12V and Lck was determined using anti-H-Ras and anti-Lck antibodies, respectively. Actin immunodetection was used as a loading control. *IB*, immunoblot.



### 6.5.8. Substitution of R398 in C-RAF and R359 in A-RAF by alanine induces mobility shift-associated hyperphosphorylation of these proteins

To elucidate the mechanism by which R398A and K399A substitutions inhibit Ras12V-induced C-RAF activation, we next investigated subcellular localization of C-RAF WT and C-RAF mutants in COS7 cells upon co-expression with Ras12V and Lck. To this end, COS7 cells were transfected with plasmids expressing Myc-tagged C-RAF wild type and C-RAF substitution mutants (C-RAF-R398A and C-RAF-K399A). 24 hours after transfection, subcellular fractions (cytosolic, membrane, nuclear and cytoskeletal fractions) were collected according to the protocol of the *ProteoExtract* subcellular proteome extraction kit. Fractionation of the COS7 cells revealed that C-RAF proteins were absent from the nuclear fraction (**Fig. 38 A and B**), and the cytoskeletal fraction contained only small portion of C-RAF. Most of the C-RAF protein was distributed between cytosolic and membrane fractions. In contrast to non-stimulated cells (**Fig. 34A**), C-RAF WT expressed in the presence of Ras12V and Lck was located preferentially in the membrane fraction (63%). Substitution of K399 to alanine did not alter the distribution of activated C-RAF (61% in the membrane fraction), whereas exchange of arginine in position 398 to alanine elevated the membrane located portion of C-RAF protein up to 78% (see also **Fig. 38A and B**).

To examine phosphorylation status of C-RAF WT and mutants in subcellular fractions, we probed the samples with anti-pS338, anti-pS259, and anti-pS621 antibodies. The immunoblotting analysis with anti-pS338 antibody revealed that 83% of the S338 phosphorylated C-RAF WT were located at the membranes (**Fig. 38A and B**). Similar results were obtained for C-RAF-K399A. In contrast, the membrane localization of the S338 phosphorylated C-RAF-R398A mutant was impaired, resulting in only 61% of C-RAF-R398A that were found within the membrane fraction. Distribution of the S259 and S621 phosphorylated C-RAF between cytoplasm and membranes was not significantly changed upon substitution of R398 or K399 by alanine (**Fig. 38A and B**). Whereas the S259 phosphorylated C-RAF was preferentially located in the cytoplasm (about 80%), the cytosol located portion of the S621 phosphorylated C-RAF was smaller than in the case of S259 phosphorylation (about 65%).

The most interesting finding disclosed by subcellular fractionation was mobility shift of C-RAF-R398A mutant in SDS-PAGE (see **Fig. 38C**). The separation of the membrane located C-RAF-R398A fraction by electrophoresis revealed two protein bands: the lower band is also present in the samples of C-RAF WT and C-RAF-K399A, whereas the upper band is C-RAF-R398A-specific. These observations suggest that the substitution of R398 by alanine induces posttranslational modifications of C-RAF resulting in mobility shift. The mobility shift of the C-RAF-R398A mutant was observed only in the samples stimulated by co-expression with Ras12V and Lck. The non-stimulated samples and samples activated with EGF (5 minutes) did not revealed electrophoretic mobility shift (data not shown). Using phosphospecific antibodies, we analyzed the phosphorylation pattern of the normal and shifted C-RAF-R398A bands. The intensity of the upper and the lower bands in the anti-pS338 immunoblots are comparable, whereas in the anti-Myc immunoblots the lower band is

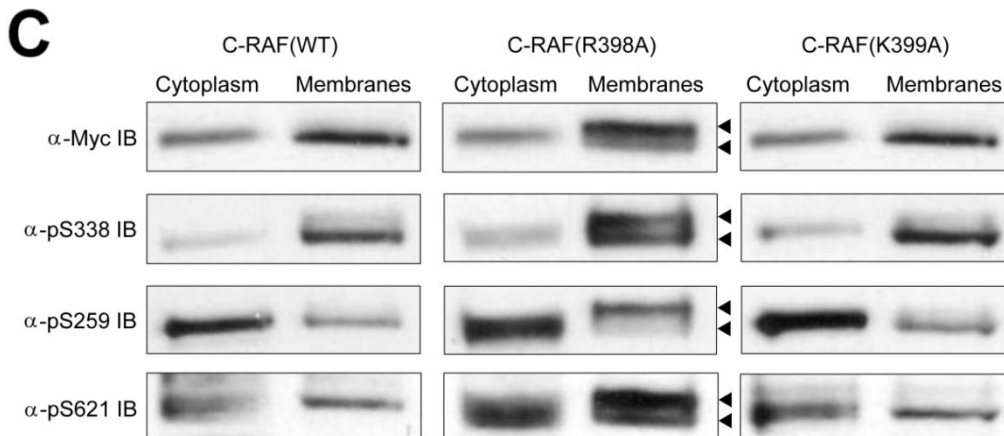
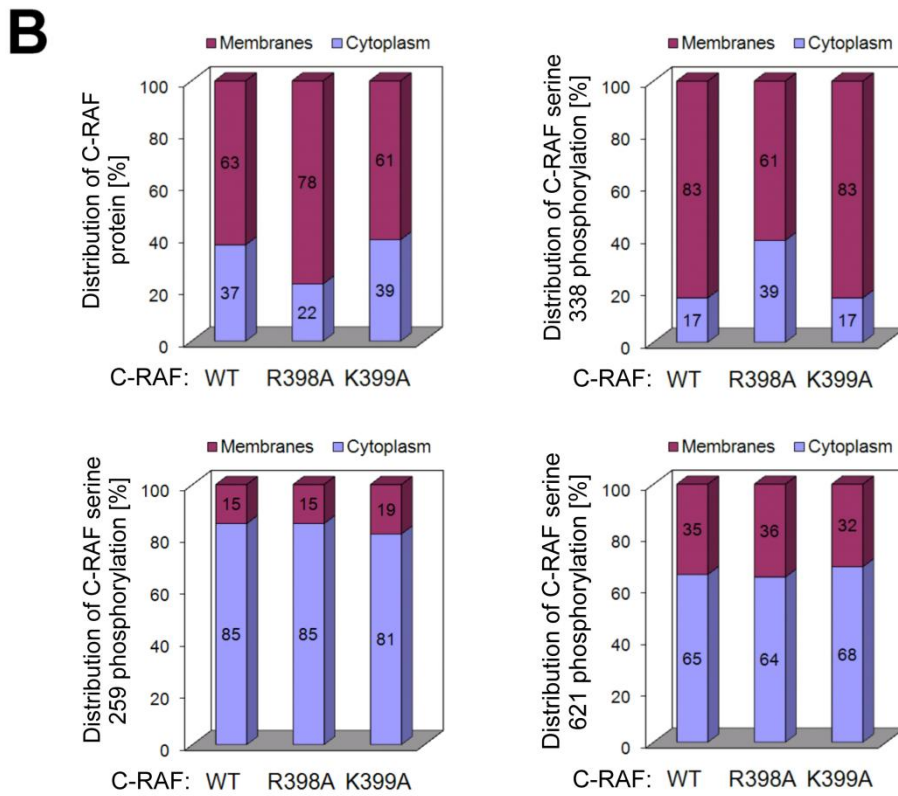
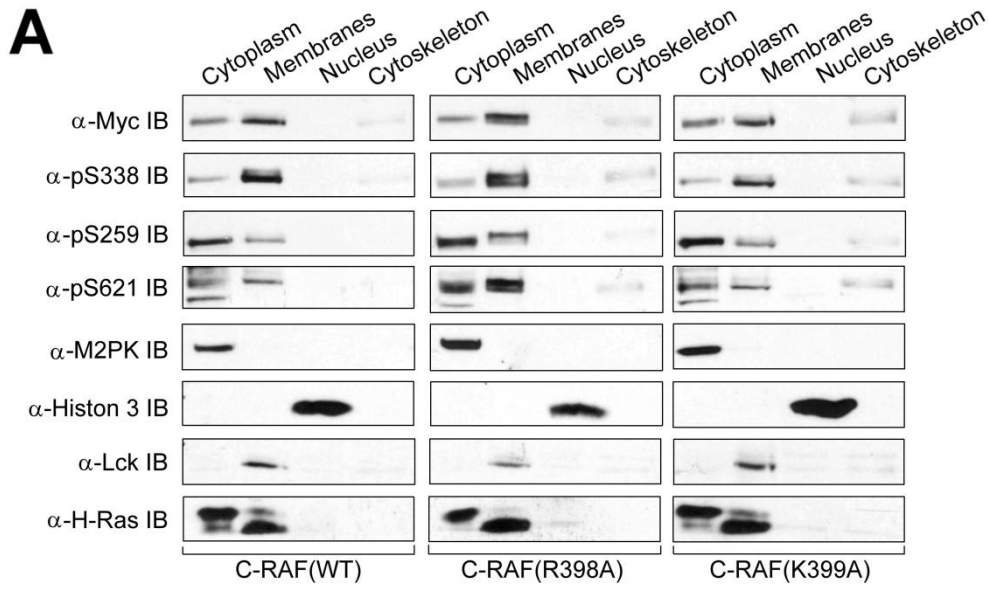


**FIGURE 38: Subcellular localization of C-RAF WT and C-RAF-R398A and -K399A mutants upon co-transfection with Ras12V and Lck.** (A) Western blot analysis of subcellular distribution of C-RAF wild type and C-RAF mutants. COS7 cells were transfected with C-RAF wild type and C-RAF substitution mutants (as indicated) carrying C-terminal Myc tag in presence of Ras12V and Lck. 24 hours after transfection, cytoplasmic, membrane, nuclear, and cytoskeletal fractions were collected according to the protocol of the *ProteoExtract* subcellular proteome extraction kit. *Fractionation control*: anti-M2PK immunodetection for cytosolic fraction, anti-Lck immunodetection for membrane fraction, anti-histon 3 immunodetection for nuclear fraction. *IB*, immunoblot. (B) Quantification of C-RAF protein distribution between cytosolic and membrane fractions and quantification of C-RAF S338, S259 and S621 phosphorylation in cytosolic and membrane fractions. Data from two independent experiments were quantified by optical densitometry. Values represent %-ratio of RAF protein in each fraction relative to the total RAF protein detected in both, cytosolic and membrane fractions together. Values of observed phosphorylation were normalized for C-RAF content. They represent %-ratio of measured S338, S259 and S621 phosphorylation in each fraction relative to the total phosphorylation in both, cytosolic and membrane fractions together. (C) Close-up view at the Western blots from A.

less intensive than the upper one (**Fig. 38C**), suggesting that the S338 phosphorylation degree of the shifted C-RAF-R398A population is decreased compared with the phosphorylation of the normal population. The S621 phosphorylation of the shifted C-RAF-R398A population is comparable with that of the normal population. In contrast, the shifted C-RAF-R398A population is strongly phosphorylated on S259, whereas the normal population is almost not phosphorylated on this site (**Fig. 38C**).

As the Ras12V-induced kinase activity of the C-RAF-R398A mutant was inhibited compared to C-RAF WT (**Fig. 36A and B**), these results demonstrate clearly that the marked electrophoretic mobility shift of C-RAF-R398A observed in response to Ras12V co-expression is not required for kinase activation. Hence, the C-RAF-R398A mobility shift is an inadequate monitor for the activation state of this kinase.

Several groups reported a casual relationship between hyperphosphorylation and C-RAF mobility shift [153,230,296-298]. Moreover, Dougherty *et al.* [153] have shown that the electrophoretic mobility shift of C-RAF is a result of a direct feedback phosphorylation by ERK. C-RAF has been suggested to be negatively regulated by ERK-mediated hyperphosphorylation that inhibits the Ras/C-RAF interaction and desensitizes C-RAF to additional stimuli [153]. To address, whether the mobility shift observed in this study may be a result of ERK-mediated feedback phosphorylation, we treated the cells expressing Ras12V, Lck and Myc-tagged C-RAF-R398A mutant with the MEK inhibitor U0126 before fractionation. The U0126-induced deactivation of ERK was validated by use of anti-phospho-ERK antibody, as shown in **Fig. 39B**. Inhibition of MEK activity by U0126 and subsequent deactivation of ERK led to a significant decrease in the intensity of the upper C-RAF band compared to control (**Fig. 39A**). This finding suggests that the shift in the electrophoretic mobility of the C-RAF-R398A mutant is a result of the ERK-mediated feedback phosphorylation.

Remarkably, subcellular fractionation of the cells expressing A-RAF WT or A-RAF mutants (A-RAF-R359A or A-RAF-K360A) in the presence of Ras12V and Lck revealed in the case of A-RAF-R359A mutant also two protein bands: the lower band that was also present in the samples of A-RAF WT and A-RAF-K360A, and the upper band that was A-RAF-R359A-specific (**Fig. 40**). These results suggest that similar to C-RAF substitution of

R359 to alanine leads to hyperphosphorylation of A-RAF kinase upon co-expression with Ras12V and Lck.

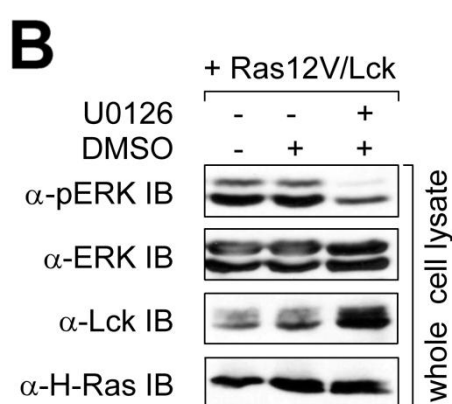
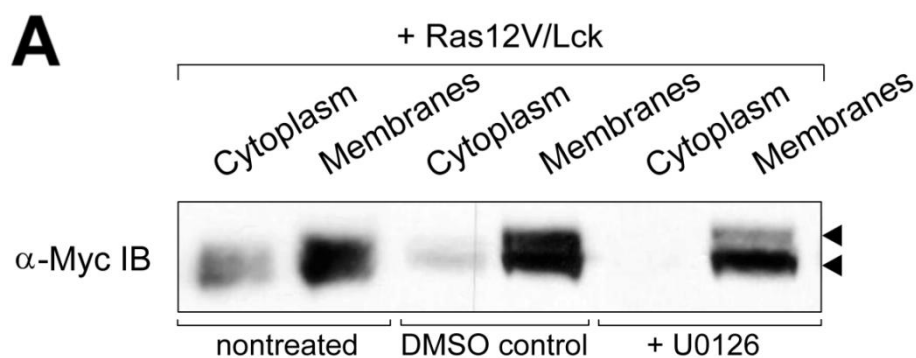


**FIGURE 39: U0126 inhibits hyperphosphorylation of the C-RAF-R398A mutant.** (A) Western blot analysis of electrophoretic mobility of C-RAF-R398A upon treatment with the MEK inhibitor U0126. COS7 cells were transfected with C-RAF-R398A carrying C-terminal Myc tag in the presence of Ras12V and Lck. 12 hours after transfection, the cells were treated with U0126 (10 μM) for further 12 hours. Cytoplasmic and membrane fractions were collected according to the protocol of the *ProteoExtract* subcellular proteome extraction kit. (B) Validation of the U0126 mediated inhibition of ERK activity by anti-pERK antibody. ERK immunodetection was used as a loading control. Expression efficiency of H-

Ras12V and Lck was determined using anti-H-Ras and anti-Lck antibodies, respectively. *IB*, immunoblot.

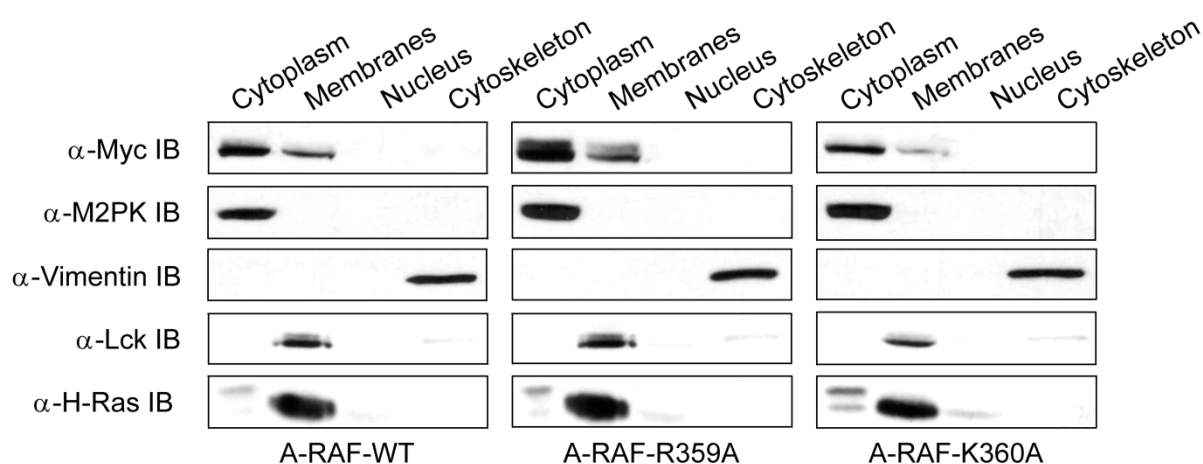


**FIGURE 40: A-RAF-R359A mutant reveals an electrophoretic mobility shift upon co-expression with Ras12V and Lck.** (A) Western blot analysis of subcellular distribution of A-RAF wild type and A-RAF mutants. COS7 cells were transfected with A-RAF wild type and A-RAF substitution mutants (as indicated) carrying C-terminal Myc-tag in presence of Ras12V and Lck. 24 hours after transfection, cytoplasmic, membrane, nuclear and cytoskeletal fractions were collected according to the protocol of the *ProteoExtract* subcellular proteome extraction kit. *Fractionation control*: anti-

M2PK immunodetection for cytosolic fraction, anti-Lck immunodetection for membrane fraction, anti-vimentin immunodetection for cytoskeleton fraction. Expression efficiency of H-Ras12V was determined using anti-H-Ras antibodies. *IB*, immunoblot.

## 6.6. Feedback regulation of A-RAF

### 6.6.1. Phosphorylation within the IH-domain positively regulates activation process of A-RAF

Whereas the initial steps of RAF activation have been investigated in detail, the mechanisms of feedback regulation are only partially understood. Recently, Dougherty *et al.* [153] discussed the possibility that ERK-induced phosphorylation may be responsible for downregulation of C-RAF kinase activity. These data are in agreement with our contribution [194], in which we identified negative regulation of C-RAF by phosphorylation at serines 296 and 301 within the isoform-specific hinge domain (IH-domain). In the case of B-RAF, phosphorylation of the evolutionarily conserved SPKTP motif located at the C-terminus has been suggested to be involved in the negative feedback regulation [299]. Regarding feedback regulation of A-RAF, no data are available so far. With the exception of the 257SP site in A-RAF that corresponds to the C-RAF 296SP motif, the amino acid sequences of the IH-segments in A- and C-RAF reveal a very low degree of similarity, suggesting that regulation of kinase activity by this segment may occur in an isoform-specific way. Indeed, our data obtained by mass spectrometry revealed that A-RAF similar to C-RAF is phosphorylated within the IH-domain. We detected several phosphorylated fragments covering the region between amino acids 248 and 288 of A-RAF (see **Fig. 20** and **Table 2**) that correspond to IH-segment. However, in contrast to C-RAF, which has been reported to be phosphorylated at only two sites (S296 and S301), the corresponding A-RAF fragment (248-267) was phosphorylated at all of the seven putative phosphorylation sites. This phosphopeptide was detected only in the Ras12V/Lck activated A-RAF protein. Other peptides derived from this region were partially phosphorylated and were found in both serum- and Ras12V/Lck-stimulated A-RAF samples. In addition, we identified two A-RAF-specific phosphorylation sites (S272 and S274) next to the IH-region (see also **Fig. 20** and **Tables 2** and **3**). Thus, these findings suggest that A-RAF becomes highly phosphorylated within the IH-region upon prolonged stimulation.

To examine the functional role of the novel phosphorylation sites for A-RAF signaling, we prepared single mutations derived from the seven phosphorylation sites present in the GGSDGTPRGSPSPASVSSGR tryptic fragment by replacing each of the six serines and threonine 253 by alanine. As depicted in **Fig. 41A** and **B** single mutations at serines 257, 262 and 264 strongly impaired the A-RAF kinase activity upon EGF stimulation. Consistent with these findings Ras/Lck-mediated A-RAF activation was almost completely abolished by the same substitutions (**Fig. 41D** and **E**). The replacement of other residues (S250, T253,

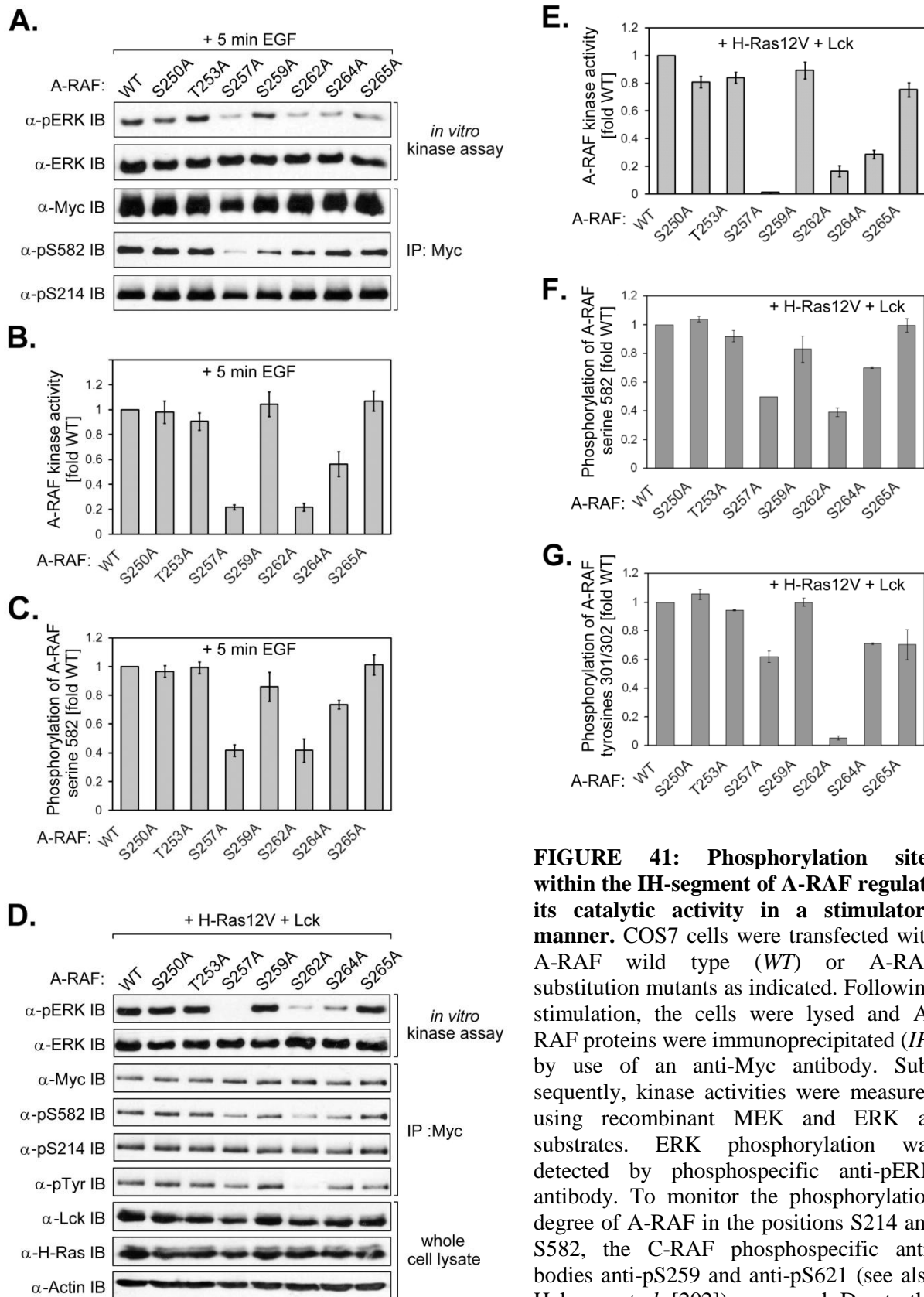


**FIGURE 41: Phosphorylation sites within the IH-segment of A-RAF regulate its catalytic activity in a stimulatory manner.** COS7 cells were transfected with A-RAF wild type (WT) or A-RAF substitution mutants as indicated. Following stimulation, the cells were lysed and A-RAF proteins were immunoprecipitated (IP) by use of an anti-Myc antibody. Subsequently, kinase activities were measured using recombinant MEK and ERK as substrates. ERK phosphorylation was detected by phosphospecific anti-pERK antibody. To monitor the phosphorylation degree of A-RAF in the positions S214 and S582, the C-RAF phosphospecific antibodies anti-pS259 and anti-pS621 (see also Hekman *et al.* [202]) were used. Due to the homology of the corresponding epitopes, these antibodies detect both RAF isoforms

with comparable affinity. Tyrosine phosphorylation of A-RAF was determined by anti-phosphotyrosine (*pTyr*) antibody 4G10. (A) Western blot analysis of A-RAF kinase activity and phosphorylation degree of S214 and S582 upon stimulation with EGF (100 ng/ml) for 5 minutes. (B)

Quantification of A-RAF kinase activity upon activation with EGF. The quantification results are expressed in terms of fold activation, where 1-fold activity represents the amount of activity determined for A-RAF wild type. Average values derived from the data of five independent experiments were used for quantification. (C) Quantification of serine 582 phosphorylation upon activation with EGF. The quantification results are expressed in terms of fold phosphorylation, where 1-fold of phosphorylation represents the amount of phosphorylation determined for A-RAF wild type. (D) Western blot analysis of A-RAF kinase activity and phosphorylation degree of S214, S582 and Y301/Y302 upon co-expression with Ras12V and Lck. (E) Quantification of A-RAF kinase activity upon co-expression with Ras12V/Lck. The quantification results are expressed in terms of fold activation, where 1-fold activity represents the amount of activity determined for A-RAF wild type. Average values derived from the data of three independent experiments were used for quantification. (F and G) Quantification of serine 582 and tyrosines 301/302 phosphorylation upon co-expression with Ras12V/Lck. The quantification results are expressed in terms of fold phosphorylation, where 1-fold of phosphorylation represents the amount of phosphorylation determined for A-RAF wild type. Expression efficiency of H-Ras12V and Lck was determined using anti-H-Ras and anti-Lck antibodies, respectively. Actin immunodetection was used as a loading control. *IB*, immunoblot.

S259 and S265) by alanine did not cause significant changes of A-RAF activity. Similarly, substitution of serines 272 and 274 by alanine did not impair kinase activity (data not shown). In this context, we examined also the degree of phosphorylation of other regulatory sites of A-RAF: e. g. serines 582 and 214 within the 14-3-3 binding domains and tyrosines 301/302 within the N-region. Whereas phosphorylation of S214 was unchanged for all of the samples, the levels of S582 phosphorylation were considerably reduced in A-RAF-S257A, A-RAF-S262A and ARAF-S264A mutants, indicating an interdependence between activity and phosphorylation of the C-terminal 14-3-3 binding site (**Fig. 41**). Regarding tyrosine phosphorylation, we did not observe any phosphorylation upon EGF stimulation in agreement with original findings [77]. In contrast, activation mediated by Ras12V/Lck resulted in efficient tyrosine phosphorylation of A-RAF WT and substitution mutants with exception of A-RAF-S262A mutant, whose tyrosine phosphorylation was completely abrogated. Although the antibody used here is directed against phosphotyrosine *per se*, tyrosine phosphorylation induced by co-expression with Ras12V and Lck can be ascribed entirely to tyrosines 301/302, because this antibody did not recognize A-RAF-Y301D-Y302D mutant (see **Fig. 42**). This finding indicates that A-RAF-S262A mutant is not phosphorylated on tyrosines 301/302 compared to wild type. Notably, it was possible to rescue partially the kinase activity of A-RAF-S262A mutant by additional introduction of aspartic acids in positions Y301 and Y302 that mimics Lck induced phosphorylation in these positions (see **Fig. 42**).

As three S/TP phosphorylation sites within the IH-segment of A-RAF (253TP, 257SP and 259SP) and two adjacent SP sites (269 and 274) reveal ERK-directed phosphorylation motifs, we expected that these sites might be involved in ERK-mediated feedback phosphorylation of A-RAF. To this end, we examined activation of A-RAF wild type in the presence and absence of the MEK inhibitor U0126. As demonstrated in **Fig. 43**, treatment of the cells with U0126 resulted in a considerable reduction of A-RAF activity induced by Ras12V/Lck. Thus, in contrast to C-RAF, in which phosphorylation within the IH-domain contributes to negative feedback regulation, phosphorylation of the IH-domain in A-RAF regulates its kinase activity in a stimulatory manner.

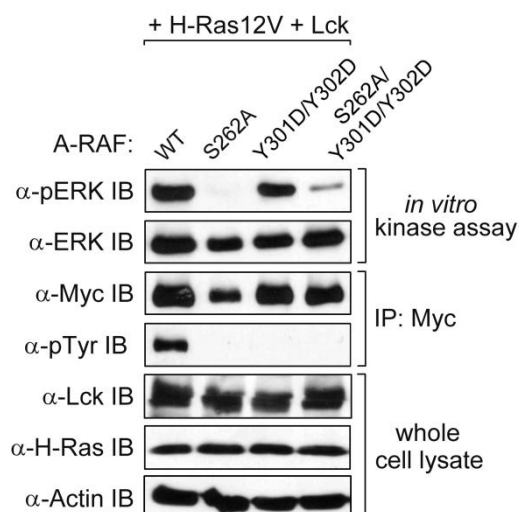


**FIGURE 42: Introduction of Y301D/Y302D substitution into the A-RAF-S262A mutant rescues partially its kinase activity.** C-terminally Myc-tagged A-RAF wild type (WT) and A-RAF substitution mutants (S262A, Y301D/Y302D and S262A/Y301D/Y302D) were expressed in COS7 cells in presence of H-Ras12V and Lck. Cell lysis, immunoprecipitation (IP) with anti-Myc antibody and kinase activity measurements were carried out as described in Fig. 41. Tyrosine phosphorylation of A-RAF was determined by anti-phosphotyrosine (*pTyr*) antibody 4G10. Expression efficiency of H-Ras12V and Lck was determined using anti-H-Ras and anti-Lck antibodies, respectively. Actin immunodetection was used as a loading control. *IB*, immunoblot.

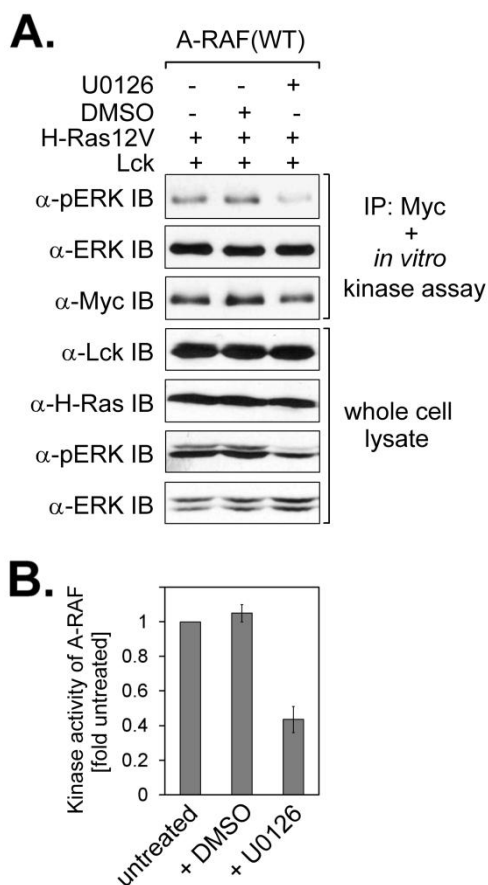


**FIGURE 43: Abolishment of ERK-mediated feedback regulation by treatment with MEK inhibitor U0126 results in reduction of A-RAF kinase activity.** C-terminally Myc-tagged A-RAF wild type (WT) was expressed in COS7 cells in the presence of H-Ras12V and Lck. Prior to lysis, the cells were treated with MEK inhibitor U0126 (10  $\mu$ M) for 12 hours. Immunoprecipitation (IP) with anti-Myc antibody and kinase activity measurements were carried out as described in Fig. 41. (A) Western blot analysis of A-RAF kinase activity. (B) Quantification of A-RAF kinase activity. The quantification results are expressed in terms of fold activation, where 1-fold activity represents the amount of activity determined for A-RAF wild type derived from the untreated cells. Average values derived from the data of two independent experiments were used for quantification. Expression efficiency of H-Ras12V and Lck was determined using anti-H-Ras and anti-Lck antibodies, respectively. Detection of phosphorylated ERK in whole cell lysates was used to verify the efficiency of MEK inhibition by U0126. ERK immunodetection was used as a loading control. *IB*, immunoblot.

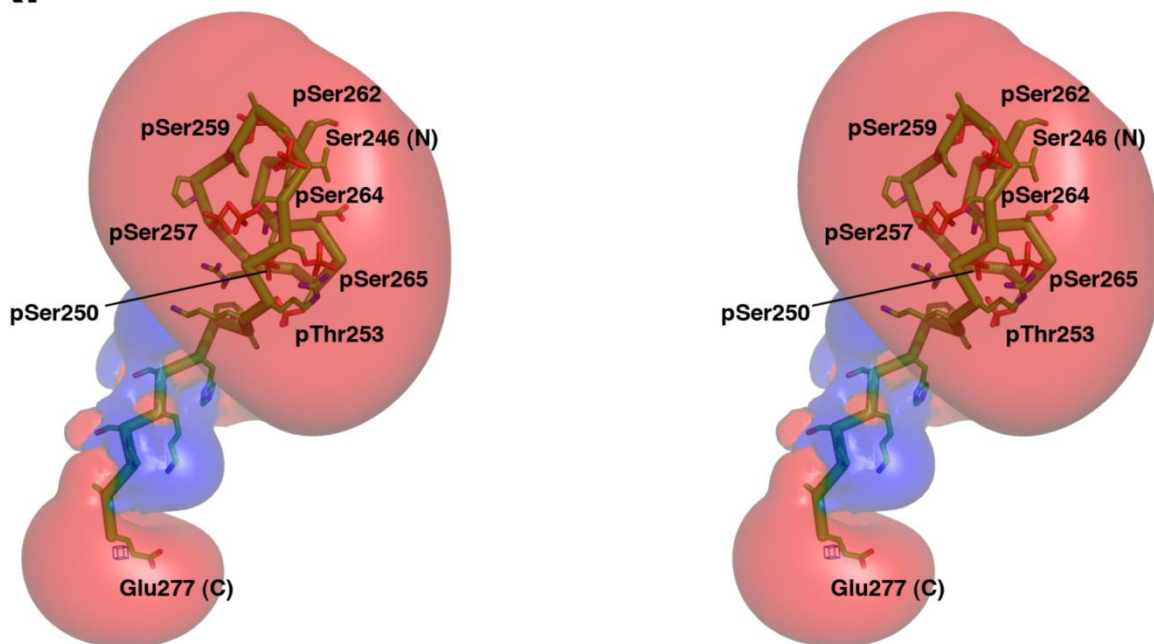


### 6.6.2. Spatial model reveals charge reversal at the molecular surface of IH-segment of A-RAF upon phosphorylation

The isoform specific IH-segment of A-RAF reveals an unusually high density of putative phosphorylation sites, but in addition also a high number of basic residues (see **Fig. 20**). To obtain a spatial image of the distribution of negative charge upon phosphorylation of these sites and to compare this with the distribution of the positive charge of the non-stimulated kinase, we performed molecular modeling of the IH-region. The three-dimensional structure of the corresponding peptide comprising residues between S246 and E277 was modeled using *Protein Design Model QUANTA2006*. Since no homologous structure templates were available, *de novo* modeling was applied using an extended peptide strand without secondary structure elements as start structure. This starting template was then submitted to molecular dynamics simulations to form a more globular structure. Several structures for the phosphorylated and non-phosphorylated form were simulated to test whether the sequence folds into a common motif, however, consistent with secondary structure prediction, neither defined secondary structure elements nor globular structures were observed. Similar results were obtained for phosphorylated and non-phosphorylated forms, indicating that phosphorylation did not influence the peptide structure in defined manner. One representative conformer for both, the phosphorylated and non-phosphorylated form is illustrated in **Fig. 44**, revealing the typical random coil structure. To analyze the changes in charge distribution upon phosphorylation, electrostatic potential maps were calculated using the non-linearized Poisson-Boltzmann equation and the software *APBS*. Upon introduction of multiple phosphorylation sites in positions S250, T253, S257, S259, S262, S264 and S265, we observed a charge reversal of a mainly positive to a strongly negative electrostatic potential map. This observation forms our current working hypothesis, in which we propose that the high accumulation of negative charges may lead to an electrostatic destabilization of protein-membrane interaction, resulting in depletion of A-RAF from the plasma membrane upon prolonged stimulation by Ras and Lck. On the other hand, C-RAF, which is lacking this multiphosphorylation stretch, may behave contrary to A-RAF.

To test this hypothesis, we performed analysis of subcellular localization of A- and C-RAF wild type expressed in the presence and absence of Ras12V and Lck. The data illustrated in **Fig. 45** indicate that in non-stimulated cells both, A- and C-RAF, were located preferentially in the cytosolic fraction. In contrast, upon co-expression with Ras and Lck, the subcellular distribution of A- and C-RAF was diametrically opposed. Whereas C-RAF has been found to be associated mainly with membranes, A-RAF was highly accumulated in the cytosolic fraction. Thus, these experiments support the view that A- and C-RAF are subject to differential regulation, most probably due to the structural differences within the N- and IH-regions.

A.



B.

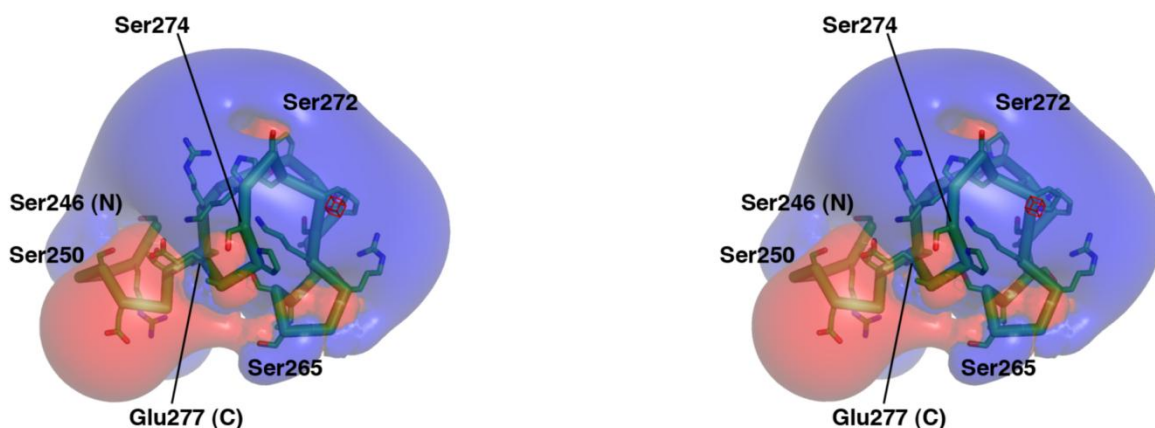


**FIGURE 44: Charge reversal at the molecular surface of IH-segment in A-RAF upon phosphorylation.** (A) Stereoview of the electrostatic potential map of the A-RAF fragment (residues between S246 and E277) containing the IH region with residues Ser250, Thr253, Ser257, Ser259, Ser262, Ser264 and Ser265 being phosphorylated. The peptide region adopts a random coil structure. One representative of five calculated structures has been chosen for quantification of the electrostatic potential. Isocontours for  $-0.5$  kT/e (red) and  $+0.5$  kT/e (blue) are shown. The region comprising the phosphoserine and -threonine residues shows a highly negative potential besides the presence of several positively charged amino acids. (B) Stereoview of the electrostatic potential of the IH-region of A-RAF in its non-phosphorylated form. In contrast to A, various basic residues cause a mainly positively charged potential, thus suggesting a switch of charge upon phosphorylation.

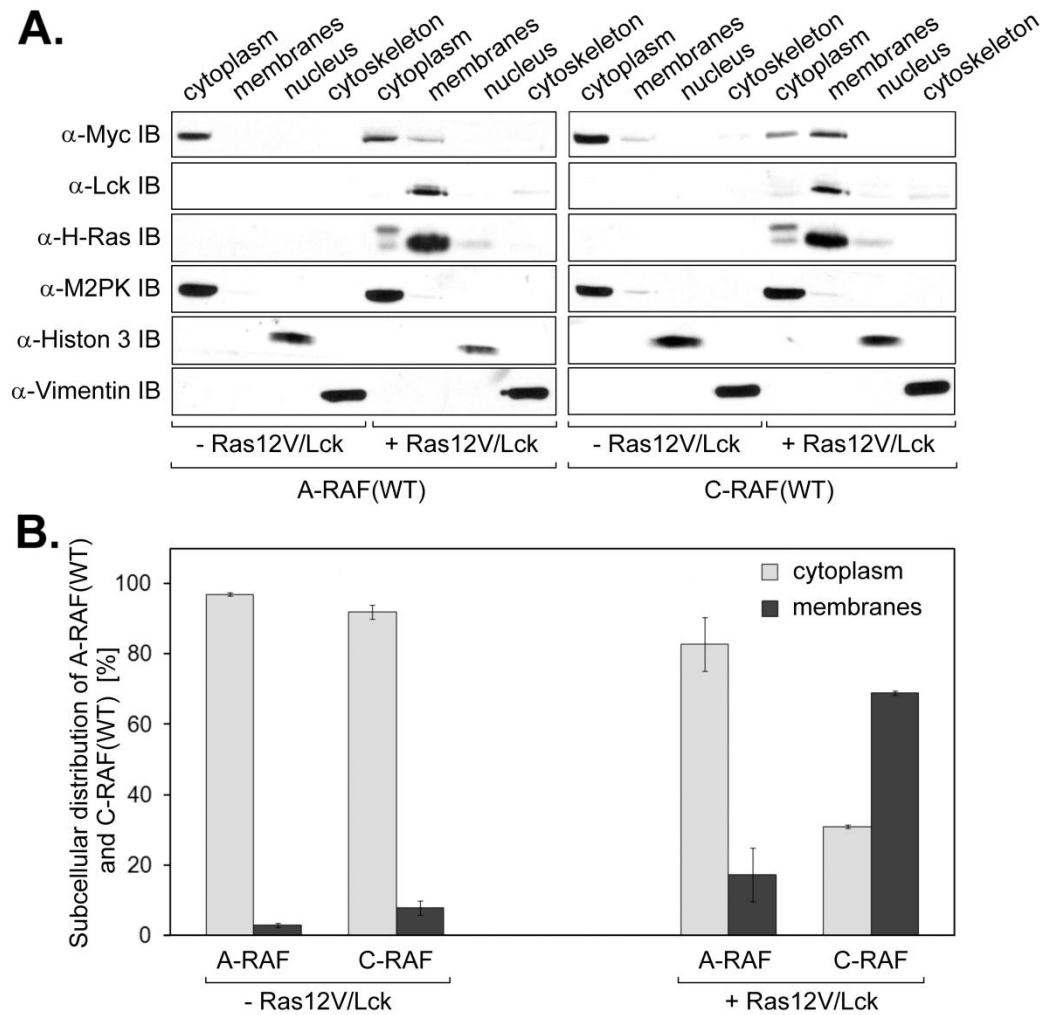


**FIGURE 45: Subcellular fractionation study reveals opposite distribution of activated A- and C-RAF.** (A) Western blot analysis of subcellular distribution of activated and non-activated A-RAF wild type (WT) (left panel) and C-RAF wild type (WT) (right panel). COS7 cells were transfected with Myc-tagged A- and C-RAF wild type in the presence and absence of H-Ras12V and Lck. After 24 hours of serum starvation, cytoplasmic, membrane, nuclear and cytoskeletal fractions were collected according to the protocol of the *ProteoExtract* subcellular proteome extraction kit. *Fractionation control*: anti-M2PK immunodetection for cytosolic fraction, anti-histon 3 immunodetection for nuclear fraction and anti-vimentin immunodetection for cytoskeletal fraction. Expression of H-Ras12V and Lck was detected using anti-H-Ras and anti-Lck antibodies, respectively. *IB*, immunoblot. (B) Quantification of A- and C-RAF protein distribution between cytosolic and membrane fractions. Data from two independent experiments were quantified by optical densitometry. Values represent %-ratio of RAF protein in each fraction relative to the total RAF protein detected in both, cytosolic and membrane fractions together.

## 7. DISCUSSION

While much attention has been devoted to the phosphorylation-mediated regulation of B- and C-RAF, with some exception little is known about the role of phosphorylation in the A-RAF activation process. In the presented work, we performed a systematic analysis of regulatory phosphorylation sites of A-RAF by mass spectrometry. The screening of the peptides derived from the serum-activated or Ras12V/Lck-stimulated A-RAF protein revealed a number of phosphorylated fragments that correspond to both, N-terminal regulatory part as well as to the kinase domain (**Fig. 20** and **Table 2**). Most of the phosphorylation sites identified within the kinase domain of A-RAF appeared to be conserved, suggesting that regulation by phosphorylation of the kinase domain occurs in a similar way for all three RAF isoforms. In contrast, the phosphorylation sites that were detected within the N-terminal regulatory part and at the very C-terminus of the protein show high degree of variability. These observations indicate that the unique regulation of each RAF isoform is specified *inter alia* by these variable regions.

### 7.1. Isoform-specific regulation of A-RAF by 14-3-3 proteins

The participation of 14-3-3 proteins in the activation-deactivation cycle of B- and C-RAF is well established [202,243,289]. Dimers of 14-3-3 proteins have been shown to interact with C- and B-RAF by binding to the internal and C-terminal 14-3-3 binding motifs [199]. Since the association of RAF with 14-3-3 proteins requires phosphorylation of the serines within the binding motifs, we investigated here by use of mass spectrometry and available phosphospecific antibodies the phosphorylation of the proposed 14-3-3 binding sites in A-RAF. The mass spectrometry data provided partial information. We detected only the tryptic fragment corresponding to the C-terminal 14-3-3 binding domain (**Fig. 20** and **Table 2**). Data from MS analysis were complemented by use of phosphospecific antibodies. As shown in **Fig. 21** and **22**, both, the internal and the C-terminal 14-3-3 binding sites of A-RAF, proved to be phosphorylated, suggesting that A-RAF may bind 14-3-3 dimers in a similar way as already described for C- and B-RAF.

#### 7.1.1. Phosphorylation of the N-region may support the association of A-RAF with 14-3-3 dimers

The presence of the serines 621 and 729 in C- and B-RAF, respectively, has been shown to be crucial for the activation of these kinases [202,243]. Regarding the internal 14-3-3 binding domain of B-RAF, the substitution of serine 365 by alanine led to a strong increase of kinase activity, indicating that phosphorylation of this 14-3-3 binding site acts

highly inhibitory [243]. Analogous observations have been made with C-RAF [202,300]. The data obtained with the A-RAF-S582A mutant isolated from Sf9 cells revealed that A-RAF behaves similar to B- and C-RAF with respect to regulation by the C-terminal 14-3-3 binding site. The basal activity of A-RAF-S582A was abolished upon substitution of S582 by alanine. Furthermore, the presence of the intact C-terminal 14-3-3 binding site was partially required for kinase stimulation by Ras12V and Lck. Similarly, Ras12V/Lck-induced activity of the A-RAF-S582A mutant isolated from COS7 cells was significantly diminished compared with wild type (**Fig. 22**). Thus, regulation of A-RAF by the C-terminal 14-3-3 binding site is common for all cell systems. Remarkably, fragmentation analysis of the phosphopeptide corresponding to the C-terminal 14-3-3 binding domain revealed an additional phosphorylation at S585 (**Table 3**). Phosphorylation of this highly conserved serine has not been observed in B- or C-RAF so far and may be A-RAF-specific. The consequence of this phosphorylation may be the prevention of 14-3-3 binding to A-RAF, resulting in the extraordinary low extent of A-RAF kinase activity as generally observed.

Regarding the internal 14-3-3 binding site, the results of the present study performed with Sf9 insect cells show that the basal kinase activity of the A-RAF-S214A mutant was elevated compared to A-RAF wild type (**Fig. 21**). This finding suggests that regulation of A-RAF by the internal 14-3-3 binding site occurs in a similar way as reported for C- and B-RAF in Sf9 cells. On the other hand, the data obtained from the COS7 cells revealed that regulation of the A-RAF activity by the internal 14-3-3 binding site differs from that of B- and C-RAF. While the substitutions of serine 259 and 365 by alanine in C-RAF and B-RAF, respectively, have been reported to cause a dramatic enhancement of the basal kinase activity [205], the analogous A-RAF mutant (A-RAF-S214A) revealed a reduction of activity compared to A-RAF wild type (**Fig. 22**). This observation could be explained by the extremely low degree of serine 582 phosphorylation in A-RAF-S214A mutant (**Fig. 22**), thus, preventing interactions with 14-3-3 proteins. The finding that S582 phosphorylation of A-RAF was not impaired by S214 to alanine substitution in Sf9 cells (**Fig. 21**) supports the accuracy of this explanation. In summary, regulation of A-RAF by the internal 14-3-3 binding site depends on cell system.

Remarkably, substitution of S214 by alanine did not have an effect on S582 phosphorylation, if this mutant was expressed in COS7 cells in the presence of Ras12V and Lck (**Fig. 22**). As the N-region of RAF kinases is highly phosphorylated upon co-transfection with Ras12V/Lck (see **Fig. 30**), prevention of S582 dephosphorylation by the N-region may be supposed. Based on the results of this study, we propose the following model for regulation of A-RAF by 14-3-3 proteins in COS7 cells. Activation of A-RAF requires binding of 14-3-3 dimers to both, the internal and the C-terminal 14-3-3 binding domains. The observation that S214A or S582A mutations impair the Ras12V/Lck-induced kinase activity of A-RAF supports this assumption. Abrogation of S582 phosphorylation in non-stimulated cells by substitution of S214 to alanine suggests that internal 14-3-3 binding site may play an initial role in the association of A-RAF with 14-3-3 dimers. This means that elimination of S214 prevents completely association of 14-3-3 with inactive A-RAF. In this case, S582 is not protected by binding of 14-3-3 and can be easily dephosphorylated. Furthermore, interdependence between phosphorylation of the N-region and phosphorylation of S582 suggests that activated N-region may support and/or even partially compensate binding of 14-3-3 to the internal S214. Binding of 14-3-3 dimers to the phosphorylated N-region would

stabilize association of 14-3-3 with the C-terminal S582 and prevent its dephosphorylation. This would explain why A-RAF-S214A mutant is highly phosphorylated at S582 upon co-expression with Ras12V and Lck. Unfortunately, the data confirming interaction between 14-3-3 proteins and the activated N-region of A-RAF are not available so far. However, this model is supported by the results of the indirect competition assay, in which we used synthetic phosphopeptides as competitive inhibitors for the RAF/14-3-3 interaction (**Fig. 24**). C-terminal peptides of RAF isoforms did not significantly differ in their ability to inhibit the RAF/14-3-3 association. In contrast, peptides corresponding to the internal binding sites exhibited differential inhibitory potential, suggesting that differences in the affinity of 14-3-3 proteins to RAF isoforms are determined by the internal 14-3-3 binding site.

In this context, recently published findings by two independent groups concerning developmental disorders caused by mutations within the 14-3-3 binding domains in C-RAF are of particular interest [301,302]. Most of the altered residues in B- and C-RAF that are associated with cancer have been found localized within the kinase domain [195]. In contrast to these data, Pandit *et al.* [301] and Razzaque *et al.* [302] reported for the first time on pathological C-RAF mutations positioned within the internal 14-3-3 binding site and in the proximity of the C-terminal 14-3-3 binding domain. These mutations lead to gain-of-function of C-RAF. The consequences of this gain-of-function are severe cardio-facio-cutaneous disorders called Noonan and LEOPARD syndrome. Most of these mutations altered the motif flanking serine 259 of the internal 14-3-3 binding domain (e.g. S257L, T260R and P261S). A displacement of the serine 259 by phenylalanine (S259F) has also been detected. Thus, mutations at these residues abolish the autoinhibitory mechanism of C-RAF resulting in a permanent active C-RAF form. Whether analogous mutations of the 14-3-3 binding sites in A-RAF lead to similar disorders remains to be investigated.

### **7.1.2. Differences in subcellular localization of RAF isoforms may explain the isoform-specific association with 14-3-3 proteins**

To address the question whether mammalian 14-3-3 isoforms reveal specificity in association with RAF kinases, we performed here systematic binding studies using purified preparations of all of the seven mammalian 14-3-3 isoforms and RAF isozymes (A-, B- and C-RAF). Data obtained by both, direct binding (**Fig. 23**) and by competition assays (**Fig. 24**), document unambiguously that 14-3-3 proteins interact with RAF and *vice versa* in an isoform-specific manner. Notably, as shown in **Fig. 23**, we observed that in contrast to B- and C-RAF, the A-RAF kinase binds with lower affinity to 14-3-3 utilizing only four of the seven mammalian 14-3-3 isoforms. The lower affinity of A-RAF binding to 14-3-3 proteins *in vitro* may explain the observation of our group that lower abundance of 14-3-3 proteins was found attached to the purified A-RAF proteins. Contrary to this finding, C- and particularly B-RAF have been found to be associated with several 14-3-3 proteins upon purification from Sf9 and HEK293 cells [205]. Furthermore, Fischer *et al.* [205] have found using MS analysis of purified RAF proteins that B-RAF associated with a much higher number of 14-3-3 isoforms compared to C-RAF. The 14-3-3 epsilon isoform was present in both samples indicating that

at least a part of 14-3-3 proteins appear in heterodimeric form. Data showing that A-, B- and C-RAF display *in vivo* differential composition of associated 14-3-3 proteins goes along with our findings that RAF isoforms fulfill different functions in the cell due to their structure and subcellular localization. While C-RAF has been detected predominantly at the plasma membrane, B-RAF localizes mainly in the cytosolic environment [216] explaining the high amount of attached 14-3-3 proteins. The fact that A-RAF associates predominantly with endosomal vesicles (Nekhoroshkova *et al.*, *PLoS ONE*, in revision) and the finding that A-RAF reveals lower affinity for 14-3-3 proteins compared to B- and C-RAF may explain the poor amount and the specific pattern of bound 14-3-3 proteins.

## 7.2. Maximal activation of A-RAF kinase requires phosphorylation of both MEK binding sites, S432 and T442

A number of protein kinases have been shown to be regulated by phosphorylation within the kinase domain. In the case of RAF proteins, phosphorylation of the MEK binding domain and the activating segment has been reported to be necessary for kinase activity of C- and B-RAF [132,239,240]. Although the entire coupling area between C-RAF and MEK has not yet been determined, it has recently been reported that serine 471 in C-RAF (and the corresponding residue S579 in B-RAF) is critical for its kinase activity and for binding to MEK [132]. These phosphorylation sites are located within the region that is highly conserved among mammalian RAF isoforms and RAF from other species (see also **Fig. 20**). In our study, we detected an A-RAF phosphopeptide located between residues 432–444 that includes the putative MEK binding domain and contains two potential phosphorylation sites, S432 and T442 (**Fig. 20** and **Table 2**). Using the functional substitution analysis, we show that S432 is strictly required for A-RAF kinase activity. In contrast, the dependence of A-RAF activity on T442 was restricted to activation by Ras12V and Lck only (**Fig. 25**). These data suggest that whereas phosphorylation of the single S432 is necessary and sufficient for EGF-mediated A-RAF activation, the maximal activation of A-RAF kinase requires phosphorylation of both residues, S432 and T442. Our observations are partially in agreement with results recently obtained by Zhu *et al.* [132] for C- and B-RAF. They reported that S471 of C-RAF and the corresponding residue of B-RAF (S579) are critical for activation of these isoforms by growth factors, whereas substitution of T481 and T589 in C- and B-RAF, respectively, does not have much effect on their kinase activities. Unfortunately, this group did not investigate the importance of the S471/T481 of C-RAF and the corresponding sites in B-RAF for the maximal activation of these isoforms by Ras12V and Lck. Thus, the role of the T481 and T589 in the functioning of C- and B-RAF isoforms, respectively, is not completely elucidated.

Additionally, Zhu *et al.* [132] report that substitution of S471 by alanine in C-RAF almost completely diminished association of this RAF isoform with MEK, whereas the C-RAF-T481A mutant bound MEK as well as wild type, suggesting that the S471 but not T481 may serve as the MEK binding site for C-RAF. However, the authors did not mention, whether the C-RAF used in the pull-down assay has been stimulated. Therefore, the question,

whether T481 may be involved in the MEK binding to C-RAF, remains to be investigated. In the case of maximal A-RAF activation, it is possible that the introduction of negative charge within the N-region caused by Ras/Lck may change the contact area between A-RAF and MEK, thus making T442 also necessary for transduction of the signals from RAF to MEK. However, other possibilities such as interaction of T442 with some RAF-activating components should also be considered.

### 7.3. Negative charge of the N-region is a prerequisite for phosphorylation of activation segment

In contrast to the MEK binding site, which serves as docking platform for substrate, phosphorylation of the activation segment has been reported to induce intramolecular rearrangement allowing RAF kinase to fold into the active conformation [195]. As phosphorylation of the residues within the activation segment has been established for C- and B-RAF only, in the present work we investigated the role of the activation segment in the regulation of A-RAF kinase activity. Identification of the phosphorylated A-RAF tryptic fragment IGDFGLATVKTR containing phosphate residues at both T452 and T455 (**Fig. 20** and **Table 2**) suggests that similar to B- and C-RAF the activation segment of A-RAF kinase may be involved in the activation process. Confirming this assumption, the results from the functional mutation study showed that, depending on stimulation conditions, either both residues or neither are necessary for A-RAF activation (**Fig. 26**). The results of kinase activity assay have revealed that EGF-mediated stimulation of A-RAF does not require phosphorylation on threonines 452 and 455 within the activation segment, whereas maximal activation by co-operation of Ras and Lck strongly depends on phosphorylation of these residues (**Fig. 26**). In part, these data are in accordance with results obtained for B- and C-RAF activation. Zhang *et al.* [239] have shown convincingly that phosphorylation of T599 and S602 is essential for B-RAF activation. In contrast, the role of phosphorylation within the activation segment of C-RAF is controversially discussed. Whereas Barnard *et al.* [303] reported that phosphorylation of the activation loop plays no significant role in C-RAF activation, the functional mutation study performed by Chong *et al.* [240] revealed that the activation of the T491A or S494A mutants was diminished, demonstrating that these residues play indeed a regulatory role in C-RAF activation. Structural studies using the crystal structure of the B-RAF kinase domain [193] provided more insight into how RAF proteins may be regulated by the activation segment. There is a hydrophobic interaction between the glycine-rich loop and the activation segment that traps RAF in an inactive conformation. Phosphorylation of the threonine within the activation segment (T599 in B-RAF) is thought to disrupt this interaction releasing the activation segment and reorienting critical residues into the correct position for catalysis [193,195]. Our results suggest that this activation model can also be applied to A-RAF. Furthermore, considering the fact that A-RAF kinase activity depends on phosphorylation of the activation segment only in the case of Ras/Lck-mediated stimulation, we suggest that the negative charge at the N-region caused by Ras/Lck is a



prerequisite for phosphorylation of activation segment, indicating a functional interdependence between phosphorylation of S299/Y302 and T452/T455 in A-RAF. Similar considerations were reported by Chong *et al.* [240] for C-RAF. They have shown that double acidic residue substitutions at either S338/Y341 or T491/S494 in C-RAF were insufficient to confer constitutive activity. In contrast, when the S338D/Y341D mutation was combined with T491E/S494D mutation, C-RAF became constitutively active. From these observations Chong *et al.* [240] concluded that the requirement for phosphorylation at S338 and Y341 in C-RAF is likely to be the reason for insufficient activation of C-RAF by the T491E/S494D substitution. Substitution of the valine 600 by glutamic acid within the activation segment of B-RAF (B-RAF-V600E) mimicking the conformational change normally induced by phosphorylation of T599 and S602 [304] leads to a highly activated B-RAF kinase that could not be further activated by Ras12V. Notably, in about 70% of malignant melanomas the highly active B-RAF-V600E mutant was detected [305,306]. Whether mutation of the corresponding A-RAF valine 453 to glutamic acid in the activation segment elevates the activity of A-RAF remains to be investigated. Emuss *et al.* [307] recently showed that C-RAF is not activated by V492E mutation presumably due to the fact that the N-region of C-RAF lacks negative charge in non-stimulated cells.

#### **7.4. Non-conserved residues within the N-region determine activation properties of RAF kinases**

Although the basic activation steps are similar for all three RAF isoforms, there are several subtle differences in the regulation of their kinase activity. These isoform-specific regulation varieties result in the enormous differences between the RAF isoforms with respect to basal activity and activities caused by external stimulation. For example, the maximal activation of B-RAF merely requires signals that generate Ras-GTP, whereas activation of C-RAF and A-RAF requires Ras-GTP together with signals that lead to their phosphorylation on tyrosines in the N-region [113]. The N-region, which contains several conserved phosphorylation sites, plays an important role in the course of RAF activation process. Phosphorylation of S338 and Y341 in the N-region initiated by activated Ras and Src family kinases, respectively, is required for full C-RAF activity, whereas S446 (the B-RAF equivalent of S338 in C-RAF) is constitutively phosphorylated, and this phosphorylation together with the aspartic acids at 448/449 (equivalent to Y340/Y341 of C-RAF) contributes to the high basal activity of B-RAF [114,182]. Comparably little is known about the phosphorylation in the N-region of A-RAF. Substitution of tyrosines 301/302 in A-RAF (equivalent to Y340/Y341 of C-RAF) with aspartic acids generated a protein, which had an elevated basal level of activity, suggesting that these residues play a similar role in the activating process as in C-RAF [113]. However, no data are available about the phosphorylation of the regulatory serine 299 (equivalent of S338 in C-RAF), and which role this serine plays in the activation process of A-RAF kinase. Furthermore, the contribution of serine 339 in C-RAF and the analogous serine 447 in B-RAF with regard to regulation of

RAF kinase activity is controversial. Serine 339 has been reported to be phosphorylated in C-RAF. However, phosphorylation of this site is not required for kinase activation, because the alanine substitution at S339 did not affect C-RAF kinase activity [182].

#### 7.4.1. PKA and RSK are predicted to phosphorylate RAF on the conserved serine within the N-region

Although the sequence of N-region is highly conserved between all three RAF isoforms, there are several amino acid variations (**Fig. 27A**). The relevance of aspartate residues in the B-RAF N-region at positions that are occupied by tyrosines in A- and C-RAF for B-RAF kinase activity is already well known. In contrast, the role of the glycine in the N-region of A-RAF in position 300, which is occupied by serine in B- and C-RAF, in activation of A-RAF has not been investigated so far. Similarly, the possible contribution of the amino acid variations at the position  $-3$  to the highly conserved serine (S299 in A-RAF, S338 in C-RAF and S446 in B-RAF) for its phosphorylation and RAF activation has not been studied. Therefore, in this study we focused on the differences in the structure of the N-region and addressed the question whether these non-conserved residues in positions  $-3$  and  $+1$  relative to the highly conserved serine participate in RAF activation. Here we report that non-conserved residues that have not been considered as regulatory sites determine to a considerable extent the RAF activation process. In particular, the residues  $X_1$  and  $X_2$  in the core structure of the N-region  $GX_1RDSX_2YY(DD)WE$  strongly influence the magnitude and dynamics of RAF activation. We found contrary to expectation that glycine in position 300 affected the activation of A-RAF in a stimulatory manner. This finding was corroborated by the observation that substitution of serine 339 by glycine in C-RAF led to a constitutively active kinase (**Fig. 32** and **Fig. 33**), thus confirming the assumption that glycine in position  $+1$  relative to S338 facilitates RAF activation. Our results demonstrate further that the substitution of glycine 300 with serine in A-RAF is inhibitory for A-RAF kinase activity (**Fig. 30A** and **B**). The importance of the glycine at this position is quite surprising, because analysis of A-RAF protein sequences from different species has shown that only mammalian A-RAF contains glycine at position 300, whereas in frogs and fishes A-RAF contains a serine residue at this position, similar to the sequences of C- and B-RAF in this region. Because the introduction of glycine instead of serine in position  $X_2$  obviously impairs the recognition sequence of the anti-pS338 antibody, we were not able using this antibody to examine whether glycine at this position enhances RAF kinase activity by facilitating the phosphorylation of the conserved serine. On the other hand, substitution of glycine with serine in A-RAF did not impair the phosphorylation of the neighboring tyrosines 301/302 upon activation with Lck (**Fig. 30D** and **Fig. 31**), suggesting that amino acid  $X_2$  influences only the Ras-GTP dependent RAF activation pathway but not the Src-dependent RAF kinase activation.

Furthermore, we also showed in this study that amino acid in the position  $-3$  relative to conserved serine influences the phosphorylation efficiency of this serine residue. Whereas glutamine in this position leads to moderate phosphorylation and tyrosine almost completely

abrogates phosphorylation of conserved serine, introduction of arginine in the same position increases enormously the phosphorylation efficiency and consequently the activity of RAF kinases (**Fig. 30, A and C, Fig. 32, Fig. 33B and D**). These results raise the following question: which of the protein kinases that phosphorylate the conserved serine in the N-region of RAF is dependent on amino acid X<sub>1</sub>? p21-activated protein kinase PAK3 has been reported to phosphorylate C-RAF on S338 *in vitro* and *in vivo* [227]. Moreover, S338 phosphorylation by PAK was found to be very sensitive to loss of N-terminal arginines resulting in decreased phosphorylation [308]. However, it was not examined whether S338 phosphorylation by PAK is also sensitive to alterations in amino acid side chains in position -3 to this serine. Furthermore, Chiloeches *et al.* [309] have shown that PAK3 is not activated under conditions where S338 is phosphorylated, but when PAK3 is strongly activated either by co-expression with Cdc42-12V or by mutations, which render it independent from Cdc42, it did stimulate S338 phosphorylation. The role of this kinase as a physiological mediator of S338 phosphorylation in growth factor-stimulated cells therefore remains highly controversial. Recently, serine-threonine kinase CK2 was identified as a RAF family N-region kinase. Using *in vitro* kinase assay it was shown that CK2 efficiently phosphorylates B-RAF on serine 446. On the other hand, CK2 can only phosphorylate C-RAF that has been co-expressed with v-Src or contained an aspartic acid residue at the position 341, indicating that the conserved serine is a target of CK2 only when a negatively charged residue is additionally present at the +3 position [310]. It is unlikely that the amino acid variations at the position -3 would impair phosphorylation of conserved serine in the N-region of RAF by CK2, because according to the consensus target sequence for this kinase ((S/T)XX(E/D/pY/pS/pT)) the negatively charged amino acids C-terminal rather than the amino acid constellation N-terminal to the phosphorylation site are crucial for substrate recognition [311]. Using *NetPhosK 1.0* server [312], which produces neural network predictions of kinase-specific eukaryotic protein phosphorylation sites, we looked for the further putative serine-threonine kinases that could be proposed to phosphorylate RAF proteins on the conserved serine within the N-region. Currently, *NetPhosK 1.0* covers the following kinases: PKA, protein kinase C, protein kinase G, CKII, Cdc2, CaM-II, ATM, DNA PK, Cdk5, p38 MAPK, GSK3, CKI, protein kinase B, RSK, INSR, EGF receptor and Src. Besides CK2, PKA and p90 ribosomal Ser-6 kinase (RSK) are also predicted to be potential kinases for phosphorylation on conserved serine within the RAF N-region (**Table 4**). B-RAF WT is predicted to be efficiently phosphorylated by both, PKA and RSK, whereas C-RAF WT is phosphorylated by PKA only and A-RAF WT is not phosphorylated at all. Introduction of arginine instead of glutamine at position 335 in C-RAF results in a protein, which is predicted to be phosphorylated on serine 338 by PKA as well as by RSK that presumably is the basis of the increased kinase activity of this mutant relative to C-RAF WT (**Table 4**). Furthermore, according to *NetPhosK 1.0* analysis, A-RAF-Y296R mutant is predicted to be highly phosphorylated by PKA kinase in contrast to A-RAF WT, which is not phosphorylated at all. These predictions are in accordance with our experimental data and may present a potential explanation, *i.e.* how the amino acid at the position -3 to the conserved serine within the N-region influences its phosphorylation in the A- and C-RAF substitution mutants examined in this study.

**TABLE 4: Prediction of kinase specific phosphorylation of S338 (C-RAF), S446 (B-RAF) and S299 (A-RAF) by *NetPhosK 1.0* server [312]**

| RAF isoforms and mutants | N-region sequence                                 | Predicted kinases   | Phosphorylation score |
|--------------------------|---|---------------------|-----------------------|
| B-RAF WT                 | (LGRRDSSDD)                                       | PKA<br>RSK          | 72%<br>63%            |
| C-RAF WT                 | (RGQRDSSYY)                                       | PKA                 | 63%                   |
| C-RAF (Q335R)            | (RGRRDSSYY)                                       | PKA<br>RSK          | 84%<br>64%            |
| A-RAF WT                 | (LGYRDSGYY)                                       | non-phosphorylated  |                       |
| A-RAF (Y296R/G300S)      | (LGRRDSSYY)                                       | PKA                 | 87%                   |
| Protein kinase           |   | Consensus sequences |                       |
| PKA                      | (R-R/K-X-S/T) > (R-X-X-S/T) = (R-X-S/T) [313,314] |                     |                       |
| RSK                      | (R-X-R-X-X-S) > (K/R-X-X-S/T) [315,316]           |                     |                       |

#### 7.4.2. Tyrosine 296 determines the low activating potency of A-RAF by sterical reasons

Taking advantage of the recently published three-dimensional structure of the B-RAF catalytic domain [193], we provide a potential answer to the following question: how to explain the effects of substitutions in positions  $X_1$  and  $X_2$  on RAF kinase activity on the molecular basis considering the three-dimensional structure of RAF kinases? Although the exact three-dimensional structure of the complete RAF protein is still unknown, it has been generally accepted that the N-terminal regulatory part in A- and C-RAF associates with the catalytic domain in the basal state forming a closed conformation of the protein [176]. On the other hand, it is very probable that contact points between N-region and both the regulatory moiety (including CR1 and CR2) and the catalytic domain exist, because N-region is positioned exactly between these two domains. Using molecular modeling, we reconstructed the possible spatial orientation of the N-region in A- and C-RAF relative to the catalytic domain utilizing three-dimensional structure of the B-RAF catalytic domain as a template.

According to the model illustrated in **Fig. 35A**, we identified contact points between N-region and the  $\alpha C$  and  $\alpha E$  helices of the catalytic domain. Taking into account our experimental results, this contact is proposed to regulate RAF kinase activity allowing tight interaction between the N-region and the catalytic domain and inhibiting RAF activation, whereas weakening of this binding enhances RAF kinase activity. Indeed, disruption of the hydrogen bond between serine 339 of the N-region and arginine 398 of the catalytic domain of C-RAF by serine to glycine substitution led to constitutively active C-RAF (C-RAF-S339G

and C-RAF-Q335Y/S339G mutants, see also **Figs. 32, 33** and **35C**), whereas induction of this interaction by reverse amino acid exchange in A-RAF inhibited kinase activity (A-RAF-G300S and A-RAF-Y296R/G300S mutants, see also **Fig. 30A** and **B**, and **Fig. 35B**). Furthermore, it should be considered that glycine is the only amino acid without a side chain. Introduction of this amino acid into a protein sequence renders its structure more flexible. In our case, the introduction of glycine into the N-region between the conserved serine and two tyrosines has a dual effect. First, as already mentioned, it disrupts a hydrogen bond to the  $\alpha$ C helix of the catalytic domain. Second, it also increases flexibility of the adjacent segment and by this means further weakens hydrogen binding to the catalytic domain. This assumption has been confirmed by the observation that anti-pS338 antibody, which recognizes pS338 in C-RAF and pS446 in B-RAF, cannot recognize pS299 in A-RAF, probably because of the difference in the structure and conformation of these epitopes.

Furthermore, the three-dimensional model presented in **Fig. 35** together with our experimental results reveal that amino acid at position 296 in A-RAF may also have a dual effect on RAF kinase activity. A tyrosine residue at this position decreases the kinase activity, because of inhibition of phosphorylation on serine 299 and additionally because of its interaction with the  $\alpha$ E helix of the catalytic domain. On the other hand, arginine at the same position facilitates serine phosphorylation and disrupts the contact to the  $\alpha$ E helix of catalytic domain; both effects reinforce the RAF kinase activity.

In contrast, according to the reconstruction model (**Fig. 35**), the phosphoserine at position 338 in C-RAF (299 in A-RAF) and phosphotyrosines at positions 340/341 in C-RAF (301/302 in A-RAF) would rather interact with the regulatory domain than with the catalytic domain, because the side chains of these residues are orientated out of the plane in which the N-region interacts with the catalytic domain. Interaction of these phosphorylated residues with the regulatory part of the protein may pull away the N-region segment and contribute to the disruption of the contact between N-region and catalytic domain, resulting in elevated kinase activity.

### **7.4.3. Disruption of interaction between the N-region and the PABR facilitates binding to lipids**

The consequences of the abolishment of the binding between the N-region and catalytic domain of RAF may be the reorganization in the complex formation between 14-3-3 proteins and RAF and subsequently preferential formation of heterodimers between C- and B-RAF [154,223,224]. Another possible consequence may involve Ras-independent recruitment of RAF to membranes. The segment in the catalytic domain of RAF, which in our reconstruction model makes contacts with the N-region (**Fig. 35**), is part of the sequence, which has been described as the phosphatidic acid-binding region (PABR) of RAF proteins. The PABR is a highly conserved 36-amino acid region, which has been reported to associate with phosphatidic acid. It contains a cluster of basic residues (R398, K399 and R401 in C-RAF) as well as a short segment of hydrophobic residues (405–408) [191,317]. Rizzo *et al.*

have shown that the PA-binding region of C-RAF is sufficient to target green fluorescent protein to membranes, and its overexpression blocked recruitment of C-RAF to membranes and disrupted insulin-dependent ERK phosphorylation. Based on these results, they concluded that the recruitment of C-RAF to membranes is mediated by direct interaction with phosphatidic acid [217]. Considering these data, it could be supposed that disruption of the contact between the N-region and the PABR of the catalytic domain may release this segment for the binding to membrane lipids. This hypothesis is in accordance with our fractionation data that show the active and the serine 338-phosphorylated C-RAF forms located preferentially at the membranes (**Fig. 34**).

#### 7.4.4. Regulation of RAF activity by PABR is similar for A- and C-RAF

To test whether disruption of the interaction between the N-region and the PABR would influence the binding to membranes and the activation of RAF kinase, we generated several C- and A-RAF point mutants with the impaired contact between N-region and PABR. The kinase activity and subcellular localization of these mutants have been investigated. Whereas the basal and the Ras12V-induced kinase activity of the C-RAF-D337A mutant was significantly reduced, the substitution of S339 to alanine led to elevated basal activity compared to wild type (**Fig. 36**). The unexpected decrease in the activity of the C-RAF-D337A mutant can be explained by the abolishment of the S338 phosphorylation in this mutant. Obviously, substitution of D337 with alanine prevents phosphorylation of S338 and subsequently prevents activation of C-RAF. In contrast, exchange of S339 with alanine enhances phosphorylation of S338 even in the basal state, thus elevating the activity of this C-RAF mutant (**Fig. 36**). These results demonstrate that regulation of RAF kinase activity by the N-region is highly complex and mutations that support one activation mechanism can handicap the other one.

The mutations in the PABR of C-RAF (R398A and K399A) displayed striking differences in their phenotypes as well. Whereas the basal and the Ras12V-induced activities of C-RAF-K399A mutant were diminished compared with wild type, the substitution of R398 to alanine led to enhancement of the basal activity on the one hand, but to decrease of the Ras12V-induced kinase activity on the other hand (**Fig. 36**). Increased phosphorylation of the S338 observed in this mutant can explain the elevated basal activity of the C-RAF-R398A, but not the reduction of the Ras12V-induced activation. These data suggest that C-RAF-R398A mutation may influence both mechanisms that are responsible for regulation of RAF activity by N-region. The first mechanism is phosphorylation of S338 and the second one is binding of phosphatidic acid (PA) and membrane targeting. The fractionation results presented in **Fig. 38** revealed that substitution of R398 with alanine did not impaired targeting of C-RAF to the membranes. Moreover, the membrane located portion of the C-RAF-R398A mutant was elevated compared to wild type protein, suggesting that R398A substitution does not prevent binding of PA to C-RAF. These observations are in accordance with data reported by Ghosh *et al.* [317], who demonstrated that replacement of the single site R398 or R401 by alanine did not affect phosphatidate binding when compared with wild type protein. Thus, the

third mechanism by which R398 regulates the Ras12V-induced activation of C-RAF is probable. The results presented in **Figs. 38** and **39** suggest that this mechanism may be the feedback phosphorylation and inactivation by ERK. As shown in **Fig. 38** we observed a mobility shift in the SDS-PAGE pattern of the C-RAF-R398A mutant. Of note, the mobility shift appears preferentially in the membrane portion of the C-RAF-R398A. Several groups have observed such a mobility shift of the C-RAF wild type in response to stimulation by mitogens [153,230,296-298]. In all cases, the decreased electrophoretic mobility was a result of hyperphosphorylation of C-RAF. Moreover, Wartmann *et al.* and Dougherty *et al.* [153,296] reported that the mobility shift-associated hyperphosphorylation of C-RAF correlates with a reduction of mitogen-stimulated C-RAF kinase activity. These data and the observations that C-RAF activation was prolonged when ERK activation was blocked by pharmacological inhibitors [318] or by an inhibitor of KSR that disrupts the RAF-MEK interaction [319] led to the conclusion that C-RAF is a target of ERK-mediated feedback inhibition. The mobility shift of the C-RAF-R398A mutant observed in this study is most likely a result of such a negative regulation by ERK-mediated phosphorylation, because treatment with the MEK inhibitor U0126 significantly reduced the shifted fraction of this mutant (**Fig. 39**). Dougherty *et al.* [153] reported that inhibition of ERK-mediated phosphorylation led to sustained kinase activity and S338 phosphorylation, and prolonged membrane localization, suggesting that down regulation of C-RAF requires dephosphorylation of S338 and depletion from membranes. Considering these data, the following model may be proposed: upon its translocation to the plasma membrane and association with Ras, C-RAF is phosphorylated at S338. The consequence is activation of C-RAF kinase that leads to accumulation of activated ERK in the cell. Feedback phosphorylation of C-RAF by activated ERK at several specific sites inhibits C-RAF activity and induces dephosphorylation of activating S338 by specific phosphatases. PP5 is a most probable candidate for pS338-directed phosphatase [320]. Feedback phosphorylation also induces phosphorylation of inhibitory S259. Dephosphorylation of the N-region and phosphorylation of the S259 leads to depletion of the kinase from the plasma membrane and, consequently, to dephosphorylation of the feedback regulation sites by PP2A [153]. This model is supported by the observation that hyperphosphorylation inhibits the Ras/RAF interaction and desensitizes C-RAF to additional stimuli [153]. The results presented in this contribution strongly suggest that substitution of R398 with alanine alters the S338 surrounding structure preventing recognition and dephosphorylation of S338 by PP5. The consequence is accumulation of hyperphosphorylated inactive C-RAF at the plasma membrane.

Similar to R398A substitution, exchange of K399 with alanine reduces kinase activity of C-RAF, however by a different mechanism. The C-RAF-K399A mutant did not revealed accumulation of the hyperphosphorylated form at the membranes upon activation with Ras12V/Lck (**Fig. 38**). Thus, the inhibiting effect of this mutation has another origin. Ghosh *et al.* [317] reported that K399A replacement resulted in reduced binding of C-RAF to phosphatidic acid. In addition, this mutation impaired Ras12V/Lck induced phosphorylation of S338 in our study (see **Fig. 36**). These data suggest that K399A substitution may have a dual effect on activation of C-RAF. It restrains phosphorylation of S338 by alteration of the surrounding structure and, concurrently, prevents association of the kinase domain with PA.

Substitution of the homologous residues in A-RAF (R359 and K360) revealed the same effects on A-RAF activity as already described for C-RAF. Single site R359A or K360A replacements strongly inhibited Ras12V/Lck-induced A-RAF kinase activity (**Fig. 37**). Moreover, R359A exchange led to accumulation of the hyperphosphorylated (shifted) form of A-RAF at the membranes as well as in cytosol (**Fig. 40**). These observations suggest that the regulation of A- and C-RAF activity share the mechanism, in which the conserved basic residues within the PABR determine the RAF activation process.

## 7.5. ERK-mediated feedback phosphorylation is proposed to participate in A-RAF activation

Regulation of kinase activity by phosphorylation within the non-conserved region, which is located between the CR2 and kinase domain, appears to be isoform-specific. For example, phosphorylation of the residues S428 and T440, which are unique for B-RAF, has been reported to regulate negatively its kinase activity [190]. Furthermore, in our current study we demonstrated that the non-conserved residues within the N-region determine partially the basal and the inducible activity of RAF isoforms. In the case of C-RAF, a domain between serine 289 and serine 301 has been reported to participate in the regulation of C-RAF activity by phosphorylation of residues S289, S296 and S301 [152,153,194]. In this study, we identified using mass spectrometry technique several novel A-RAF phosphorylation sites within the non-conserved region between the CR2 and the kinase domain. Data obtained by MS (see **Fig. 20** and **Table 2**) provided eight phosphorylated fragments covering the region between the residues G248 and K288. Importantly, one of these fragments has been found to be phosphorylated at seven putative phosphorylation sites and was detected only in the Ras12V/Lck-stimulated A-RAF, whereas other fragments carrying one, two or four phosphate residues have been detected in both serum-activated and Ras12V/Lck-stimulated proteins (**Fig. 20** and **Table 2**). These data suggest that the prolonged stimulation of A-RAF kinase may be accompanied with hyperphosphorylation of the regulatory IH-domain. The role of the intermediate phosphorylations and their progression during activation remain to be elucidated. In addition, the activity state of such differentially phosphorylated intermediates is a matter of speculation.

On the other hand, we show here that single point mutations within the IH-domain generated by substitution of serines or threonine with alanine resulted in some cases in reduction of induced A-RAF kinase activity (**Fig. 41A, B, D and E**). In contrast to A-RAF mutants S250A, T253A, S259A and S265A, whose catalytic activity was not significantly diminished, substitutions of S257, S262 and S264 led to almost complete inactivation of A-RAF kinase, suggesting that these three residues are crucial for its regulation. Considering these observations, it is tempting to speculate that phosphorylation of S257, S262 or S264 might be a prerequisite for phosphorylation of further sites within the IH-domain. If that would be the case, then replacement of each of these crucial sites would partially or even



completely abrogate the hyperphosphorylation of the IH-domain. At present, however, we can only speculate about the hierarchy of phosphorylation events within this domain.

Furthermore, by use of phosphospecific antibodies, we observed a relationship between different regulatory phosphorylation sites. Although phosphorylation of S214 was unchanged in all IH-mutants, the level of pS582 was diminished in the samples that displayed reduced kinase activity (**Fig. 41A, C, D and F**). The homologous serine in C-RAF (S621) has been proposed to function as an autophosphorylation site [202]. A similar consideration may apply to serine 582 of A-RAF. In this case, the reduced S582 phosphorylation of A-RAF IH-point mutants would be the result of their low kinase activity. However, other possibilities, such as dephosphorylation by phosphatases should also be considered. Although tyrosine phosphorylation of several A-RAF IH-mutants was slightly diminished, only the A-RAF-S262A mutant almost completely abrogated Y301/Y302 phosphorylation (**Fig. 41D and G**), indicating that interplay between these two phosphorylation sites may exist. Interestingly, introduction of the additional Y301D/Y302D substitution into the A-RAF-S262A mutant rescued only partially the kinase activity (**Fig. 42**). The partial rescue suggests that phosphorylation at S262 of the IH-domain may be required for activating tyrosine phosphorylation within the N-region. The current phosphopeptide screening revealed that A-RAF WT is phosphorylated not only at Y301/Y302 but also at additional tyrosines, Y24, Y155 and Y419 (**Fig. 20 and Table 2**). Although Y24 and Y155 are A-RAF-specific, Y419 is highly conserved among all RAF proteins. Y419 is equivalent to Y538 of D-RAF (*Drosophila* RAF), which together with Y510 (Y391 in human A-RAF) was recently discussed by Xia *et al.* [321] as targets for Src-mediated phosphorylation. However, experimental results confirmed only Y510 but not Y538 as a proper target for phosphorylation by Src. Whether A-RAF Y24, Y155 and Y419 are substrates for human Src family kinases and whether phosphorylation of these sites is impaired by S262A substitution remains to be investigated.

From seven phosphorylation sites within the A-RAF-(248–267) tryptic fragment, three are part of the ERK-specific (S/T)P phosphorylation motifs (**Fig. 20**). Based on this observation, ERK-mediated feedback phosphorylation of T253, S257 and S259 in the IH-domain of A-RAF should be considered. ERK-mediated feedback phosphorylation has already been found to modulate kinase activity of B- and C-RAF [152,153,299]. However, entirely different motifs have been described to be involved in this process. Although in B-RAF the evolutionarily conserved SPKTP motif at the C-terminus has been made responsible for feedback regulation [299], C-RAF has the sequence SPRLP in this location. Although an SP site is present in this fragment, other regions that are not present in B-RAF have been proposed to be involved in feedback regulation of C-RAF. The positions S289, S296 and S301 in C-RAF are targets of ERK proline-directed kinase phosphorylation (**Fig. 20**). The consequences of phosphorylation at these positions for C-RAF activity were described as negative by Dougherty *et al.* [153] and Hekman *et al.* [194] and positive by Balan *et al.* [152]. Perhaps some of the differences in results relate to the fact that Dougherty *et al.* [153] and Balan *et al.* [152] did not use single site mutants for their evaluation. As it stands, definitive conclusions regarding the role of ERK-mediated phosphorylation in C-RAF require additional investigation. Regarding feedback regulation of A-RAF, our present results demonstrate that the putative ERK-induced phosphorylation of T253/S257/S259 is involved in the positive regulation of its kinase activity (**Fig. 41**). Of these three sites, serine 257 showed the most

pronounced effect on A-RAF catalytic activity. Whereas T253 and S259 do not possess counterparts in C-RAF, S257 of A-RAF is analogous to S296 of C-RAF. However, although this residue is conserved in both isoforms, the relative position of S257 in A-RAF protein may differ considerably. The sequence surrounding the S296 in C-RAF is six amino acids shorter than the corresponding region in A-RAF (see **Fig. 20**).

The suggestion that ERK-mediated feedback phosphorylation of T253/S257/S259 may positively regulate A-RAF activity is further supported by the results obtained using MEK inhibitor U0126. A-RAF wild type isolated from the U0126-treated cells displayed considerably decreased catalytic activity compared with the protein derived from the untreated cells (**Fig. 43**), suggesting that ERK-mediated feedback regulation is required for effective activation of A-RAF. This raises the possibility that ERK regulates A-RAF activation by feedback phosphorylation at these SP motifs. In addition, adjacent to the T253/S257/S259 sites, two other SP motifs are present in A-RAF, *i.e.* 269SP and 274SP, and should also be considered as putative ERK phosphorylation sites. One of them (S274) has indeed been identified in its phosphorylated state (**Fig. 20** and **Table 3**).

## 7.6. Molecular modeling of the IH-segment suggests a “switch-of-charge” mechanism for A-RAF regulation

Recruitment of RAF kinases to the plasma membrane was initially proposed to be mediated by Ras proteins via interaction with the RAF-RBD. However, data published by our group and others showed that Ras-independent association with membrane lipids is involved in the RAF translocation pathway as well [11,191,217]. Interaction of B- and C-RAF with negatively charged phospholipids has been documented by several studies. Besides the ability to interact with Ras and 14-3-3 proteins, C-RAF-CRD has been shown to associate with phosphatidylserine at the plasma membrane [187,322]. In addition, a phosphatidic acid binding domain has been identified within the CR3 of C-RAF kinase [11,191,323]. This domain is highly conserved in all three RAF isoforms and comprises an RKTR motif, which is rich in positively charged amino acids. In the case of A-RAF, lysine 50 and arginine 52 within the RBD as well as several basic residues within the region between amino acids 200 and 606 have been suggested to be implicated in binding of negatively charged phospholipids, such as phosphatidic acid and phosphorylated phosphoinositides [192]. However, although several basic residues of A-RAF were included in this study, Johnson *et al.* [192] did not examine the role of positively charged residues within the IH-segment. Because of the fact that the IH-region comprises six basic residues, the modeling of the non-phosphorylated form of the IH-region revealed a relatively high density of positive charge that may facilitate A-RAF association with plasma membrane before and during activation. On the other hand, in the case that all of the seven phosphorylation sites located within the tryptic fragment 248–267 were considered to carry a phosphate residue (as suggested by the MS findings presented in **Fig. 20** and **Table 2**), a high accumulation of negative charge at the surface of the molecule emerged in the three-dimensional reconstruction (**Fig. 44**). This observation prompts us to

speculate that the complete phosphorylation of the IH-region may result in depletion of A-RAF from membranes. Indeed, data obtained by subcellular fractionation revealed that in contrast to C-RAF, which was enriched preferentially in the membrane fraction, the majority of A-RAF was located in the cytosolic fraction upon stimulation with Ras12V/Lck (**Fig. 45**). This observation is consistent with data of Yuryev and Wennogle [261] and Mazurek *et al.* [324], who reported that A-RAF regulates a number of cytosolic proteins.

Although all three RAF family members (A-, B- and C-RAF) overlap in their regulation and choice of substrate, there are significant differences in their activation-deactivation profiles and in the degree of ERK activation [293]. Based on results presented here and data published by Wixler *et al.* [293], we suggest a model for A-RAF activation that differs from models proposed for B- and C-RAF. According to this model, the rapid A-RAF stimulation that is of short duration (1–2 minutes) takes place at the plasma membrane, where Ras-GTPases and Src family kinases are located. The association of inactive A-RAF with the plasma membrane may be facilitated by the high density of positive charge at the IH-region, as demonstrated by molecular modeling (see **Fig. 44**). Activating phosphorylations, such as phosphorylation of the N-region upon growth factor stimulation, would moderately enhance the catalytic activity of A-RAF in this location. Sustained activation would be delayed relative to B- and C-RAF that first generate active ERK needed for feedback phosphorylation of A-RAF in the IH-region. Such a delay may facilitate the function of A-RAF in endocytosis that has recently become evident [266]. We further propose that the stimulatory phosphorylation of residues S257 and/or S262, and/or S264 within the IH-domain may have a dual effect. On the one hand, it facilitates and accelerates activation of A-RAF at the plasma or endocytic membranes. On the other hand, it may also recruit phosphorylation of further residues within the IH-domain, resulting in hyperphosphorylation of this region. Upon multiple phosphorylation events at the IH-region catalyzed by Ras and Lck, we propose a switch of charge in the IH-region that may be responsible for dissociation of A-RAF from the plasma membrane. Nevertheless, the exact fate and physiological function of the hyperphosphorylated A-RAF fraction remain unknown. For C-RAF, a negative modulation of membrane localization by hyperphosphorylation was discussed [153,297]. However, the proposed inactivation mechanism of C-RAF differs considerably from the model discussed here. Contrary to A-RAF, displacement of C-RAF from the plasma membranes requires phosphorylation of six serine residues distributed across the whole molecule. Moreover, four of these sites are C-RAF-specific and are not present in A-RAF. Therefore, the most important message of our modeling and fractionation studies is that A-RAF behaves distinct from C-RAF upon hyperphosphorylation. Nevertheless, to obtain more insight into the complex activation cycle of A-RAF, development of phosphospecific antibodies directed against the regulatory sites within the IH-domain is necessary. The generation of these antibodies is in progress.

Results presented in this contribution raise the old questions: why do most vertebrates have three RAF genes and what is the gain of function of this situation relative to insects and nematodes that make do with just one RAF gene? One possibility is that having three RAF enzymes with widely differing basal and inducible activities [307] could significantly improve the fine-tuning of the mitogenic cascade. This principle is reminiscent

of the EGF receptor family, which has four members, which are strikingly different in their regulation. Because of its similarities with D-RAF and Lin-45, B-RAF is most closely related to solitary RAFs and is therefore proposed to be the founder kinase gene. The transition of B-RAF to C- and A-RAF probably required an attenuation of the extraordinary high basal activity of B-RAF. This has been primarily achieved by replacement of the two aspartic acids of the N-region at the positions 448 and 449 (D448 and D449) by tyrosines that could now be regulated. Our data presented here indicate that the replacement of arginine 443 of B-RAF by glutamine, as is the case in C-RAF (Q335), led to further reduction of basal and inducible activation because of lower phosphorylation efficiency of serine 338 (**Fig. 33B and D**). In B-RAF this phosphorylation is constitutive and contributes to the high basal activity. The third member of the RAF kinase family, A-RAF, lost the aspartic acids D448 and D449 as well and instead contains, similar to C-RAF, tyrosines in positions 301 and 302. Moreover, the introduction of tyrosine in position 296 instead of arginine or glutamine (as is the case in B- and C-RAF, respectively) resulted in extremely low basal activity caused probably by poor phosphorylation of serine 299. However, to facilitate the Ras-induced activation of A-RAF, it was apparently necessary in the course of evolution to introduce glycine instead of serine in the position +1 relative to S299. As demonstrated by our data, maintaining serine in this position leads to a completely inactive kinase with respect to Ras-induced activation (see **Fig. 30A and B**). Only the co-operative action of Ras and Src family kinases (such as Lck that has been used in our experiments) allows the activation of the A-RAF-G300S mutant (**Fig. 29**). Apart from differences in the regulation of the N-region, which are responsible for the gradual reduction of kinase activity from B-RAF to A-RAF, the net values of binding affinities of Ras proteins to RBD of A-, B- and C-RAF are the second parameter affecting RAF activation efficiency. As recently found by our group, the GTP-loaded H-Ras binds to the isolated RBD of B-RAF with highest affinity followed by RBDs of C- and A-RAF [216]. These differences were much more pronounced in the experiments where full-length RAF kinases were used in binding assays. Furthermore, it was demonstrated that the higher accessibility of Ras for B-RAF is caused by its prolonged N-terminal tail, probably keeping RBD of B-RAF in an “open” conformation, because truncation of this region resulted in a protein that changed its kinase properties and closely resembles C-RAF [216]. Thus, the length of the extreme N-termini of RAF kinases plays an important role with regard to RAF activation. In addition, isoform specific feedback regulation of RAF kinases determine the duration of the signals transmitted by Ras/RAF/MEK/ERK cascade. Whereas, C-RAF is inactivated by the negative feedback regulation immediately after stimulation, the positive feedback regulation of A-RAF allows prolonged activation of this isoform. It appears that in the course of evolution the consecutive shortening of the N-terminal part together with specific mutations in the N- and the IH-regions resulted in the fine regulation of the basal and inducible kinase activities of RAF isoforms.

## 8. REFERENCES

- [1] Pearson, G., Robinson, F., Beers Gibson, T., Xu, B.E., Karandikar, M., Berman, K. and Cobb, M.H. (2001). Mitogen-activated protein (MAP) kinase pathways: regulation and physiological functions. *Endocr Rev* 22, 153-83.
- [2] Chen, R.E. and Thorner, J. (2007). Function and regulation in MAPK signaling pathways: lessons learned from the yeast *Saccharomyces cerevisiae*. *Biochim Biophys Acta* 1773, 1311-40.
- [3] Avruch, J. (2007). MAP kinase pathways: the first twenty years. *Biochim Biophys Acta* 1773, 1150-60.
- [4] Boulton, T.G., Yancopoulos, G.D., Gregory, J.S., Slaughter, C., Moomaw, C., Hsu, J. and Cobb, M.H. (1990). An insulin-stimulated protein kinase similar to yeast kinases involved in cell cycle control. *Science* 249, 64-7.
- [5] Boulton, T.G. et al. (1991). ERKs: a family of protein-serine/threonine kinases that are activated and tyrosine phosphorylated in response to insulin and NGF. *Cell* 65, 663-75.
- [6] Lewis, T.S., Shapiro, P.S. and Ahn, N.G. (1998). Signal transduction through MAP kinase cascades. *Adv Cancer Res* 74, 49-139.
- [7] Hunter, T. (1995). Protein kinases and phosphatases: the yin and yang of protein phosphorylation and signaling. *Cell* 80, 225-36.
- [8] Seger, R. and Krebs, E.G. (1995). The MAPK signaling cascade. *FASEB J* 9, 726-35.
- [9] Robbins, D.J., Zhen, E., Owaki, H., Vanderbilt, C.A., Ebert, D., Geppert, T.D. and Cobb, M.H. (1993). Regulation and properties of extracellular signal-regulated protein kinases 1 and 2 in vitro. *J Biol Chem* 268, 5097-106.
- [10] Rapp, U.R., Gotz, R. and Albert, S. (2006). BuCy RAFs drive cells into MEK addiction. *Cancer Cell* 9, 9-12.
- [11] Hekman, M., Hamm, H., Villar, A.V., Bader, B., Kuhlmann, J., Nickel, J. and Rapp, U.R. (2002). Associations of B- and C-Raf with cholesterol, phosphatidylserine, and lipid second messengers: preferential binding of Raf to artificial lipid rafts. *J Biol Chem* 277, 24090-102.
- [12] Rajalingam, K., Schreck, R., Rapp, U.R. and Albert, S. (2007). Ras oncogenes and their downstream targets. *Biochim Biophys Acta* 1773, 1177-95.
- [13] Zhang, J., Zhang, F., Ebert, D., Cobb, M.H. and Goldsmith, E.J. (1995). Activity of the MAP kinase ERK2 is controlled by a flexible surface loop. *Structure* 3, 299-307.
- [14] Canagarajah, B.J., Khokhlatchev, A., Cobb, M.H. and Goldsmith, E.J. (1997). Activation mechanism of the MAP kinase ERK2 by dual phosphorylation. *Cell* 90, 859-69.
- [15] Coulombe, P. and Meloche, S. (2007). Atypical mitogen-activated protein kinases: structure, regulation and functions. *Biochim Biophys Acta* 1773, 1376-87.
- [16] Davis, R.J. (1994). MAPKs: new JNK expands the group. *Trends Biochem Sci* 19, 470-3.
- [17] Avruch, J. (1998). Insulin signal transduction through protein kinase cascades. *Mol Cell Biochem* 182, 31-48.
- [18] Matsuda, S., Kawasaki, H., Moriguchi, T., Gotoh, Y. and Nishida, E. (1995). Activation of protein kinase cascades by osmotic shock. *J Biol Chem* 270, 12781-6.
- [19] Vojtek, A.B. and Cooper, J.A. (1995). Rho family members: activators of MAP kinase cascades. *Cell* 82, 527-9.

- [20] Waskiewicz, A.J. and Cooper, J.A. (1995). Mitogen and stress response pathways: MAP kinase cascades and phosphatase regulation in mammals and yeast. *Curr Opin Cell Biol* 7, 798-805.
- [21] Woodgett, J.R., Avruch, J. and Kyriakis, J. (1996). The stress activated protein kinase pathway. *Cancer Surv* 27, 127-38.
- [22] Robinson, M.J. and Cobb, M.H. (1997). Mitogen-activated protein kinase pathways. *Curr Opin Cell Biol* 9, 180-6.
- [23] Whitmarsh, A.J. (2007). Regulation of gene transcription by mitogen-activated protein kinase signaling pathways. *Biochim Biophys Acta* 1773, 1285-98.
- [24] Minden, A., Lin, A., Claret, F.X., Abo, A. and Karin, M. (1995). Selective activation of the JNK signaling cascade and c-Jun transcriptional activity by the small GTPases Rac and Cdc42Hs. *Cell* 81, 1147-57.
- [25] Herlaar, E. and Brown, Z. (1999). p38 MAPK signalling cascades in inflammatory disease. *Mol Med Today* 5, 439-47.
- [26] Ichijo, H. (1999). From receptors to stress-activated MAP kinases. *Oncogene* 18, 6087-93.
- [27] Kyriakis, J.M. (1999). Making the connection: coupling of stress-activated ERK/MAPK (extracellular-signal-regulated kinase/mitogen-activated protein kinase) core signalling modules to extracellular stimuli and biological responses. *Biochem Soc Symp* 64, 29-48.
- [28] Li, S. and Wattenberg, E.V. (1999). Cell-type-specific activation of p38 protein kinase cascades by the novel tumor promoter palytoxin. *Toxicol Appl Pharmacol* 160, 109-19.
- [29] Roberson, M.S., Zhang, T., Li, H.L. and Mulvaney, J.M. (1999). Activation of the p38 mitogen-activated protein kinase pathway by gonadotropin-releasing hormone. *Endocrinology* 140, 1310-8.
- [30] Tibbles, L.A. and Woodgett, J.R. (1999). The stress-activated protein kinase pathways. *Cell Mol Life Sci* 55, 1230-54.
- [31] Wysk, M., Yang, D.D., Lu, H.T., Flavell, R.A. and Davis, R.J. (1999). Requirement of mitogen-activated protein kinase kinase 3 (MKK3) for tumor necrosis factor-induced cytokine expression. *Proc Natl Acad Sci U S A* 96, 3763-8.
- [32] Cohen, P. (1997). The search for physiological substrates of MAP and SAP kinases in mammalian cells. *Trends Cell Biol* 7, 353-61.
- [33] Kyriakis, J.M. and Avruch, J. (2001). Mammalian mitogen-activated protein kinase signal transduction pathways activated by stress and inflammation. *Physiol Rev* 81, 807-69.
- [34] Cuenda, A., Cohen, P., Buee-Scherrer, V. and Goedert, M. (1997). Activation of stress-activated protein kinase-3 (SAPK3) by cytokines and cellular stresses is mediated via SAPKK3 (MKK6); comparison of the specificities of SAPK3 and SAPK2 (RK/p38). *EMBO J* 16, 295-305.
- [35] Cuenda, A., Alonso, G., Morrice, N., Jones, M., Meier, R., Cohen, P. and Nebreda, A.R. (1996). Purification and cDNA cloning of SAPKK3, the major activator of RK/p38 in stress- and cytokine-stimulated monocytes and epithelial cells. *EMBO J* 15, 4156-64.
- [36] Derijard, B., Raingeaud, J., Barrett, T., Wu, I.H., Han, J., Ulevitch, R.J. and Davis, R.J. (1995). Independent human MAP-kinase signal transduction pathways defined by MEK and MKK isoforms. *Science* 267, 682-5.
- [37] Raingeaud, J., Whitmarsh, A.J., Barrett, T., Derijard, B. and Davis, R.J. (1996). MKK3- and MKK6-regulated gene expression is mediated by the p38 mitogen-activated protein kinase signal transduction pathway. *Mol Cell Biol* 16, 1247-55.

- [38] Cheung, P.C., Campbell, D.G., Nebreda, A.R. and Cohen, P. (2003). Feedback control of the protein kinase TAK1 by SAPK2a/p38alpha. *EMBO J* 22, 5793-805.
- [39] Gallo, K.A. and Johnson, G.L. (2002). Mixed-lineage kinase control of JNK and p38 MAPK pathways. *Nat Rev Mol Cell Biol* 3, 663-72.
- [40] Ichijo, H. et al. (1997). Induction of apoptosis by ASK1, a mammalian MAPKKK that activates SAPK/JNK and p38 signaling pathways. *Science* 275, 90-4.
- [41] Yamaguchi, K. et al. (1995). Identification of a member of the MAPKKK family as a potential mediator of TGF-beta signal transduction. *Science* 270, 2008-11.
- [42] Marinissen, M.J., Chiariello, M. and Gutkind, J.S. (2001). Regulation of gene expression by the small GTPase Rho through the ERK6 (p38 gamma) MAP kinase pathway. *Genes Dev* 15, 535-53.
- [43] Sakabe, K., Teramoto, H., Zohar, M., Behbahani, B., Miyazaki, H., Chikumi, H. and Gutkind, J.S. (2002). Potent transforming activity of the small GTP-binding protein Rit in NIH 3T3 cells: evidence for a role of a p38gamma-dependent signaling pathway. *FEBS Lett* 511, 15-20.
- [44] Zhang, S., Han, J., Sells, M.A., Chernoff, J., Knaus, U.G., Ulevitch, R.J. and Bokoch, G.M. (1995). Rho family GTPases regulate p38 mitogen-activated protein kinase through the downstream mediator Pak1. *J Biol Chem* 270, 23934-6.
- [45] Marinissen, M.J., Chiariello, M., Pallante, M. and Gutkind, J.S. (1999). A network of mitogen-activated protein kinases links G protein-coupled receptors to the c-jun promoter: a role for c-Jun NH2-terminal kinase, p38s, and extracellular signal-regulated kinase 5. *Mol Cell Biol* 19, 4289-301.
- [46] Cuenda, A. and Rousseau, S. (2007). p38 MAP-kinases pathway regulation, function and role in human diseases. *Biochim Biophys Acta* 1773, 1358-75.
- [47] Lee, J.D., Ulevitch, R.J. and Han, J. (1995). Primary structure of BMK1: a new mammalian map kinase. *Biochem Biophys Res Commun* 213, 715-24.
- [48] Abe, J., Kusuhara, M., Ulevitch, R.J., Berk, B.C. and Lee, J.D. (1996). Big mitogen-activated protein kinase 1 (BMK1) is a redox-sensitive kinase. *J Biol Chem* 271, 16586-90.
- [49] Kato, Y., Kravchenko, V.V., Tapping, R.I., Han, J., Ulevitch, R.J. and Lee, J.D. (1997). BMK1/ERK5 regulates serum-induced early gene expression through transcription factor MEF2C. *EMBO J* 16, 7054-66.
- [50] Kamakura, S., Moriguchi, T. and Nishida, E. (1999). Activation of the protein kinase ERK5/BMK1 by receptor tyrosine kinases. Identification and characterization of a signaling pathway to the nucleus. *J Biol Chem* 274, 26563-71.
- [51] Chao, T.H., Hayashi, M., Tapping, R.I., Kato, Y. and Lee, J.D. (1999). MEKK3 directly regulates MEK5 activity as part of the big mitogen-activated protein kinase 1 (BMK1) signaling pathway. *J Biol Chem* 274, 36035-8.
- [52] Sun, W., Kesavan, K., Schaefer, B.C., Garrington, T.P., Ware, M., Johnson, N.L., Gelfand, E.W. and Johnson, G.L. (2001). MEKK2 associates with the adapter protein Lad/RIBP and regulates the MEK5-BMK1/ERK5 pathway. *J Biol Chem* 276, 5093-100.
- [53] English, J.M., Pearson, G., Baer, R. and Cobb, M.H. (1998). Identification of substrates and regulators of the mitogen-activated protein kinase ERK5 using chimeric protein kinases. *J Biol Chem* 273, 3854-60.
- [54] Pearson, G., English, J.M., White, M.A. and Cobb, M.H. (2001). ERK5 and ERK2 cooperate to regulate NF-kappaB and cell transformation. *J Biol Chem* 276, 7927-31.
- [55] Nishimoto, S. and Nishida, E. (2006). MAPK signalling: ERK5 versus ERK1/2. *EMBO Rep* 7, 782-6.

- [56] Turgeon, B., Saba-El-Leil, M.K. and Meloche, S. (2000). Cloning and characterization of mouse extracellular-signal-regulated protein kinase 3 as a unique gene product of 100 kDa. *Biochem J* 346 Pt 1, 169-75.
- [57] Kant, S., Schumacher, S., Singh, M.K., Kispert, A., Kotlyarov, A. and Gaestel, M. (2006). Characterization of the atypical MAPK ERK4 and its activation of the MAPK-activated protein kinase MK5. *J Biol Chem* 281, 35511-9.
- [58] Seternes, O.M. et al. (2004). Activation of MK5/PRAK by the atypical MAP kinase ERK3 defines a novel signal transduction pathway. *EMBO J* 23, 4780-91.
- [59] Abe, M.K., Kuo, W.L., Hershenson, M.B. and Rosner, M.R. (1999). Extracellular signal-regulated kinase 7 (ERK7), a novel ERK with a C-terminal domain that regulates its activity, its cellular localization, and cell growth. *Mol Cell Biol* 19, 1301-12.
- [60] Abe, M.K., Saelzler, M.P., Espinosa, R., 3rd, Kahle, K.T., Hershenson, M.B., Le Beau, M.M. and Rosner, M.R. (2002). ERK8, a new member of the mitogen-activated protein kinase family. *J Biol Chem* 277, 16733-43.
- [61] Bogoyevitch, M.A. and Court, N.W. (2004). Counting on mitogen-activated protein kinases--ERKs 3, 4, 5, 6, 7 and 8. *Cell Signal* 16, 1345-54.
- [62] Krens, S.F., Spaink, H.P. and Snaar-Jagalska, B.E. (2006). Functions of the MAPK family in vertebrate-development. *FEBS Lett* 580, 4984-90.
- [63] Kanei-Ishii, C. et al. (2004). Wnt-1 signal induces phosphorylation and degradation of c-Myb protein via TAK1, HIPK2, and NLK. *Genes Dev* 18, 816-29.
- [64] Ohkawara, B., Shirakabe, K., Hyodo-Miura, J., Matsuo, R., Ueno, N., Matsumoto, K. and Shibuya, H. (2004). Role of the TAK1-NLK-STAT3 pathway in TGF-beta-mediated mesoderm induction. *Genes Dev* 18, 381-6.
- [65] Smit, L., Baas, A., Kuipers, J., Korswagen, H., van de Wetering, M. and Clevers, H. (2004). Wnt activates the Tak1/Nemo-like kinase pathway. *J Biol Chem* 279, 17232-40.
- [66] Kojima, H. et al. (2005). STAT3 regulates Nemo-like kinase by mediating its interaction with IL-6-stimulated TGFbeta-activated kinase 1 for STAT3 Ser-727 phosphorylation. *Proc Natl Acad Sci U S A* 102, 4524-9.
- [67] Yarden, Y. and Sliwkowski, M.X. (2001). Untangling the ErbB signalling network. *Nat Rev Mol Cell Biol* 2, 127-37.
- [68] Olayioye, M.A., Neve, R.M., Lane, H.A. and Hynes, N.E. (2000). The ErbB signaling network: receptor heterodimerization in development and cancer. *EMBO J* 19, 3159-67.
- [69] Wieduwilt, M.J. and Moasser, M.M. (2008). The epidermal growth factor receptor family: biology driving targeted therapeutics. *Cell Mol Life Sci* 65, 1566-84.
- [70] Bouyain, S., Longo, P.A., Li, S., Ferguson, K.M. and Leahy, D.J. (2005). The extracellular region of ErbB4 adopts a tethered conformation in the absence of ligand. *Proc Natl Acad Sci U S A* 102, 15024-9.
- [71] Garrett, T.P. et al. (2002). Crystal structure of a truncated epidermal growth factor receptor extracellular domain bound to transforming growth factor alpha. *Cell* 110, 763-73.
- [72] Ogiso, H. et al. (2002). Crystal structure of the complex of human epidermal growth factor and receptor extracellular domains. *Cell* 110, 775-87.
- [73] Garrett, T.P. et al. (2003). The crystal structure of a truncated ErbB2 ectodomain reveals an active conformation, poised to interact with other ErbB receptors. *Mol Cell* 11, 495-505.
- [74] Zhang, X., Gureasko, J., Shen, K., Cole, P.A. and Kuriyan, J. (2006). An allosteric mechanism for activation of the kinase domain of epidermal growth factor receptor. *Cell* 125, 1137-49.



- [75] Salomon, D.S., Brandt, R., Ciardiello, F. and Normanno, N. (1995). Epidermal growth factor-related peptides and their receptors in human malignancies. *Crit Rev Oncol Hematol* 19, 183-232.
- [76] Hagemann, C. and Rapp, U.R. (1999). Isotype-specific functions of Raf kinases. *Exp Cell Res* 253, 34-46.
- [77] App, H., Hazan, R., Zilberstein, A., Ullrich, A., Schlessinger, J. and Rapp, U. (1991). Epidermal growth factor (EGF) stimulates association and kinase activity of Raf-1 with the EGF receptor. *Mol Cell Biol* 11, 913-9.
- [78] Burgering, B.M. and Coffey, P.J. (1995). Protein kinase B (c-Akt) in phosphatidylinositol-3-OH kinase signal transduction. *Nature* 376, 599-602.
- [79] Liu, W., Li, J. and Roth, R.A. (1999). Heregulin regulation of Akt/protein kinase B in breast cancer cells. *Biochem Biophys Res Commun* 261, 897-903.
- [80] Muthuswamy, S.K., Gilman, M. and Brugge, J.S. (1999). Controlled dimerization of ErbB receptors provides evidence for differential signaling by homo- and heterodimers. *Mol Cell Biol* 19, 6845-57.
- [81] Slater, E.P., Stubig, T., Lau, Q.C., Achenbach, T.V., Rapp, U.R. and Muller, R. (2003). C-Raf controlled pathways in the protection of tumor cells from apoptosis. *Int J Cancer* 104, 425-32.
- [82] Chan, T.O., Rittenhouse, S.E. and Tsichlis, P.N. (1999). AKT/PKB and other D3 phosphoinositide-regulated kinases: kinase activation by phosphoinositide-dependent phosphorylation. *Annu Rev Biochem* 68, 965-1014.
- [83] Ceteci, F., Ceteci, S., Karreman, C., Kramer, B.W., Asan, E., Gotz, R. and Rapp, U.R. (2007). Disruption of tumor cell adhesion promotes angiogenic switch and progression to micrometastasis in RAF-driven murine lung cancer. *Cancer Cell* 12, 145-59.
- [84] Engebraaten, O., Bjerkvig, R., Pedersen, P.H. and Laerum, O.D. (1993). Effects of EGF, bFGF, NGF and PDGF(bb) on cell proliferative, migratory and invasive capacities of human brain-tumour biopsies in vitro. *Int J Cancer* 53, 209-14.
- [85] Shibata, T., Kawano, T., Nagayasu, H., Okumura, K., Arisue, M., Hamada, J., Takeichi, N. and Hosokawa, M. (1996). Enhancing effects of epidermal growth factor on human squamous cell carcinoma motility and matrix degradation but not growth. *Tumour Biol* 17, 168-75.
- [86] Petit, A.M., Rak, J., Hung, M.C., Rockwell, P., Goldstein, N., Fendly, B. and Kerbel, R.S. (1997). Neutralizing antibodies against epidermal growth factor and ErbB-2/neu receptor tyrosine kinases down-regulate vascular endothelial growth factor production by tumor cells in vitro and in vivo: angiogenic implications for signal transduction therapy of solid tumors. *Am J Pathol* 151, 1523-30.
- [87] Goldman, C.K., Kim, J., Wong, W.L., King, V., Brock, T. and Gillespie, G.Y. (1993). Epidermal growth factor stimulates vascular endothelial growth factor production by human malignant glioma cells: a model of glioblastoma multiforme pathophysiology. *Mol Biol Cell* 4, 121-33.
- [88] Colicelli, J. (2004). Human RAS superfamily proteins and related GTPases. *Sci STKE* 2004, RE13.
- [89] Chiu, V.K. et al. (2002). Ras signalling on the endoplasmic reticulum and the Golgi. *Nat Cell Biol* 4, 343-50.
- [90] Rocks, O. et al. (2005). An acylation cycle regulates localization and activity of palmitoylated Ras isoforms. *Science* 307, 1746-52.
- [91] Hancock, J.F. and Parton, R.G. (2005). Ras plasma membrane signalling platforms. *Biochem J* 389, 1-11.
- [92] Hancock, J.F., Paterson, H. and Marshall, C.J. (1990). A polybasic domain or palmitoylation is required in addition to the CAAX motif to localize p21ras to the plasma membrane. *Cell* 63, 133-9.

- [93] Bourne, H.R., Sanders, D.A. and McCormick, F. (1990). The GTPase superfamily: a conserved switch for diverse cell functions. *Nature* 348, 125-32.
- [94] Bourne, H.R., Sanders, D.A. and McCormick, F. (1991). The GTPase superfamily: conserved structure and molecular mechanism. *Nature* 349, 117-27.
- [95] Kinbara, K., Goldfinger, L.E., Hansen, M., Chou, F.L. and Ginsberg, M.H. (2003). Ras GTPases: integrins' friends or foes? *Nat Rev Mol Cell Biol* 4, 767-76.
- [96] John, J., Sohmen, R., Feuerstein, J., Linke, R., Wittinghofer, A. and Goody, R.S. (1990). Kinetics of interaction of nucleotides with nucleotide-free H-ras p21. *Biochemistry* 29, 6058-65.
- [97] Gideon, P., John, J., Frech, M., Lautwein, A., Clark, R., Scheffler, J.E. and Wittinghofer, A. (1992). Mutational and kinetic analyses of the GTPase-activating protein (GAP)-p21 interaction: the C-terminal domain of GAP is not sufficient for full activity. *Mol Cell Biol* 12, 2050-6.
- [98] Eccleston, J.F., Moore, K.J., Morgan, L., Skinner, R.H. and Lowe, P.N. (1993). Kinetics of interaction between normal and proline 12 Ras and the GTPase-activating proteins, p120-GAP and neurofibromin. The significance of the intrinsic GTPase rate in determining the transforming ability of ras. *J Biol Chem* 268, 27012-9.
- [99] Klebe, C., Prinz, H., Wittinghofer, A. and Goody, R.S. (1995). The kinetic mechanism of Ran--nucleotide exchange catalyzed by RCC1. *Biochemistry* 34, 12543-52.
- [100] Lowy, D.R. and Willumsen, B.M. (1993). Function and regulation of ras. *Annu Rev Biochem* 62, 851-91.
- [101] Barbacid, M. (1987). ras genes. *Annu Rev Biochem* 56, 779-827.
- [102] Romero, F., Martinez, A.C., Camonis, J. and Rebollo, A. (1999). Aiolos transcription factor controls cell death in T cells by regulating Bcl-2 expression and its cellular localization. *EMBO J* 18, 3419-30.
- [103] Singh, A., Sowjanya, A.P. and Ramakrishna, G. (2005). The wild-type Ras: road ahead. *FASEB J* 19, 161-9.
- [104] Sicheri, F. and Kuriyan, J. (1997). Structures of Src-family tyrosine kinases. *Curr Opin Struct Biol* 7, 777-85.
- [105] Boggon, T.J. and Eck, M.J. (2004). Structure and regulation of Src family kinases. *Oncogene* 23, 7918-27.
- [106] Palacios, E.H. and Weiss, A. (2004). Function of the Src-family kinases, Lck and Fyn, in T-cell development and activation. *Oncogene* 23, 7990-8000.
- [107] Zamoyska, R., Basson, A., Filby, A., Legname, G., Lovatt, M. and Seddon, B. (2003). The influence of the src-family kinases, Lck and Fyn, on T cell differentiation, survival and activation. *Immunol Rev* 191, 107-18.
- [108] Yu, X.Z., Levin, S.D., Madrenas, J. and Anasetti, C. (2004). Lck is required for activation-induced T cell death after TCR ligation with partial agonists. *J Immunol* 172, 1437-43.
- [109] Samraj, A.K., Stroh, C., Fischer, U. and Schulze-Osthoff, K. (2006). The tyrosine kinase Lck is a positive regulator of the mitochondrial apoptosis pathway by controlling Bak expression. *Oncogene* 25, 186-97.
- [110] Reed, J.C., Torigoe, T., Turner, B.C., Merida, I., Gaulton, G., Saragovi, H.U., Rapp, U.R. and Taichman, R. (1993). Protooncogene-encoded protein kinases in interleukin-2 signal transduction. *Semin Immunol* 5, 327-36.
- [111] Thompson, P.A., Ledbetter, J.A., Rapp, U.R. and Bolen, J.B. (1991). The Raf-1 serine-threonine kinase is a substrate for the p56lck protein tyrosine kinase in human T-cells. *Cell Growth Differ* 2, 609-17.
- [112] Li, M., Ong, S.S., Rajwa, B., Thieu, V.T., Geahlen, R.L. and Harrison, M.L. (2008). The SH3 domain of Lck modulates T-cell receptor-dependent activation of

- extracellular signal-regulated kinase through activation of Raf-1. *Mol Cell Biol* 28, 630-41.
- [113] Marais, R., Light, Y., Paterson, H.F., Mason, C.S. and Marshall, C.J. (1997). Differential regulation of Raf-1, A-Raf, and B-Raf by oncogenic ras and tyrosine kinases. *J Biol Chem* 272, 4378-83.
- [114] Fabian, J.R., Daar, I.O. and Morrison, D.K. (1993). Critical tyrosine residues regulate the enzymatic and biological activity of Raf-1 kinase. *Mol Cell Biol* 13, 7170-9.
- [115] Marais, R., Light, Y., Mason, C., Paterson, H., Olson, M.F. and Marshall, C.J. (1998). Requirement of Ras-GTP-Raf complexes for activation of Raf-1 by protein kinase C. *Science* 280, 109-12.
- [116] Crews, C.M., Alessandrini, A. and Erikson, R.L. (1992). The primary structure of MEK, a protein kinase that phosphorylates the ERK gene product. *Science* 258, 478-80.
- [117] Seger, R. et al. (1992). Human T-cell mitogen-activated protein kinase kinases are related to yeast signal transduction kinases. *J Biol Chem* 267, 25628-31.
- [118] Zheng, C.F. and Guan, K.L. (1993). Properties of MEKs, the kinases that phosphorylate and activate the extracellular signal-regulated kinases. *J Biol Chem* 268, 23933-9.
- [119] Shaul, Y.D. and Seger, R. (2007). The MEK/ERK cascade: from signaling specificity to diverse functions. *Biochim Biophys Acta* 1773, 1213-26.
- [120] Ohren, J.F. et al. (2004). Structures of human MAP kinase kinase 1 (MEK1) and MEK2 describe novel noncompetitive kinase inhibition. *Nat Struct Mol Biol* 11, 1192-7.
- [121] Alessi, D.R. et al. (1994). Identification of the sites in MAP kinase kinase-1 phosphorylated by p74raf-1. *EMBO J* 13, 1610-9.
- [122] Gomez, N. and Cohen, P. (1991). Dissection of the protein kinase cascade by which nerve growth factor activates MAP kinases. *Nature* 353, 170-3.
- [123] Matsuda, S., Gotoh, Y. and Nishida, E. (1993). Phosphorylation of Xenopus mitogen-activated protein (MAP) kinase kinase by MAP kinase kinase kinase and MAP kinase. *J Biol Chem* 268, 3277-81.
- [124] Brunet, A., Pages, G. and Pouyssegur, J. (1994). Growth factor-stimulated MAP kinase induces rapid retrophosphorylation and inhibition of MAP kinase kinase (MEK1). *FEBS Lett* 346, 299-303.
- [125] Nantel, A., Mohammad-Ali, K., Sherk, J., Posner, B.I. and Thomas, D.Y. (1998). Interaction of the Grb10 adapter protein with the Raf1 and MEK1 kinases. *J Biol Chem* 273, 10475-84.
- [126] Frost, J.A., Steen, H., Shapiro, P., Lewis, T., Ahn, N., Shaw, P.E. and Cobb, M.H. (1997). Cross-cascade activation of ERKs and ternary complex factors by Rho family proteins. *EMBO J* 16, 6426-38.
- [127] Slack-Davis, J.K. et al. (2003). PAK1 phosphorylation of MEK1 regulates fibronectin-stimulated MAPK activation. *J Cell Biol* 162, 281-91.
- [128] Eblen, S.T., Slack-Davis, J.K., Tarcsafalvi, A., Parsons, J.T., Weber, M.J. and Catling, A.D. (2004). Mitogen-activated protein kinase feedback phosphorylation regulates MEK1 complex formation and activation during cellular adhesion. *Mol Cell Biol* 24, 2308-17.
- [129] Sontag, E., Fedorov, S., Kamibayashi, C., Robbins, D., Cobb, M. and Mumby, M. (1993). The interaction of SV40 small tumor antigen with protein phosphatase 2A stimulates the map kinase pathway and induces cell proliferation. *Cell* 75, 887-97.
- [130] Seger, R., Ahn, N.G., Posada, J., Munar, E.S., Jensen, A.M., Cooper, J.A., Cobb, M.H. and Krebs, E.G. (1992). Purification and characterization of mitogen-activated protein

- kinase activator(s) from epidermal growth factor-stimulated A431 cells. *J Biol Chem* 267, 14373-81.
- [131] Xiang, X., Zang, M., Waelde, C.A., Wen, R. and Luo, Z. (2002). Phosphorylation of 338SSYY341 regulates specific interaction between Raf-1 and MEK1. *J Biol Chem* 277, 44996-5003.
- [132] Zhu, J. et al. (2005). Identification of Raf-1 S471 as a novel phosphorylation site critical for Raf-1 and B-Raf kinase activities and for MEK binding. *Mol Biol Cell* 16, 4733-44.
- [133] Wang, D., Boerner, S.A., Winkler, J.D. and LoRusso, P.M. (2007). Clinical experience of MEK inhibitors in cancer therapy. *Biochim Biophys Acta* 1773, 1248-55.
- [134] Ray, L.B. and Sturgill, T.W. (1987). Rapid stimulation by insulin of a serine/threonine kinase in 3T3-L1 adipocytes that phosphorylates microtubule-associated protein 2 in vitro. *Proc Natl Acad Sci U S A* 84, 1502-6.
- [135] Yung, Y., Yao, Z., Hanoch, T. and Seger, R. (2000). ERK1b, a 46-kDa ERK isoform that is differentially regulated by MEK. *J Biol Chem* 275, 15799-808.
- [136] Aebbersold, D.M., Shaul, Y.D., Yung, Y., Yarom, N., Yao, Z., Hanoch, T. and Seger, R. (2004). Extracellular signal-regulated kinase 1c (ERK1c), a novel 42-kilodalton ERK, demonstrates unique modes of regulation, localization, and function. *Mol Cell Biol* 24, 10000-15.
- [137] Gonzalez, F.A., Raden, D.L., Rigby, M.R. and Davis, R.J. (1992). Heterogeneous expression of four MAP kinase isoforms in human tissues. *FEBS Lett* 304, 170-8.
- [138] Rubinfeld, H., Hanoch, T. and Seger, R. (1999). Identification of a cytoplasmic-retention sequence in ERK2. *J Biol Chem* 274, 30349-52.
- [139] Chuderland, D. and Seger, R. (2005). Protein-protein interactions in the regulation of the extracellular signal-regulated kinase. *Mol Biotechnol* 29, 57-74.
- [140] Tanoue, T., Adachi, M., Moriguchi, T. and Nishida, E. (2000). A conserved docking motif in MAP kinases common to substrates, activators and regulators. *Nat Cell Biol* 2, 110-6.
- [141] Cobb, M.H. and Goldsmith, E.J. (2000). Dimerization in MAP-kinase signaling. *Trends Biochem Sci* 25, 7-9.
- [142] Zhang, F., Strand, A., Robbins, D., Cobb, M.H. and Goldsmith, E.J. (1994). Atomic structure of the MAP kinase ERK2 at 2.3 Å resolution. *Nature* 367, 704-11.
- [143] Cobb, M.H. and Goldsmith, E.J. (1995). How MAP kinases are regulated. *J Biol Chem* 270, 14843-6.
- [144] Gonzalez, F.A., Raden, D.L. and Davis, R.J. (1991). Identification of substrate recognition determinants for human ERK1 and ERK2 protein kinases. *J Biol Chem* 266, 22159-63.
- [145] Corbalan-Garcia, S., Yang, S.S., Degenhardt, K.R. and Bar-Sagi, D. (1996). Identification of the mitogen-activated protein kinase phosphorylation sites on human Sos1 that regulate interaction with Grb2. *Mol Cell Biol* 16, 5674-82.
- [146] Jacobs, D., Glossip, D., Xing, H., Muslin, A.J. and Kornfeld, K. (1999). Multiple docking sites on substrate proteins form a modular system that mediates recognition by ERK MAP kinase. *Genes Dev* 13, 163-75.
- [147] Lee, T. et al. (2004). Docking motif interactions in MAP kinases revealed by hydrogen exchange mass spectrometry. *Mol Cell* 14, 43-55.
- [148] Casar, B., Pinto, A. and Crespo, P. (2008). Essential role of ERK dimers in the activation of cytoplasmic but not nuclear substrates by ERK-scaffold complexes. *Mol Cell* 31, 708-21.

- [149] Alessi, D.R., Gomez, N., Moorhead, G., Lewis, T., Keyse, S.M. and Cohen, P. (1995). Inactivation of p42 MAP kinase by protein phosphatase 2A and a protein tyrosine phosphatase, but not CL100, in various cell lines. *Curr Biol* 5, 283-95.
- [150] Pulido, R., Zuniga, A. and Ullrich, A. (1998). PTP-SL and STEP protein tyrosine phosphatases regulate the activation of the extracellular signal-regulated kinases ERK1 and ERK2 by association through a kinase interaction motif. *EMBO J* 17, 7337-50.
- [151] Sun, H., Charles, C.H., Lau, L.F. and Tonks, N.K. (1993). MKP-1 (3CH134), an immediate early gene product, is a dual specificity phosphatase that dephosphorylates MAP kinase in vivo. *Cell* 75, 487-93.
- [152] Balan, V. et al. (2006). Identification of novel in vivo Raf-1 phosphorylation sites mediating positive feedback Raf-1 regulation by extracellular signal-regulated kinase. *Mol Biol Cell* 17, 1141-53.
- [153] Dougherty, M.K. et al. (2005). Regulation of Raf-1 by direct feedback phosphorylation. *Mol Cell* 17, 215-24.
- [154] Rushworth, L.K., Hindley, A.D., O'Neill, E. and Kolch, W. (2006). Regulation and role of Raf-1/B-Raf heterodimerization. *Mol Cell Biol* 26, 2262-72.
- [155] Morrison, D.K. and Davis, R.J. (2003). Regulation of MAP kinase signaling modules by scaffold proteins in mammals. *Annu Rev Cell Dev Biol* 19, 91-118.
- [156] Therrien, M., Chang, H.C., Solomon, N.M., Karim, F.D., Wassarman, D.A. and Rubin, G.M. (1995). KSR, a novel protein kinase required for RAS signal transduction. *Cell* 83, 879-88.
- [157] Kornfeld, K., Hom, D.B. and Horvitz, H.R. (1995). The *ksr-1* gene encodes a novel protein kinase involved in Ras-mediated signaling in *C. elegans*. *Cell* 83, 903-13.
- [158] Claperon, A. and Therrien, M. (2007). KSR and CNK: two scaffolds regulating RAS-mediated RAF activation. *Oncogene* 26, 3143-58.
- [159] Raabe, T. and Rapp, U.R. (2003). Ras signaling: PP2A puts Ksr and Raf in the right place. *Curr Biol* 13, R635-7.
- [160] Morrison, D.K. (2001). KSR: a MAPK scaffold of the Ras pathway? *J Cell Sci* 114, 1609-12.
- [161] Muller, J., Ory, S., Copeland, T., Piwnicka-Worms, H. and Morrison, D.K. (2001). C-TAK1 regulates Ras signaling by phosphorylating the MAPK scaffold, KSR1. *Mol Cell* 8, 983-93.
- [162] Sternberg, P.W. and Alberola-Ila, J. (1998). Conspiracy theory: RAS and RAF do not act alone. *Cell* 95, 447-50.
- [163] Rajakulendran, T., Sahmi, M., Kurinov, I., Tyers, M., Therrien, M. and Sicheri, F. (2008). CNK and HYP form a discrete dimer by their SAM domains to mediate RAF kinase signaling. *Proc Natl Acad Sci U S A* 105, 2836-41.
- [164] Kolch, W. (2005). Coordinating ERK/MAPK signalling through scaffolds and inhibitors. *Nat Rev Mol Cell Biol* 6, 827-37.
- [165] Schaeffer, H.J., Catling, A.D., Eblen, S.T., Collier, L.S., Krauss, A. and Weber, M.J. (1998). MP1: a MEK binding partner that enhances enzymatic activation of the MAP kinase cascade. *Science* 281, 1668-71.
- [166] Wunderlich, W., Fialka, I., Teis, D., Alpi, A., Pfeifer, A., Parton, R.G., Lottspeich, F. and Huber, L.A. (2001). A novel 14-kilodalton protein interacts with the mitogen-activated protein kinase scaffold mp1 on a late endosomal/lysosomal compartment. *J Cell Biol* 152, 765-76.
- [167] Kurzbauer, R. et al. (2004). Crystal structure of the p14/MP1 scaffolding complex: how a twin couple attaches mitogen-activated protein kinase signaling to late endosomes. *Proc Natl Acad Sci U S A* 101, 10984-9.

- [168] DeWire, S.M., Ahn, S., Lefkowitz, R.J. and Shenoy, S.K. (2007). Beta-arrestins and cell signaling. *Annu Rev Physiol* 69, 483-510.
- [169] Rapp, U.R., Goldsborough, M.D., Mark, G.E., Bonner, T.I., Groffen, J., Reynolds, F.H., Jr. and Stephenson, J.R. (1983). Structure and biological activity of v-raf, a unique oncogene transduced by a retrovirus. *Proc Natl Acad Sci U S A* 80, 4218-22.
- [170] Jansen, H.W., Lurz, R., Bister, K., Bonner, T.I., Mark, G.E. and Rapp, U.R. (1984). Homologous cell-derived oncogenes in avian carcinoma virus MH2 and murine sarcoma virus 3611. *Nature* 307, 281-4.
- [171] Sutrave, P., Bonner, T.I., Rapp, U.R., Jansen, H.W., Patschinsky, T. and Bister, K. (1984). Nucleotide sequence of avian retroviral oncogene v-mil: homologue of murine retroviral oncogene v-raf. *Nature* 309, 85-8.
- [172] Kieber, J.J., Rothenberg, M., Roman, G., Feldmann, K.A. and Ecker, J.R. (1993). CTR1, a negative regulator of the ethylene response pathway in Arabidopsis, encodes a member of the raf family of protein kinases. *Cell* 72, 427-41.
- [173] Han, M., Golden, A., Han, Y. and Sternberg, P.W. (1993). *C. elegans* lin-45 raf gene participates in let-60 ras-stimulated vulval differentiation. *Nature* 363, 133-40.
- [174] Mark, G.E., MacIntyre, R.J., Digan, M.E., Ambrosio, L. and Perrimon, N. (1987). *Drosophila melanogaster* homologs of the raf oncogene. *Mol Cell Biol* 7, 2134-40.
- [175] Bonner, T.I., Kerby, S.B., Sutrave, P., Gunnell, M.A., Mark, G. and Rapp, U.R. (1985). Structure and biological activity of human homologs of the raf/mil oncogene. *Mol Cell Biol* 5, 1400-7.
- [176] Daum, G., Eisenmann-Tappe, I., Fries, H.W., Troppmair, J. and Rapp, U.R. (1994). The ins and outs of Raf kinases. *Trends Biochem Sci* 19, 474-80.
- [177] Huleihel, M., Goldsborough, M., Cleveland, J., Gunnell, M., Bonner, T. and Rapp, U.R. (1986). Characterization of murine A-raf, a new oncogene related to the v-raf oncogene. *Mol Cell Biol* 6, 2655-62.
- [178] Ikawa, S., Fukui, M., Ueyama, Y., Tamaoki, N., Yamamoto, T. and Toyoshima, K. (1988). B-raf, a new member of the raf family, is activated by DNA rearrangement. *Mol Cell Biol* 8, 2651-4.
- [179] Storm, S.M., Cleveland, J.L. and Rapp, U.R. (1990). Expression of raf family proto-oncogenes in normal mouse tissues. *Oncogene* 5, 345-51.
- [180] Shiu, S.H. and Bleecker, A.B. (2001). Receptor-like kinases from Arabidopsis form a monophyletic gene family related to animal receptor kinases. *Proc Natl Acad Sci U S A* 98, 10763-8.
- [181] Diaz, B., Barnard, D., Filson, A., MacDonald, S., King, A. and Marshall, M. (1997). Phosphorylation of Raf-1 serine 338-serine 339 is an essential regulatory event for Ras-dependent activation and biological signaling. *Mol Cell Biol* 17, 4509-16.
- [182] Mason, C.S., Springer, C.J., Cooper, R.G., Superti-Furga, G., Marshall, C.J. and Marais, R. (1999). Serine and tyrosine phosphorylations cooperate in Raf-1, but not B-Raf activation. *EMBO J* 18, 2137-48.
- [183] Chong, H., Vikis, H.G. and Guan, K.L. (2003). Mechanisms of regulating the Raf kinase family. *Cell Signal* 15, 463-9.
- [184] Beck, T.W., Huleihel, M., Gunnell, M., Bonner, T.I. and Rapp, U.R. (1987). The complete coding sequence of the human A-raf-1 oncogene and transforming activity of a human A-raf carrying retrovirus. *Nucleic Acids Res* 15, 595-609.
- [185] Vojtek, A.B., Hollenberg, S.M. and Cooper, J.A. (1993). Mammalian Ras interacts directly with the serine/threonine kinase Raf. *Cell* 74, 205-14.
- [186] Morrison, D.K. and Cutler, R.E. (1997). The complexity of Raf-1 regulation. *Curr Opin Cell Biol* 9, 174-9.

- [187] Improt-Brears, T., Ghosh, S. and Bell, R.M. (1999). Mutational analysis of Raf-1 cysteine rich domain: requirement for a cluster of basic aminoacids for interaction with phosphatidylserine. *Mol Cell Biochem* 198, 171-8.
- [188] Kerkhoff, E. and Rapp, U.R. (2001). The Ras-Raf relationship: an unfinished puzzle. *Adv Enzyme Regul* 41, 261-7.
- [189] Morrison, D.K., Heidecker, G., Rapp, U.R. and Copeland, T.D. (1993). Identification of the major phosphorylation sites of the Raf-1 kinase. *J Biol Chem* 268, 17309-16.
- [190] Guan, K.L., Figueroa, C., Brtva, T.R., Zhu, T., Taylor, J., Barber, T.D. and Vojtek, A.B. (2000). Negative regulation of the serine/threonine kinase B-Raf by Akt. *J Biol Chem* 275, 27354-9.
- [191] Ghosh, S., Strum, J.C., Sciorra, V.A., Daniel, L. and Bell, R.M. (1996). Raf-1 kinase possesses distinct binding domains for phosphatidylserine and phosphatidic acid. Phosphatidic acid regulates the translocation of Raf-1 in 12-O-tetradecanoylphorbol-13-acetate-stimulated Madin-Darby canine kidney cells. *J Biol Chem* 271, 8472-80.
- [192] Johnson, L.M., James, K.M., Chamberlain, M.D. and Anderson, D.H. (2005). Identification of key residues in the A-Raf kinase important for phosphoinositide lipid binding specificity. *Biochemistry* 44, 3432-40.
- [193] Wan, P.T. et al. (2004). Mechanism of activation of the RAF-ERK signaling pathway by oncogenic mutations of B-RAF. *Cell* 116, 855-67.
- [194] Hekman, M., Fischer, A., Wennogle, L.P., Wang, Y.K., Campbell, S.L. and Rapp, U.R. (2005). Novel C-Raf phosphorylation sites: serine 296 and 301 participate in Raf regulation. *FEBS Lett* 579, 464-8.
- [195] Wellbrock, C., Karasarides, M. and Marais, R. (2004). The RAF proteins take centre stage. *Nat Rev Mol Cell Biol* 5, 875-85.
- [196] Aitken, A. (2006). 14-3-3 proteins: a historic overview. *Semin Cancer Biol* 16, 162-72.
- [197] Gardino, A.K., Smerdon, S.J. and Yaffe, M.B. (2006). Structural determinants of 14-3-3 binding specificities and regulation of subcellular localization of 14-3-3-ligand complexes: a comparison of the X-ray crystal structures of all human 14-3-3 isoforms. *Semin Cancer Biol* 16, 173-82.
- [198] Obsil, T., Ghirlando, R., Klein, D.C., Ganguly, S. and Dyda, F. (2001). Crystal structure of the 14-3-3zeta:serotonin N-acetyltransferase complex. a role for scaffolding in enzyme regulation. *Cell* 105, 257-67.
- [199] Dougherty, M.K. and Morrison, D.K. (2004). Unlocking the code of 14-3-3. *J Cell Sci* 117, 1875-84.
- [200] Dumaz, N. and Marais, R. (2003). Protein kinase A blocks Raf-1 activity by stimulating 14-3-3 binding and blocking Raf-1 interaction with Ras. *J Biol Chem* 278, 29819-23.
- [201] Clark, G.J., Drugan, J.K., Rossman, K.L., Carpenter, J.W., Rogers-Graham, K., Fu, H., Der, C.J. and Campbell, S.L. (1997). 14-3-3 zeta negatively regulates raf-1 activity by interactions with the Raf-1 cysteine-rich domain. *J Biol Chem* 272, 20990-3.
- [202] Hekman, M., Wiese, S., Metz, R., Albert, S., Troppmair, J., Nickel, J., Sendtner, M. and Rapp, U.R. (2004). Dynamic changes in C-Raf phosphorylation and 14-3-3 protein binding in response to growth factor stimulation: differential roles of 14-3-3 protein binding sites. *J Biol Chem* 279, 14074-86.
- [203] Ory, S., Zhou, M., Conrads, T.P., Veenstra, T.D. and Morrison, D.K. (2003). Protein phosphatase 2A positively regulates Ras signaling by dephosphorylating KSR1 and Raf-1 on critical 14-3-3 binding sites. *Curr Biol* 13, 1356-64.
- [204] Light, Y., Paterson, H. and Marais, R. (2002). 14-3-3 antagonizes Ras-mediated Raf-1 recruitment to the plasma membrane to maintain signaling fidelity. *Mol Cell Biol* 22, 4984-96.

- [205] Fischer, A. et al. (2008). Regulation of RAF activity by 14-3-3 proteins - RAF kinases associate functionally with both homo- and heterodimeric forms of 14-3-3 proteins. *J Biol Chem*
- [206] Le Mellay, V. et al. (2002). Regulation of glycolysis by Raf protein serine/threonine kinases. *Adv Enzyme Regul* 42, 317-32.
- [207] Hagemann, C. (1999). Raf-Isoform spezifische Protein-Protein Wechselwirkungen, detektiert mit dem Hefe Two-Hybrid System. Dissertation zur Erlangung des naturwissenschaftlichen Doktorgrades der Bayerischen Julius-Maximilians-Universität Würzburg
- [208] Nassar, N., Horn, G., Herrmann, C., Scherer, A., McCormick, F. and Wittinghofer, A. (1995). The 2.2 Å crystal structure of the Ras-binding domain of the serine/threonine kinase c-Raf1 in complex with Rap1A and a GTP analogue. *Nature* 375, 554-60.
- [209] Weber, C.K., Slupsky, J.R., Herrmann, C., Schuler, M., Rapp, U.R. and Block, C. (2000). Mitogenic signaling of Ras is regulated by differential interaction with Raf isozymes. *Oncogene* 19, 169-76.
- [210] Nassar, N., Horn, G., Herrmann, C., Block, C., Janknecht, R. and Wittinghofer, A. (1996). Ras/Rap effector specificity determined by charge reversal. *Nat Struct Biol* 3, 723-9.
- [211] Bruder, J.T., Heidecker, G. and Rapp, U.R. (1992). Serum-, TPA-, and Ras-induced expression from Ap-1/Ets-driven promoters requires Raf-1 kinase. *Genes Dev* 6, 545-56.
- [212] Zhang, X.F. et al. (1993). Normal and oncogenic p21ras proteins bind to the amino-terminal regulatory domain of c-Raf-1. *Nature* 364, 308-13.
- [213] Roy, S., Lane, A., Yan, J., McPherson, R. and Hancock, J.F. (1997). Activity of plasma membrane-recruited Raf-1 is regulated by Ras via the Raf zinc finger. *J Biol Chem* 272, 20139-45.
- [214] Luo, Z., Diaz, B., Marshall, M.S. and Avruch, J. (1997). An intact Raf zinc finger is required for optimal binding to processed Ras and for ras-dependent Raf activation in situ. *Mol Cell Biol* 17, 46-53.
- [215] Hu, C.D., Kariya, K., Tamada, M., Akasaka, K., Shirouzu, M., Yokoyama, S. and Kataoka, T. (1995). Cysteine-rich region of Raf-1 interacts with activator domain of post-translationally modified Ha-Ras. *J Biol Chem* 270, 30274-7.
- [216] Fischer, A., Hekman, M., Kuhlmann, J., Rubio, I., Wiese, S. and Rapp, U.R. (2007). B- and C-RAF display essential differences in their binding to Ras: the isotype-specific N terminus of B-RAF facilitates Ras binding. *J Biol Chem* 282, 26503-16.
- [217] Rizzo, M.A., Shome, K., Watkins, S.C. and Romero, G. (2000). The recruitment of Raf-1 to membranes is mediated by direct interaction with phosphatidic acid and is independent of association with Ras. *J Biol Chem* 275, 23911-8.
- [218] Rajalingam, K., Wunder, C., Brinkmann, V., Churin, Y., Hekman, M., Sievers, C., Rapp, U.R. and Rudel, T. (2005). Prohibitin is required for Ras-induced Raf-MEK-ERK activation and epithelial cell migration. *Nat Cell Biol* 7, 837-43.
- [219] Tzivion, G., Luo, Z. and Avruch, J. (1998). A dimeric 14-3-3 protein is an essential cofactor for Raf kinase activity. *Nature* 394, 88-92.
- [220] Avruch, J., Khokhlatchev, A., Kyriakis, J.M., Luo, Z., Tzivion, G., Vavvas, D. and Zhang, X.F. (2001). Ras activation of the Raf kinase: tyrosine kinase recruitment of the MAP kinase cascade. *Recent Prog Horm Res* 56, 127-55.
- [221] Denouel-Galy, A., Douville, E.M., Warne, P.H., Papin, C., Laugier, D., Calothy, G., Downward, J. and Eychene, A. (1998). Murine Ksr interacts with MEK and inhibits Ras-induced transformation. *Curr Biol* 8, 46-55.



- [222] Yu, W., Fantl, W.J., Harrowe, G. and Williams, L.T. (1998). Regulation of the MAP kinase pathway by mammalian Ksr through direct interaction with MEK and ERK. *Curr Biol* 8, 56-64.
- [223] Weber, C.K., Slupsky, J.R., Kalmes, H.A. and Rapp, U.R. (2001). Active Ras induces heterodimerization of cRaf and BRaf. *Cancer Res* 61, 3595-8.
- [224] Garnett, M.J., Rana, S., Paterson, H., Barford, D. and Marais, R. (2005). Wild-type and mutant B-RAF activate C-RAF through distinct mechanisms involving heterodimerization. *Mol Cell* 20, 963-9.
- [225] Schlegel, A., Volonte, D., Engelman, J.A., Galbiati, F., Mehta, P., Zhang, X.L., Scherer, P.E. and Lisanti, M.P. (1998). Crowded little caves: structure and function of caveolae. *Cell Signal* 10, 457-63.
- [226] Kikuchi, A. and Williams, L.T. (1996). Regulation of interaction of ras p21 with RalGDS and Raf-1 by cyclic AMP-dependent protein kinase. *J Biol Chem* 271, 588-94.
- [227] King, A.J., Sun, H., Diaz, B., Barnard, D., Miao, W., Bagrodia, S. and Marshall, M.S. (1998). The protein kinase Pak3 positively regulates Raf-1 activity through phosphorylation of serine 338. *Nature* 396, 180-3.
- [228] Stokoe, D. and McCormick, F. (1997). Activation of c-Raf-1 by Ras and Src through different mechanisms: activation in vivo and in vitro. *EMBO J* 16, 2384-96.
- [229] Ritt, D.A., Daar, I.O. and Morrison, D.K. (2006). KSR regulation of the Raf-MEK-ERK cascade. *Methods Enzymol* 407, 224-37.
- [230] Morrison, D.K., Kaplan, D.R., Rapp, U. and Roberts, T.M. (1988). Signal transduction from membrane to cytoplasm: growth factors and membrane-bound oncogene products increase Raf-1 phosphorylation and associated protein kinase activity. *Proc Natl Acad Sci U S A* 85, 8855-9.
- [231] Morrison, D.K., Heidecker, G., Rapp, U.R. and Copeland, T.D. (1993). Identification of the major phosphorylation sites of the Raf-1 kinase. *J Biol Chem* 268, 17309-16.
- [232] Yaffe, M.B. et al. (1997). The structural basis for 14-3-3:phosphopeptide binding specificity. *Cell* 91, 961-71.
- [233] Reusch, H.P., Zimmermann, S., Schaefer, M., Paul, M. and Moelling, K. (2001). Regulation of Raf by Akt controls growth and differentiation in vascular smooth muscle cells. *J Biol Chem* 276, 33630-7.
- [234] Moelling, K., Schad, K., Bosse, M., Zimmermann, S. and Schweneker, M. (2002). Regulation of Raf-Akt Cross-talk. *J Biol Chem* 277, 31099-106.
- [235] Dhillon, A.S., Pollock, C., Steen, H., Shaw, P.E., Mischak, H. and Kolch, W. (2002). Cyclic AMP-dependent kinase regulates Raf-1 kinase mainly by phosphorylation of serine 259. *Mol Cell Biol* 22, 3237-46.
- [236] Yip-Schneider, M.T., Miao, W., Lin, A., Barnard, D.S., Tzivion, G. and Marshall, M.S. (2000). Regulation of the Raf-1 kinase domain by phosphorylation and 14-3-3 association. *Biochem J* 351, 151-9.
- [237] Mischak, H., Seitz, T., Janosch, P., Eulitz, M., Steen, H., Schellerer, M., Philipp, A. and Kolch, W. (1996). Negative regulation of Raf-1 by phosphorylation of serine 621. *Mol Cell Biol* 16, 5409-18.
- [238] Dumaz, N., Light, Y. and Marais, R. (2002). Cyclic AMP blocks cell growth through Raf-1-dependent and Raf-1-independent mechanisms. *Mol Cell Biol* 22, 3717-28.
- [239] Zhang, B.H. and Guan, K.L. (2000). Activation of B-Raf kinase requires phosphorylation of the conserved residues Thr598 and Ser601. *Embo J* 19, 5429-39.
- [240] Chong, H., Lee, J. and Guan, K.L. (2001). Positive and negative regulation of Raf kinase activity and function by phosphorylation. *Embo J* 20, 3716-27.

- [241] Stephens, R.M., Sithanandam, G., Copeland, T.D., Kaplan, D.R., Rapp, U.R. and Morrison, D.K. (1992). 95-kilodalton B-Raf serine/threonine kinase: identification of the protein and its major autophosphorylation site. *Mol Cell Biol* 12, 3733-42.
- [242] Xing, H.R. and Kolesnick, R. (2001). Kinase suppressor of Ras signals through Thr269 of c-Raf-1. *J Biol Chem* 276, 9733-41.
- [243] Brummer, T., Martin, P., Herzog, S., Misawa, Y., Daly, R.J. and Reth, M. (2006). Functional analysis of the regulatory requirements of B-Raf and the B-Raf(V600E) oncoprotein. *Oncogene* 25, 6262-76.
- [244] Huebner, K. et al. (1986). Actively transcribed genes in the raf oncogene group, located on the X chromosome in mouse and human. *Proc Natl Acad Sci U S A* 83, 3934-8.
- [245] Derry, J.M. and Barnard, P.J. (1992). Physical linkage of the A-raf-1, properdin, synapsin I, and TIMP genes on the human and mouse X chromosomes. *Genomics* 12, 632-8.
- [246] Mahtani, M.M., Lafreniere, R.G., Kruse, T.A. and Willard, H.F. (1991). An 18-locus linkage map of the pericentromeric region of the human X chromosome: genetic framework for mapping X-linked disorders. *Genomics* 10, 849-57.
- [247] Grant, S.G. and Chapman, V.M. (1991). Detailed genetic mapping of the A-raf proto-oncogene on the mouse X chromosome. *Oncogene* 6, 397-402.
- [248] Kirchgessner, C.U., Trofatter, J.A., Mahtani, M.M., Willard, H.F. and DeGennaro, L.J. (1991). A highly polymorphic dinucleotide repeat on the proximal short arm of the human X chromosome: linkage mapping of the synapsin I/A-raf-1 genes. *Am J Hum Genet* 49, 184-91.
- [249] Lee, J.E., Beck, T.W., Brennscheidt, U., DeGennaro, L.J. and Rapp, U.R. (1994). The complete sequence and promoter activity of the human A-raf-1 gene (ARAF1). *Genomics* 20, 43-55.
- [250] Wadewitz, A.G., Winer, M.A. and Wolgemuth, D.J. (1993). Developmental and cell lineage specificity of raf family gene expression in mouse testis. *Oncogene* 8, 1055-62.
- [251] Lee, J.E., Beck, T.W., Wojnowski, L. and Rapp, U.R. (1996). Regulation of A-raf expression. *Oncogene* 12, 1669-77.
- [252] Yokoyama, T., Takano, K., Yoshida, A., Katada, F., Sun, P., Takenawa, T., Andoh, T. and Endo, T. (2007). DA-Raf1, a competent intrinsic dominant-negative antagonist of the Ras-ERK pathway, is required for myogenic differentiation. *J Cell Biol* 177, 781-93.
- [253] Luckett, J.C., Huser, M.B., Giagtzoglou, N., Brown, J.E. and Pritchard, C.A. (2000). Expression of the A-raf proto-oncogene in the normal adult and embryonic mouse. *Cell Growth Differ* 11, 163-71.
- [254] Winer, M.A. and Wolgemuth, D.J. (1995). The segment-specific pattern of A-raf expression in the mouse epididymis is regulated by testicular factors. *Endocrinology* 136, 2561-72.
- [255] Zmuidzinas, A., Gould, G.W. and Yager, J.D. (1989). Expression of c-raf-1 and A-raf-1 during differentiation of 3T3-L1 preadipocyte fibroblasts into adipocytes. *Biochem Biophys Res Commun* 162, 1180-7.
- [256] Kalvelyte, A.V. and Pabrezaite, L.C. (1998). Proto-oncogene expression in bovine peripheral blood leukemic lymphocytes during their spontaneous proliferation, differentiation and apoptosis in vitro. *Leuk Res* 22, 135-43.
- [257] McCubrey, J.A. et al. (1998). Differential abilities of activated Raf oncoproteins to abrogate cytokine dependency, prevent apoptosis and induce autocrine growth factor synthesis in human hematopoietic cells. *Leukemia* 12, 1903-29.

- [258] Mahon, E.S., Hawrysh, A.D., Chagpar, R.B., Johnson, L.M. and Anderson, D.H. (2005). A-Raf associates with and regulates platelet-derived growth factor receptor signalling. *Cell Signal* 17, 857-68.
- [259] Rybin, V.O., Xu, X. and Steinberg, S.F. (1999). Activated protein kinase C isoforms target to cardiomyocyte caveolae : stimulation of local protein phosphorylation. *Circ Res* 84, 980-8.
- [260] Yuryev, A., Ono, M., Goff, S.A., Macaluso, F. and Wennogle, L.P. (2000). Isoform-specific localization of A-RAF in mitochondria. *Mol Cell Biol* 20, 4870-8.
- [261] Yuryev, A. and Wennogle, L.P. (2003). Novel raf kinase protein-protein interactions found by an exhaustive yeast two-hybrid analysis. *Genomics* 81, 112-25.
- [262] Galmiche, A. et al. (2008). Isoform-specific interaction of C-RAF with mitochondria. *J Biol Chem*
- [263] Pritchard, C.A., Bolin, L., Slattery, R., Murray, R. and McMahon, M. (1996). Post-natal lethality and neurological and gastrointestinal defects in mice with targeted disruption of the A-Raf protein kinase gene. *Curr Biol* 6, 614-7.
- [264] Mercer, K., Chiloeches, A., Huser, M., Kiernan, M., Marais, R. and Pritchard, C. (2002). ERK signalling and oncogene transformation are not impaired in cells lacking A-Raf. *Oncogene* 21, 347-55.
- [265] Pelkmans, L., Fava, E., Grabner, H., Hannus, M., Habermann, B., Krausz, E. and Zerial, M. (2005). Genome-wide analysis of human kinases in clathrin- and caveolae/raft-mediated endocytosis. *Nature* 436, 78-86.
- [266] Pelkmans, L. and Zerial, M. (2005). Kinase-regulated quantal assemblies and kiss-and-run recycling of caveolae. *Nature* 436, 128-33.
- [267] Yin, X.L., Chen, S. and Gu, J.X. (2002). Identification of TH1 as an interaction partner of A-Raf kinase. *Mol Cell Biochem* 231, 69-74.
- [268] Rual, J.F. et al. (2005). Towards a proteome-scale map of the human protein-protein interaction network. *Nature* 437, 1173-8.
- [269] Boldyreff, B. and Issinger, O.G. (1997). A-Raf kinase is a new interacting partner of protein kinase CK2 beta subunit. *FEBS Lett* 403, 197-9.
- [270] Benzinger, A., Muster, N., Koch, H.B., Yates, J.R., 3rd and Hermeking, H. (2005). Targeted proteomic analysis of 14-3-3 sigma, a p53 effector commonly silenced in cancer. *Mol Cell Proteomics* 4, 785-95.
- [271] Ewing, R.M. et al. (2007). Large-scale mapping of human protein-protein interactions by mass spectrometry. *Mol Syst Biol* 3, 89.
- [272] Fang, Y., Johnson, L.M., Mahon, E.S. and Anderson, D.H. (2002). Two phosphorylation-independent sites on the p85 SH2 domains bind A-Raf kinase. *Biochem Biophys Res Commun* 290, 1267-74.
- [273] Bradford, M.M. (1976). A rapid and sensitive method for the quantitation of microgram quantities of protein utilizing the principle of protein-dye binding. *Anal Biochem* 72, 248-54.
- [274] Cech, N.B. and Enke, C.G. (2001). Practical implications of some recent studies in electrospray ionization fundamentals. *Mass Spectrom Rev* 20, 362-87.
- [275] Neuhoff, V., Arold, N., Taube, D. and Ehrhardt, W. (1988). Improved staining of proteins in polyacrylamide gels including isoelectric focusing gels with clear background at nanogram sensitivity using Coomassie Brilliant Blue G-250 and R-250. *Electrophoresis* 9, 255-62.
- [276] Wilm, M., Shevchenko, A., Houthaeve, T., Breit, S., Schweigerer, L., Fotsis, T. and Mann, M. (1996). Femtomole sequencing of proteins from polyacrylamide gels by nano-electrospray mass spectrometry. *Nature* 379, 466-9.

- [277] Reinders, J. et al. (2007). Profiling phosphoproteins of yeast mitochondria reveals a role of phosphorylation in assembly of the ATP synthase. *Mol Cell Proteomics* 6, 1896-906.
- [278] Zahedi, R.P. et al. (2008). Phosphoproteome of resting human platelets. *J Proteome Res* 7, 526-34.
- [279] Gruenwald, S., Heitz, J. . (1993) Baculovirus expression vector system: Procedures and methods manual. Pharmingen
- [280] King., L.A., Possee, R.D. (1992). The baculovirus expression system: A laboratory guid. Chapman and Hall.
- [281] O'Reilley, D.R., Miller, L. K., Luckow, V. A. (1994). Baculovirus expression vectors. Oxford University Press, Oxford.
- [282] Rost, B. and Liu, J. (2003). The PredictProtein server. *Nucleic Acids Res* 31, 3300-4.
- [283] Cuff, J.A., Clamp, M.E., Siddiqui, A.S., Finlay, M. and Barton, G.J. (1998). JPred: a consensus secondary structure prediction server. *Bioinformatics* 14, 892-3.
- [284] Baker, N.A., Sept, D., Joseph, S., Holst, M.J. and McCammon, J.A. (2001). Electrostatics of nanosystems: application to microtubules and the ribosome. *Proc Natl Acad Sci U S A* 98, 10037-41.
- [285] Homeyer, N., Horn, A.H., Lanig, H. and Sticht, H. (2006). AMBER force-field parameters for phosphorylated amino acids in different protonation states: phosphoserine, phosphothreonine, phosphotyrosine, and phosphohistidine. *J Mol Model* 12, 281-9.
- [286] Suen, K.L., Bustelo, X.R. and Barbacid, M. (1995). Lack of evidence for the activation of the Ras/Raf mitogenic pathway by 14-3-3 proteins in mammalian cells. *Oncogene* 11, 825-31.
- [287] Hekman, M., Hamm, H., Villar, A.V., Bader, B., Kuhlmann, J., Nickel, J. and Rapp, U.R. (2002). Associations of B- and C-Raf with cholesterol, phosphatidylserine, and lipid second messengers: preferential binding of Raf to artificial lipid rafts. *J Biol Chem* 277, 24090-102.
- [288] Kubicek, M., Pacher, M., Abraham, D., Podar, K., Eulitz, M. and Baccarini, M. (2002). Dephosphorylation of Ser-259 regulates Raf-1 membrane association. *J Biol Chem* 277, 7913-9.
- [289] Tzivion, G. and Avruch, J. (2002). 14-3-3 proteins: active cofactors in cellular regulation by serine/threonine phosphorylation. *J Biol Chem* 277, 3061-4.
- [290] Payne, D.M. et al. (1991). Identification of the regulatory phosphorylation sites in pp42/mitogen-activated protein kinase (MAP kinase). *Embo J* 10, 885-92.
- [291] Blom, N., Gammeltoft, S. and Brunak, S. (1999). Sequence and structure-based prediction of eukaryotic protein phosphorylation sites. *J Mol Biol* 294, 1351-62.
- [292] Zang, M., Waelde, C.A., Xiang, X., Rana, A., Wen, R. and Luo, Z. (2001). Microtubule integrity regulates Pak leading to Ras-independent activation of Raf-1. insights into mechanisms of Raf-1 activation. *J Biol Chem* 276, 25157-65.
- [293] Wixler, V., Smola, U., Schuler, M. and Rapp, U. (1996). Differential regulation of Raf isozymes by growth versus differentiation inducing factors in PC12 pheochromocytoma cells. *FEBS Lett* 385, 131-7.
- [294] Stokoe, D., Macdonald, S.G., Cadwallader, K., Symons, M. and Hancock, J.F. (1994). Activation of Raf as a result of recruitment to the plasma membrane. *Science* 264, 1463-7.
- [295] Noble, C. et al. (2008). CRAF autophosphorylation of serine 621 is required to prevent its proteasome-mediated degradation. *Mol Cell* 31, 862-72.
- [296] Wartmann, M. and Davis, R.J. (1994). The native structure of the activated Raf protein kinase is a membrane-bound multi-subunit complex. *J Biol Chem* 269, 6695-701.

- [297] Wartmann, M., Hofer, P., Turowski, P., Saltiel, A.R. and Hynes, N.E. (1997). Negative modulation of membrane localization of the Raf-1 protein kinase by hyperphosphorylation. *J Biol Chem* 272, 3915-23.
- [298] Chen, C. and Sytkowski, A.J. (2004). Erythropoietin regulation of Raf-1 and MEK: evidence for a Ras-independent mechanism. *Blood* 104, 73-80.
- [299] Brummer, T., Naegele, H., Reth, M. and Misawa, Y. (2003). Identification of novel ERK-mediated feedback phosphorylation sites at the C-terminus of B-Raf. *Oncogene* 22, 8823-34.
- [300] Kubicek, M., Pacher, M., Abraham, D., Podar, K., Eulitz, M. and Baccarini, M. (2002). Dephosphorylation of Ser-259 regulates Raf-1 membrane association. *J Biol Chem* 277, 7913-9.
- [301] Pandit, B. et al. (2007). Gain-of-function RAF1 mutations cause Noonan and LEOPARD syndromes with hypertrophic cardiomyopathy. *Nat Genet* 39, 1007-12.
- [302] Razzaque, M.A. et al. (2007). Germline gain-of-function mutations in RAF1 cause Noonan syndrome. *Nat Genet* 39, 1013-7.
- [303] Barnard, D., Diaz, B., Clawson, D. and Marshall, M. (1998). Oncogenes, growth factors and phorbol esters regulate Raf-1 through common mechanisms. *Oncogene* 17, 1539-47.
- [304] Garnett, M.J. and Marais, R. (2004). Guilty as charged: B-RAF is a human oncogene. *Cancer Cell* 6, 313-9.
- [305] Houben, R., Becker, J.C., Kappel, A., Terheyden, P., Brocker, E.B., Goetz, R. and Rapp, U.R. (2004). Constitutive activation of the Ras-Raf signaling pathway in metastatic melanoma is associated with poor prognosis. *J Carcinog* 3, 6.
- [306] Davies, H. et al. (2002). Mutations of the BRAF gene in human cancer. *Nature* 417, 949-54.
- [307] Emuss, V., Garnett, M., Mason, C. and Marais, R. (2005). Mutations of C-RAF are rare in human cancer because C-RAF has a low basal kinase activity compared with B-RAF. *Cancer Res* 65, 9719-26.
- [308] King, A.J., Wireman, R.S., Hamilton, M. and Marshall, M.S. (2001). Phosphorylation site specificity of the Pak-mediated regulation of Raf-1 and cooperativity with Src. *FEBS Lett* 497, 6-14.
- [309] Chiloeches, A., Mason, C.S. and Marais, R. (2001). S338 phosphorylation of Raf-1 is independent of phosphatidylinositol 3-kinase and Pak3. *Mol Cell Biol* 21, 2423-34.
- [310] Ritt, D.A., Zhou, M., Conrads, T.P., Veenstra, T.D., Copeland, T.D. and Morrison, D.K. (2007). CK2 Is a component of the KSR1 scaffold complex that contributes to Raf kinase activation. *Curr Biol* 17, 179-84.
- [311] Meggio, F. and Pinna, L.A. (2003). One-thousand-and-one substrates of protein kinase CK2? *FASEB J* 17, 349-68.
- [312] Blom, N., Sicheritz-Ponten, T., Gupta, R., Gammeltoft, S. and Brunak, S. (2004). Prediction of post-translational glycosylation and phosphorylation of proteins from the amino acid sequence. *Proteomics* 4, 1633-49.
- [313] Pinna, L.A. and Ruzzene, M. (1996). How do protein kinases recognize their substrates? *Biochim Biophys Acta* 1314, 191-225.
- [314] Zhou, J., Shin, H.G., Yi, J., Shen, W., Williams, C.P. and Murray, K.T. (2002). Phosphorylation and putative ER retention signals are required for protein kinase A-mediated potentiation of cardiac sodium current. *Circ Res* 91, 540-6.
- [315] Alessi, D.R., Caudwell, F.B., Andjelkovic, M., Hemmings, B.A. and Cohen, P. (1996). Molecular basis for the substrate specificity of protein kinase B; comparison with MAPKAP kinase-1 and p70 S6 kinase. *FEBS Lett* 399, 333-8.
- [316] Leighton, I.A., Dalby, K.N., Caudwell, F.B., Cohen, P.T. and Cohen, P. (1995). Comparison of the specificities of p70 S6 kinase and MAPKAP kinase-1 identifies a

- relatively specific substrate for p70 S6 kinase: the N-terminal kinase domain of MAPKAP kinase-1 is essential for peptide phosphorylation. *FEBS Lett* 375, 289-93.
- [317] Ghosh, S., Moore, S., Bell, R.M. and Dush, M. (2003). Functional analysis of a phosphatidic acid binding domain in human Raf-1 kinase: mutations in the phosphatidate binding domain lead to tail and trunk abnormalities in developing zebrafish embryos. *J Biol Chem* 278, 45690-6.
- [318] Alessi, D.R., Cuenda, A., Cohen, P., Dudley, D.T. and Saltiel, A.R. (1995). PD 098059 is a specific inhibitor of the activation of mitogen-activated protein kinase kinase in vitro and in vivo. *J Biol Chem* 270, 27489-94.
- [319] Matheny, S.A., Chen, C., Kortum, R.L., Razidlo, G.L., Lewis, R.E. and White, M.A. (2004). Ras regulates assembly of mitogenic signalling complexes through the effector protein IMP. *Nature* 427, 256-60.
- [320] von Kriegsheim, A., Pitt, A., Grindlay, G.J., Kolch, W. and Dhillon, A.S. (2006). Regulation of the Raf-MEK-ERK pathway by protein phosphatase 5. *Nat Cell Biol* 8, 1011-6.
- [321] Xia, F. et al. (2008). Raf activation is regulated by tyrosine 510 phosphorylation in *Drosophila*. *PLoS Biol* 6, e128.
- [322] Ghosh, S., Xie, W.Q., Quest, A.F., Mabrouk, G.M., Strum, J.C. and Bell, R.M. (1994). The cysteine-rich region of raf-1 kinase contains zinc, translocates to liposomes, and is adjacent to a segment that binds GTP-ras. *J Biol Chem* 269, 10000-7.
- [323] Rizzo, M.A., Kraft, C.A., Watkins, S.C., Levitan, E.S. and Romero, G. (2001). Agonist-dependent traffic of raft-associated Ras and Raf-1 is required for activation of the mitogen-activated protein kinase cascade. *J Biol Chem* 276, 34928-33.
- [324] Mazurek, S., Drexler, H.C., Troppmair, J., Eigenbrodt, E. and Rapp, U.R. (2007). Regulation of pyruvate kinase type M2 by A-Raf: a possible glycolytic stop or go mechanism. *Anticancer Res* 27, 3963-71.

Nekhoroshkova, E., Albert, S., Becker, M. and Rapp, U.R. A-RAF kinase functions in ARF6 regulated endocytotic membrane traffic. (2008) *PLOS One*, in revision.

## 9. APPENDIX

### 9.1. Mascot<sup>TM</sup> results pages of the phosphopeptide spectra from Table 3

#### **Mascot Search Results**

1/13

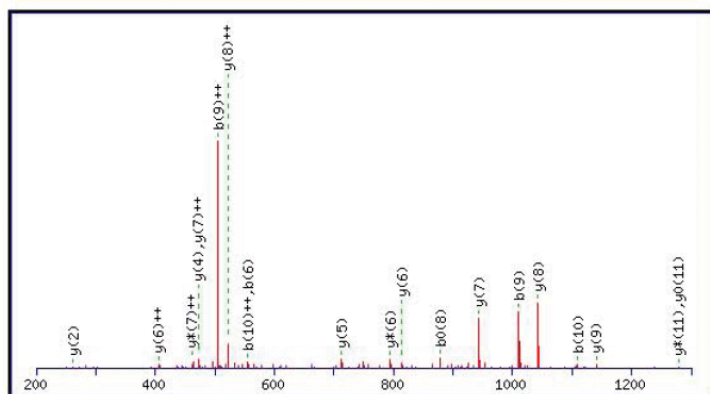
##### Peptide View

MS/MS Fragmentation of **AVGTVKVVYLPNK**Found in **gi|000**, AG Rapp

Match to Query 1151: 1367.976724 from(684.995638,2+)

Title: LTQ11188.3096.3096.2.dta

Click mouse within plot area to zoom in by factor of two about that point

Or, Plot from  to  Da Monoisotopic mass of neutral peptide  $M_r(\text{calc})$ : 1367.72

Fixed modifications: Carbamidomethyl (C)

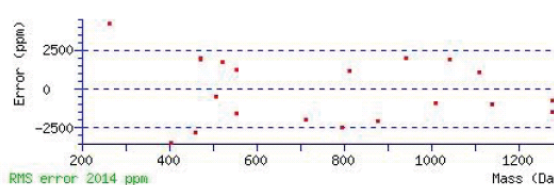
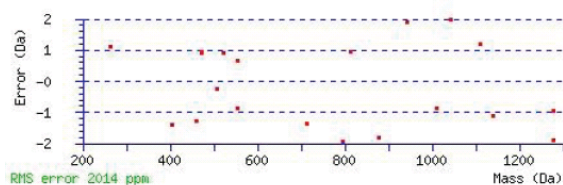
Variable modifications:

Y8 : Phospho (Y)

Ions Score: 29 Expect: 0.046

Matches (**Bold Red**): 20/100 fragment ions using 33 most intense peaks

| #  | b              | b <sup>++</sup> | b <sup>+</sup> | b <sup>+++</sup> | b <sup>0</sup> | b <sup>0++</sup> | Seq. | y              | y <sup>++</sup> | y <sup>+</sup> | y <sup>+++</sup> | y <sup>0</sup> | y <sup>0++</sup> | #  |
|----|----------------|-----------------|----------------|------------------|----------------|------------------|------|----------------|-----------------|----------------|------------------|----------------|------------------|----|
| 1  | 72.04          | 36.53           |                |                  |                |                  | A    |                |                 |                |                  |                |                  | 12 |
| 2  | 171.11         | 86.06           |                |                  |                |                  | V    | 1297.69        | 649.35          | <b>1280.67</b> | 640.84           | <b>1279.68</b> | 640.34           | 11 |
| 3  | 228.13         | 114.57          |                |                  |                |                  | G    | 1198.62        | 599.82          | 1181.60        | 591.30           | 1180.61        | 590.81           | 10 |
| 4  | 329.18         | 165.09          |                |                  | 311.17         | 156.09           | T    | <b>1141.60</b> | 571.30          | 1124.58        | 562.79           | 1123.59        | 562.30           | 9  |
| 5  | 428.25         | 214.63          |                |                  | 410.24         | 205.62           | V    | <b>1040.55</b> | <b>520.78</b>   | 1023.53        | 512.27           |                |                  | 8  |
| 6  | <b>556.35</b>  | 278.68          | 539.32         | 270.16           | 538.33         | 269.67           | K    | <b>941.49</b>  | <b>471.25</b>   | 924.46         | <b>462.73</b>    |                |                  | 7  |
| 7  | 655.41         | 328.21          | 638.39         | 319.70           | 637.40         | 319.21           | V    | <b>813.39</b>  | <b>407.20</b>   | <b>796.36</b>  | 398.69           |                |                  | 6  |
| 8  | 898.44         | 449.73          | 881.42         | 441.21           | <b>880.43</b>  | 440.72           | Y    | <b>714.32</b>  | 357.66          | 697.30         | 349.15           |                |                  | 5  |
| 9  | <b>1011.53</b> | <b>506.27</b>   | 994.50         | 497.75           | 993.52         | 497.26           | L    | <b>471.29</b>  | 236.15          | 454.27         | 227.64           |                |                  | 4  |
| 10 | <b>1108.58</b> | <b>554.79</b>   | 1091.55        | 546.28           | 1090.57        | 545.79           | P    | 358.21         | 179.61          | 341.18         | 171.09           |                |                  | 3  |
| 11 | 1222.62        | 611.82          | 1205.60        | 603.30           | 1204.61        | 602.81           | N    | <b>261.16</b>  | 131.08          | 244.13         | 122.57           |                |                  | 2  |
| 12 |                |                 |                |                  |                |                  | K    | 147.11         | 74.06           | 130.09         | 65.55            |                |                  | 1  |



**Mascot Search Results**  
2/13

**Peptide View**

MS/MS Fragmentation of **QQFYHSVQDLSGGSR**

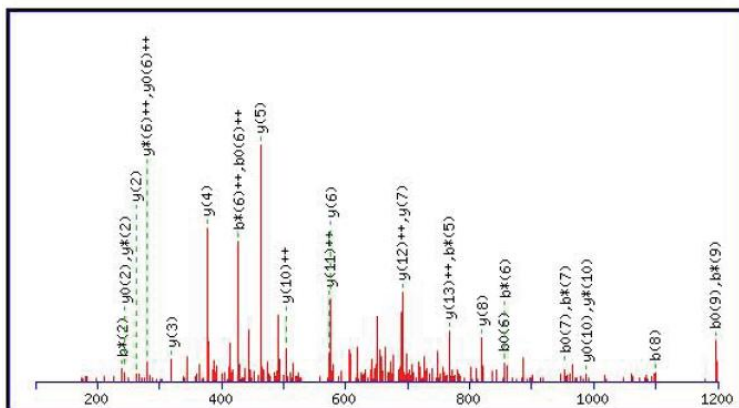
Found in **gi000**, AG Rapp

Match to Query 1830: 1788.615723 from(597.212517,3+)

Title: LTQ11184.1447.1447.3.dta

Click mouse within plot area to zoom in by factor of two about that point

Or,  100 to  Da



**Monoisotopic mass of neutral peptide Mr(calc):** 1787.76

**Fixed modifications:** Carbamidomethyl (C)

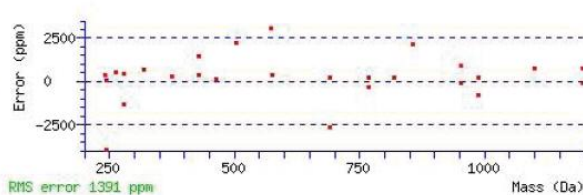
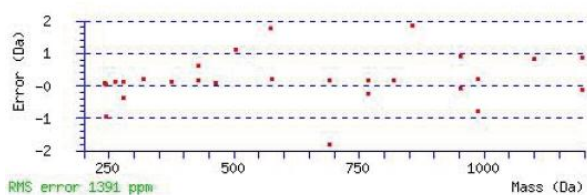
**Variable modifications:**

**Y4** : Phospho (Y)

**Ions Score:** 31 **Expect:** 0.065

**Matches (Bold Red):** 28/156 fragment ions using 33 most intense peaks

| #  | b              | b <sup>++</sup> | b <sup>*</sup> | b <sup>*++</sup> | b <sup>0</sup> | b <sup>0++</sup> | Seq. | y             | y <sup>++</sup> | y <sup>*</sup> | y <sup>*++</sup> | y <sup>0</sup> | y <sup>0++</sup> | #  |
|----|----------------|-----------------|----------------|------------------|----------------|------------------|------|---------------|-----------------|----------------|------------------|----------------|------------------|----|
| 1  | 129.07         | 65.04           | 112.04         | 56.52            |                |                  | Q    |               |                 |                |                  |                |                  | 15 |
| 2  | 257.12         | 129.07          | <b>240.10</b>  | 120.55           |                |                  | Q    | 1660.71       | 830.86          | 1643.68        | 822.35           | 1642.70        | 821.85           | 14 |
| 3  | 404.19         | 202.60          | 387.17         | 194.09           |                |                  | F    | 1532.65       | <b>766.83</b>   | 1515.63        | 758.32           | 1514.64        | 757.82           | 13 |
| 4  | 647.22         | 324.11          | 630.20         | 315.60           |                |                  | Y    | 1385.58       | <b>693.30</b>   | 1368.56        | 684.78           | 1367.57        | 684.29           | 12 |
| 5  | 784.28         | 392.64          | <b>767.25</b>  | 384.13           |                |                  | H    | 1142.55       | <b>571.78</b>   | 1125.53        | 563.27           | 1124.54        | 562.78           | 11 |
| 6  | 871.31         | 436.16          | <b>854.29</b>  | <b>427.65</b>    | <b>853.30</b>  | <b>427.16</b>    | S    | 1005.50       | <b>503.25</b>   | <b>988.47</b>  | 494.74           | <b>987.49</b>  | 494.25           | 10 |
| 7  | 970.38         | 485.69          | <b>953.36</b>  | 477.18           | <b>952.37</b>  | 476.69           | V    | 918.46        | 459.74          | 901.44         | 451.22           | 900.45         | 450.73           | 9  |
| 8  | <b>1098.44</b> | 549.72          | 1081.41        | 541.21           | 1080.43        | 540.72           | Q    | <b>819.40</b> | 410.20          | 802.37         | 401.69           | 801.38         | 401.20           | 8  |
| 9  | 1213.47        | 607.24          | <b>1196.44</b> | 598.72           | <b>1195.46</b> | 598.23           | D    | <b>691.34</b> | 346.17          | 674.31         | 337.66           | 673.33         | 337.17           | 7  |
| 10 | 1326.55        | 663.78          | 1309.52        | 655.27           | 1308.54        | 654.77           | L    | <b>576.31</b> | 288.66          | 559.28         | <b>280.15</b>    | 558.30         | <b>279.65</b>    | 6  |
| 11 | 1413.58        | 707.30          | 1396.56        | 698.78           | 1395.57        | 698.29           | S    | <b>463.23</b> | 232.12          | 446.20         | 223.60           | 445.22         | 223.11           | 5  |
| 12 | 1470.60        | 735.81          | 1453.58        | 727.29           | 1452.59        | 726.80           | G    | <b>376.19</b> | 188.60          | 359.17         | 180.09           | 358.18         | 179.60           | 4  |
| 13 | 1527.63        | 764.32          | 1510.60        | 755.80           | 1509.62        | 755.31           | G    | <b>319.17</b> | 160.09          | 302.15         | 151.58           | 301.16         | 151.08           | 3  |
| 14 | 1614.66        | 807.83          | 1597.63        | 799.32           | 1596.65        | 798.83           | S    | <b>262.15</b> | 131.58          | <b>245.12</b>  | 123.07           | <b>244.14</b>  | 122.57           | 2  |
| 15 |                |                 |                |                  |                |                  | R    | 175.12        | 88.06           | 158.09         | 79.55            |                |                  | 1  |



NCBI BLAST search of **QQFYHSVQDLSGGSR**

(Parameters: blastp, nr protein database, expect=20000, no filter, PAM30)

Other BLAST [web gateways](#)



# MASCOT SEARCH RESULTS

3/13

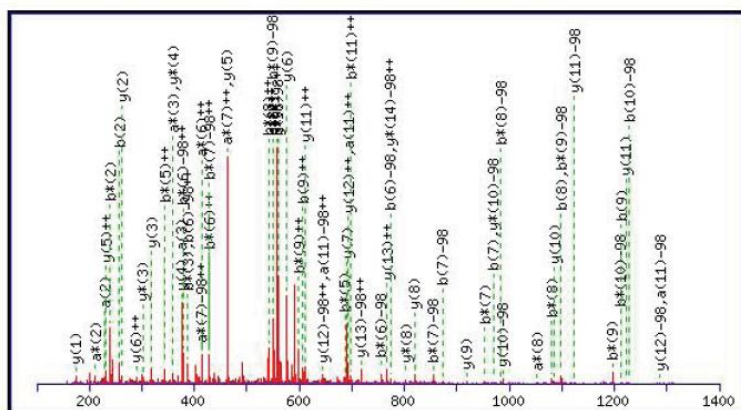
## Peptide View

MS/MS Fragmentation of **QQFYHVSVDLSGGSR**Found in **gi|000**, AG Rapp

Match to Query 490: 1787.761410 from(596.927746,3+)

Title: File: QstarE04014.wiff, Sample: GST-A-Raf 080617 Bande 2.2 (sample number 1), Elution: 45.498 to 45.507 min, Period: 1, Cycle(s): 1796

Click mouse within plot area to zoom in by factor of two about that point

Or, Plot from  to  Da Monoisotopic mass of neutral peptide **Mr(calc)**: 1787.76

Fixed modifications: Carbamidomethyl (C)

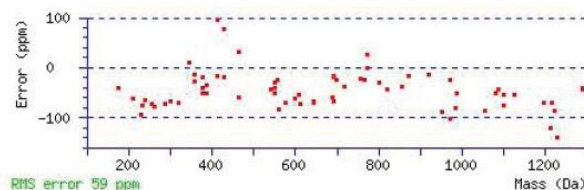
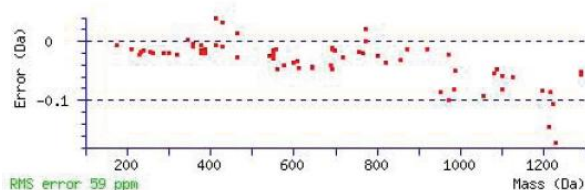
Variable modifications:

S6 : Phospho (ST), with neutral losses 97.98 (shown in table), 0.00

Ions Score: 49 Expect: 0.00052

Matches (Bold Red): 69/260 fragment ions using 123 most intense peaks

| #  | a              | a <sup>++</sup> | a <sup>*</sup> | a <sup>++</sup> | b              | b <sup>++</sup> | b <sup>*</sup> | b <sup>++</sup> | Seq. | y              | y <sup>++</sup> | y <sup>*</sup> | y <sup>++</sup> | #  |
|----|----------------|-----------------|----------------|-----------------|----------------|-----------------|----------------|-----------------|------|----------------|-----------------|----------------|-----------------|----|
| 1  | 101.07         | 51.04           | 84.04          | 42.53           | 129.07         | 65.04           | 112.04         | 56.52           | Q    |                |                 |                |                 | 15 |
| 2  | <b>229.13</b>  | 115.07          | <b>212.10</b>  | 106.56          | <b>257.12</b>  | 129.07          | <b>240.10</b>  | 120.55          | Q    | 1562.73        | 781.87          | 1545.71        | <b>773.36</b>   | 14 |
| 3  | <b>376.20</b>  | 188.60          | <b>359.17</b>  | 180.09          | 404.19         | 202.60          | <b>387.17</b>  | 194.09          | F    | 1434.68        | <b>717.84</b>   | 1417.65        | 709.33          | 13 |
| 4  | 539.26         | 270.13          | 522.23         | 261.62          | 567.26         | 284.13          | <b>550.23</b>  | 275.62          | Y    | <b>1287.61</b> | <b>644.31</b>   | 1270.58        | 635.79          | 12 |
| 5  | 676.32         | 338.66          | 659.29         | 330.15          | 704.32         | 352.66          | <b>687.29</b>  | <b>344.15</b>   | H    | <b>1124.54</b> | 562.78          | 1107.52        | 554.26          | 11 |
| 6  | 745.34         | 373.17          | 728.32         | 364.66          | <b>773.34</b>  | <b>387.17</b>   | <b>756.31</b>  | <b>378.66</b>   | S    | <b>987.49</b>  | 494.25          | <b>970.46</b>  | 485.73          | 10 |
| 7  | 844.41         | 422.71          | 827.38         | <b>414.20</b>   | <b>872.40</b>  | 436.71          | <b>855.38</b>  | <b>428.19</b>   | V    | <b>918.46</b>  | 459.74          | 901.44         | 451.22          | 9  |
| 8  | 972.47         | 486.74          | 955.44         | 478.22          | 1000.46        | 500.74          | <b>983.44</b>  | 492.22          | Q    | <b>819.40</b>  | 410.20          | <b>802.37</b>  | 401.69          | 8  |
| 9  | 1087.50        | 544.25          | 1070.47        | 535.74          | 1115.49        | <b>558.25</b>   | <b>1098.46</b> | <b>549.74</b>   | D    | <b>691.34</b>  | 346.17          | 674.31         | 337.66          | 7  |
| 10 | 1200.58        | 600.79          | 1183.55        | 592.28          | <b>1228.57</b> | 614.79          | <b>1211.55</b> | 606.28          | L    | <b>576.31</b>  | <b>288.66</b>   | <b>559.28</b>  | 280.15          | 6  |
| 11 | <b>1287.61</b> | <b>644.31</b>   | 1270.59        | 635.80          | 1315.61        | 658.31          | 1298.58        | 649.79          | S    | <b>463.23</b>  | <b>232.12</b>   | 446.20         | 223.60          | 5  |
| 12 | 1344.63        | 672.82          | 1327.61        | 664.31          | 1372.63        | 686.82          | 1355.60        | 678.30          | G    | <b>376.19</b>  | 188.60          | <b>359.17</b>  | 180.09          | 4  |
| 13 | 1401.65        | 701.33          | 1384.63        | 692.82          | 1429.65        | 715.33          | 1412.62        | 706.82          | G    | <b>319.17</b>  | 160.09          | <b>302.15</b>  | 151.58          | 3  |
| 14 | 1488.69        | 744.85          | 1471.66        | 736.33          | 1516.68        | 758.84          | 1499.65        | 750.33          | S    | <b>262.15</b>  | 131.58          | 245.12         | 123.07          | 2  |
| 15 |                |                 |                |                 |                |                 |                |                 | R    | <b>175.12</b>  | 88.06           | 158.09         | 79.55           | 1  |



**MASCOT SEARCH RESULTS**

4/13

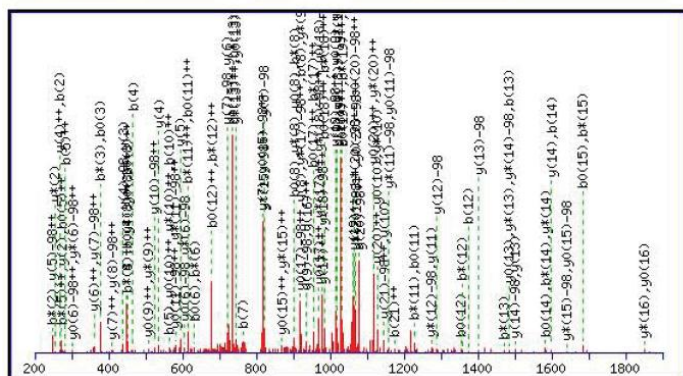
**Peptide View**

MS/MS Fragmentation of **QHEAPSNRFLNELLTPQGSPR**  
 Found in **gi000**, AG Rapp

Match to Query 3273: 2518.418724 from(840.480184,3+)  
 Title: LTQ11188.1682.1682.3.dta

Click mouse within plot area to zoom in by factor of two about that point

Or, Plot from  to  Da



Monoisotopic mass of neutral peptide Mr(calc): 2517.21

Fixed modifications: Carbamidomethyl (C)

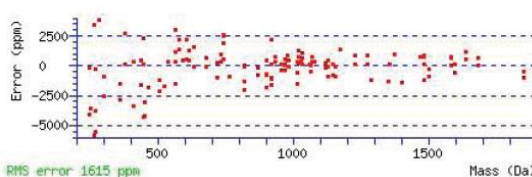
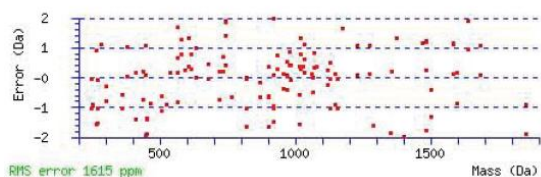
Variable modifications:

S20 : Phospho (ST), with neutral losses 0.00(shown in table), 97.98

Ions Score: 56 Expect: 0.00014

Matches (Bold Red): 134/370 fragment ions using 125 most intense peaks

| #  | b              | b <sup>++</sup> | b <sup>+</sup> | b <sup>+++</sup> | b <sup>0</sup> | b <sup>0++</sup> | Seq. | y              | y <sup>++</sup> | y <sup>+</sup> | y <sup>+++</sup> | y <sup>0</sup> | y <sup>0++</sup> | #  |
|----|----------------|-----------------|----------------|------------------|----------------|------------------|------|----------------|-----------------|----------------|------------------|----------------|------------------|----|
| 1  | 129.07         | 65.04           | 112.04         | 56.52            |                |                  | Q    |                |                 |                |                  |                |                  | 22 |
| 2  | <b>266.12</b>  | 133.57          | <b>249.10</b>  | 125.05           |                |                  | H    | 2390.16        | 1195.58         | 2373.13        | 1187.07          | 2372.15        | 1186.58          | 21 |
| 3  | 395.17         | 198.09          | <b>378.14</b>  | 189.57           | <b>377.16</b>  | 189.08           | E    | 2253.10        | <b>1127.05</b>  | 2236.08        | <b>1118.54</b>   | 2235.09        | <b>1118.05</b>   | 20 |
| 4  | <b>466.20</b>  | 233.61          | <b>449.18</b>  | 225.09           | <b>448.19</b>  | 224.60           | A    | 2124.06        | <b>1062.53</b>  | 2107.03        | 1054.02          | 2106.05        | 1053.53          | 19 |
| 5  | <b>563.26</b>  | <b>282.13</b>   | 546.23         | <b>273.62</b>    | 545.25         | <b>273.13</b>    | P    | 2053.02        | <b>1027.01</b>  | 2036.00        | <b>1018.50</b>   | 2035.01        | <b>1018.01</b>   | 18 |
| 6  | 650.29         | 325.65          | <b>633.26</b>  | 317.13           | <b>632.28</b>  | 316.64           | S    | 1955.97        | <b>978.49</b>   | 1938.94        | <b>969.98</b>    | 1937.96        | <b>969.48</b>    | 17 |
| 7  | <b>764.33</b>  | 382.67          | 747.31         | 374.16           | 746.32         | 373.66           | N    | 1868.94        | <b>934.97</b>   | <b>1851.91</b> | 926.46           | <b>1850.93</b> | 925.97           | 16 |
| 8  | <b>920.43</b>  | 460.72          | <b>903.41</b>  | <b>452.21</b>    | <b>902.42</b>  | <b>451.72</b>    | R    | 1754.89        | 877.95          | 1737.87        | <b>869.44</b>    | 1736.88        | <b>868.95</b>    | 15 |
| 9  | <b>1017.49</b> | 509.25          | 1000.46        | 500.73           | 999.48         | 500.24           | P    | <b>1598.79</b> | 799.90          | <b>1581.77</b> | 791.39           | 1580.78        | 790.90           | 14 |
| 10 | 1130.57        | <b>565.79</b>   | 1113.54        | 557.28           | 1112.56        | 556.78           | L    | <b>1501.74</b> | 751.37          | <b>1484.71</b> | <b>742.86</b>    | <b>1483.73</b> | <b>742.37</b>    | 13 |
| 11 | 1244.61        | 622.81          | <b>1227.59</b> | <b>614.30</b>    | <b>1226.60</b> | <b>613.80</b>    | N    | 1388.66        | 694.83          | 1371.63        | 686.32           | 1370.65        | 685.83           | 12 |
| 12 | <b>1373.66</b> | 687.33          | <b>1356.63</b> | <b>678.82</b>    | <b>1355.65</b> | <b>678.33</b>    | E    | <b>1274.61</b> | 637.81          | 1257.59        | 629.30           | 1256.60        | 628.81           | 11 |
| 13 | <b>1486.74</b> | <b>743.87</b>   | <b>1469.71</b> | <b>735.36</b>    | 1468.73        | <b>734.87</b>    | L    | <b>1145.57</b> | 573.29          | <b>1128.54</b> | <b>564.78</b>    | <b>1127.56</b> | <b>564.28</b>    | 10 |
| 14 | <b>1599.82</b> | 800.42          | <b>1582.80</b> | 791.90           | <b>1581.81</b> | 791.41           | L    | <b>1032.49</b> | 516.75          | <b>1015.46</b> | <b>508.23</b>    | <b>1014.48</b> | <b>507.74</b>    | 9  |
| 15 | 1700.87        | 850.94          | <b>1683.84</b> | 842.43           | <b>1682.86</b> | 841.93           | T    | <b>919.40</b>  | 460.21          | <b>902.38</b>  | <b>451.69</b>    | <b>901.39</b>  | <b>451.20</b>    | 8  |
| 16 | 1797.92        | 899.47          | 1780.90        | 890.95           | 1779.91        | 890.46           | P    | <b>818.36</b>  | <b>409.68</b>   | 801.33         | 401.17           | 800.35         | 400.68           | 7  |
| 17 | 1925.98        | 963.50          | 1908.96        | <b>954.98</b>    | 1907.97        | <b>954.49</b>    | Q    | <b>721.30</b>  | <b>361.16</b>   | 704.28         | 352.64           | 703.29         | 352.15           | 6  |
| 18 | 1983.00        | 992.01          | 1965.98        | <b>983.49</b>    | 1964.99        | <b>983.00</b>    | G    | <b>593.24</b>  | 297.13          | 576.22         | 288.61           | 575.23         | 288.12           | 5  |
| 19 | 2080.06        | 1040.53         | 2063.03        | <b>1032.02</b>   | 2062.05        | <b>1031.53</b>   | P    | <b>536.22</b>  | <b>268.62</b>   | 519.20         | 260.10           | 518.21         | 259.61           | 4  |
| 20 | 2247.06        | 1124.03         | 2230.03        | 1115.52          | 2229.04        | 1115.03          | S    | <b>439.17</b>  | 220.09          | 422.14         | 211.58           | 421.16         | 211.08           | 3  |
| 21 | 2344.11        | <b>1172.56</b>  | 2327.08        | 1164.04          | 2326.10        | 1163.55          | P    | <b>272.17</b>  | 136.59          | <b>255.15</b>  | 128.08           |                |                  | 2  |
| 22 |                |                 |                |                  |                |                  | R    | 175.12         | 88.06           | 158.09         | 79.55            |                |                  | 1  |



**{MATRIX}**  
**{SCIENCE}** Mascot Search Results  
5/13

**Peptide View**

MS/MS Fragmentation of **GSPSPASVSSGR**

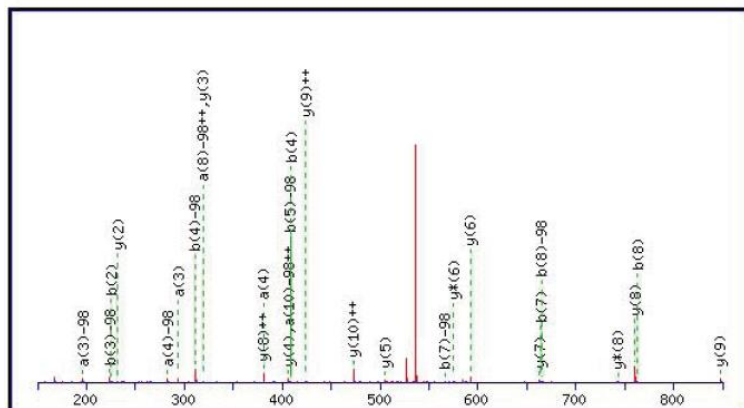
Found in **gi000**, AG Rapp

Match to Query 361: 1167.489932 from(584.752242,2+)

Title: File: QstarE04010.wiff, Sample: GST-A-Raf 080617 Bande 1.2 (sample number 1), Elution: 25.785 to 26.209 min, Period: 1, Cycle(s): 2235

Click mouse within plot area to zoom in by factor of two about that point

Or, Plot from  to  Da



**Monoisotopic mass of neutral peptide Mr(calc):** 1167.49

**Fixed modifications:** Carbamidomethyl (C)

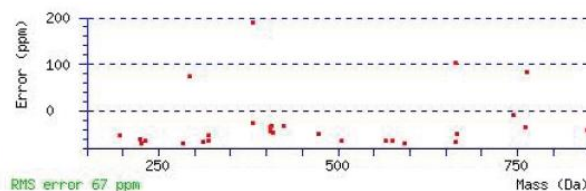
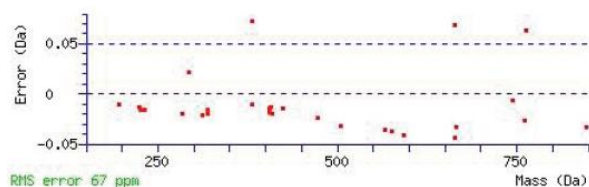
**Variable modifications:**

S2 : Phospho (ST), with neutral losses 97.98 (shown in table), 0.00

**Ions Score:** 39 **Expect:** 0.0044

**Matches (Bold Red):** 28/132 fragment ions using 66 most intense peaks

| #  | a             | a <sup>++</sup> | b             | b <sup>++</sup> | Seq. | y             | y <sup>++</sup> | y <sup>+</sup> | y <sup>++</sup> | #  |
|----|---------------|-----------------|---------------|-----------------|------|---------------|-----------------|----------------|-----------------|----|
| 1  | 30.03         | 15.52           | 58.03         | 29.52           | G    |               |                 |                |                 | 12 |
| 2  | 99.06         | 50.03           | 127.05        | 64.03           | S    | 1013.50       | 507.25          | 996.47         | 498.74          | 11 |
| 3  | <b>196.11</b> | 98.56           | <b>224.10</b> | 112.56          | P    | 944.48        | <b>472.74</b>   | 927.45         | 464.23          | 10 |
| 4  | <b>283.14</b> | 142.07          | <b>311.13</b> | 156.07          | S    | <b>847.43</b> | <b>424.22</b>   | 830.40         | 415.70          | 9  |
| 5  | 380.19        | 190.60          | <b>408.19</b> | 204.60          | P    | <b>760.39</b> | <b>380.70</b>   | <b>743.37</b>  | 372.19          | 8  |
| 6  | 451.23        | 226.12          | 479.22        | 240.12          | A    | <b>663.34</b> | 332.17          | 646.32         | 323.66          | 7  |
| 7  | 538.26        | 269.63          | <b>566.26</b> | 283.63          | S    | <b>592.30</b> | 296.66          | <b>575.28</b>  | 288.14          | 6  |
| 8  | 637.33        | <b>319.17</b>   | <b>665.33</b> | 333.17          | V    | <b>505.27</b> | 253.14          | 488.25         | 244.63          | 5  |
| 9  | 724.36        | 362.68          | 752.36        | 376.68          | S    | <b>406.20</b> | 203.61          | 389.18         | 195.09          | 4  |
| 10 | 811.39        | <b>406.20</b>   | 839.39        | 420.20          | S    | <b>319.17</b> | 160.09          | 302.15         | 151.58          | 3  |
| 11 | 868.42        | 434.71          | 896.41        | 448.71          | G    | <b>232.14</b> | 116.57          | 215.11         | 108.06          | 2  |
| 12 |               |                 |               |                 | R    | 175.12        | 88.06           | 158.09         | 79.55           | 1  |



**MASCOT** Mascot Search Results  
6/13

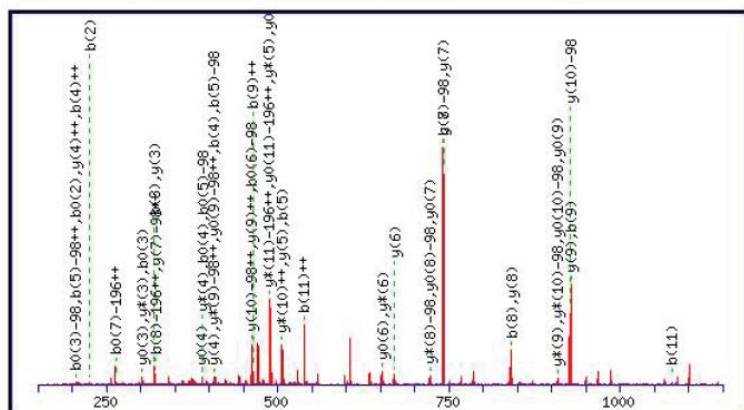
**Peptide View**

MS/MS Fragmentation of **GSPSPASVSSGR**  
Found in **gi000**, AG Rapp

Match to Query 902: 1247.644724 from(624.829638,2+)  
Title: LTQ11188.1455.1457.2.dta

Click mouse within plot area to zoom in by factor of two about that point

Or, Plot from  to  Da



**Monoisotopic mass of neutral peptide Mr(calc):** 1247.46

**Fixed modifications:** Carbamidomethyl (C)

**Variable modifications:**

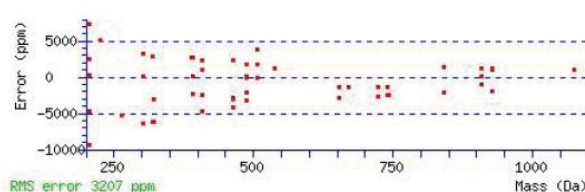
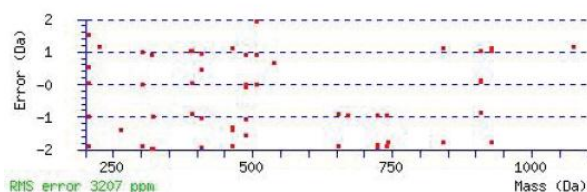
S2 : Phospho (ST), with neutral losses 0.00(shown in table), 97.98

S7 : Phospho (ST), with neutral losses 0.00(shown in table), 97.98

**Ions Score:** 39 **Expect:** 0.011

**Matches (Bold Red):** 55/180 fragment ions using 63 most intense peaks

| #  | b              | b <sup>++</sup> | b <sup>0</sup> | b <sup>0++</sup> | Seq. | y             | y <sup>++</sup> | y <sup>*</sup> | y <sup>++</sup> | y <sup>0</sup> | y <sup>0++</sup> | #  |
|----|----------------|-----------------|----------------|------------------|------|---------------|-----------------|----------------|-----------------|----------------|------------------|----|
| 1  | 58.03          | 29.52           |                |                  | G    |               |                 |                |                 |                |                  | 12 |
| 2  | <b>225.03</b>  | 113.02          | <b>207.02</b>  | 104.01           | S    | 1191.44       | 596.23          | 1174.42        | 587.71          | 1173.43        | 587.22           | 11 |
| 3  | <b>322.08</b>  | 161.54          | <b>304.07</b>  | 152.54           | P    | 1024.45       | 512.73          | 1007.42        | <b>504.21</b>   | 1006.44        | 503.72           | 10 |
| 4  | <b>409.11</b>  | <b>205.06</b>   | <b>391.10</b>  | 196.05           | S    | <b>927.39</b> | <b>464.20</b>   | <b>910.37</b>  | 455.69          | <b>909.38</b>  | 455.19           | 9  |
| 5  | <b>506.16</b>  | 253.59          | <b>488.15</b>  | 244.58           | P    | <b>840.36</b> | 420.68          | 823.33         | 412.17          | 822.35         | 411.68           | 8  |
| 6  | 577.20         | 289.10          | 559.19         | 280.10           | A    | <b>743.31</b> | 372.16          | 726.28         | 363.64          | <b>725.30</b>  | 363.15           | 7  |
| 7  | <b>744.20</b>  | 372.60          | 726.19         | 363.60           | S    | <b>672.27</b> | 336.64          | <b>655.24</b>  | 328.13          | <b>654.26</b>  | 327.63           | 6  |
| 8  | <b>843.27</b>  | 422.14          | 825.26         | 413.13           | V    | <b>505.27</b> | 253.14          | <b>488.25</b>  | 244.63          | <b>487.26</b>  | 244.13           | 5  |
| 9  | <b>930.30</b>  | <b>465.65</b>   | 912.29         | 456.65           | S    | <b>406.20</b> | <b>203.61</b>   | <b>389.18</b>  | 195.09          | <b>388.19</b>  | 194.60           | 4  |
| 10 | 1017.33        | 509.17          | 999.32         | 500.16           | S    | <b>319.17</b> | 160.09          | <b>302.15</b>  | 151.58          | <b>301.16</b>  | 151.08           | 3  |
| 11 | <b>1074.35</b> | <b>537.68</b>   | 1056.34        | 528.68           | G    | 232.14        | 116.57          | 215.11         | 108.06          |                |                  | 2  |
| 12 |                |                 |                |                  | R    | 175.12        | 88.06           | 158.09         | 79.55           |                |                  | 1  |



**MASCOT**  
**SCIENCE** Mascot Search Results  
7/13

**Peptide View**

MS/MS Fragmentation of **GSPSPASVSSGR**

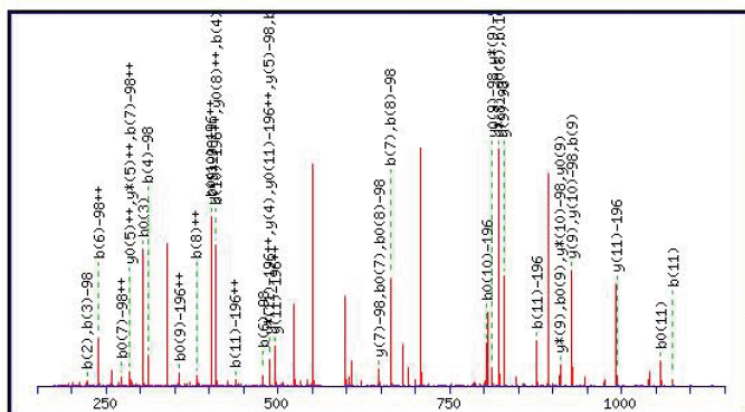
Found in **gi|000**, AG Rapp

Match to Query 731: 1248.680724 from(625.347638,2+)

Title: LTQ11184.1299.1299.2.dta

Click mouse within plot area to zoom in by factor of two about that point

Or,  150 to  Da



**Monoisotopic mass of neutral peptide Mr(calc):** 1247.46

**Fixed modifications:** Carbamidomethyl (C)

**Variable modifications:**

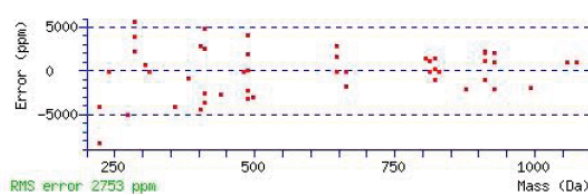
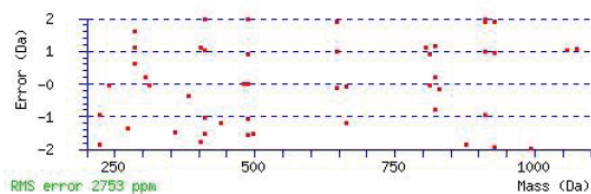
S2 : Phospho (ST), with neutral losses 97.98 (shown in table), 0.00

S9 : Phospho (ST), with neutral losses 97.98 (shown in table), 0.00

**Ions Score:** 32 **Expect:** 0.056

**Matches (Bold Red):** 48/192 fragment ions using 50 most intense peaks

| #  | b             | b <sup>++</sup> | b <sup>0</sup> | b <sup>0++</sup> | Seq. | y             | y <sup>++</sup> | y <sup>*</sup> | y <sup>++</sup> | y <sup>0</sup> | y <sup>0++</sup> | #  |
|----|---------------|-----------------|----------------|------------------|------|---------------|-----------------|----------------|-----------------|----------------|------------------|----|
| 1  | 58.03         | 29.52           |                |                  | G    |               |                 |                |                 |                |                  | 12 |
| 2  | 127.05        | 64.03           | 109.04         | 55.02            | S    | <b>995.49</b> | <b>498.25</b>   | 978.46         | <b>489.74</b>   | 977.48         | <b>489.24</b>    | 11 |
| 3  | <b>224.10</b> | 112.56          | 206.09         | 103.55           | P    | <b>926.47</b> | 463.74          | <b>909.44</b>  | 455.22          | 908.46         | 454.73           | 10 |
| 4  | <b>311.13</b> | 156.07          | 293.12         | 147.07           | S    | <b>829.42</b> | 415.21          | <b>812.39</b>  | 406.70          | <b>811.41</b>  | <b>406.21</b>    | 9  |
| 5  | <b>408.19</b> | 204.60          | 390.18         | 195.59           | P    | 742.38        | 371.70          | 725.36         | 363.18          | 724.37         | 362.69           | 8  |
| 6  | <b>479.22</b> | <b>240.12</b>   | 461.21         | 231.11           | A    | <b>645.33</b> | 323.17          | 628.30         | 314.66          | 627.32         | 314.16           | 7  |
| 7  | 566.26        | <b>283.63</b>   | 548.25         | <b>274.63</b>    | S    | 574.29        | 287.65          | 557.27         | 279.14          | 556.28         | 278.65           | 6  |
| 8  | <b>665.33</b> | 333.17          | <b>647.31</b>  | 324.16           | V    | <b>487.26</b> | 244.13          | 470.24         | 235.62          | 469.25         | 235.13           | 5  |
| 9  | 734.35        | 367.68          | 716.34         | <b>358.67</b>    | S    | 388.19        | 194.60          | 371.17         | 186.09          | 370.18         | 185.60           | 4  |
| 10 | <b>821.38</b> | <b>411.19</b>   | <b>803.37</b>  | <b>402.19</b>    | S    | 319.17        | 160.09          | 302.15         | 151.58          | 301.16         | 151.08           | 3  |
| 11 | <b>878.40</b> | <b>439.70</b>   | 860.39         | 430.70           | G    | 232.14        | 116.57          | 215.11         | 108.06          |                |                  | 2  |
| 12 |               |                 |                |                  | R    | 175.12        | 88.06           | 158.09         | 79.55           |                |                  | 1  |



**MASCOT** Mascot Search Results  
8/13

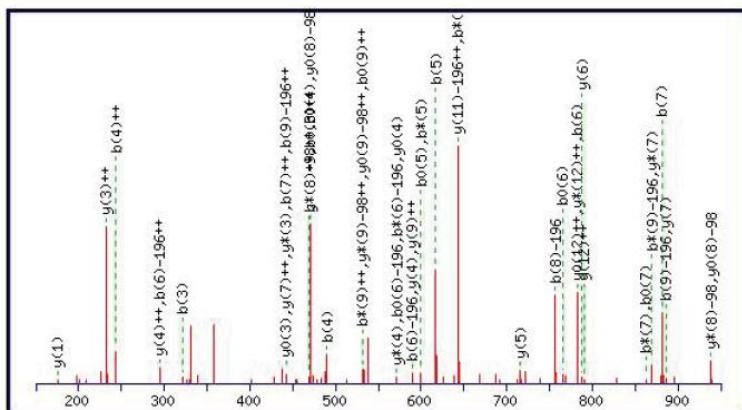
**Peptide View**

MS/MS Fragmentation of **SPHSKSPAEQRER**  
Found in **gi000**, AG Rapp

Match to Query 2204: 1667.724723 from(556.915517,3+)  
Title: LTQ11186.2554.2554.3.dta

Click mouse within plot area to zoom in by factor of two about that point

Or, Plot from  to  Da



**Monoisotopic mass of neutral peptide Mr(calc): 1667.68**

**Fixed modifications:** Carbamidomethyl (C)

**Variable modifications:**

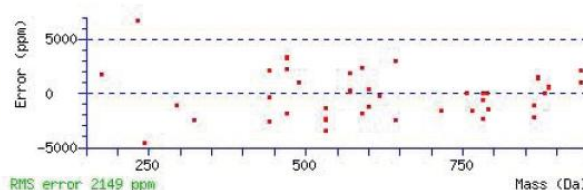
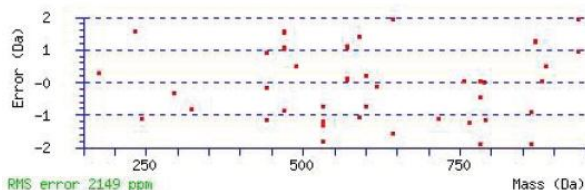
**S4** : Phospho (ST), with neutral losses 0.00(shown in table), 97.98

**S6** : Phospho (ST), with neutral losses 0.00(shown in table), 97.98

**Ions Score:** 28 **Expect:** 0.18

**Matches (Bold Red):** 50/216 fragment ions using 48 most intense peaks

| #  | b             | b <sup>++</sup> | b <sup>*</sup> | b <sup>***</sup> | b <sup>0</sup> | b <sup>0++</sup> | Seq. | y             | y <sup>++</sup> | y <sup>*</sup> | y <sup>***</sup> | y <sup>0</sup> | y <sup>0++</sup> | #  |
|----|---------------|-----------------|----------------|------------------|----------------|------------------|------|---------------|-----------------|----------------|------------------|----------------|------------------|----|
| 1  | 88.04         | 44.52           |                |                  | 70.03          | 35.52            | S    |               |                 |                |                  |                |                  | 13 |
| 2  | 185.09        | 93.05           |                |                  | 167.08         | 84.04            | P    | 1581.66       | <b>791.33</b>   | 1564.63        | <b>782.82</b>    | 1563.65        | <b>782.33</b>    | 12 |
| 3  | <b>322.15</b> | 161.58          |                |                  | 304.14         | 152.57           | H    | 1484.60       | 742.81          | 1467.58        | 734.29           | 1466.59        | 733.80           | 11 |
| 4  | <b>489.15</b> | <b>245.08</b>   |                |                  | <b>471.14</b>  | 236.07           | S    | 1347.55       | 674.28          | 1330.52        | 665.76           | 1329.53        | 665.27           | 10 |
| 5  | <b>617.24</b> | 309.13          | <b>600.22</b>  | 300.61           | <b>599.23</b>  | 300.12           | K    | 1180.55       | <b>590.78</b>   | 1163.52        | 582.26           | 1162.54        | 581.77           | 9  |
| 6  | <b>784.24</b> | 392.62          | 767.22         | 384.11           | <b>766.23</b>  | 383.62           | S    | 1052.45       | 526.73          | 1035.43        | 518.22           | 1034.44        | 517.72           | 8  |
| 7  | <b>881.30</b> | <b>441.15</b>   | <b>864.27</b>  | 432.64           | <b>863.28</b>  | 432.15           | P    | <b>885.45</b> | <b>443.23</b>   | <b>868.43</b>  | 434.72           | 867.44         | 434.23           | 7  |
| 8  | 952.33        | 476.67          | 935.31         | <b>468.16</b>    | 934.32         | <b>467.66</b>    | A    | <b>788.40</b> | 394.70          | 771.37         | 386.19           | 770.39         | 385.70           | 6  |
| 9  | 1081.38       | 541.19          | 1064.35        | <b>532.68</b>    | 1063.36        | <b>532.19</b>    | E    | <b>717.36</b> | 359.19          | 700.34         | 350.67           | 699.35         | 350.18           | 5  |
| 10 | 1209.43       | 605.22          | 1192.41        | 596.71           | 1191.42        | 596.22           | Q    | <b>588.32</b> | <b>294.66</b>   | <b>571.29</b>  | 286.15           | <b>570.31</b>  | 285.66           | 4  |
| 11 | 1365.53       | 683.27          | 1348.51        | 674.76           | 1347.52        | 674.27           | R    | 460.26        | <b>230.63</b>   | <b>443.24</b>  | 222.12           | <b>442.25</b>  | 221.63           | 3  |
| 12 | 1494.58       | 747.79          | 1477.55        | 739.28           | 1476.57        | 738.79           | E    | 304.16        | 152.58          | 287.13         | 144.07           | 286.15         | 143.58           | 2  |
| 13 |               |                 |                |                  |                |                  | R    | <b>175.12</b> | 88.06           | 158.09         | 79.55            |                |                  | 1  |



**MASCOT**  
**SCIENCE** Mascot Search Results  
9/13

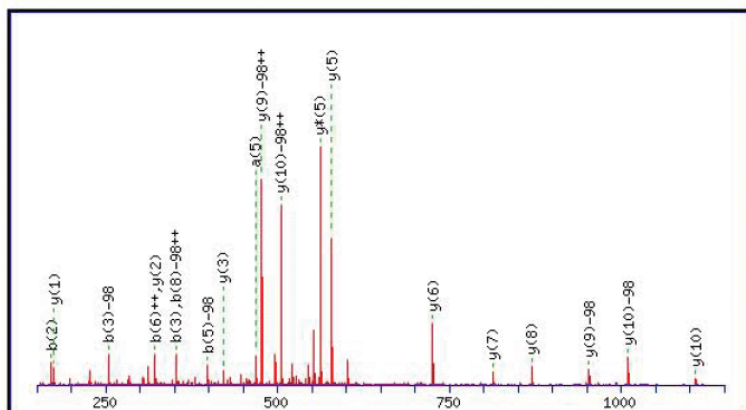
## Peptide View

MS/MS Fragmentation of **IGTGSFGTVFR**Found in **gi000**, AG Rapp

Match to Query 268: 1220.575388 from(611.294970,2+)

Title: File: QstarE04014.wiff, Sample: GST-A-Raf 080617 Bande 2.2 (sample number 1), Elution: 68.374 to 68.691 min, Period: 1, Cycle(s): 2074-

Click mouse within plot area to zoom in by factor of two about that point

Or, Plot from  to  Da 

Monoisotopic mass of neutral peptide Mr(calc): 1220.56

Fixed modifications: Carbamidomethyl (C)

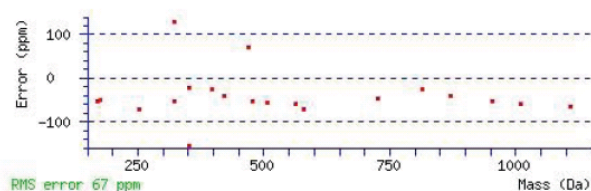
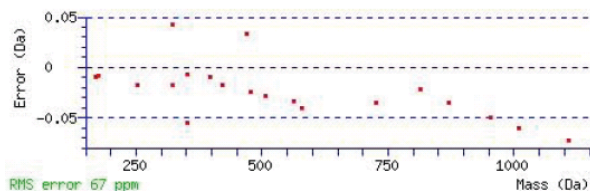
Variable modifications:

T3 : Phospho (ST), with neutral losses 97.98 (shown in table), 0.00

Ions Score: 87 Expect: 8.1e-008

Matches (Bold Red): 20/120 fragment ions using 22 most intense peaks

| #  | a      | a <sup>++</sup> | b             | b <sup>++</sup> | Seq. | y              | y <sup>++</sup> | y <sup>*</sup> | y <sup>*++</sup> | #  |
|----|--------|-----------------|---------------|-----------------|------|----------------|-----------------|----------------|------------------|----|
| 1  | 86.10  | 43.55           | 114.09        | 57.55           | I    |                |                 |                |                  | 11 |
| 2  | 143.12 | 72.06           | <b>171.11</b> | 86.06           | G    | <b>1010.51</b> | <b>505.76</b>   | 993.48         | 497.24           | 10 |
| 3  | 226.15 | 113.58          | <b>254.15</b> | 127.58          | T    | <b>953.48</b>  | <b>477.25</b>   | 936.46         | 468.73           | 9  |
| 4  | 283.18 | 142.09          | 311.17        | 156.09          | G    | <b>870.45</b>  | 435.73          | 853.42         | 427.21           | 8  |
| 5  | 370.21 | 185.61          | <b>398.20</b> | 199.61          | S    | <b>813.43</b>  | 407.22          | 796.40         | 398.70           | 7  |
| 6  | 517.28 | 259.14          | 545.27        | 273.14          | F    | <b>726.39</b>  | 363.70          | 709.37         | 355.19           | 6  |
| 7  | 574.30 | 287.65          | 602.29        | 301.65          | G    | <b>579.32</b>  | 290.17          | <b>562.30</b>  | 281.65           | 5  |
| 8  | 675.35 | 338.18          | 703.34        | <b>352.17</b>   | T    | 522.30         | 261.66          | 505.28         | 253.14           | 4  |
| 9  | 774.41 | 387.71          | 802.41        | 401.71          | V    | <b>421.26</b>  | 211.13          | 404.23         | 202.62           | 3  |
| 10 | 921.48 | 461.25          | 949.48        | 475.24          | F    | <b>322.19</b>  | 161.60          | 305.16         | 153.08           | 2  |
| 11 |        |                 |               |                 | R    | <b>175.12</b>  | 88.06           | 158.09         | 79.55            | 1  |



**MASCOT**  
**SCIENCE** Mascot Search Results

10/13

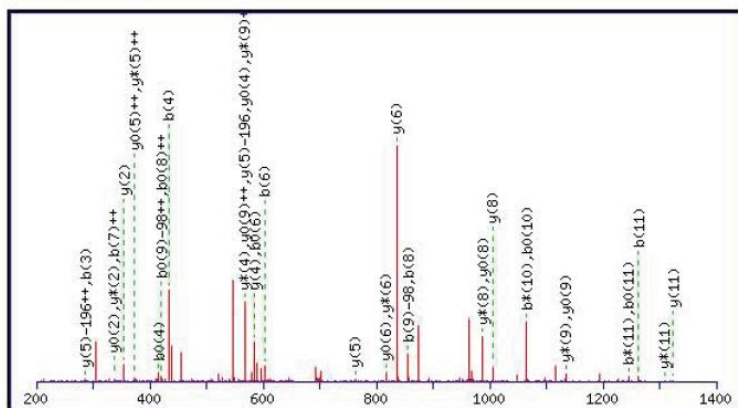
## Peptide View

MS/MS Fragmentation of **IGDFGLATVKTR**Found in **gi000**, AG Rapp

Match to Query 1083: 1436.396724 from(719.205638,2+)

Title: LTQ11184.1561.1563.2.dta

Click mouse within plot area to zoom in by factor of two about that point

Or, Plot from  to  Da Monoisotopic mass of neutral peptide  $M_r(\text{calc})$ : 1436.65

Fixed modifications: Carbamidomethyl (C)

Variable modifications:

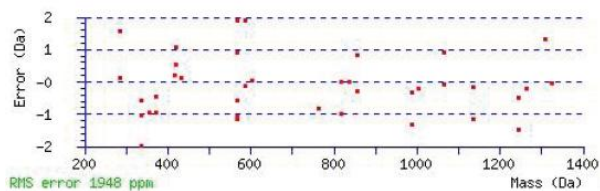
T8 : Phospho (ST), with neutral losses 0.00 (shown in table), 97.98

T11 : Phospho (ST), with neutral losses 0.00 (shown in table), 97.98

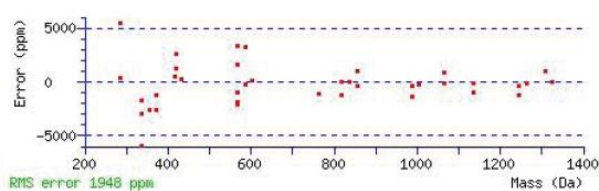
Ions Score: 28 Expect: 0.089

Matches (**Bold Red**): 38/188 fragment ions using 47 most intense peaks

| #  | b              | b <sup>++</sup> | b <sup>*</sup> | b <sup>*++</sup> | b <sup>0</sup> | b <sup>0++</sup> | Seq. | y              | y <sup>++</sup> | y <sup>*</sup> | y <sup>*++</sup> | y <sup>0</sup> | y <sup>0++</sup> | #  |
|----|----------------|-----------------|----------------|------------------|----------------|------------------|------|----------------|-----------------|----------------|------------------|----------------|------------------|----|
| 1  | 114.09         | 57.55           |                |                  |                |                  | I    |                |                 |                |                  |                |                  | 12 |
| 2  | 171.11         | 86.06           |                |                  |                |                  | G    | <b>1324.57</b> | 662.79          | <b>1307.54</b> | 654.28           | 1306.56        | 653.78           | 11 |
| 3  | <b>286.14</b>  | 143.57          |                |                  | 268.13         | 134.57           | D    | 1267.55        | 634.28          | 1250.52        | 625.76           | 1249.54        | 625.27           | 10 |
| 4  | <b>433.21</b>  | 217.11          |                |                  | <b>415.20</b>  | 208.10           | F    | 1152.52        | 576.76          | <b>1135.49</b> | <b>568.25</b>    | <b>1134.51</b> | <b>567.76</b>    | 9  |
| 5  | 490.23         | 245.62          |                |                  | 472.22         | 236.61           | G    | <b>1005.45</b> | 503.23          | <b>988.43</b>  | 494.72           | <b>987.44</b>  | 494.22           | 8  |
| 6  | <b>603.31</b>  | 302.16          |                |                  | <b>585.30</b>  | 293.16           | L    | 948.43         | 474.72          | 931.40         | 466.21           | 930.42         | 465.71           | 7  |
| 7  | 674.35         | <b>337.68</b>   |                |                  | 656.34         | 328.67           | A    | <b>835.35</b>  | 418.18          | <b>818.32</b>  | 409.66           | <b>817.34</b>  | 409.17           | 6  |
| 8  | <b>855.36</b>  | 428.19          |                |                  | 837.35         | <b>419.18</b>    | T    | <b>764.31</b>  | 382.66          | 747.28         | <b>374.15</b>    | 746.30         | <b>373.65</b>    | 5  |
| 9  | 954.43         | 477.72          |                |                  | 936.42         | 468.71           | V    | <b>583.30</b>  | 292.15          | <b>566.27</b>  | 283.64           | <b>565.29</b>  | 283.15           | 4  |
| 10 | 1082.53        | 541.77          | <b>1065.50</b> | 533.25           | <b>1064.52</b> | 532.76           | K    | 484.23         | 242.62          | 467.20         | 234.10           | 466.22         | 233.61           | 3  |
| 11 | <b>1263.54</b> | 632.27          | <b>1246.52</b> | 623.76           | <b>1245.53</b> | 623.27           | T    | <b>356.13</b>  | 178.57          | <b>339.11</b>  | 170.06           | <b>338.12</b>  | 169.56           | 2  |
| 12 |                |                 |                |                  |                |                  | R    | 175.12         | 88.06           | 158.09         | 79.55            |                |                  | 1  |



RMS error 1948 ppm



RMS error 1948 ppm



**Mascot Search Results**  
11/13

**Peptide View**

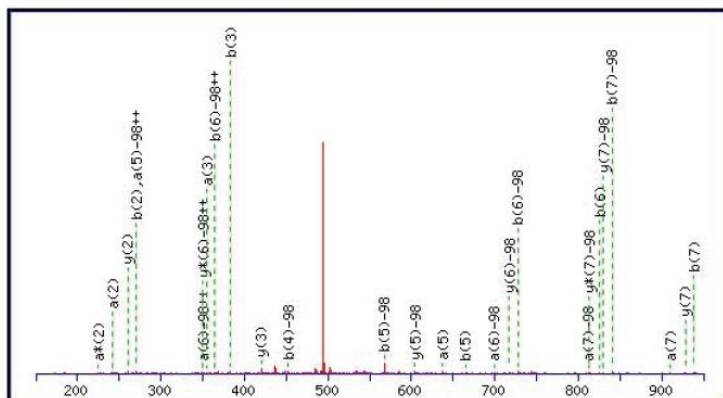
MS/MS Fragmentation of **RLLSDCLK**  
Found in **gi000**, AG Rapp

Match to Query 188: 1083.514100 from(542.764326,2+)

Title: File: QstarE04014.wiff, Sample: GST-A-Raf 080617 Bande 2.2 (sample number 1), Elution: 48.226 min, Period: 1, Cycle(s): 1830 (Experiment 3)

Click mouse within plot area to zoom in by factor of two about that point

Or, Plot from  to  Da



**Monoisotopic mass of neutral peptide Mr(calc): 1083.51**

**Fixed modifications:** Carbamidomethyl (C)

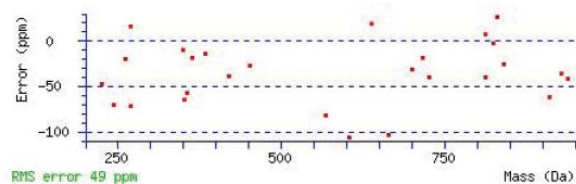
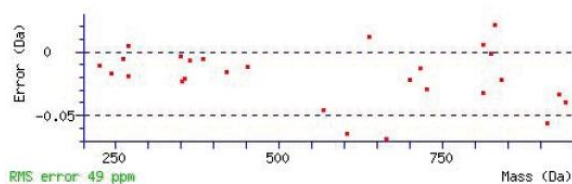
**Variable modifications:**

**S4** : Phospho (ST), with neutral losses 97.98 (shown in table), 0.00

**Ions Score: 23 Expect: 0.18**

**Matches (Bold Red): 27/128 fragment ions using 65 most intense peaks**

| # | a             | a <sup>++</sup> | a <sup>*</sup> | a <sup>*++</sup> | b             | b <sup>++</sup> | b <sup>*</sup> | b <sup>*++</sup> | Seq.     | y             | y <sup>++</sup> | y <sup>*</sup> | y <sup>*++</sup> | #        |
|---|---------------|-----------------|----------------|------------------|---------------|-----------------|----------------|------------------|----------|---------------|-----------------|----------------|------------------|----------|
| 1 | 129.11        | 65.06           | 112.09         | 56.55            | 157.11        | 79.06           | 140.08         | 70.54            | <b>R</b> |               |                 |                |                  | <b>8</b> |
| 2 | <b>242.20</b> | 121.60          | <b>225.17</b>  | 113.09           | <b>270.19</b> | 135.60          | 253.17         | 127.09           | <b>L</b> | <b>830.44</b> | 415.73          | <b>813.42</b>  | 407.21           | 7        |
| 3 | <b>355.28</b> | 178.14          | 338.26         | 169.63           | <b>383.28</b> | 192.14          | 366.25         | 183.63           | <b>L</b> | <b>717.36</b> | 359.18          | 700.33         | <b>350.67</b>    | 6        |
| 4 | 424.30        | 212.66          | 407.28         | 204.14           | <b>452.30</b> | 226.65          | 435.27         | 218.14           | <b>S</b> | <b>604.28</b> | 302.64          | 587.25         | 294.13           | 5        |
| 5 | 539.33        | <b>270.17</b>   | 522.30         | 261.66           | <b>567.32</b> | 284.17          | 550.30         | 275.65           | <b>D</b> | 535.25        | 268.13          | 518.23         | 259.62           | 4        |
| 6 | <b>699.36</b> | <b>350.18</b>   | 682.33         | 341.67           | <b>727.36</b> | <b>364.18</b>   | 710.33         | 355.67           | <b>C</b> | <b>420.23</b> | 210.62          | 403.20         | 202.10           | 3        |
| 7 | <b>812.44</b> | 406.73          | 795.42         | 398.21           | <b>840.44</b> | 420.72          | 823.41         | 412.21           | <b>L</b> | <b>260.20</b> | 130.60          | 243.17         | 122.09           | 2        |
| 8 |               |                 |                |                  |               |                 |                |                  | <b>K</b> | 147.11        | 74.06           | 130.09         | 65.55            | 1        |



# {MATRIX} Mascot Search Results

12/13

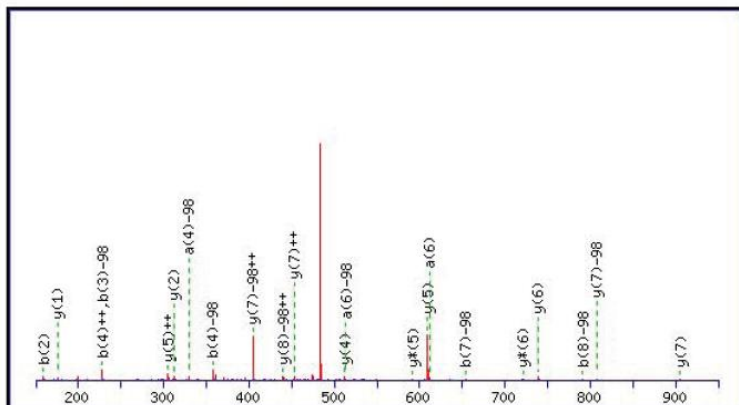
## Peptide View

MS/MS Fragmentation of **SASEPSLHR**Found in **gi000**, AG Rapp

Match to Query 192: 1062.443942 from(532.229247,2+)

Title: File: QstarE04012.wiff, Sample: GST-A-Raf 080617 Bande 1.3 (sample number 1), Elution: 24.099 to 24.611 min, Period: 1, Cycle(s): 2455,

Click mouse within plot area to zoom in by factor of two about that point

Or,  150  950  Monoisotopic mass of neutral peptide  $M_r(\text{calc})$ : 1062.45

Fixed modifications: Carbamidomethyl (C)

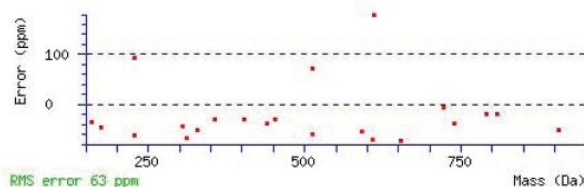
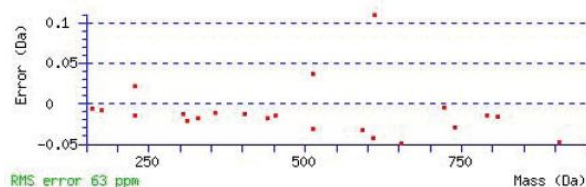
Variable modifications:

S3 : Phospho (ST), with neutral losses 97.98 (shown in table), 0.00

Ions Score: 33 Expect: 0.019

Matches (**Bold Red**): 22/96 fragment ions using 42 most intense peaks

| # | a             | a <sup>++</sup> | b             | b <sup>++</sup> | Seq. | y             | y <sup>++</sup> | y <sup>*</sup> | y <sup>+++</sup> | # |
|---|---------------|-----------------|---------------|-----------------|------|---------------|-----------------|----------------|------------------|---|
| 1 | 60.04         | 30.53           | 88.04         | 44.52           | S    |               |                 |                |                  | 9 |
| 2 | 131.08        | 66.04           | <b>159.08</b> | 80.04           | A    | 878.45        | <b>439.73</b>   | 861.42         | 431.21           | 8 |
| 3 | 200.10        | 100.56          | <b>228.10</b> | 114.55          | S    | <b>807.41</b> | <b>404.21</b>   | 790.38         | 395.70           | 7 |
| 4 | <b>329.15</b> | 165.08          | <b>357.14</b> | 179.07          | E    | <b>738.39</b> | 369.70          | <b>721.36</b>  | 361.19           | 6 |
| 5 | 426.20        | 213.60          | 454.19        | 227.60          | P    | <b>609.35</b> | <b>305.18</b>   | <b>592.32</b>  | 296.66           | 5 |
| 6 | <b>513.23</b> | 257.12          | 541.23        | 271.12          | S    | <b>512.29</b> | 256.65          | 495.27         | 248.14           | 4 |
| 7 | 626.31        | 313.66          | <b>654.31</b> | 327.66          | L    | 425.26        | 213.13          | 408.24         | 204.62           | 3 |
| 8 | 763.37        | 382.19          | <b>791.37</b> | 396.19          | H    | <b>312.18</b> | 156.59          | 295.15         | 148.08           | 2 |
| 9 |               |                 |               |                 | R    | <b>175.12</b> | 88.06           | 158.09         | 79.55            | 1 |



**MASCOT**  
**SCIENCE** Mascot Search Results  
13/13

**Peptide View**

MS/MS Fragmentation of **SASEPSLHR**

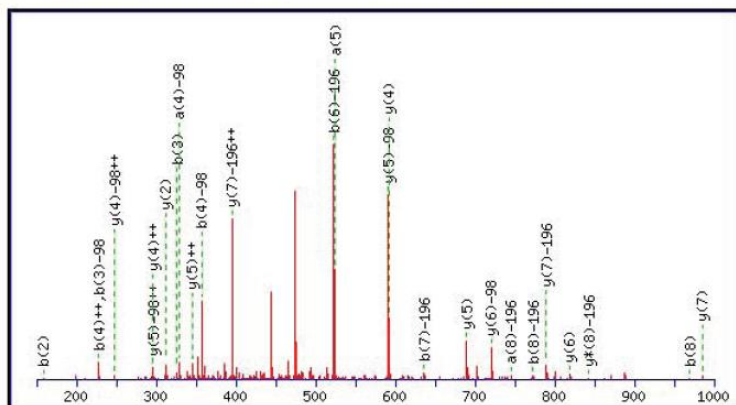
Found in **gi|000**, AG Rapp

Match to Query 30: 1142.395350 from(572.204951,2+)

Title: File: QstarE04163.wiff, Sample: H-Raf Gel02 Probe 3 TiO2 (sample number 1), Elution: 34.022 to 34.066 min, Period: 1, Cycle(s): 3874-3875

Click mouse within plot area to zoom in by factor of two about that point

Or, Plot from  to  Da



**Monoisotopic mass of neutral peptide Mr(calc):** 1142.42

**Fixed modifications:** Carbamidomethyl (C)

**Variable modifications:**

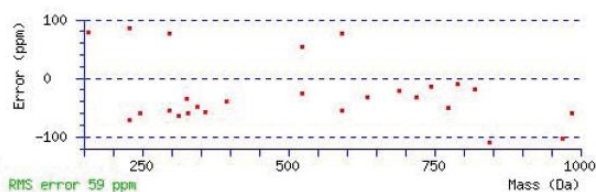
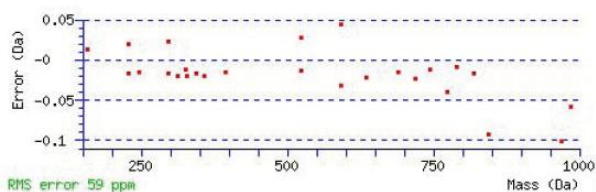
S3 : Phospho (ST), with neutral losses 97.98 (shown in table), 0.00

S6 : Phospho (ST), with neutral losses 97.98 (shown in table), 0.00

**Ions Score:** 26 **Expect:** 0.083

**Matches (Bold Red):** 26/108 fragment ions using 55 most intense peaks

| # | a             | a <sup>++</sup> | b             | b <sup>++</sup> | Seq. | y             | y <sup>++</sup> | y <sup>*</sup> | y <sup>*++</sup> | # |
|---|---------------|-----------------|---------------|-----------------|------|---------------|-----------------|----------------|------------------|---|
| 1 | 60.04         | 30.53           | 88.04         | 44.52           | S    |               |                 |                |                  | 9 |
| 2 | 131.08        | 66.04           | <b>159.08</b> | 80.04           | A    | 860.44        | 430.72          | <b>843.41</b>  | 422.21           | 8 |
| 3 | 200.10        | 100.56          | <b>228.10</b> | 114.55          | S    | <b>789.40</b> | <b>395.20</b>   | 772.37         | 386.69           | 7 |
| 4 | <b>329.15</b> | 165.08          | <b>357.14</b> | 179.07          | E    | <b>720.38</b> | 360.69          | 703.35         | 352.18           | 6 |
| 5 | 426.20        | 213.60          | 454.19        | 227.60          | P    | <b>591.34</b> | <b>296.17</b>   | 574.31         | 287.66           | 5 |
| 6 | 495.22        | 248.11          | <b>523.21</b> | 262.11          | S    | 494.28        | <b>247.65</b>   | 477.26         | 239.13           | 4 |
| 7 | 608.30        | 304.66          | <b>636.30</b> | 318.65          | L    | 425.26        | 213.13          | 408.24         | 204.62           | 3 |
| 8 | <b>745.36</b> | 373.19          | <b>773.36</b> | 387.18          | H    | <b>312.18</b> | 156.59          | 295.15         | 148.08           | 2 |
| 9 |               |                 |               |                 | R    | 175.12        | 88.06           | 158.09         | 79.55            | 1 |



## 9.2. Abbreviations

|                    |   |
|--------------------|---|
| AcNPV              | <i>Autographa californica</i> nuclear polyhedrosis virus                    |
| AICD               | Activation-induced T-cell death   |
| API                | Atmospheric Pressure Ionization   |
| APS                | Ammonium peroxydisulfate  |
| ATP                | Adenosine-5'-triphosphate   |
| bp                 | Base pairs  |
| BSA                | Bovine serum albumin  |
| C-terminal         | Carboxy-terminal  |
| ca.                | Circa   |
| cAMP               | Cyclic adenosine monophosphate  |
| cDNA               | Complementary DNA   |
| CNK                | Connector enhancer of KSR   |
| COS7 cells         | African green monkey SV40-transfected kidney fibroblast cell line           |
| CR                 | Conserved region  |
| CRD                | Cysteine rich domain  |
| Da                 | Dalton  |
| DBD                | DNA binding domain  |
| ddH <sub>2</sub> O | Double distilled water  |
| DFG                | Deutsche Forschungsgemeinschaft   |
| D-MEM              | Dulbecco's Modified Eagle Medium  |
| DMSO               | Dimethyl sulfoxide  |
| DNA                | Deoxyribonucleic acid   |
| dNTP               | Deoxyribonucleoside triphosphate  |
| dsDNA              | Double-stranded DNA   |
| DTT                | Dithiothreitol  |
| <i>E. coli</i>     | <i>Escherichia coli</i>   |
| ECL                | Enhanced chemiluminescence  |
| EDTA               | Ethylenediaminetetraacetic acid-disodium salt                               |
| e. g.              | <i>exempli gratia</i>   |
| EGF                | Epidermal growth factor   |
| EGFR               | Epidermal growth factor receptor  |
| EGTA               | Ethylene glycol-bis-( $\beta$ -aminoethylether)-N,N,N',N'-tetraacetic acid) |
| ER                 | Endoplasmic reticulum   |
| ERK                | Extracellular signal-regulated protein kinase                               |
| ESI                | Electrospray Ionization   |
| FCS                | Fetal calf serum  |
| <i>et al.</i>      | <i>et alii</i>  |
| FTase              | Farnesyl transferase  |
| GAP                | GTPas-activating proteins   |
| GDP                | Guanosine diphosphate   |
| GEF                | Guanine nucleotide exchange factor  |
| GGTase I           | Geranylgeranyltransferase type I  |
| GPCR               | G-protein-coupled receptor  |
| Grb2               | Growth-factor-receptor-binding protein 2                                    |
| GRE                | Glucocorticoid response element   |

---

|              |   |
|--------------|---|
| GRK          | GPCR kinases  |
| GST          | Glutathione <i>S</i> -transferase                         |
| GTP          | Guanosine-5'-triphosphate                                 |
| h            | Hours   |
| HEK293 cells | Human Embryonic Kidney 293 cells                          |
| HIPK2        | Homeodomain-interacting protein kinase                    |
| HVR          | Hypervariable region                                      |
| IB           | Immunoblot  |
| Icmt         | Isoprenylcysteine carboxyl methyltransferase              |
| IH-region    | Isoform-specific hinge region                             |
| IL-2R        | Inreleukin-2 receptor                                     |
| IP           | Immunoprecipitation                                       |
| ITAM         | Immunoreceptor tyrosine-based activation motif            |
| JBC          | Journal of Biological Chemistry                           |
| JNK          | c-Jun N-terminal kinases                                  |
| kb           | Kilobase  |
| kDa          | Kilodalton  |
| L            | Liter   |
| LB           | Luria Bertani   |
| KSR          | Kinase suppressor of Ras                                  |
| M2PK         | Pyruvate kinase isoenzyme type M2                         |
| MALDI        | Matrix Assisted Laser Desorption Ionization               |
| MAPK         | Mitogen-activated protein kinase                          |
| MAP2K        | MAPK kinase   |
| MAP3K        | MAPK kinase kinase  |
| MEF2         | Myocyte enhancer factor 2                                 |
| MEK          | MAPK kinase   |
| MEKK         | MAPK kinase kinase  |
| MHC          | Major histocompatibility complex                          |
| min          | Minutes   |
| MOI          | Multiplicity of infection                                 |
| MORG1        | MAPK organizer-1  |
| MP1          | MEK-partner 1   |
| mRNA         | Messenger RNA   |
| MS           | Mass spectrometry   |
| MSZ          | Institut für Medizinische Strahlenkunde und Zellforschung |
| MW           | Molecular weight  |
| N-terminal   | Amino-terminal  |
| N-region     | Negative-charge regulatory region                         |
| NES          | Nuclear-export sequences                                  |
| NGF          | Nerve growth factor                                       |
| NLK          | Nemo-like kinase  |
| NLS          | Nuclear-localization sequences                            |
| NP-40        | Nonidet P40   |
| NUP          | Nuclear pore protein                                      |
| OD           | Optical density   |
| PAK          | p21-activated kinases                                     |
| PABR         | Phosphatidic acid-binding region                          |
| PARP-1       | Poly-[ADP-ribose]-polymerase 1                            |

|           |  |
|-----------|--|
| PBS       | Phosphate buffered saline  |
| PFTase    | Protein farnesyltransferase  |
| PI3K      | Phosphatidylinositol 3-kinase  |
| PKA       | Protein kinase A   |
| PKB       | Protein kinase B   |
| PKC       | Protein kinase C   |
| PP5       | Protein phosphatase 5  |
| PP2A      | Protein phosphatase 2A   |
| PRS       | Proline-rich sequences   |
| pS (pSer) | Phosphoserine  |
| pT (pThr) | Phosphothreonine   |
| PTK       | Protein tyrosine kinase  |
| pY (pTyr) | Phosphotyrosine  |
| RA domain | Ras association domain   |
| RalGDS    | Ral guanine nucleotide dissociation stimulator                             |
| RBD       | Ras binding domain   |
| Rce 1     | Ras converting enzyme 1  |
| RKIP      | RAF kinase inhibitor protein   |
| PA        | Phosphatidic acid  |
| PCR       | Polymerase chain reaction  |
| PFC       | Serum glycoprotein properdin   |
| pfu       | Plaque forming unit  |
| PHB       | Prohibitin   |
| PKC       | Protein kinase C   |
| RLK       | Receptor-like kinase   |
| PMSF      | Phenylmethylsulfonylfluorid  |
| PVDF      | Polyvinylidene difluoride  |
| RNA       | Ribonucleic acid   |
| Rpm       | Rotations per minute   |
| RPT       | Ras palmitoyltransferase   |
| RSK       | Ribosomal S6 kinase  |
| RT        | Room temperature   |
| RTK       | Receptor tyrosine kinase   |
| RU        | Resonance unit   |
| SAPK      | Stress activated protein kinase  |
| SDS       | Sodium dodecyl sulfate   |
| SDS-PAGE  | Sodium dodecyl sulfate polyacrylamide gel electrophoresis                  |
| sec       | Seconds  |
| Sf9 cells | Insect cell line derived from pupal ovarian tissue of <i>S. frugiperda</i> |
| SH2       | Src homology 2   |
| SOS       | “Son of sevenless”   |
| SPR       | Surface plasmon resonance  |
| SRF       | Serum response factor  |
| SUR-8     | Suppressor of Ras-8  |
| SYN1      | Synapsin I   |
| TAB1      | TAK1-binding protein 1   |
| TAK1      | TGF- $\beta$ -activated kinase 1   |
| TCR       | T-cell receptor  |
| TEMED     | N,N,N',N'-Tetramethylethylenediamine                                       |

|                |  |
|----------------|--|
| TERT           | Telomerase reverse transcriptase       |
| TGF- $\beta$   | Transforming growth factor- $\beta$    |
| TIMP           | Tissue inhibitor of metalloproteinases |
| T <sub>m</sub> | Melting temperature                    |
| TPA            | 12-O-Tetradecanoylphorbol 13-acetate   |
| TRE            | Thyroid hormone response element       |
| U              | Unit                                   |
| UV-light       | Ultraviolet light                      |
| vs.            | <i>versus</i>                          |
| v/v            | Volume/Volume                          |
| v              | Viral                                  |
| WT             | Wild type                              |
| w/v            | Weight/Volume                          |

## **ACKNOWLEDGMENTS**

This dissertation would not have been possible without the contribution of many people who not only influenced my work, but also supported me in many ways in obtaining a doctoral degree.

First of all, I would like to express my deepest gratitude to my supervisor Prof. Dr. Ulf R. Rapp for providing an opportunity to express myself as a young scientist doing my research, for giving me the important lessons in conducting an independent and fruitful research and for the strong scientific guidance. I would also like to extend my appreciation to Prof. Dr. Ricardo Benavente for accepting me to the faculty of biology and his support during my research.

I am very grateful to my first co-supervisors Dr. Hannes Drexler, who accompanied me through the first two years, for his involvement in my research work and sharing his fruitful ideas. I want to extend my gratitude to my second co-supervisor Dr. Mirko Hekman for his support during these years. He participated actively in many steps that were necessary to achieve the goals of this dissertation.

I would like to thank Prof. Dr. Thomas Müller for his help in protein modeling, many thanks also to Dr. Werner Schmitz and Dr. René Zahedi for their help in mass spectrometrical analysis.

I wish to thank all the past and present members of the “MSZ’s Biochemistry Club” for their important contribution and constructive discussions. Furthermore, I would like to thank them for the many social and scientific events we have shared and for providing an uncomplicated and stimulating environment. I would not forget to thank our technicians Renate Metz, Barbara Bauer and Reinhold Krug for their persistent readiness to help and their excellent technical assistance.

I appreciate Prof. Dr. Thomas Raabe and all the past and present members of his group for giving me an opportunity to work in their laboratories during the first year of my research and for their help at the first steps of my work. Furthermore, I wish to thank them for the friendly and enjoyable atmosphere during the lunchtime we spent together.

I am grateful to many other co-workers in MSZ-Institute for the nice and friendly atmosphere, for support and helpful suggestions and for the time we shared also outside of the institute.

My final and most heartfelt acknowledgment go to my family for their everlasting love and support, and particularly to my mother for spending her whole life just in tuning a good future for me and for instilling in me the belief that I could do absolutely anything to which I applied myself and making the option of giving up an unlikely one.



## CURRICULUM VITAE

### Personal data

|                |  |
|----------------|--|
| Name           | Baljuls                                  |
| Given name     | Angela                                   |
| Previous name  | Baljuls                                  |
| Postal address | Erthalstr. 46, D-97074 Würzburg, Germany |
| Phone          | +49-931-4651985                          |
| Email          | angela_baljuls@gmx.de                    |
| Date of birth  | January 24, 1978                         |
| Place of birth | Kokshetau, Kazakhstan                    |
| Marital status | unmarried                                |
| Children       | none                                     |
| Nationality    | German                                   |

### Education

#### Lower Education

---

|                   |   |
|-------------------|---|
| 1985–1995         | Secondary school, Kokshetau, Kazakhstan   |
| Aug 1996–Feb 1997 | Language school (Interkulturelle Bildung Hamburg e. V.), Hamburg, Germany   |
| 1997–1999         | Secondary school “Sonderlehrgang für Berechtigte nach dem Bundesvertriebenengesetz (BVFG)”, Göttingen, Germany<br>Degree: General qualification for university entrance |

#### Higher Education

---

|                   |  |
|-------------------|--|
| 2000–2004         | Study of Biology, Julius-Maximilian-University of Würzburg, Germany<br>Degree: Diploma<br>Diploma thesis at the Institute of Biochemistry of the University of Würzburg, Germany; Supervisor: Prof. Dr. Hildburg Beier; Title: “Characterization of the tRNA splice endonuclease of higher plants” |
| 2004–present time | PhD student at the Institute for Medical Radiation and Cell Research, University of Würzburg, Germany; Supervisor: Prof. Dr. Ulf R. Rapp   |

## List of publications

- **Baljuls, A.**, Mueller, T., Drexler, H.C.A., Hekman, M. and Rapp, U.R. (2007) Unique N-region determines low basal activity and limited inducibility of A-RAF kinase – The role of N-region in the evolutionary divergence of RAF kinase function in vertebrates. *J. Biol. Chem.*, Vol. 282, Issue 36, 26575–26590.
- **Baljuls, A.**, Schmitz, W., Mueller, T., Zahedi, R.P., Sickmann, A., Hekman, M. and Rapp, U.R. (2008) Positive regulation of A-RAF by phosphorylation of isoform-specific hinge segment and identification of novel phosphorylation sites. *J. Biol. Chem.*, Vol. 283, Issue 40, 27239–27254.
- Fischer, A., **Baljuls, A.**, Reinders, J., Nekhoroshkova, E., Sibilski, C., Metz, R., Albert, S., Hekman, M. and Rapp, U.R. (2008) Regulation of RAF activity by 14-3-3 proteins – RAF kinases associate functionally with both homo- and heterodimeric forms of 14-3-3 proteins. *J. Biol. Chem.*, in press.
- Beck, M., Klingauf, M., Robubi, A., **Baljuls, A.**, Hekman, M., Heinzer, S., Turgay, Y., Rapp, U.R. and Kroschewski, R. (2008) The Ras-like tumor suppressor DiRas3 (Noey2, ARHI) downregulates specifically RAF and MEK signaling. *Molecular cell*, in revision.
- **Baljuls, A.** and Rapp, U. R. “A-RAF – the RAF isoform shrouded in mystery.” Review, in preparation.

## Poster abstracts

- **Baljuls, A.**, Schmitz, W., Mueller, T., Zahedi, R.P., Sickmann, A., Hekman, M. and Rapp, U. R. Positive regulation of A-RAF by phosphorylation of isoform-specific hinge segment. EMBO Workshop: Can Epigenetics Influence Reprogramming & Metastatic Progression? Banz Monastery, Bad Staffelstein, Germany. September 6–9, 2008.
- Klingauf, M., Beck, M., Robubi, A., Hekman, M., **Baljuls, A.**, Heinzer, S., Turgay, Y., Rapp, U.R. and Kroschewski, R. The Ras-like tumor suppressor DiRas3 (Noey2, ARHI) downregulates specifically the RAF-MEK-ERK signaling pathway by inhibiting MEK. ELSO Meeting: Frontiers of Cellular, Developmental and Molecular Biology. Nice, France, August 30–September 2, 2008.
- **Baljuls, A.**, Müller, T., Drexler, H.C.A., Hekman, M. and Rapp, U.R. Nonconserved residues within the N-region determine activation properties of RAF kinases. 9th Young Scientist Meeting of the DGZ: Signaling Cascades in Development and Disease. Max-Planck-Institute for Molecular Biomedicine, Münster, Westphalia, Germany, September 20–21, 2007.

- Hekman, M., Fischer, A., Rubio, I., Wiese, S., Kuhlmann, J., **Baljuls, A.** and Rapp, U.R. Regulation of RAF kinases by Ras and 14-3-3 proteins. International Symposium of the SFB 487: Membrane Proteins and Diseases. Würzburg, Germany, June 7–9, 2007.
- Englert, M., **Baljuls, A.**, Akama, K. and Beier, H. Structure and function of tRNA splicing enzymes from wheat germ. 29th FEBS Congress, Warsaw, Poland, June 26–July 1, 2004.

## Oral presentations

- “Mutations of non-conserved residues within the N-region reverse activation properties of RAF kinases.” 9th Young Scientist Meeting of the DGZ: Signaling Cascades in Development and Disease. Max-Planck-Institute for Molecular Biomedicine, Münster, Westphalia, Germany, 20–21 September, 2007.

Würzburg, den \_\_\_\_\_

---

(Angela Baljuls)

Erklärung gemäß § 4 Absatz 3 der Promotionsordnung der  
Fakultät für Biologie der Bayerischen Julius-Maximilians-  
Universität Würzburg vom 15. März 1999.

Hiermit erkläre ich ehrenwörtlich, dass ich die vorliegende Dissertation selbständig angefertigt und keine anderen als die angegebenen Quellen und Hilfsmittel benutzt habe.

Weiterhin erkläre ich, dass die vorliegende Dissertation noch in keinem anderen Prüfungsverfahren in gleicher oder ähnlicher Form vorgelegen hat.

Außer den in dem Zulassungsgesuch urkundlich vorgelegten Graden habe ich keine weiteren Grade erworben oder zu erwerben versucht.

Würzburg, den \_\_\_\_\_

---

(Angela Baljuls)